Genome-wide molecular characterisation of central nervous system primitive neuroectodermal tumours and pineoblastomas

Suzanne Miller

Thesis presented for the degree of
Doctor of Philosophy

The University of Nottingham
June 2010

This thesis is dedicated to the children and their families whose lives have been affected by brain tumours

ABSTRACT

CNS PNET and pineoblastomas are highly malignant embryonal brain tumours of poor prognosis. Current treatment strategies are based on the histologically similar medulloblastoma; however, patients with CNS PNET and pineoblastoma have significantly worse outcomes. Specific therapies based on the underlying biology and genetics of CNS PNET and pineoblastoma are needed. To provide evidence of the fundamental genetics driving tumour pathogenesis and to identify novel targets for therapy, 46 CNS PNETs and pineoblastomas were analysed using the Affymetrix 100K/500K mapping sets to identify genome-wide copy number alterations and loss of heterozygosity. Overall, frequent gains of 1q, 2p and 21q and frequent loss of 16q were identified. Unsupervised hierarchical clustering showed marked differences in the frequency of genetic imbalance in the CNS PNETs and pineoblastomas, with pineoblastomas containing fewer genomic changes clustering separately to the CNS PNETs. Novel gene copy number alterations were identified; gain of *PCDHGA3* (5q31.3) and *FAM129A* (1q25) and losses of *OR4C12* (11p11.12), *CADPS* (3p14.2), and *SALL1* (16q12.1). Loss of *CDKN2A* and *CDKN2B* was also identified, in keeping with previous genetic studies of CNS PNET. Linking gene copy number data with patient clinical information, loss of *CADPS* was associated with poor prognosis in patients with primary CNS PNETs ($p = 0.033$ and $p = 0.046$, by SNP array and real time qPCR analyses, respectively). On comparison of 5 primary and recurrent CNS PNET pairs, gain of 2p21 was the most common alteration maintained in 80% of cases. Immunohistochemistry for p15INK4B (encoded by *CDKN2B*) was performed which demonstrated the loss in gene copy number had lowered the expression of the encoded protein. Finally an immunohistochemical and mutational screen for INI1 (commonly lost in the malignant embryonal brain tumour, ATRT) was performed in the CNS PNET/pineoblastoma cohort which showed the loss of INI1 protein expression in the tumour cohort was not due to mutations residing in the mutational hotspots of exons 5 and 9 of the *INI1* gene. Patients with INI1 immunonegative CNS PNETs had a worse prognosis than those with INI1 immunopositive CNS PNETs ($p < 0.0001$). This project demonstrated the first application of SNP array technology in the analysis of the largest cohort of CNS PNETs and pineoblastomas to date, identified novel gene copy number alterations, linked genetic alterations with clinical factors and identified 2 potential markers of prognosis.

ACKNOWLEDGEMENTS

I wish to express my sincere thanks to many people who have supported and helped me during my study. First and foremost I would like to thank my supervisor Professor Richard Grundy for his encouragement, patience and enthusiasm throughout this period of research. Always on hand with expert guidance and advice, it was a pleasure to work with such a dedicated person and I am very proud to have been one of his students.

I am also very grateful to Dr Beth Coyle for her knowledgeable support and help with preparing this thesis. I would also like to thank Dr Vikki Rand for support whilst using the Affymetrix and Spotfire programs and a special thank you goes to my two office buddies Dr Hazel Rogers and Dr Martyna Adamovicz-Brice for their scientific help and for keeping me sane. I received invaluable help from the staff at the West Midlands Regional Genetics Laboratory where the SNP array work was performed. I am indebted to Dr Emma Prebble and Dr Sara Dyer for their specialist help with the SNP array work whilst working at the Birmingham Women's Hospital.

I would like to thank the team at the Children's Brain Tumour Research Centre for technical support and lively scientific discussions. In particular Dr Lisa Storer for sample collection and Mr Lee Ridley for sample collection and construction of the tissue microarray. Prof James Lowe, Dr Keith Robson and Dr Marie-anne Brundler for careful histopathological review of the tumours and also with the interpretation of immunohistochemical results. Mr Stuart Smith and Dr Jo-Fen Lui for help with statistical analysis.

A special thank you is reserved for The Samantha Dickson Brain Tumour Trust for the funding of this PhD. Tirelessly campaigning for better research into brain tumours and providing funding, I am very thankful for the support they have given me.

Finally a big thank you to my family and friends who have supported me on this journey. To my parents and brother who have encouraged me to achieve my goals in life. Mostly I would like to thank my partner Lee for his love, encouragement and support throughout this journey.

LIST OF ILLUSTRATIONS

LIST OF TABLES

LIST OF ABBREVIATIONS

3’ UTR	3’ untranslated region
A	Adenine
aCGH	Array comparative genomic hybridisation
ATCC	American type culture collection
ATP	Adenosine triphosphate
ATRT	Atypical teratoid rhabdoid tumour
aUPD	Acquired uniparental disomy
BAC	Bacterial artificial chromosome
BBB	Blood brain barrier
bp	Basepair
BRLMM	Bayesian robust linear model with mahalanobis distance classifier
BSA	Bovine serum albumin
C	Cytosine
CBTRC	Children’s brain tumour research centre
CCG	Children’s cancer group
CGH	Comparative genomic hybridisation
CHTN	Cooperative human tissue network
Ck	Cytokeratin
CML	Chronic myeloid leukaemia
CN	Copy number
CNAG	Copy number analyser for genechip
CNS	Central nervous system
CNS PNET	Central nervous system primitive neuroectodermal tumour
CSI	Craniospinal irradiation
Ct	Threshold cycle
CT	Chemotherapy
d	Downstream
DAB	3,3-diaminobenzidine
DAPI	4’,6-diamidino-2-phenylindole

DIM	Diminished
DM	Dynamic model
DMSO	Dimethyl sulphoxide
DNA	Deoxyribonucleic acid
dNTP	Deoxyribonucleotide triphosphate
DPX	Depex-polystyrene dissolved in Xylene
E	Efficiency
EB	Elution buffer
EDTA	Ethylenediaminetetraacetic acid
EFS	Event-free survival
EGL	External granular layer
EMA	Epithelial membrane antigen
ENH	Enhanced
FAP	Familial adenomatous polypopsis
FB	Foetal Brain
FFPE	Formalin fixed paraffin embedded
FISH	Fluoresence in situ hybridisation
FITC	Fluorescein isothiocyanate
G	Guanine
GBM	Glioblastoma multiforme
GCOS	Genechip operating software
GFAP	Glial fibrillary acidic protein
GTR	Gross total resection
GTYPE	Genechip genotyping analysis software
H and E	Haematoxylin and eosin
HMM	Hidden markov model
HNPCC	Hereditary nonpolyposis colorectal cancer
HSDNA	Herring sperm DNA
i	Intronic
i17q	Isochromosome 17q
IHC	Immunohistochemistry
iHDAC	Histone deactylase inhibitor
ISCN	International system for human cytogenetic nomenclature
ISH	In situ hybridisation

Kb	Kilobase
KV	Kilovolt
LOH	Loss of heterozygosity
MB	Medulloblastoma
Mb	Megabase
MES	4-morpholine ethanesulfonic acid
MgSO4	Magnesium sulphate
MRI	Magnetic resonance imaging
mRNA	Messenger RNA
NaAc	Sodium acetate
NaB	Sodium butyrate
NaCl	Sodium chloride
NF	Neurofilament
Ng	Nanogram
NS	Nervous system
NSE	Neuron specific enolase
OCR	Oligo control reagent
OS	Overall survival
PAC	P1 artificial chromosome
PBS	Phosphate buffered saline
PCR	Polymerase chain reaction
PFS	Progression-free survival
PLG	Phase lock gel
PNET	Primitive neuroectodermal tumour
QC	Quality control
Rb	Retinoblastoma
RNAi	Ribonucleic acid interference
RT	Radiotherapy
SAHA	Suberoylanilide hydroxamic acid
SAPE	Streptavidin-phycoerythrin
SDS	Sodium dodecyl sulfate
Seq	Sequence
SFOP	Societé française oncologie pédiatrique
SHH	Sonic hedgehog

SIOP	International society of paediatric oncology
SMA	Smooth muscle actin
SNP	Single nucleotide polymorphism
SPSS	Statistical package for the social sciences
SRCC	Spearman's rank correlation coefficient
T	Thymine
TdT	Terminal deoxynucleotidyl transferase
TMA	Tissue microarray
TMACl	Tetramethyl ammonium chloride
TSA	Trichostatin A
u	Upstream
UKCCSG/CCLG	United Kingdom Children's Cancer Study Group/Children's Cancer and Leukaemia group
UPGMA	Unweighted pair group method with arithmetic mean
WHO	World health organisation
Wt	Wildtype
Yr	Year

CHAPTER 1

INTRODUCTION

1.1 Paediatric brain tumours

1.1.1 General background and epidemiology

Cancer of the brain is the most common solid tumour of childhood, with 450 new cases in the UK each year (McKinney, 2004). Although brain tumours in adults are rare (approximately 8% of adult cancers), they account for nearly 25% of all childhood cancers (Figure 1.1). The incidence of brain tumours in children has risen in the past 20 years. This may in part be due to the introduction of MRI scanning; with clinicians now better equipped to correctly diagnose a brain tumour. Of all paediatric cancers, tumours of the central nervous system (CNS) are second in frequency only to leukaemia. However, whereas 80% of leukaemias are now successfully treated, this is not the case for children diagnosed with a brain tumour where an overall survival of only 50-60% is obtainable (Stiller 2004). Thus, whereas the rates for children surviving leukaemia have dramatically improved in the past 20 years, the rates for children surviving a brain tumour has only moderately improved (Figure 1.2) (Ries 1999). Brain tumours are the leading cause of mortality from diease in children aged less than 15 years (Kleihues, Louis et al. 2002). Over 100 children in the UK die each year due to cancer of the CNS and in England and Wales alone, over 10,000 life years are lost each year. Of the paediatric brain tumour patients who survive, 60% will acquire disabilities, which are usually life long and progressive. Intensive treatment regimes including radiotherapy frequently damage the normal brain leaving patients with a reduced quality of life. A reduction in the use of radiotherapy given to children is essential to limit neurocognitive damage which includes a decline in IQ and short term memory. Additionally the use of radiotherapy has been linked with the increased occurrence of secondary malignancies and endocrinopathies (Lannering, Marky et al. 1990; Duffner, Krischer et al. 1998; Copeland, deMoor et al. 1999; Riva and Giorgi 2000; Mulhern, Merchant et al. 2004; Spiegler, Bouffet et al. 2004; Spoudeaus 2004).

Paediatric brain tumours are complicated neoplasms to study, with challenges in classification due to the diverse histological spectra. Presently treatment is empirical rather than based on an understanding of the underlying tumour biology. Increased knowledge of the genetics and better understanding of the underlying biology

contributing to the development and progression of brain tumours is needed to identify novel targets for therapy. New evidence based treatments will ultimately lead to increases in patient survival and a meaningful decrease in morbidity.

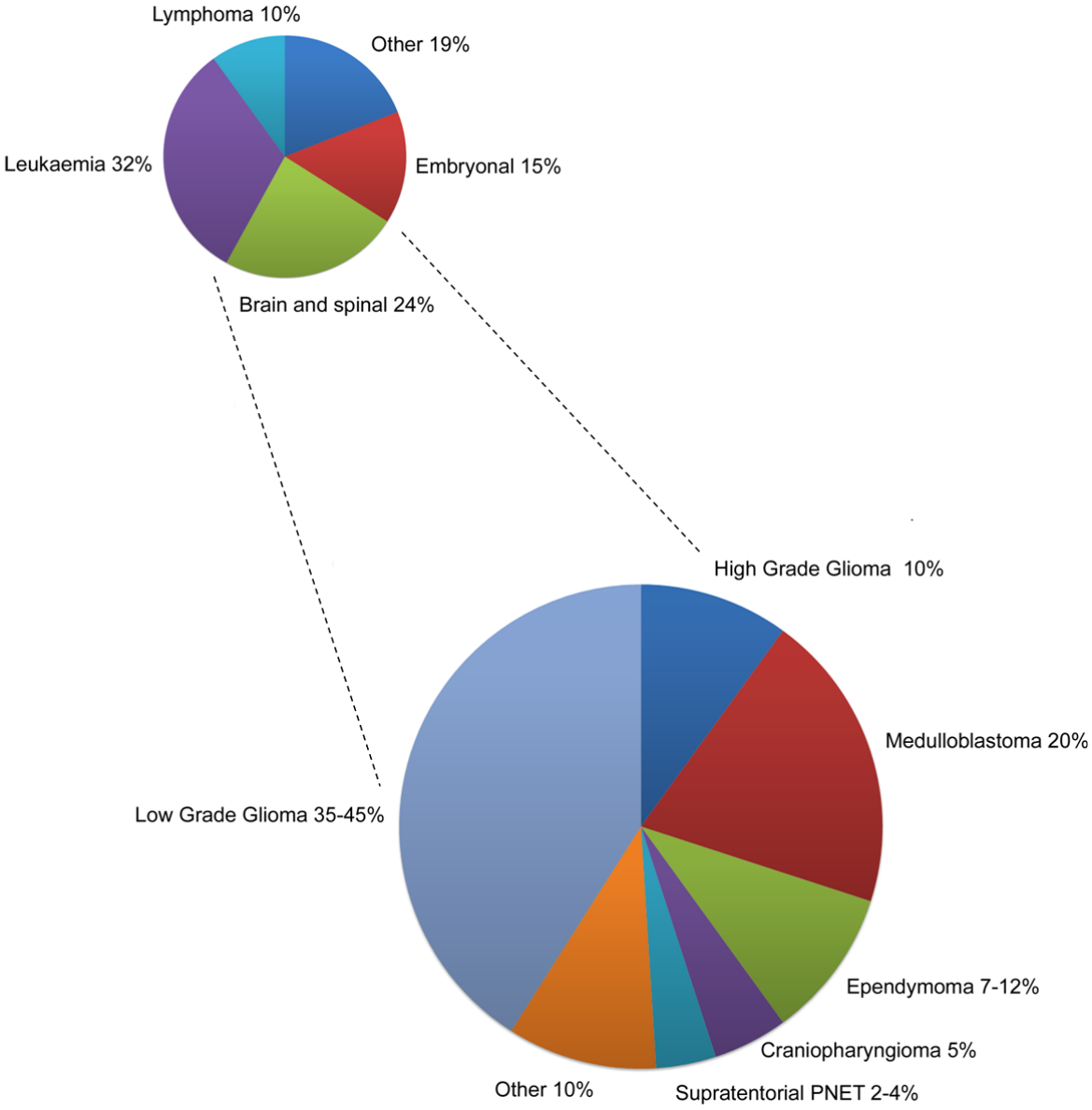

Figure 1.1 The relative incidence of paediatric cancers and paediatric brain tumours in industrialised countries (Stiller, 2004).

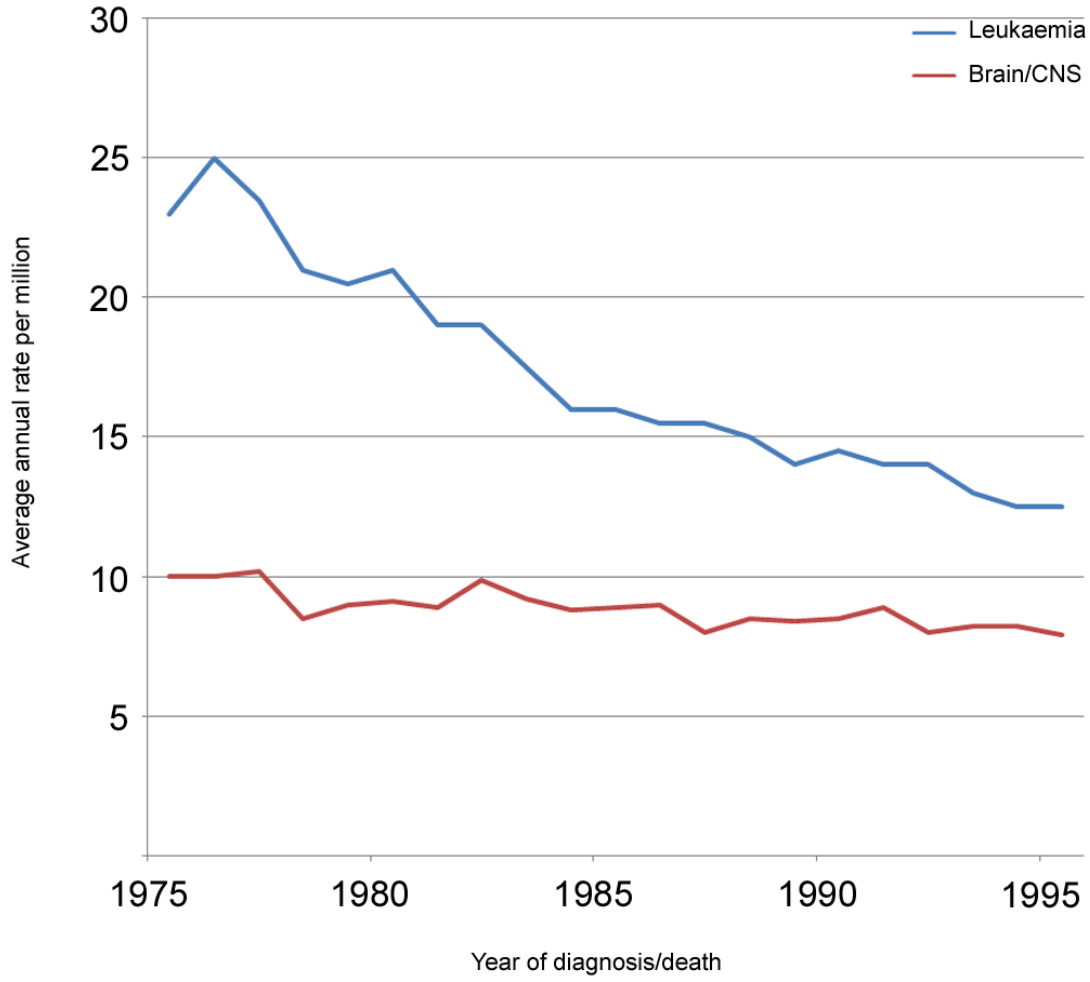

Figure 1.2 Comparison of the trends in mortality between paediatric leukaemia and paediatric brain tumours. Data reproduced from the SEER Program, 'Cancer Incidence and Survival among Children and Adolescents: United States 1975-1995' (Ries, 1999).

1.1.2 Neuroembryology

It has long been proposed that tumours of childhood are the result of abnormal development, with defects present in key regulatory pathways leading to tumourigenesis (Scotting, Walker et al. 2005). Loss in control of cell division, differentiation and apoptosis can all lead to the tumourigenic transformation of a cell. Thus, a comprehensive understanding of normal brain development is essential in the understanding of tumourigenic events leading to the development of brain tumours. At present it is not known at what stage of brain development cells can become tumourigenic. Current knowledge of the development, growth and processes of which cells in the brain go through during normal brain development has led to many hypotheses, many of which cannot at present be answered. Further characterisation of brain tumour cells will undoubtedly lead to evidence towards answering these questions.

The CNS is generated from the maturation and differentiation of the cells of the ectoderm ultimately producing the brain and spinal cord. Normal neurogenesis comprises of multipotent neural stem cells originating from the ectoderm giving rise to progenitor cells. Thus, the mature CNS is generated from the differentiation of these progenitors into neurons or glia. A more detailed account of normal neurogenesis is described in chapter 4a, (Scotting and Appleby, 2004).

During the third week of embryogenesis, 3 germ layers are produced (termed gastrulation), giving rise to the endoderm, mesoderm and ectoderm. The notochord (formed during gastrulation) induces the development of the neural plate by the thickening of the ectoderm (neuralation). In the 4^{th} week of embryonic development, the neural plate folds to form the neural tube (Figure 1.3).

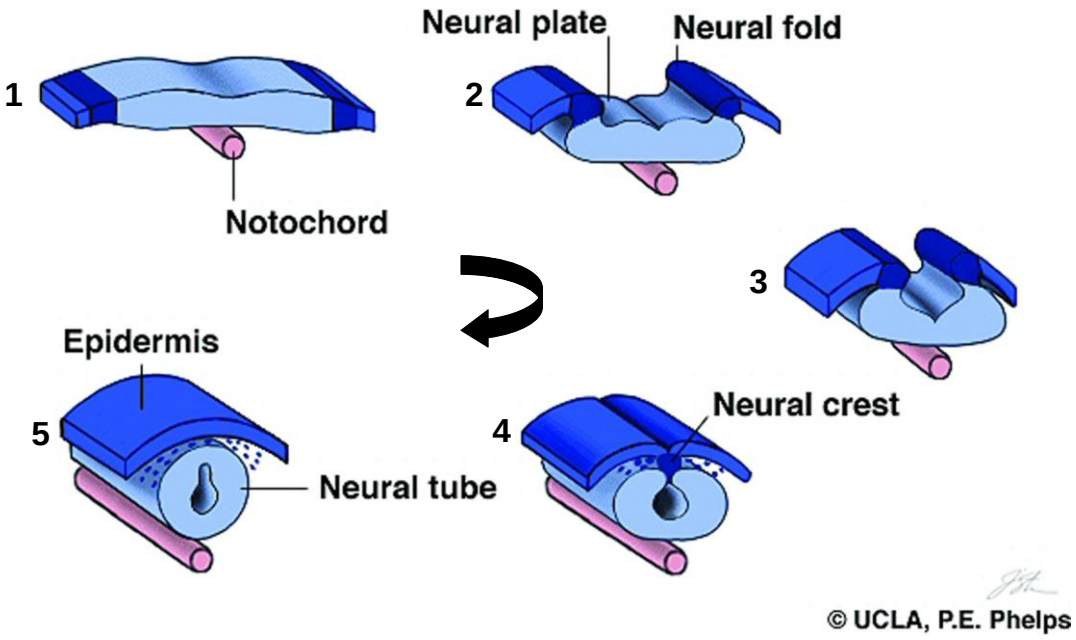

Figure 1.3 Development of the CNS. The ectoderm thickens (1) forming the neural plate (2). Fusion of the 2 ends of the neural plate (3 and 4), gives rise to the neural tube (5). Figure reproduced from P. E. Phelps, UCLA.

By the 4th week the 'head' region of the embryo flexs and 3 early cranial regions are visible – the proencephalon (forebrain), the mesencephalon (midbrain) and the rhombencephalon (hindbrain). Proliferation of the neuroepithelium continues and the neural tube forms 3 layers, the ventricular, mantle and marginal layers (Figure 1.4).

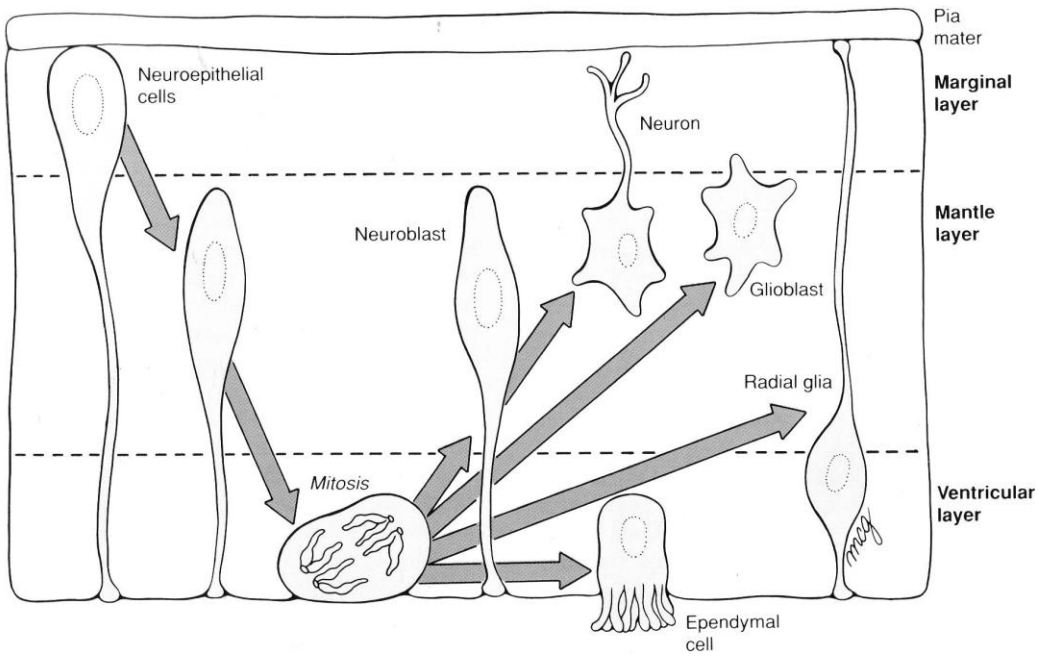

Figure 1.4 Cytodifferentiation of the neural tube. Reproduced from Larsen (1993).

In the 5th week of embryonic development, 5 brain regions are visible, with the proencephalon and rhombencephalon each subdiving further to produce the telencephalon and diencephalon and the metencephalon and myencephalon, respectively (Figure 1.5).

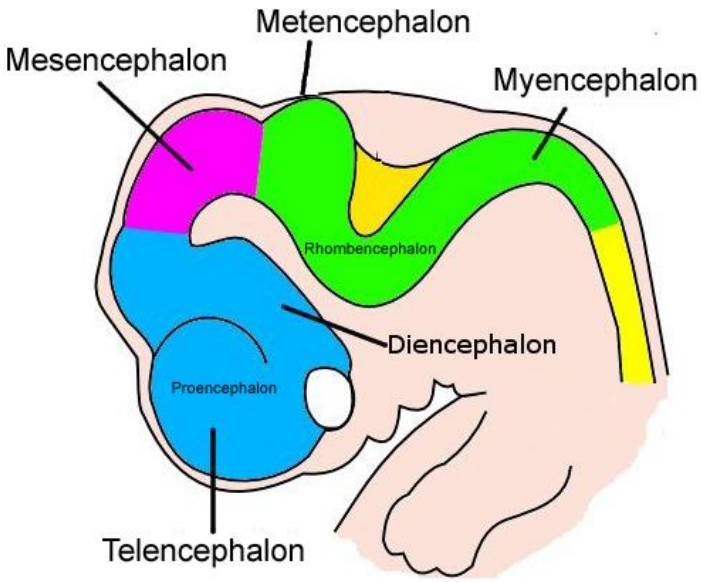

Figure 1.5 The brain of a 5 week embryo. Adapted from Figure by Kurzon, www.en.wikipedia.org/wiki/Neural-development_in_humans

As development of the brain continues 15 smaller regions are formed (neuromeres). On approximately day 32 of embryonic development, the 2 cerebral hemispheres are formed from the telencephalon. Due to rapid cell profileration and migration, the hemispheres expand, covering both the diencephalon and mesencephalon. As the cortex folds, gyri are formed. By the 4th month the temporal lobe is visable and in the 8th and 9th months, the frontal and then parietal and occipital lobes are visable. Neuroblasts progress through vast cell division, with apoptosis an essential control process. Developing cells prone to tumourigenic transformation (due to the accumulation of genetic aberrations), are usually apoptosed, however, the evasion of apoptosis at this stage could potentially lead to the development of a brain tumour (Scotting 2004).

The cellular proliferation, migration and differentiation of the cerebral cortex are both complex and unique. The architechtural complexity of the cortex arises upon cellular proliferation in the ventricular layer (Figure 1.6) Waves of neuroblasts migrate peripherally forming layers of cells. When the production of neuroblasts gradually

decreases, the ventricular layer then gives rise to both glioblasts and ependyma. Essentially there are 2 main types of brain cell; glia and neurons. Astrocytes, oligodendrocytes, ependymal cells, radial glia and migroglia are all types of glial cell and provide support, protection, nutrition and aid cell migration, whereas neurons process and transmit information through the nervous system.

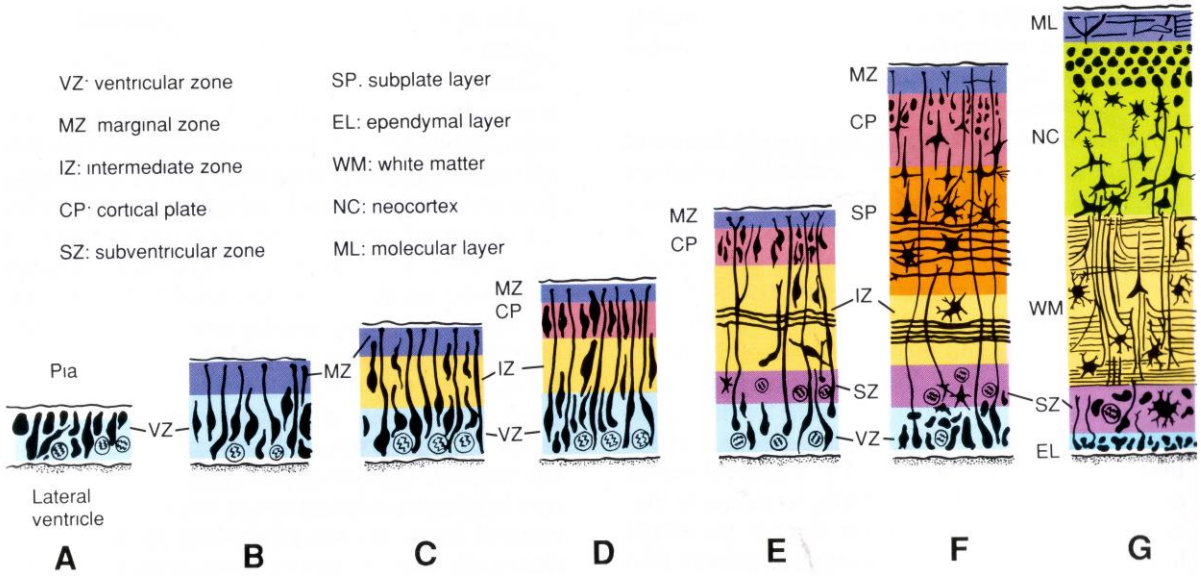

Figure 1.6 Cytodifferentiation of the cerebral neocortex. Adapted from (Larsen 1993). Neuroblasts of the ventricular zone (A) migrate forming an intermediate layer (between the ventricular layer and marginal zone) (C). In addition to some cells of the intermediate zone, new neuroblasts of the ventricular layer also migrate to form a layer called the cortical plate (D). As the production of neuroblasts gradually decreases in the ventricular zone, the production is taken over by proliferating cells within the subventricular zone (between the ventricular and intermediate zones) (E). The subplate layer is formed by the peripheral migration of neuroblasts from the subventricular zone (F). The cerebral cortex arises from the cortical and subplate layers (G). Whilst the grey matter (molecular layer and neocortex) contains neuroblast cell bodies, the white matter mostly contains myelinated axon tracts.

Originally stem cells were thought not to be present in adult tissue, thus, neurogenesis in adult life was not thought possible, however, recent experiments have found evidence to question this assumption (Hemmati, Nakano et al. 2003; Singh, Clarke et al. 2003; Vescovi, Galli et al. 2006). The properties a cell must possess to be called a stem cell include the potential to self renew and divide, in addition to being

multipotent. The cancer stem cell hypothesis claims tumour progression, recurrence and resistance to treatment is due to the existence of resistant cancer stem cells (Sakariassen, 2007). This subpopulation of cells could have been left behind following surgery and are resistant to adjuvant therapy becoming resistant to further therapy. Tumours can comprise of a heterogenous population of cells, with cancer stem cells a small subpopulation. CD133 has been hypothesised as a marker of brain tumour initiating cells (Hemmati, Nakano et al. 2003; Singh, Hawkins et al. 2004), however other studies have shown that CD133 negative tumour cells are also capable of tumour formation (Beier, Hau et al. 2007; Zheng, Shen et al. 2007). Clearly the study of stem cell populations within the normal brain contributing to the development of a brain tumour is a controversial subject needing further investigation. If proved correct, treatment tailored toward the stem cell populations could be developed to target the self renewal properties of this cell population, thereby inhibiting tumour progression and recurrence.

1.1.3 WHO grading and classification

The World Health Organisation (WHO) classifies and grades tumours of the CNS. There are many different sub-types of brain tumour and a correct diagnosis is essential for optimal patient treatment and management. Currently brain tumours are classified by histopathological examination of a biopsy taken from surgery. In addition to a histological diagnosis of the tumour tissue, other factors are also taken into account, for example, patient age, the tumour's location, evidence of metastasis and clinical history.

Grading is an important predictive factor of malignancy and outcome, thus a tumour's grade is invaluable when considering treatment options. The current WHO classification of tumours of the CNS, released in 2007, documents the grades of all tumours of the CNS (Table 1.1) (Louis, 2007). Grade I tumours contain cells with a low proliferative index, which can generally be treated by surgery alone if a complete resection is obtained. Grade II tumours have the potential to infiltrate and recur, with a number, particularly astrocytomas, having the capacity to transform to grade IV glioblastoma multiforme (GBM), although this is more commonly seen in adults rather than children (Ohgaki, Dessen et al. 2004). Patients with grade II brain tumours usually

survive over 5 years post-diagnosis. Grade III brain tumours are potentially fatal. They are treated with surgery and typically warrant additional therapies including chemotherapy and radiotherapy. Evidence of malignancy is observed with differences in nuclear morphology and increased mitotic activity. Grade IV tumours are also potentially fatal; containing mitotically active and necrotic cells, with infiltration into the surrounding tissue. Therefore, depending on patient age, where the tumour is located and how well the tumour responds to treatment, patients with grade IV tumours (including central nervous system primitive neuroectodermal tumours (CNS PNET)) may have a very poor prognosis. The outcome of grade IV medulloblastoma is however dependent on histological subtype, with standard risk medulloblastoma patient survival increasing over the years and currently a 70% cure rate is achieveable (Oyharcabal-Bourden, Kalifa et al. 2005). Patients diagnosed with desmoplastic/nodular medulloblastoma have a better outcome than those diagnosed with classic medulloblastoma, whilst patients with anaplastic/large cell medulloblastoma have the worst outcome (Giangaspero, Perilongo et al. 1999; Eberhart, Kepner et al. 2002; Ellison 2002; McManamy, Lamont et al. 2003; McManamy, Pears et al. 2007).

Table 1.1 WHO grading system of CNS tumours, reproduced from Louis (2007).

	I	II	III	IV
Astrocytic tumours				
Subependymal giant cell astrocytoma	•			
Pilocytic astrocytoma	•			
Pilomyxoid astrocytoma		•		
Diffuse astrocytoma		•		
Pleomorphic xanthoastrocytoma		•		
Anaplastic astrocytoma			•	
Glioblastoma				•
Giant cell glioblastoma				•
Gliosarcoma				•
Oligodendroglial tumours				
Oligodendroglioma		•		
Anaplastic oligodendroglioma			•	
Oligoastrocytic tumours				
Oligoastrocytoma		•		
Anaplastic oligoastrocytoma			•	
Ependymal tumours				
Subependymoma	•			
Myxopapillary ependymoma	•			
Ependymoma		•		
Anaplastic ependymoma			•	
Choroid plexus tumours				
Choroid plexus papilloma	•			
Atypical choroid plexus papilloma		•		
Choroid plexus carcinoma			•	
Other neuroepithelial tumours				
Angiocentric glioma	•			
Chordoid glioma of the third ventricle		•		
Neuronal and mixed neuronal-glial tumours				
Gangliocytoma	•			
Ganglioglioma	•			
Anaplastic ganglioglioma			•	
Desmoplastic infantile astrocytoma and ganglioglioma	•			
Dysembryoplastic neuroepithelial tumour	•			

	I	II	III	IV
Central neurocytoma		•		
Extraventricular neurocytoma		•		
Cerebellar liponeurocytoma		•		
Paraganglioma of the spinal cord	•			
Papillary glioneuronal tumour	•			
Rosette-forming glioneuronal tumour of the fourth ventricle	•			
Pineal tumours				
Pineocytoma	•			
Pineal parenchymal tumour of intermediate differentiation		•	•	
Pineoblastoma				•
Papillary tumour of the pineal region		•	•	
Embryonal tumours				
Medulloblastoma				•
CNS primitive neuroectodermal tumour (PNET)				•
Atypical teratoid / rhabdoid tumour				•
Tumours of the cranial and paraspinal nerves				
Schwannoma	•			
Neurofibroma	•			
Perineurioma	•	•	•	
Malignant peripheral nerve sheath tumour (MPNST)		•	•	•
Meningeal tumours				
Meningioma	•			
Atypical meningioma		•		
Anaplastic / malignant meningioma			•	
Haemangiopericytoma		•		
Anaplastic haemangiopericytoma			•	
Haemangioblastoma	•			
Tumours of the sellar region				
Craniopharyngioma	•			
Granular cell tumour of the neurohypophysis	•			
Pituicytoma	•			
Spindle cell oncocytoma of the adenohypophysis	•			

1.1.4 Embryonal CNS tumours

Embryonal CNS tumours are classically high grade tumours of childhood. WHO grade IV brain tumours include the embryonal tumours, CNS PNET, pineoblastoma, medulloblastoma (MB), atypical teratoid/rhabdoid tumour (ATRT) and the astrocytic tumour glioblastoma multiforme (GBM) (Figure 1.7).

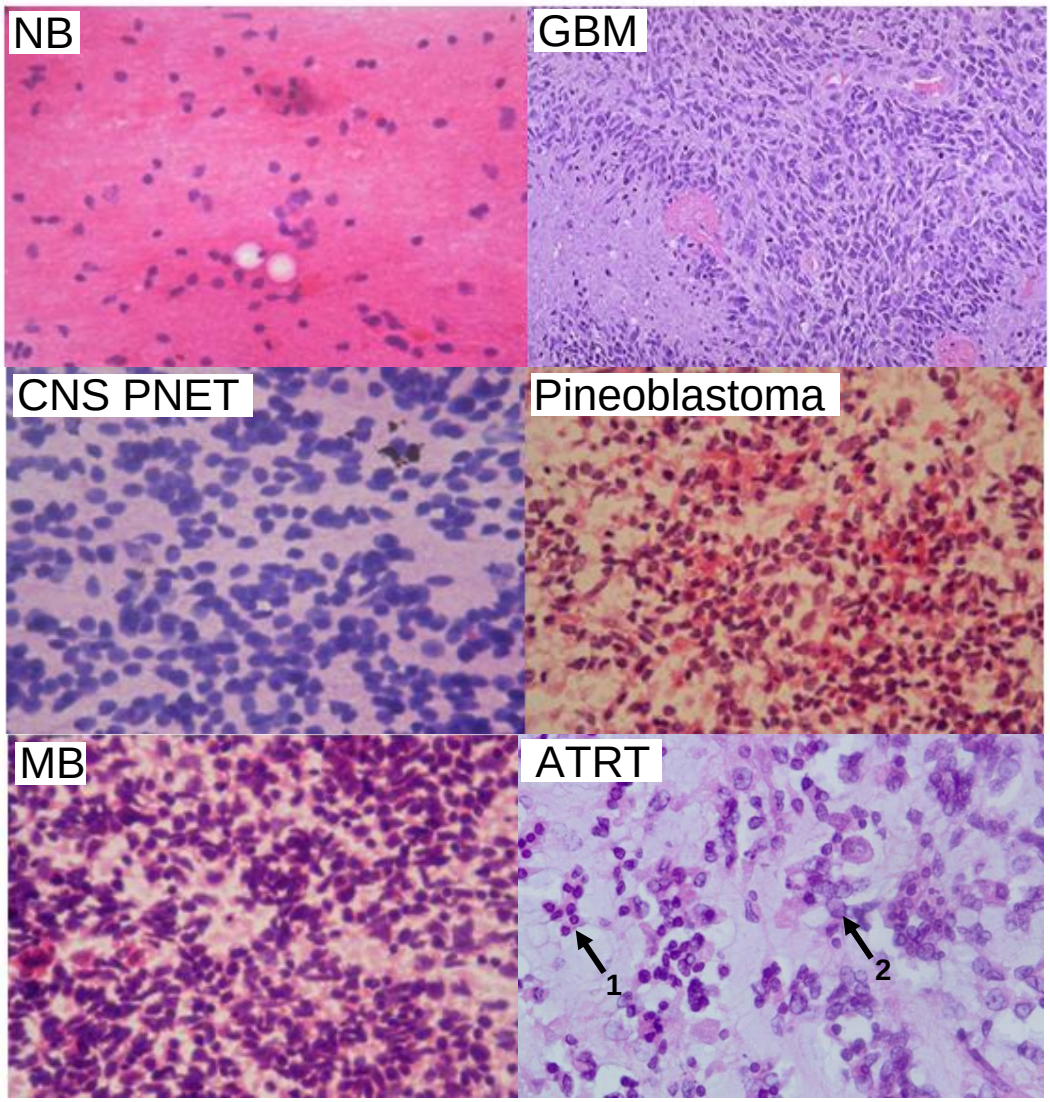

Figure 1.7 Haematoxylin and eosin (H and E) stained grade IV brain tumour Sections. Whereas the tumour Sections contain densely packed nuclei in a small area consistent with grade IV tumours, the normal brain (NB) contains only few haematoxylin stained nuclei (purple) within a small area with a large amount of eosin stained cytoplasm present (pink). Glioblastoma multiforme (GBM) contains poorly differentiated astrocytic tumour cells and can show areas of anaplasia. CNS PNETs contain undifferentiated or poorly differentiated neuroepithelial cells which have the capacity for neuronal, astrocytic, muscular and melanocytic differentiation. Only scant cytoplasm is present. Pineoblastomas are dense, highly cellular tumours with scant cytoplasm and contain patternless sheets of small cells. Classic medulloblastoma (MB) contain densely packed PNET cells, have scant cytoplasm and the most common differentiation is along the neuronal lineage. Atypical teratoid rhabdoid tumours (ATRT) typically contains rhabdoid cells and can have differentiation along epithelial, mesenchymal, neuronal or glial lines. Arrow 1 shows an area of the tumour containing PNET cells, whilst arrow 2 shows a region of rhabdoid cells present in the ATRT. Maginification of x40 for NB, CNS PNET, pineoblastoma, MB and ATRT and x10 for GBM.

The histopathological diagnosis distinguishing between different high grade paediatric brain tumour types remains a challenge. Whilst all of the tumours featured in Figure 1.7 can contain primitive cells, they also can differentiate along many different lineages. For example a CNS PNET harbouring glial differentiation could be mistaken for a GBM, whilst an ATRT can contain <5% of rhabdoid cells within the tumour and the

diagnosis of a PNET can prevail. Therefore, definitive immunohistological and genetic markers are needed to help elucidate between different tumour types.

Brain tumours of childhood most commonly occur in the cerebellum, with this region developing postnatally. Grade IV brain tumours of the cerebellar region include medulloblastoma, ATRT and in rare cases GBM. Grade IV brain tumours can also arise in the cerebral hemispheres (frontal, parietal, occipital and temporal lobes) and include GBM, CNS PNET and ATRT whilst the pineoblastoma occurs in the pineal gland (Figure 1.8).

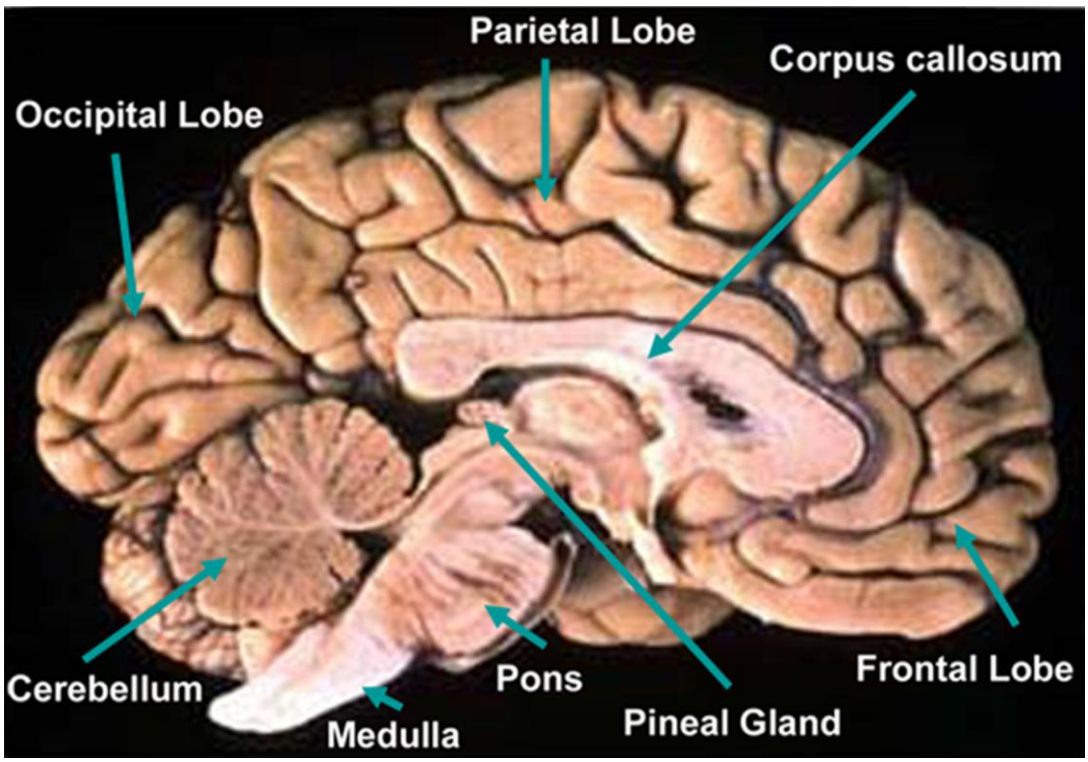

Figure 1.8 Cross Section of the brain
www.psychology.uoguelph.ca/lrnlinks/hubrain.html

Whereas GBM is predominantly a brain tumour of adults, ATRT occurs early in childhood (Dohrmann, Farwell et al. 1976; Bhattacharjee, Hicks et al. 1997). Patients with GBM and ATRT have extremely poor outcomes with the majority dying within 2 years of diagnosis (Chen, McComb et al. 2005). Table 1.2 documents the differences in mean age at diagnosis and survival outcomes for paediatric WHO grade IV tumours of the CNS.

Table 1.2 Clinical features observed in high grade (WHO grade IV) brain tumours of childhood.

Brain Tumour	**Medulloblastoma (MB)**	**CNS PNET**	**Pineoblastoma**	**Glioblastoma Multiforme (GBM)**	**Atypical Teratoid/Rhabdoid Tumour (ATRT)**
WHO grade	IV	IV	IV	IV	IV
Anatomical location	Posterior fossa, cerebellum	Cerebral hemispheres, suprasellar	Pineal region	65% Posterior fossa, 35% cerebral	65% Posterior fossa, 35% cerebral
Male/Female (%)	1.86:1	2:1	1.56:1	1.5:1	1.5:1
Symptoms*	Truncal ataxia, disturbed gait, lethargy	Seizures, disturbance of conciousness,motor deficit, visual/endocrine problems, depends on which lobe the tumour affects	Changes in mental state, endocrine abnormalities, parinaud syndrome – loss of vertical gaze and sluggish reaction to light	Dependent on location	Dependent on location
Mean age at diagnosis (years)	7	5.5	5	9	1.8
5yr overall survival	70%	34%	58%	33%	<1%

A slight predominance for brain tumours is observed for males. The mean age at diagnosis for medulloblastoma was higher than that of CNS PNET and pineoblastoma patients. 5 year overall survival was highest for medulloblastoma, with CNS PNET and GBM both incurring a poorer survival. The poorest survival rate was observed in ATRT, with a minimal percentage of patients surviving 5 years post diagnosis. *The most common symptom observed within all brain tumours is a headache due to raised intracranial pressure. Information summarised from (Louis, 2007).

The most common grade IV paediatric brain tumours are shown in Table 1.2; however, two rarer entities are also described. Medulloepithelioma is characterised by papillary, tubular arrangements of neoplastic neuroepithelium mimicking the embryonic neural tube (Louis, 2007). Generally affecting children between the ages of 6 months and 5 years, a limited number of 37 cases have been published in the literature to date (Molloy, Yachnis et al. 1996; Sharma, Mahapatra et al. 1998; Vincent, Dhellemmes et al. 2002; Norris, Snodgrass et al. 2005). Prognosis is poor, with most patients dying within a year of diagnosis. Medulloepitheliomas can occur anywhere in the brain and may have multiple lines of differentiation. Ependymoblastomas are histologically characterised by distinctive multilayered rosettes (Louis, 2007). Occurring in young children and neonates, these large and generally supratentorial tumours are usually fatal within a year of diagnosis. When considering the diagnosis of a CNS PNET, knowledge of other childhood brain tumours is essential, particularly as PNET, GBM and ATRT have similar histological appearances and frequently present difficulties to neuropathologists with classification. From the clinical perspective, factors other than histological grade need to be taken into account including patient age, tumour location and genetic alterations. Further knowledge is needed to elucidate differences in the cells of origin and the genetic components leading to particular subtypes of brain tumour. Only then will clearly separate tumour classifications be made, thus providing the information needed for the correct diagnoses and patients can receive the optimal targeted treatments needed.

1.1.5 The ‘PNET’ entity - A historical perspective

PNETs are thought to be embryonal tumours arising from the germinal matrix of the primitive neural tube during embryonic development (Hart and Earle 1973). The intracranial ‘primitive neuroectodermal tumour (PNET)’ has historically been hard to classify and is still surrounded by controversy. Modern understanding of the ‘PNET’ is limited with little genetic or pathobiologic understanding. One structure within the brain is important in the distinction between the diagnosis of infratentorial and supratentorial PNETs (termed medulloblastoma and CNS PNET, respectively). The tentorium is a fold of the dura mater separating the cerebellum from the cerebrum (Figure 1.9).

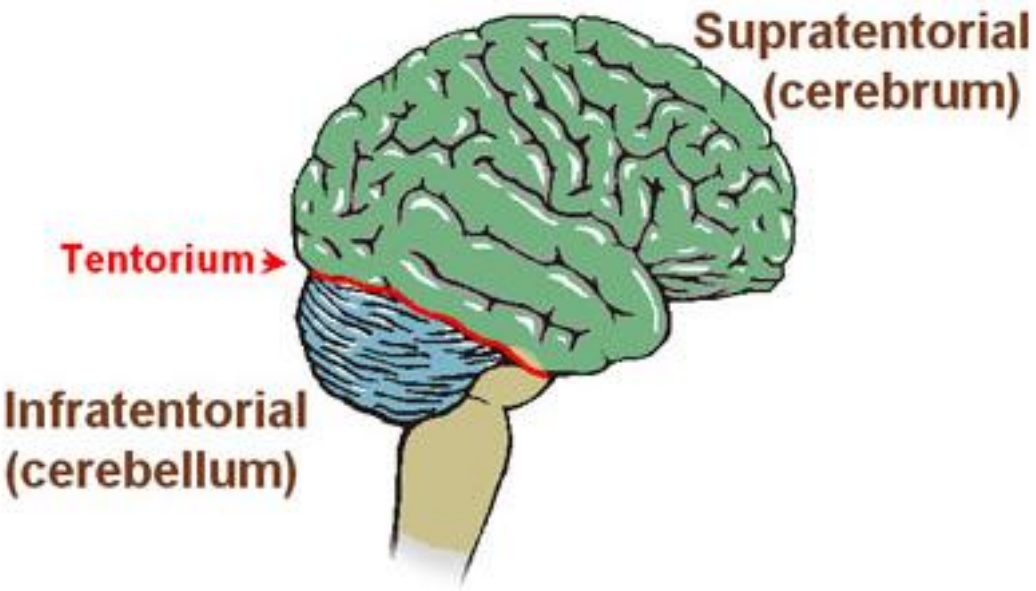

Figure 1.9 The tentorium of the brain. Whereas CNS PNETs arise in the cerebrum and pineoblastomas arise in the pineal region (both supratentorial regions), medulloblastomas arise infratentorially within the cerebellum.
www.training.seer.cancer.gov

The WHO has provided a classification and grading system of brain tumours for over 30 years. To date, 4 editions of the WHO classification of tumours of the nervous system have been published. Although previous editions of the WHO classifications of CNS tumours grouped together all small round blue cell tumours of the brain irrespective of tumour location, current editions now classify medulloblastoma, CNS PNET and pineoblastoma as separate entities.

Firstly in 1979, Zülch *et al* published the histological features of tumours of the nervous system (Zulch 1979). Following this in 1993, Kleihues *et al* introduced the use of immunohistochemistry (IHC) to better define differences in the diagnosis of nervous system tumours (Kleihues, Burger et al. 1993). The year 2000 saw the release of the 3rd WHO classification of nervous system tumours and with the advent of CGH techniques, cytogenetic profiles of each tumour type started to emerge (Kleihues 2000). Additional Sections were included comprising of epidemiology, clinical symptoms,

imaging and predictive factors. New information on specific embryonal tumours of the CNS was reviewed in 2005, highlighting both immunological and genetic differences between these tumour types (Table 1.3) (Sarkar, Deb et al. 2005). Five embryonal tumours were included, medulloblastoma, CNS PNET, ATRT and the extremely rare medulloepithelioma and ependymoblastoma.

For many years, PNETs were grouped together irrespective of anatomical location within the brain. More recently it has become apparent that PNETs occurring in the supratentorial region have a different clinical behaviour than those arising in the cerebellum (Cohen, Zeltzer et al. 1995; Pizer, Weston et al. 2006; Sung, Yoo et al. 2007). Medulloblastomas are the more common PNET of the brain, constituting 80% of all PNETs compared to 20% arising in the supratentorial region. Histologically the two PNETs are indistinguishable, with small round blue cells and scanty cytoplasm (as shown in Figure 1.7).

Grouping PNETs into a single group solely due to the similarity of tumour histology is controversial. Such a grouping implies a common cell of origin (which has never been proven) and there is evidence suggesting medulloblastomas and CNS PNETs harbour different underlying genetic defects (Section 1.7). The possible differences in the cell of origin and underlying genetics between medulloblastoma and CNS PNET could explain the differences in clinical behaviour and outcome, with CNS PNET patients having a poorer prognosis.

In 1983, Rorke *et al*., hypothesised that both medulloblastoma and CNS PNET arose from a common cell of origin within the subventricular matrix, however, more recent research has provided evidence that this is not the case (Rorke 1983; Marino, Vooijs et al. 2000; Pomeroy, Tamayo et al. 2002; Inda, Perot et al. 2005; McCabe, Ichimura et al. 2006; Pfister, Remke et al. 2007). Firstly a study by Marino *et al.*, showed that medulloblastomas and not CNS PNETs originate from multipotent precursor cells of the cerebellar external granular layer (Marino, Vooijs et al. 2000). Secondly, a study by Pomeroy *et al.*, compared the gene expression profiles of a variety of paediatric brain tumours and identified differences in both the hierarchical cluster groups and individual gene expressions between the medulloblastomas and CNS PNETs studied (Pomeroy, Tamayo et al. 2002). Whereas the majority of medulloblastomas clustered together,

suggestive of similar gene expression profiles, the CNS PNETs did not form a cluster group suggesting heterogeneity in expression profiles within the CNS PNETs (Section 1.5.7, Figure 1.18). Interestingly, two genes encoding transcription factors specific for cerebellar granule cells were found to be highly expressed in the medulloblastomas and not the CNS PNET samples, providing further evidence of a cerebellar granule cell origin for medulloblastoma and not CNS PNET (Section 1.5.7, Figure 1.19). The increasing evidence that medulloblastomas and CNS PNETs are not the same entity highlights that these two separate PNETs could be biologically distinct and may respond differently to treatment, thus warranting different therapeutic regimes. In 1997, Rorke *et al.*, reviewed both the historical and current understanding of PNET classification (Figure 1.10) (Rorke, Trojanowski et al. 1997).

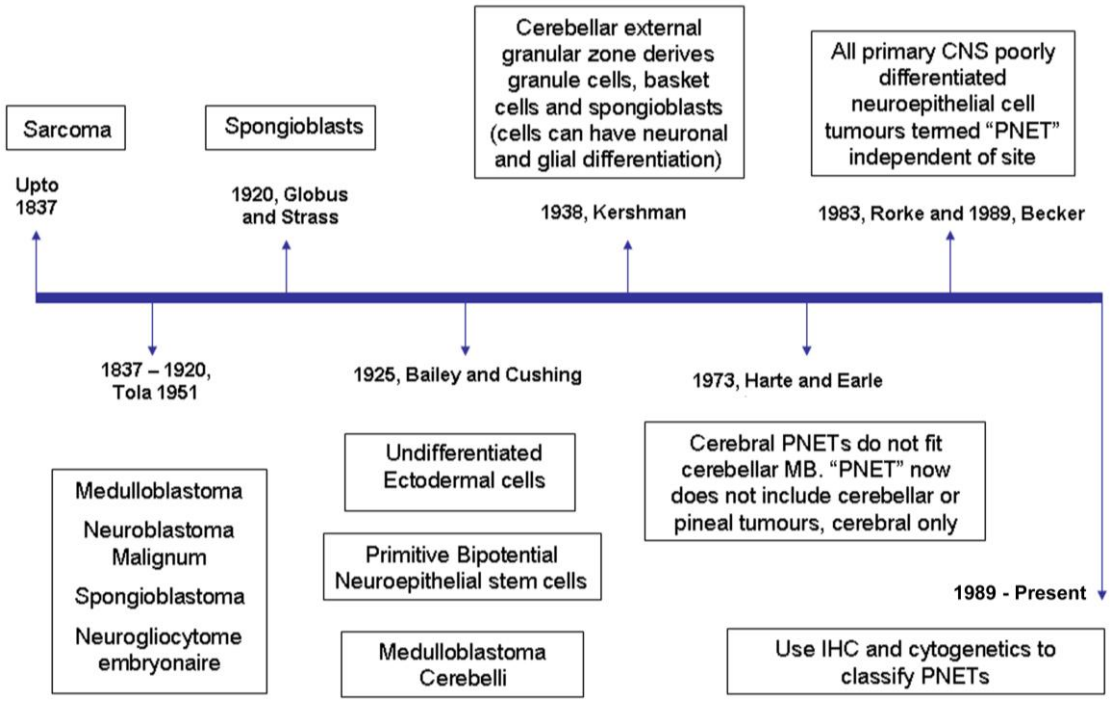

Figure 1.10 Historical and current conceptions of the intracranial PNET. This timeline highlights the difficulty still present in what to call a primitive neuroectodermal tumour located at different regions of the brain. Derived from the review (Rorke, Trojanowski et al. 1997).

Table 1.3 Comparison of the 5 embryonal tumour types from the 3rd edition of the WHO classification of tumours of the nervous system.

	Medulloblastoma	**CNS PNET**	**ATRT**	**Medulloepithelioma**	**Ependymoblastoma**
Age	<16 years (70%; mean 7 years)	1st decade (80%; mean 5.5 years)	<5 years (94%; mean 17 months)	<5 years	<5 years
Location	Cerebellum	Cerebrum, suprasellar	Posterior fossa (52%), supratentorial (40%), pineal, spinal	Periventricular, cerebral hemispheric	Supratentorial, intraparenchymal
Histopathology	Undifferentiated cells ± neuronal/glial differentiation, six variants	Undifferentiated cells ± neuronal/glial differentiation	Rhabdoid cells + PNET, glial, epithelial and mesenchymal components	Resemblance to embryonic neural tube cyto-architecture	Multilayered ependymoblastic rosettes
Immunohistological features	Synaptophysin + vimentin + GFAP/NF±	Synaptophysin + GFAP/NF ±	EMA and vimentin + SMA, CK, GFAP, NF ±	Nestin and vimentin	Vimentin + GFAP, S100 ±, EMA and NF negative
Loss of Chr 17p/ I17q	+	-	-	-	-
Mutation of *PTCH* locus	+	-	-	-	-
ZIC and *NSCL1* genes	+	-	-	-	-
Neurogenic basic helix loop genes (*HASH1*)	-	+	-	-	-
Loss of 14q and 19q	-	+	-	-	-
Mutation of *INI1* gene	-	-	+	-	-
Histogenesis	EGL and medullary velum	Primitive neuroepithelial cells	Stem/germ cells	Subependymal primitive cells	Periventricular neuroepithelial cells
Outcome	50-70% (5 years)	34% (5 years)	Mean 1 year (<20%)	6 months to 1 year	6 months to 1 year

GFAP glial fibrillary acidic protein, NF neurofilament, EGL external granular layer, EMA epithelial membrane antigen, SMA smooth muscle actin, CK cytokeratin. Whereas medulloblastoma harboured alterations including i17q, mutation of the *PTCH* gene and high expression of cerebellar precursor cells *ZIC* and *NSCL1*, CNS PNETs were found to contain loss of chromosome arms 14q and 19q and express *HASH1*. ATRT was the sole brain tumour to have loss of *INI1* (22q11.2). These genetic factors differentiating between brain tumours will aid in the correct diagnosis, which is especially important when in dispute due to similar tumour histologies. Reproduced from (Sarkar 2005).

The current 4th edition of the WHO classification of tumours of the central nervous system, published in 2007, was limited to tumours of the central nervous system, not including tumours of the peripheral nervous system (Louis, Ohgaki et al. 2007). New Sections included molecular genetics rather than cytogenetics, in addition to prognostic factors relating to individual tumour types. To avoid confusion with other PNETs at extracerebellar sites, the authors of the 4th edition of the WHO classification system for CNS tumours designated new terminology for the formerly known sPNET due to the existence of similar but not identical tumours present at these sites. The new term 'CNS PNET' is now used for the former classification. Moreover, whereas the 3rd edition of the WHO classification of nervous system tumours classified embryonal PNETs of the cerebrum and suprasellar regions as 'sPNET', the 4th edition of the WHO classification of CNS tumours used the new term 'CNS PNET' to corresponded only to PNETs found in the cerebral hemispheres, brain stem and spinal cord, with undifferentiated or poorly differentiated neuroepithelial cells (Table 1.4). The term pineoblastoma (PNET of the pineal region) was classified separately to CNS PNET in both the WHO 3rd edition and 4th editions. Although no recent advancements have been made in histological or genetic subgroups for CNS PNET between the 3rd and 4th WHO editions, this is in contrast to progress made in the histologically similar medulloblastoma. The publication of the 4th edition of the WHO classification of tumours of the CNS contained expanded information of the medulloblastoma variants: anaplastic, desmoplastic, large cell and extensive nodularity. The histological subtype of medulloblastoma has important clinical consequences with large cell/anaplastic tumours having a poorer prognosis than classic medulloblastoma and the desmoplastic/nodular variant having the best overall outcome (Giangaspero, Perilongo et al. 1999; Eberhart, Kepner et al. 2002; Ellison 2002; McManamy, Lamont et al. 2003; McManamy, Pears et al. 2007).

Table 1.4 Differences in the classification of embryonal CNS tumours from the 3rd and 4th editions of the WHO tumours of the CNS.

WHO NS 3rd edition	WHO CNS 4th edition	Tumour subtype
sPNET Cerebral Neuroblastoma Cerebral Ganglioneuroblastoma	CNS PNET	CNS/Supratentorial PNET CNS Neuroblastoma CNS Ganglioneuroblastoma Medulloepithelioma Ependymoblastoma
Pineoblastoma	Pineoblastoma	
ATRT	ATRT	
Medulloblastoma Medullomyoblastoma Melanotic Medulloblastoma Medulloepithelioma Ependymoblastoma	Medulloblastoma	Desmoplastic/nodular Extensive nodularity Anaplastic Large cell Myogenic differentiation Melanotic differentiation

NS = Nervous system. Table summarised from (Louis, D. N. *et al*., 2007).

1.1.6 Histological subtypes and markers

The term CNS PNET incorporates all PNETs of the supratentorial compartment of the brain irrespective of anatomical location (frontal lobe, occipital lobe, parietal lobe, temporal lobe) and is independent of specific histological markers. By contrast, a variety of histological subtypes for medulloblastoma have recently been described in the WHO classification of tumours of the CNS including classic, desmoplastic, medulloblastoma with extensive nodularity, anaplastic and large cell (Louis, 2007). The large cell variant, making up 2-4% of medulloblastoma cases, contains large monomorphic vesicular nuclei (Figure 1.11d) (Giangaspero, Rigobello et al. 1992; Ellison 2002). Whilst classic medulloblastomas make up 64-78%, the anaplastic variant makes up 10-22% of cases, the desmoplastic variant makes up 7% and the medulloblastoma with extensive nodularity accounts for 3% of medulloblastoma (Ellison 2002; McManamy, Pears et al. 2007). On histological evaluation, classic medulloblastoma illustrates the common high cell density of 'small round blue cells' whereas desmoplastic medulloblastoma is characterised by 'pale islands' of reticulin free areas (Figure 1.11a). medulloblastoma with extensive nodularity is characterised by large lobular areas of reticulin free zones (Figure 1.11b) and anaplastic

medulloblastoma is marked by pleiomorphic nuclei with increased size (Figure 1.11c). Remarkably, the prognoses of patients depend on the subtype of medulloblastoma classified, with patients diagnosed with a desmoplastic/nodular medulloblastoma having a better outcome than those diagnosed with classic medulloblastoma, whilst patients with an anaplastic/large cell medulloblastoma have the worst outcome (Giangaspero, Perilongo et al. 1999; Eberhart, Kepner et al. 2002; Ellison 2002; McManamy, Lamont et al. 2003; McManamy, Pears et al. 2007). Thus, the identification of medulloblastoma subtypes is of clinical significance and is also genetically important. This raises the possibility of histological subgroups within CNS PNET, although the heterogeneity of CNS PNETs might prevent subtypes being identified. It will be important in the future for histopathological review of a large cohort of CNS PNETs to test this hypothesis and potentially link histopathology/cell morphology and also genetics with patient prognosis.

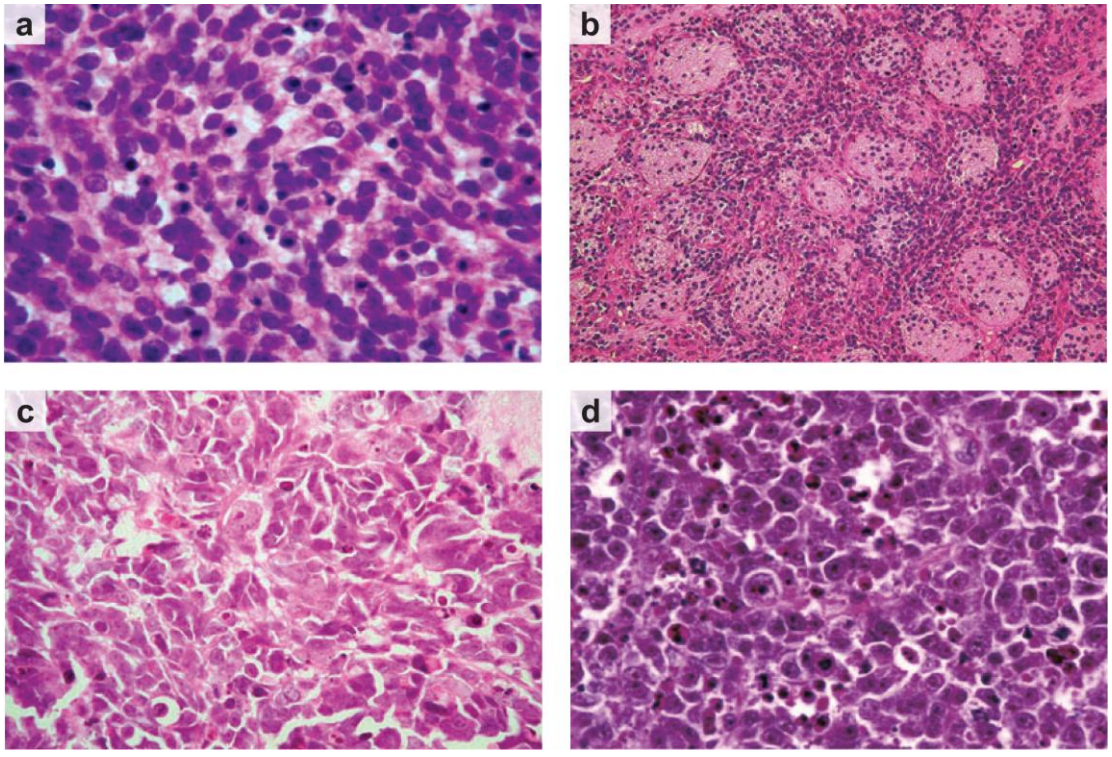

Figure 1.11 Histological variants of medulloblastoma. (a) Classic medulloblastoma, (b) Nodular/Desmoplastic, (c) Anaplastic medulloblastoma, (d) Large cell medulloblastoma. Reproduced from (Gilbertson and Ellison, 2008). Magification of x40 for a, c and d, and x10 for b.

In addition to histological tumour classification, the use of immunohistological markers to distinguish between paediatric brain tumours is common practice. It is recognised that GBM and ATRT, composed of poorly differentiated neoplastic cells, can on occasion appear morphologically very similar to PNETs. At the histological level, immunohistochemical markers usually facilitate the discrimination of different histological subtypes of brain tumours, although expression of these markers is not absolute and further histological markers distinguishing between brain tumours is still required (Table 1.5). Glial fibrillary acidic protein (GFAP), an intermediate filament protein found in glial cells, can assist in the distinction of neoplasms of astrocytic origin (Louis, 2007), whereas synaptophysin, a membrane glycoprotein of synaptic vesicles expressed in all neurons is expressed in tumours of neuroectodermal origin, as in the PNET (Table 1.6).

Table 1.5 Histological markers commonly used to distinguish between brain tumour types

Marker	**Element stained**	**Cells expressed in**
GFAP – Glial fibrillary acidic protein	Type III intermediate filament glial marker	Astrocytes
MIB1 (Ki67) – Marker of proliferation	Not expressed in G0	Proliferating cells
Synaptophysin	Differentiated neurons	Neurons/neuroendocrine cells
NF – Neurofilament	Intermediate filaments	Neuronal processes
NSE – Neuron specific enolase	Neurons	Neurons
Vimentin	Type III intermediate filament	Soft tissue/glial marker
CD31 – Platelet endothelial cell adhesion molecule 1	Vascular structures	Endothelium
EMA – Epithelial membrane antigen	Epithelium	Epithelial cells
Keratin	Intermediate filaments	Filaments
Desmin	Type III intermediate filaments	Soft tissue/muscle cells
INI1 – Integrase interactor 1	Negative	Rhabdoid cells/ATRT

Table 1.6 Histological markers expressed in individual brain tumour types

Brain tumour	**Immunohistochemical markers expressed**
CNS PNET	GFAP, NF, synaptophysin, vimentin, keratin, desmin
Medulloblastoma	GFAP, synaptophysin, nestin, vimentin
Glioblastoma	Variable GFAP (gemistocytes +ve, undifferentiated –ve), vimentin
ATRT	GFAP, EMA, vimentin, NF, keratin, desmin –ve, INI1 –ve

Information summarised from (Louis, 2007).

1.1.7 Genetic subtypes and markers

The recent discovery of the loss of *INI1* in the majority of ATRT cases has made an important contribution to the diagnosis of childhood brain tumours. *INI1* (also known as *BAF47*, *SNF5* and *SMARCB1*) is a newly recognised tumour suppressor gene located on chromosome 22q11.2 and is normally expressed in all tissues of the body. However, *INI1* expression is lost in peripheral rhabdoid tumours and ATRTs (Judkins, Mauger et al. 2004). *INI1* is related to the SWI/SNF family, with the encoded protein engaging in a complex relieving repressive chromatin structures and limiting aberrant cell division. Hence, the loss of INI1 inhibits the normal transcriptional machineries access to its target. ATRT is a highly malignant brain tumour containing both rhabdoid and primitive neuroectodermal cells, commonly occuring in patients under the age of 3 years. The morphology of ATRT may overlap with CNS PNET and the status of INI1 expression can aid in the correct diagnosis of embryonal tumours (Figure 1.12). When a diagnosis between ATRT, GBM and PNET cannot easily be distinguished by morphology and immunohistochemistry, the loss of INI1 expression supports the diagnosis of ATRT. A recent study examined INI1 expression in a large series of malignant paediatric brain tumours to determine the immunohistochemical expression of the INI1 protein (Haberler, Laggner et al. 2006). Lack of nuclear INI1 protein expression was observed in all tumours displaying characteristic morphological features of ATRT which include eccentric vesicular nuclei, prominent nucleoli and eosinophilic cytoplasmic inclusions. The majority of CNS PNETs and medulloblastomas displayed nuclear INI1 immunoreactivity throughout the whole tumour tissue (25/27, 92.6% and 152/158 96.2%, respectively), however, a small number of CNS PNETs and medulloblastomas lacked INI1 protein expression despite the absence of the rhabdoid phenotype when assessed by light microscopy. Bourdeaut *et al.*, also identified 4 paediatric brain tumours (possible choroid plexus carcinomas) with biallelic *INI1* alteration and loss of protein expression, lacking the histological features suggestive of ATRT (Bourdeaut, Freneaux et al. 2007). This highlights the possible existence of a subset of brain tumours lacking both INI1 expression and rhabdoid features. The aggressive biological behaviour of tumours lacking INI1 protein expression and the poor patient outcome if treated by conventional therapy regimens means PNET patients

with a lack of INI1 would therefore potentially benefit from intensified therapies administered to rhabdoid tumour patients.

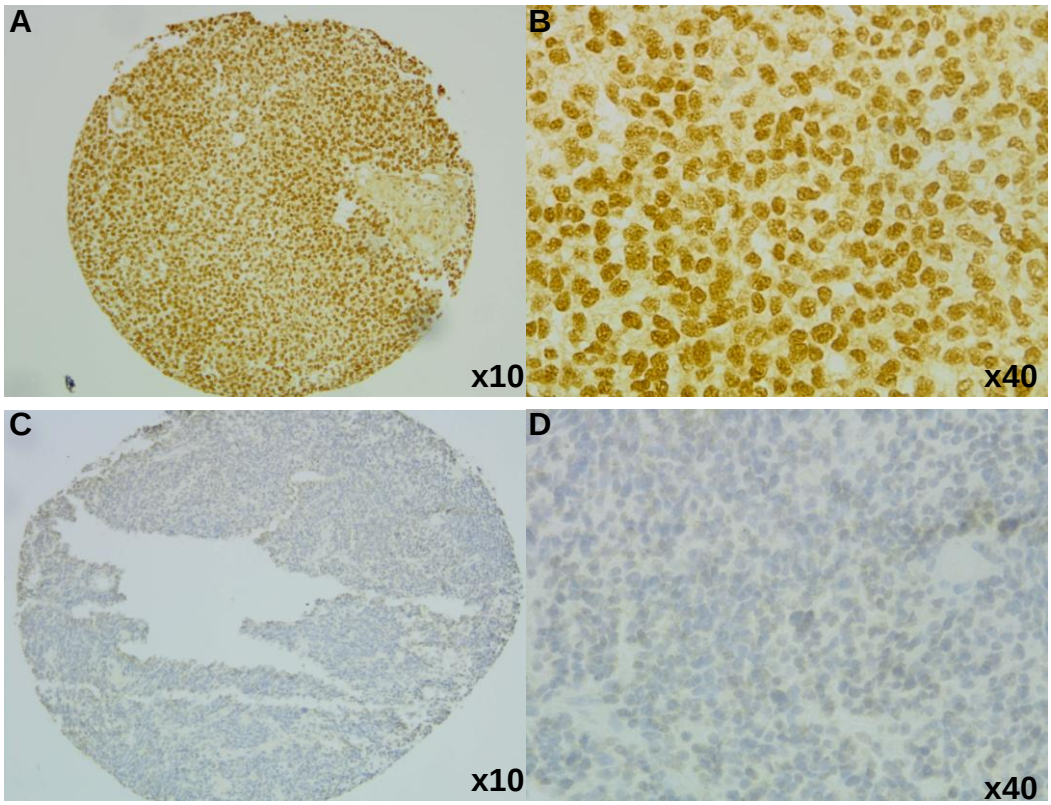

Figure 1.12 Evaluation of INI1 protein expression for brain tumours of unknown diagnosis. Both tumours were from the supratentorial region of the brain and contained 'small round blue cells' denoting PNET as a candidate classification. On immunohistochemical analysis, INI1 was expressed in the first tumour examined (A and B) which indicated the tumour classification as CNS PNET, whereas for the second tumour shown, INI1 protein expression was absent, indicative of the ATRT classification (C and D).

Grouping subtypes of CNS PNETs by histological features or genetics will be important in the future to test whether specific variants respond better to treatment and have different outcomes. Although CNS PNETs can contain cells differentiated along neuronal, astrocytic and ependymal lines, the majority of tumour samples contain the classic small round blue cells with no differentiation detected, thus grouping CNS PNETs histologically may not be an option. Advancements in the understanding of the potential histological groupings, biology and genetics of brain tumours, especially the

under-researched CNS PNET, will enable clearer tumour demographics relating to outcome to be established.

In addition to seperating medulloblastoma subtypes on histology and related patient prognosis, researchers have also identified a number of genomic aberrations linked with outcome. A recent study by Pfister *et al.,* identified gains of 6q or 17q and genomic amplification of *MYC* or *MYCN* each associated with a poor prognosis (Pfister, Remke et al. 2009). Amplification of *MYC* has also previously been linked with poor survival in medulloblastoma patients (Eberhart, Kratz et al. 2004; Lamont, McManamy et al. 2004; Aldosari, Bigner et al. 2002). In addition, isochromosome 17q (i17q), identified in ~40% of medulloblastomas, is associated with a poor prognosis (Cogen 1991; Batra, McLendon et al. 1995; Scheurlen, Schwabe et al. 1998; Gilbertson, Wickramasinghe et al. 2001; Pan, Pellarin et al. 2005). Loss of 17p has been investigated as an indicator of prognosis (Biegel, Janss et al. 1997), however, whereas some studies have shown loss on 17p and poor therapeutic response (Cogen 1991; Cogen, Daneshvar et al. 1992; Scheurlen, Schwabe et al. 1998), and poor survival (Batra, McLendon et al.1995), others failed to identify an association between loss of 17p and survival (Emadian, McDonald et al. 1996). Conversely, activation of the WNT/β-catenin pathway (in the majority of cases by an activating mutation in *CTNNB1*) has been linked to a favourable prognosis in some studies of medulloblastoma (Ellison, Onilude et al. 2005; Clifford, Lusher et al. 2006). These findings, although in medulloblastomas, gives rise to the theory that specific genetic aberrations linked to patient prognosis could well be identified in CNS PNET. Analysis of the genetic alterations within a large cohort of CNS PNETs with clinical information is now needed. Due to increased research efforts and a wealth of new genetic technologies able to probe the cancer genome, the genetic alterations of the WHO grade IV brain tumour, GBM, have now started to emerge. In adults, not only can GBM arise as a primary grade IV neoplasm, the grade II astrocytoma and grade III anaplastic astrocytoma can also progress and transform to a secondary grade IV GBM (Figure 1.13). Further characterisation of CNS PNET genetics will undoubtedly increase our understanding of this presently understudied tumour.

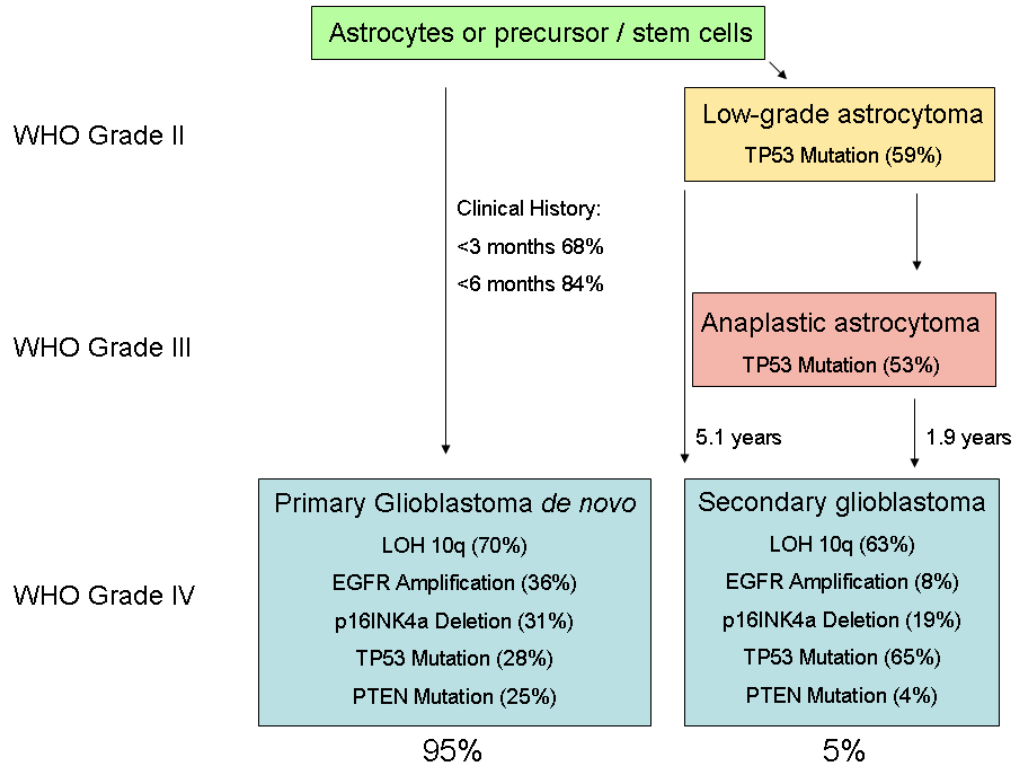

Figure 1.13 The genetics leading to primary and secondary GBMs. Modified from (Ohgaki, Dessen et al. 2004).

A well characterised abnormality distinguishing between brain tumour classifications includes the loss of chromosome arms 1p and 19q in 60% of adult oligodendrogliomas (Reifenberger, Reifenberger et al. 1994). Although the misdiagnosis of paediatric brain tumours is uncommon, additional prognostic markers linked to specific tumour classifications and sub-grouping of individual tumour types is needed to better distinguish between tumours and potentially be used to predict the response to certain therapies. Firstly the underlying genetics of each tumour type needs to be elucidated and secondly molecular sub classifications of individual tumour types need to be identified, linking genetic alterations with patient outcomes and response to treatment. Examples include loss of 1p and 19q in oligodendroglioma affording patients with a survival advantage (Cairncross, Ueki et al. 1998), while on temozolomide chemotherapy; methylation of the *MGMT* promoter is predictive of response to temozolomide and radiation therapy for patients with GBM (Donson, Addo-Yobo et al. 2007; Schlosser, Wagner et al. 2010) and loss of 22q11 establishes the diagnosis of

ATRT (Biegel 1999; Packer, Biegel et al. 2002). Genetic and prognostic markers of CNS PNET and pineoblastoma now need to be established.

1.2 Familial syndromes predisposing to paediatric brain tumours

Brain tumours can arise due to the genetic predispositions of a familial syndrome (Table 1.7). Investigation into the genetic basis of brain tumours arising within a syndrome could potentially highlight aberrent genes and pathways involved in sporadic brain tumours. The syndromes described here are of particular interest due to the incidence of an embryonal brain tumour arising as part of the disorder. Other rarer syndromes have been associated with the occurrence of a brain tumour including Fancomi anemia and Rubinstein taybi (Dewire, Ellison et al. 2009; Sari, Akyuz et al. 2009; Tischkowitz, Chisholm et al. 2004; Evans, Burnell et al. 1993).

Table 1.7 Familial tumour syndromes involving the nervous system. Adapted from (Louis, 2007).

Syndrome	**Gene**	**Chromosome**	**Manifestation**
Neurofibromatosis type 1	*NF1*	17q11	Optic nerve glioma, astrocytoma
Neurofibromatosis type 2	*NF2*	22q12	Meningioma, spinal ependymoma, astrocytoma
Von hippel-lindau	*VHL*	3p25	Haemangioblastoma
Tuberous sclerosis	*TSC1, TSC2*	9p34, 16p13	Subependymal giant cell astrocytoma
Li-Fraumeni	*TP53*	17p13	Astrocytoma, PNET
Cowden	*PTEN*	10q23	Dysplastic gangliocytoma of the cerebellum (Lhermitte-Duclos)
Turcot	*APC, hMLH1, hPMS2*	5q21, 3p21, 7p22	Medulloblastoma, Glioblastoma, CNS PNET
Naevoid basal cell carcinoma syndrome (Gorlin)	*PTCH*	9q31	Medulloblastoma
Rhabdoid tumour predispostion syndrome	*INI1*	22q11.2	ATRT

1.2.1 Li-Fraumeni syndrome

Li-Fraumeni syndrome is characterised by the germline mutation of the *p53* gene (17p13) (Malkin, Li et al. 1990; Frebourg, Barbier et al. 1995; Varley, McGown et al. 1997). It is well known that mutation of *p53* induces malignant transformation and the loss of this key tumour suppressor gene in the germline predisposes to a wide variety of different tumour types including medulloblastoma, with a mean age at diagnosis of 6 years. *p53* plays important roles in critical cell cycle pathways including the control of cell fate, activating effectors to induce cell cycle arrest, controlling the repair of damaged DNA and the promotion apoptosis in response to oncogenic stress. Interestingly, *p53* mutations have previously been identified in sporadic medulloblastoma (Ohgaki, Eibl et al. 1991; Ohgaki, Eibl et al. 1993) and it is important to note the histology of sporadic medulloblastoma and those arising from germline mutations are indistinguishable. Mutation of *p53* has also previously been identified in sporadic CNS PNETs (Kraus, Felsberg et al. 2002; Postovsky, Ben Arush et al. 2003).

1.2.2 Turcot syndrome

Turcot syndrome is characterised by the occurrence of a brain tumour secondary to the diagnosis of carcinomas and polyps of the colon. Mutations in DNA mismatch repair genes within the germline are commonly observed in Turcots. There are two types of turcot syndrome, type 1; associating hereditary non-polyposis colon carcinoma (HNPCC) and glioblastoma and the second; type 2, associating familial adenomatous polypopsis (FAP) and medulloblastoma. Mutations in the *APC* gene (5q21) are commonly involved in Turcots syndrome when the associated brain tumour is medulloblastoma (Lasser, DeVivo et al. 1994; Hamilton, Liu et al. 1995). Interestingly, medulloblastoma arising in patients with Turcots syndrome usually occurs after the age of 10 years which differs from sporadic medulloblastoma which has a mean age at diagnosis of 7 years. Although commonly associated with either glioblastoma or medulloblastoma, CNS PNETs have also been identified in patients with Turcots (De Vos, Hayward et al. 2004), highlighting a possible role for *APC* in the tumourigenesis of CNS PNET. *APC* plays a central role in regulating β-catenin levels in the WNT signalling pathway (Hamilton, Liu et al. 1995). Whilst only 5% of sporadic

medulloblastomas contain a mutation of the *APC* gene, 10% either have loss of heterozygosity or mutation of *CTNNB1* (3p21). Ultimately, loss of *APC* increases levels of Cyclin D1 (11q13), an activator of the cell cycle, thus promoting uncontrolled cell proliferation. Mutations in *CTNNB1* usually occur at phosphorylation sites which would normally be targeted by GSK-3β promoting the degradation of β-catenin. Thus, a *CTNNB1* mutation near or within a phosphorlyation site prevents β-catenin degradation and the WNT pathway remains active promoting aberrent proliferation. A recent investigation of sporadic CNS PNETs revealed the WNT pathway to be active in over a third of CNS PNETs, although not through mutation of either *APC* or *CTNNB1* in the majority of cases (Rogers, Miller et al. 2009).

1.2.3 Gorlin syndrome

Naevoid basal cell carcinoma, also known as Gorlin syndrome, comprises of cancers of the skin and CNS, particularly medulloblastoma. Caused by germline mutations of the *PTCH* gene (9q22.3), this abnormality has also been observed in 9% of sporadic medulloblastomas (Pietsch, Waha et al. 1997; Raffel, Jenkins et al. 1997; Vorechovsky, Tingby et al. 1997; Wolter, Reifenberger et al. 1997; Xie, Johnson et al. 1997; Zurawel, Allen et al. 2000; Thompson, Fuller et al. 2006). PTCH controls the sonic hedgehog signalling (SHH) pathway by inhibition of smoothened (SMO) (Murone, Rosenthal et al. 1999). Mutation of *PTCH* leads to its constitutive activation and continued SHH signalling promotes uncontrolled proliferation. SHH is an important pathway in embryonal development and the linkage between aberrations in this pathway and brain tumours adds evidence to the hypothesis that brain tumours of childhood are due to the deregulation of pathways involved in normal brain development. Further investigation of the pathways involved in normal brain development will potentially provide important pathway alterations leading to tumourigenesis in paediatric brain tumours.

1.2.4 Rhabdoid tumour predisposition

Rhabdoid tumour predisposition syndrome is characterised by the increased risk of developing malignant rhabdoid tumours. Generally occurring in infants, rhabdoid tumours can develop in any location of the body, however, are more commonly found

in the CNS (Rorke, Packer et al. 1996) or kidney (Beckwith and Palmer 1978; Weeks, Beckwith et al. 1989). Patients can be predisposed to the condition due to the constitutional loss or inactivation of one allele of the *INI1* gene (22q11.2). Younger patients with germline *INI1* mutations tend to develop rhabdoid tumours in the first year of life. Although *INI1* associated brain tumours are usually diagnosed as ATRT due to patient age (generally first diagnosed under the age of 2 years) and the existence of rhabdoid morphology on histological examination, other CNS tumours have been associated with this syndrome including choroid plexus carcinoma (Gessi, Giangaspero et al. 2003), meningioma (Schmitz, Mueller et al. 2001), medulloblastoma and CNS PNET (Sevenet, Sheridan et al. 1999). This variance could however be due to histopathological errors in the correct classification of brain tumour which can on occasion be hard to distinguish between.

Although ATRT can be a sporadic tumour, germline mutations occur in up to a third of patients diagnosed (Biegel 2006). It is important to screen the status of *INI1* in newly diagnosed ATRT patients. Familial cases of the syndrome have occasionally been reported in the literature (Proust, Laquerriere et al. 1999; Sevenet, Sheridan et al. 1999; Taylor, Gokgoz et al. 2000; Fernandez, Bouvier et al. 2002; Janson, Nedzi et al. 2006). The *INI1* tumour suppressor gene encodes a protein which is a member of the ATP dependent SWI-SNF chromatin remodelling complex and has important roles in the regulation of the cell cycle, growth and differentiation. As the function of INI1 is not yet fully understood, further research is needed to elucidate its role in the development of rhabdoid tumours within this syndrome.

1.3 Clinical aspects of CNS PNET and pineoblastoma

1.3.1 Patient age

CNS PNETs and pineoblastomas predominantly arise in childhood but can also arise in young adults. The mean age at diagnosis is 5.5 years (Louis, 2007). Up to 50% of all CNS PNETs present in very young children (<3 years of age). To date, only 57 cases of adult CNS PNET have been reported in the literature (Ohba, Yoshida et al. 2008). Currently there is insufficient evidence to determine whether the biological and genetic alterations in adult and paediatric CNS PNETs are related or differ, however, a small study by Kim *et al.*, found the 3 year OS for 12 adults diagnosed with CNS PNET to be 75% whereas studies of paediatric cases have previously identified a 3 year OS of approximately 35% (Albright, Wisoff et al. 1995; Dirks, Harris et al. 1996; Kim, Lee et al. 2002). The enhanced survival amongst adult CNS PNET patients could indicate that the tumours arising in childhood are biologically distinct entities to those arising later in life or this could relate to treatment (see Section 1.3.4). A separate issue is the age limitation for the use of radiotherapy in the treatment of paediatric CNS PNET. Special consideration needs to be given for the use of radiotherapy in children less than 3 years of age. Due to the harmful effects to the young developing brain (neuroendocrine and neurophysiological deficits), radiotherapy is generally avoided in patients less than 3 years of age (Duffner, Horowitz et al. 1993). Several studies have identified significantly poorer survival in CNS PNET patients diagnosed before the age of 3 years than those diagnosed after the age of 3 years. Dirks *et al.*, found a 5 year OS of just 5.8% in 18 CNS PNET patients <3 years old at diagnosis compared to a 5 year OS of 29% in the patients >3 years of age at diagnosis (Dirks, Harris et al. 1996). Other studies have corroborated this significant outcome, however small sample numbers and differing treatment regimes do provide limitations of the true effect that age at diagnosis has on survival (Geyer, Zeltzer et al. 1994; Albright, Wisoff et al. 1995; Cohen, Zeltzer et al. 1995). Although young age at diagnosis has been identified as a factor of poor survival, the reasons for this could be multifactorial as a higher incidence of pineoblastomas are observed in younger patients and a high proportion of younger patients have metastases (Cohen, Zeltzer et al. 1995).

1.3.2 Tumour location

Of PNETs arising in the supratentorial compartment of the brain, 70% arise in cerebral or suprasellar regions (CNS PNET), whereas 30% are located in the pineal region (pineoblastoma) (Dirks, Harris et al. 1996; Timmermann, Kortmann et al. 2002). There seems to be an age related anatomical distribution of tumours with pineoblastomas more commonly arising in children under 3 years (Table 1.8). Evaluation of the studies reported showed a prognostic difference depending on the location of the CNS PNET. In 2006, Pizer *et al.,* found that patients with a pineoblastoma had a significantly better prognosis than those with a CNS PNET, OS ($p = 0.05$) and EFS ($p = 0.03$) in children >3 years of age (Pizer, Weston et al. 2006). The 5 year EFS of patients with pineoblastomas was superior to those with CNS PNETs (71.4% and 40.7%, respectively). Also, in the CCG 921 study of CNS PNET patients >3 years of age with treatment regimens including radiotherapy and two different chemotherapies, children with pineoblastoma had a 3 year PFS of 61% compared to patients with CNS PNET with a 3yr PFS of 33% (Cohen, Zeltzer et al. 1995). This difference based on anatomical location has further been described in other studies (Dirks, Harris et al. 1996; Timmermann, Kortmann et al. 2002). In CNS PNETs, the extent of resection is a good prognostic marker and given the fact that many pineal based tumours are inoperable, the better survival of the pineoblastoma patients is somewhat suprising and could be due to differences in the cell of origin and biology of these differentially located tumours. The data suggests tumours of the pineal region could be more chemosensitive than those arising in the cerebral and suprasellar brain regions. It has also been suggested that the possible reason for the better prognosis of a pineoblastoma was due to the earlier presentation of the tumour and the smaller tumour size at diagnosis. Contrary to previous studies, the recent Headstart I and II trials concluded that patients with CNS PNET had a significantly better prognosis than patients with pineoblastoma (Fangusaro, Finlay et al. 2008). A previous study by Jakacki *et al* also found that patients with CNS PNETs had a better prognosis than those diagnosed with pineoblastoma. All patients were under the age of 18 months and whilst 46 CNS PNETs had a 3 year PFS of 55%, the 8 pineoblastoma patients had a 3 year PFS of 0% (Jakacki, Zeltzer et al. 1995). The prognostic difference between these studies is likely to be due to the variation in patient cohorts. Larger trials involving both CNS PNETs

and pineoblastoma are needed to decipher whether there are in fact differences in prognoses depending on tumour location.

Table 1.8 Previous CNS PNET and pineoblastoma studies illustrating clinical variables. A number of studies have analysed patient age, location of tumour and metastatic status at diagnosis. Metastatic stages are as shown in Table 1.9.

Author and year	Age range (m)	Average age (m)	Tumour location	Metastatic stage
Dirks, *et al*., 1996	<36 = 18, >36 = 18	Mean 53, median 35	26 (72.2%) cerebral, 10 (27.8%) pineal	N/A
Timmermann, *et al*., 2002	35 - 212	Median 76	52 (82.5%) cerebral, 11 (17.5%) pineal	46 (73%) M0, 6 (9.5%) M1, 11 (17.5%) M2/3
Pizer, *et al*., 2006	35 - 199	Median 87	54 (79.4%) cerebral, 14 (20.6%) pineal	14 (22%) M0, 41 (64%) M1, 1 (1.5%) M2, 7 (11%) M3, 1 (1.5%) M4
Fangusaro, *et al*., 2008	<36 = 20, >36 = 23	Mean 37, median 37	30 (70%) cerebral, 13 (30%) pineal	35 (82%) M0, 1 (2%) M1, 3 (7%) M2, 4 (9%) M3
Gilheeney, *et al*., 2008	4 - 194	Mean 93	11 (100%) pineal	8 (80%) M0, 1 (10%) M1, 1 (10%) M3
Johnston, *et al*., 2008	0 – 214 cerebral, 8 – 175 pineal	Mean 67.2 cerebral, 55.7 pineal	39 (81%) cerebral, 9 (19%) pineal	Cerebral 26 (84%) M0, 1 (3%) M1, 1 (3%) M2, 3 (10%) M3, Pineal 4 (66.7%) M0, 1 (16.7%) M2, 1 (16.7%) M3

1.3.3 Metastatic disease

Metastasis (Greek for displacement) is the spread of disease from the originating organ to another part of the body. A hallmark of malignancy, cells from the primary tumour site enter lymphatic and blood vessels and move to distal areas of the body. Residing within the normal tissues, secondary tumours develop. Staging for metastatic disease in patients with CNS PNET and pineoblastoma is based on the Chang staging system which was originally used for medulloblastoma, with 5 metastatic stages (Table 1.9) (Chang, Housepian et al. 1969).

Table 1.9 Chang staging system for metastasis.
Adapted from (Chang, Housepian et al. 1969).

Metastatic stage	**Definition**
M0	No evidence of metastasis
M1	Presence of tumour cells in CSF
M2	Tumour cells beyond primary site but within brain
M3	Tumour deposit in spine
M4	Tumour spread outside the CNS

Of the data given in Table 1.8, metastatic disease at diagnosis was present in over a third of cases (39%) (Timmermann, et al. 2002, Pizer, et al. 2006, Fangusaro, et al. 2008, Gilheeney, et al. 2008, Johnston, et al. 2008). Two studies have identified metastatic disease status to be a factor of poor outcome in CNS PNET (Reddy, Janss et al. 2000; Hong, Mehta et al. 2004). In 2000, Reddy *et al* reported the 5 year PFS for 5 CNS PNET patients with metastatic disease to be 0% whilst 17 patients free of metastasis had a 5 year PFS of 49%, ($p = 0.04$). A separate study by Hong *et al* in 2004 also identified a significant difference in the prognosis of 44 CNS PNET patients depending on metastatic status. In this study the 3 year PFS for patients with metastatic stages M1-4 was 14% (±9.4%) and the 3 year PFS for M0 patients was 53% (±8.5%), ($p < 0.038$). Thus, the metastatic status of CNS PNET patients is potentially an important indicator of prognosis; however, with only limited case numbers for

statistical analysis, further research is needed into the prognostic value of metastatic status in both CNS PNETs pineoblastoma.

1.3.4 Treatments and survival

Three main strategies are considered for the treatment of a brain tumour, surgery, chemotherapy and radiotherapy. Following an MRI scan to ascertain the tumour's size, location and metastatic status, surgery is typically the first treatment option for children diagnosed with a brain tumour. At this stage debulking of the tumour may be feasible to primarily alleviate the patients' symptoms. Sub-total surgical resection for CNS PNET and pineoblastoma is common due to tumour location, often occurring deep within the brain at surgically inaccessible sites such as paraventricular, thalamic or pineal sites (Dai, Backstrom et al. 2003). Complete surgical resection of deep seated locations can potentially lead to unaccepTable neurological morbidity.

In general, children diagnosed with CNS PNET or pineoblastoma have a very poor prognosis which is considerably worse than those diagnosed with medulloblastoma, and treatment strategies for CNS PNET and high risk medulloblastoma have in the past been similar (Dirks, Harris et al. 1996; Kuhl 1998; McNeil, Cote et al. 2002; Timmermann, Kortmann et al. 2002). Previous studies have suggested enhanced survival for CNS PNET patients who received either a GTR ($p = 0.08$ and $p = 0.010$) or those who had $<1.5cm^2$ of residual tumour remaining following surgery ($p = 0.19$), although these trends did not reach statistical significance (Albright, Wisoff et al. 1995; Dirks, Harris et al. 1996; McBride, Daganzo et al. 2008).

Adjuvant therapy is introduced post operatively to treat minimal residual disease. Multiagent chemotherapy drugs can be administered for cytoreduction. The therapy used is dependent on the age of the patient and the extent of dissemination. Due to the tendency of CNS PNETs to disseminate through the subarachnoid space, craniospinal radiation is recommended (Timmermann, Kortmann et al. 2002). Until recently all CNS PNETs were regarded as 'high risk' when considering therapeutic intervention, irrespective of a patients demographics. In contrast, medulloblastomas are stratified as 'average risk' or 'high risk' with different treatment options considered depending on

patient age at diagnosis, the extent of tumour resection and metastatic status (MacDonald, Rood et al. 2003). A recent study by Chintagumpala *et al* published in 2009, stratified the treatment given to CNS PNET patients depending on tumour dissemination and tumour size (Chintagumpala, Hassall et al. 2008). 8 CNS PNETs were classified as either 'average risk' or 'high risk' with the average risk patients receiving less craniospinal irradiation (CSI). The 5yr EFS and OS of the average risk patients were 75% (±17%) and 88% (±13%), respectively; whilst for the high risk patients the EFS and OS were 60% (±19%) and 58% (±19%). Thus, the average risk patients were able to receive less CSI without compromising EFS. This highlights the need for novel CNS PNET-specific treatment strategies to be developed to improve the prognosis for patients with CNS PNET. The difference in clinical outcomes and response to treatment suggests that both the underlying genetics and cells of origin of CNS PNETs and medulloblastomas are distinct.

In the UK and America, recent clinical trials in the treatment of CNS PNET have had differing levels of success. In 2006, results of the SIOP/UKCCSG PNETIII study were published (Pizer, Weston et al. 2006). The trial tested whether 10 weeks of intensive chemotherapy given after surgery and before radiotherapy would improve patient outcome when compared to patients treated with radiotherapy alone. In total 68 patients were treated, 54 had a CNS PNET whilst 14 had pineoblastoma. None of the patients had radiological evidence of metastatic disease. 44 patients had the chemotherapy regime before radiotherapy and 24 received radiotherapy alone. At a median follow-up of 7.4 years (0.2-10.8 years), 36 patients had died whilst 32 remained alive. Comparing the survival of patients receiving the different regimes, there was no evidence to suggest that pre-radiation chemotherapy improved outcome. The 44 patients receiving pre-radiation chemotherapy had 3 and 5 year overall survivals of 52.3% and 45%, respectively, compared to the 24 patients treated with radiation alone (3 and 5 year overall survivals of 58.3% and 54.2%).

The year 2008 saw the results of the Headstart trials published, which utilized intensified induction chemotherapy and myeloblative chemotherapy with autologous hematopoietic cell rescue (Fangusaro, Finlay et al. 2008). 43 paediatric CNS PNET patients were entered, with the study identifying 5 year overall and event free survivals of 49% and 39%, respectively; suggesting high dose chemotherapy is equivalent to

standard dose chemotherapy and radiotherapy. At the time of publication, 20/43 (46.5%) patients remained alive. A summary of the survival of patients diagnosed with CNS PNET in a number of clinical trials and institutional studies is shown in Table 1.10. A recent study has shown that the use of up front radiotherapy provided patients with CNS PNET a much improved outcome ($p = 0.048$) (McBride, Daganzo et al. 2008). Thus the use of radiotherapy is an important factor in the treatment of CNS PNET. A separate issue in treating paediatric brain tumour patients with therapeutic agents is the incidence of secondary malignancies due to treatment. In a study by the Pediatric Oncology Group, 5/198 (2.5%) children treated primarily for a brain tumour developed a second malignancy (Duffner, Krischer et al. 1998).

Table 1.10 Compilation of the survival rates in CNS PNET and pineoblastoma patients.

Author	**Trial**	**Year**	**Survival**
Geyer	CCG	1994	3yr PFS PB (0%), CNS PNET (55%)
Jakacki	CCG	1995	3yr PFS 61% (all PB)
Albright	CCG	1995	5yr OS 34%
Cohen	CCG	1995	3yr OS PB (73%), CNS PNET (57%)
Paulino*	-	1999	5yr OS 46.9%
Reddy	-	2000	5yr PFS 37%
Marec-Berard**	SFOP	2002	5yr OS 14%
Timmermann	HIT 88/89/91	2002	3yr OS 48.4%
Hong	CCG921	2004	3yr PFS M0 (53%), M+ (14%)
Pizer	PNETIII	2006	5yr OS CTRT (45%) 5yr OS RT (54.2%)
Timmermann	HIT-SKK87/92	2006	3yr OS 17.2%
Fangusaro	Headstart I and II	2008	5yr OS 49%

CCG = Children's cancer study group, SFOP = Societé française oncologie pédiatrique, HIT = German trial group, PFS = progression free survival, OS = overall survival, PB = pineoblastoma, M0 = no metastasis, M+ = metastasis, CTRT = chemotherapy and radiotherapy, RT = radiotherapy only. *(Paulino and Melian 1999), **(Marec-Berard, Jouvet et al. 2002).

It is clear that new targeted therapies are needed due to the poor survival of patients with CNS PNET and pineoblastoma using current treatment options. At present, treatment options in CNS PNET and pineoblastoma are limited and debilitating, with few patients (especially those under the age of 3 years) surviving with a good quality of life. One study has investigated the use of histone deacytlase inhibitors (iHDAC) in CNS PNET cell lines which can cause both differentiation and apoptosis in cancer cells. Kumar *et al.*, investigated novel therapeutic agents in cell lines derived from CNS

PNETs. The viability of CNS PNET PFSK1 cells were shown to reduce on treatment with 3 HDAC inhibitors, suberoylanilide hydroxamic acid (SAHA), trichostatin A (TSA) and sodium butyrate (NaB) (Kumar, Sonnemann et al. 2006). Cell death was triggered on treatment with each agent and the results indicated caspase 3 and 9 were activated on the induction of cell death. This evidence suggests HDAC inhibitors are potential therapeutic agents in the treatment of CNS PNET. CNS PNET-specific therapies based on scientific evidence are needed to improve survival rates in CNS PNET; however, new targeted therapies can only be identified upon the elucidation of candidate oncogenes and tumour suppressor genes playing important roles in CNS PNET pathogenesis.

1.4 Cancer genetics

Cancer is a genetic disease of somatic cells and results from the disruption of normal cellular processes which include cell proliferation, differentiation and apoptosis. Cancer is a multistep process progressing by the accumulation of genetic 'hits'. It is now recognised that 2 main categories of genes are involved in the development of cancer, oncogenes and tumour suppressor genes (Tamarin 2002). Characterised by an increase in cell proliferation, loss of cell cycle control and evasion of apoptosis, cancer involves both the activation of oncogenes and the inactivation of tumour suppressor genes. In general, oncogenes have a dominant role in a cells transformation leading to cancer. When gained, high expressions of genes encoding, growth and transcription factors lead to increased mitosis (Tamarin 2002). In contrast, tumour suppressor genes generally suppress or inhibit pathways, and when lost, the inactivation of tumour suppressor gene function can lead to loss of control over the cell at many levels. With key roles in the control of the cell cycle, control of DNA repair mechanisms and promoting apoptosis, the loss of any one of these critical actions due to gene loss can lead to the development of cancer. Hence, in cancer the critical balance between oncogene activation and the suppression by tumour suppressors is jointly defective (King 2000). Mechanisms involved in the genetic alterations of oncogenes and tumour suppressor genes identified in cancer include altered gene copy number, gene mutation, translocation, LOH and epigenetic silencing via gene methylation.

1.4.1 Oncogenes

Generally, oncogenes are the mutated form of proto-oncogenes (normal genes usually encoding proteins with roles in the regulation of cell growth and differentiation). Mechanisms of oncogene activation include amplification (*MYC*), translocation (*BCR/ABL* fusion) and point mutation (*RAS*). There are 5 main categories of oncogene, (i) growth factors, (ii) tyrosine kinases, (iii) serine/threonine kinases, (iv) regulatory GTPases and (v) transcription factors. Growth factors (e.g *PDGF, EGF, VEGF, FGF* and *BMP*) stimulate cell growth, proliferation and differentiation. Tyrosine kinases can be either cytoplasmic or membranous (as receptors). Receptor tyrosine kinases (e.g *EGFR, PDGFR, VEGFR*) add phosphate groups to receptor proteins and can cause constitutive pathway activation. Transcription factors (e.g *MYC*) are proteins that bind to specific DNA sequences and control transcription. In the case of *MYC*, a mutation can cause *MYC* to be overexpressed leading to the upregulated expression of genes involved in proliferation.

1.4.2 Tumour suppressor genes

Tumour suppressor genes encode proteins involved in both cell cycle regulation and the promotion of apoptosis. Cyclin dependent kinase inhibitor 2A (*CDKN2A*) is a tumour suppressor which represses genes essential for the continuation of the cell cycle, thus inhibiting cell divison. *TP53* functions as a tumour suppressor by activating DNA repair proteins in response to damage, in addition to initiating apoptosis if the damaged DNA is irrepairable. Mechanisms by which tumour suppressor genes can be inactivated or lost include point mutation, deletion and LOH.

A major turning point in the understanding of cancer came from the two-hit hypothesis. Dr A. Knudson compared the prevalence of familial and sporadic retinoblastoma (a tumour of the eye), and found that the retinoblastomas of younger children were more likely to be familial, with an inherited first ‘hit’ within the germline, and a second ‘hit’ more likely to occur since all cells already carried the first ‘hit’ (Knudson 1971). The retinoblastomas of older children were more commonly sporadic, with the 2 ‘hits’ needed for oncogenic transformation occurring post-zygotically. Knudson also noted

that the patients with familial retinoblastoma often had bilateral retinoblastoma. Not all tumour suppressor genes fit into this 2 'hit' hypothesis, however. Haploinsufficiency occurs when a single (remaining) copy of a gene does not produce enough gene product to provide the wild type condition. This results in an abnormal or diseased state. *CDKN1B* (a cell-cycle inhibitor encoding $p27^{Kip1}$) has been shown to be haploinsufficient for tumour suppression, with mutation in one allele causing an increase in tumour susceptibility (Fero, Randel et al. 1998). Dominant negativity is a second exception to the 2 'hit' hypothesis. Dominant negativity arises when the altered gene product of a mutant allele adversely affects the wild type gene product, usually blocking some aspect of its function. *TP53* mutations can function as dominant negatives, whereby the mutated protein prevents the function of the protein encoded for by the wild type allele (Baker, Markowitz et al. 1990).

New adaptations to Knudsons two hit hypothesis have now arisen due to advances in genetic and epigenetic analyses which have increased the understanding of mechanisms leading to cancer. Tomlinson *et al.,* reviewed aspects of the advancement within our knowledge since the now 38 year old '2 hit hypothesis' was proposed. Updating the hypothesis, Tomlinson *et al.,* identified areas needing further consideration when proposing the 2 hit hypothesis (Tomlinson, Roylance et al. 2001). These included more than 2 'hits' occuring at tumour suppressor loci (Miyaki, Konishi et al. 1994; Varley, Thorncroft et al. 1997; Spirio, Samowitz et al. 1998; Varley, McGown et al. 1999), that second hits are dependent on where the first hit arose and what type of hit it was (Varley, Thorncroft et al. 1997; Birch, Blair et al. 1998; Spirio, Samowitz et al. 1998; Lamlum, Ilyas et al. 1999) and thirdly, new concepts, including promoter methylation now need to be incorporated into the 2 hit hypothesis (Kane, Loda et al. 1997; Jones and Laird 1999). Further research and new technological advances will undoubtedly add to the generation of new information characterising the development of brain cancer.

1.4.3 Loss of heterozygosity

Loss of heterozygosity (LOH) occurs in a variety of cancers and represents the loss of one allele at a particular locus (as predicted by the 2 'hit hypothesis). These lost regions may harbour putative tumour suppressor genes and frequently the remaining copy of the

gene is inactivated by point mutation. Four main mechanisms of LOH are observed in cancer: - mitotic recombination, gene conversion, gene deletion and whole chromosomal loss (Tamarin 2002). During cell division, homologous chromosomes line up to exchange DNA by mitotic recombination and this process may result in LOH, although the mechanisms of this are at present largely unknown (Figure 1.14). A second mechanism in which LOH can occur is gene conversion. This non-reciprocal transfer of DNA alters the DNA sequence of the recipient strand, whereas the donor strand remains unchanged. Conversion of one allele to the other can cause this loss in heterozygosity (Figure 1.15) (Zhang, Lindroos et al. 2006). Both mitotic recombination and gene conversion produce LOH with no net loss of genomic material, more commonly known as copy number neutral LOH. Acquired uniparental disomy (aUPD) is an example of this whereby both alleles of a gene are derived from a single parental copy, leading to the generation of two daughter cells each with common chromosomal products. In leukaemias and lymphomas, aUPD has been shown to result in homozygosity, and hence can be the basis of gene dosage for pre-existing mutations. Interestingly, in leukaemia and lymphoma, aUPD of *FLT3* (13q12) has been shown to confer an adverse patient prognosis (Fitzgibbon, Iqbal et al. 2007; Gupta, Raghavan et al. 2008). Therefore, identifying regions of aUPD in tumours could provide an insight into potential mutational targets. Finally whole chromosome or single gene deletions can be the cause of LOH, although these do result in copy number loss.

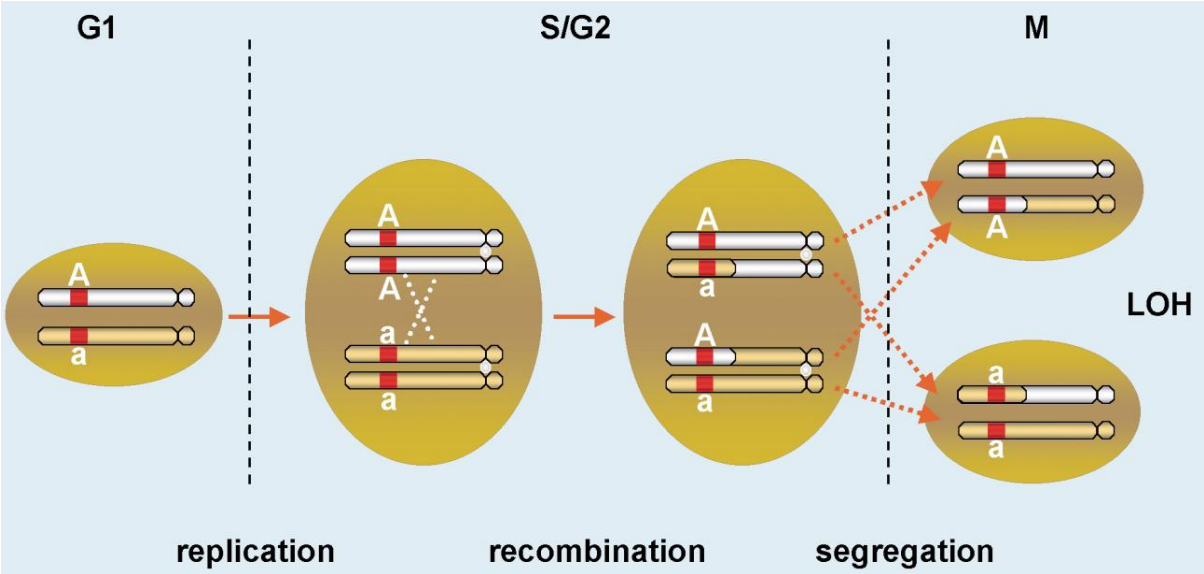

Figure 1.14 LOH due to mitotic recombination. Mitotic recombination can be caused by a recombinational exchange between two sister chromatids of homologus chromosomes during late S or G2 phase of the cell cycle. When resolution of the recombinational intermediate results in a cross-over event, daughter cells may, following mitosis (M), show LOH of numerous genetic markers on the involved chromosome. Adapted from 'Mitotic maneuvers in the light' (Vrieling 2001). A; allele 1, a; allele 2, G1; Gap 1, (cells increase in size and the G1 checkpoint ensures DNA is accepTable for synthesis), S; synthesis (DNA is replicated), G2; Gap 2, (the cell continues to grow and the G2 checkpoint ensures DNA is accepTable for mitosis), M; mitosis, (cell growth stops and the cell divides into 2 daughter cells).

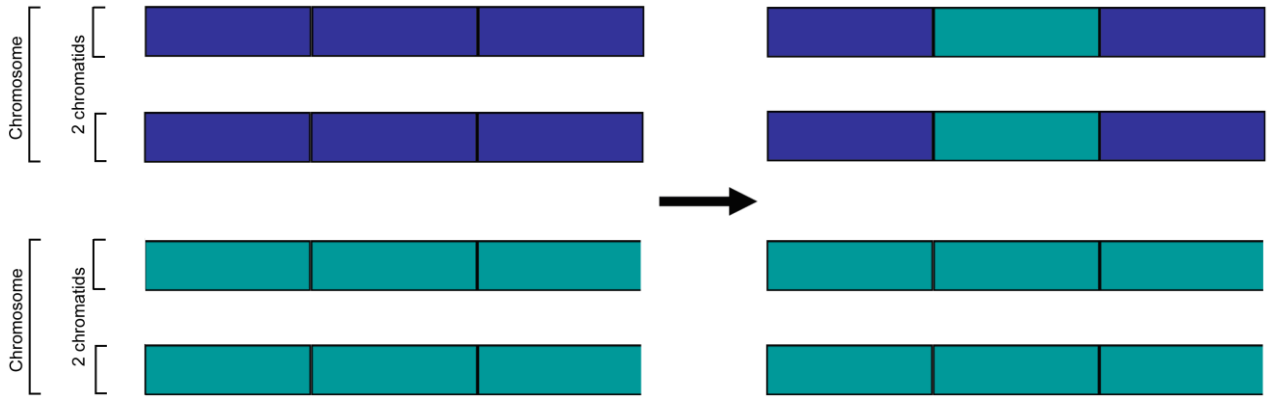

Figure 1.15 Gene conversion. The mechanism of gene conversion, where one chromosome (light blue) donates part of its genetic information to the other chromosome (dark blue) and heterozygosity is lost. During replication, a DNA strand being elongated can form a hybrid with the complementary DNA strand present in the second homologous chromosome due to DNA polymerase moving strands.

1.4.4 Epigenetics

Cancer epigenetics is the study of tumourigenic events contributing to neoplastic transformation through sTable changes in gene expression. Epigenetic mechanisms involved in cancer include DNA methylation, histone modification, nucleosome positioning and miRNA expression. Although not altering the DNA structure, epigenetic alteration by DNA methylation (where a methyl group is enzymatically added to a carbon-5 of a cytosine residue) plays a major role in tumourigenesis, alongside the genetic alterations of DNA (Goelz, et al. 1985). Transcriptional silencing due to promoter-associated CpG island hypermethylation of tumour suppressor genes is involved in the development of cancer (Momparler, et al. 2000, Yan, et al. 2001). DNA methylation impacts gene transcription in 2 ways. Firstly, the methylation of DNA physically obstructs the binding of transcriptional proteins to the gene, and secondly, methylated DNA may be bound by methyl-CpG-binding domain proteins (MBDs), which can recruit additional proteins to the site, including histone deacetylases and chromation remodelling proteins. These make the chromatin compact and inactive, causing both chromatin and gene silencing. DNA methylation occurs due to the enzymatic activity of DNA methyltransferases (DNMTs). Tumour suppressors shown to be methylated include genes implicated in the control of the cell cycle and DNA mismatch repair (Merlo, Herman et al. 1995; Herman, Umar et al. 1998; Jones and Laird 1999; Simpkins, Bocker et al. 1999). The reversibility of methylation represents a potential therapeutic target. Demethylating agents and inhibitors of methyltransferases are two candidates to reverse the process of methylation (Egger, Liang et al. 2004). An example of where the methylation status of a gene represents a marker of response to chemotherapy is the gene, *MGMT* (10q26). Patients with glioma had an increased response to the alkylating agent temozolomide when the promoter region of *MGMT* was methylated and this was also associated with a favourable outcome (Hegi, Diserens et al. 2005; Donson, Addo-Yobo et al. 2007). Thus, when characterising the components leading to tumourigenesis, both genetic and epigenetic mechanisms should be considered.

1.5 Genetic alterations of CNS PNET and pineoblastoma

Limited genetic research has been performed for CNS PNET and pineoblastoma. With less than 20 new cases diagnosed in the UK each year, the overall rarity of tumour tissue has led to difficulties obtaining large sample cohorts to analyse at the genetic level, thus previous studies have contained only small sample sets. Also, the collection of tissue samples is hindered by the fact that many pineoblastomas are surgically unresectable or, if resectable, only small biopsies are taken.

1.5.1 Cytogenetics – CNS PNET and pineoblastoma karyotypes

Karyotyping is a cytogenetic method used to visualise both the size and number of chromosomes. In cancer research, karyotyping is utilized to define large regions of genetic alteration which include gain, loss and translocation of genetic material in tumour samples. Although karyotyping is a useful cytogenetic tool in the elucidation of a tumour's genetic profile, the relatively low resolution technique has limitations. The correct assignment of chromosome breakpoints of karyotypes in the literature can be inaccurate due to the low resolution and the quality of metaphase cells from solid tumour preparations is often poor.

Previous cytogenetic studies using karyotyping have been performed on 24 CNS PNETs and 12 pineoblastomas (Griffin, Hawkins et al. 1988; Sreekantaiah, Jockin et al. 1989; Chadduck, Boop et al. 1991; Fujii, Hongo et al. 1994; Agamanolis and Malone 1995; Bhattacharjee, Armstrong et al. 1997; Bigner, McLendon et al. 1997; Burnett, White et al. 1997; Bayani, Zielenska et al. 2000; Roberts, Chumas et al. 2001; Uematsu, Takehara et al. 2002; Batanian, Havlioglu et al. 2003; Sawyer, Sammartino et al. 2003; Brown, Leibundgut et al. 2006). To date, 9 studies containing CNS PNET karyotypes have been published (Table 1.11). Patient ages ranged from <1 – 16 years and the studies were undertaken between 1991 and 2003. 9 CNS PNETs had normal karyotypes, whereas 13 CNS PNETs contained complex karyotypes. Interestingly, 2 CNS PNET karyotypes contained only a single aberration, with one containing monosomy 22, whilst a separate case contained a translocation between chromosomes 6 and 13 (t(6;13)(q25;q14)) (Chadduck, Boop et al. 1991; Bayani, Zielenska et al. 2000).

Monosomy 22 has previously been identified as a common imbalance in ATRT, usually occurring with a mutation or deletion at the *INI1* locus (22q11.2) (Versteege, Sevenet et al. 1998; Biegel 1999; Packer, Biegel et al. 2002). In addition, aberrations involving chromosome 22, are the most frequent genetic alteration in ependymomas, especially those arising in the spine (Hamilton and Pollack 1997). The 9/22 (40.9%) CNS PNETs harbouring normal karyotypes could harbour subtle genetic changes not detected by this low resolution analysis. Other reasons for a normal karyotype could be that the biopsy contained normal brain tissue, or that only normal cells survived the short term culture prior to karyotyping. The most common chromosome abnormalities were gains of chromosome 7 (4/22, 18.2%), gain or loss of chromosome 11 (7/22, 31.8%), gain or loss of chromosome 13 (4/22, 18.2% each) and gain of chromosome 18 (3/22 13.6%). Interestingly, 4 of the 6 translocations (66.7%) identified in the CNS PNETs involved chromosome 11. The loss of chromosome 11q has previously been reported in medulloblastoma (Vagner-Capodano, Gentet et al. 1992; Reardon, Michalkiewicz et al. 1997; Avet-Loiseau, Venuat et al. 1999; Rickert and Paulus 2004). It has previously been proposed that the subset of medulloblastomas harbouring 11q loss are distinct to those containing isochromosome 17q (Vagner-Capodano, Gentet et al. 1992).

Table 1.11 CNS PNET karyotypes from the literature. * = recurrent tumour. Karyotypes described using International System for Human Cytogenetic Nomenclature (ISCN) 1995.

Authors and year	Age (Yrs), sex	Location	Karyotype
Chadduck, *et al*., 1991	<1		Normal
	<1		Normal
	<1		Normal
	<1		45,XY,-22
Fujii, *et al*., 1994	9, F		Normal
	11, M		43-44;XY;+2,-6;der(10)t(10,11)(q26;q21),del(11)(q21),-12,-13,=mar,(8)/84/90,XXYY,der(10)t(10;11)(q26;q21),der(10)t(10;11)(q26;q21),der(11)(q21),=mar/(8)
	14, M		Normal
Bhattacharjee, *et al*., 1997		Parietal	46,XY,i(1)(q10);-9,t(9;11)(q34;q13),8?/90;idemx2,-X,Y1/46;XY
Bigner, *et al*., 1997	2, M		46;XY,t(6;9)(q21;q13),del(10)(q22)2/45,t(11;13)(q15;q11),-13
			Normal
			Normal
			Normal
Burnett, *et al*., 1997	7	Parietal	49,XX,add(3)(q23orq24),+5,+8,dup(11)(q12q22.3or13q23),del(16)(q22q24),add(19)(p13),+21[8]/49,idem,i(1)(q10)[1]/49,idem,add(13)(q34)[1]
	16*	Parietal	90,XX,add(X)(p22)x2,dic(1;9)(q42;p21)x2,dic(4;9)(q3?5;p2?2),-6,add(6)(p24),-9,add(11)(p15)x2,-15x2,add(16)(q2?2),+mar1,+mar2[11]
Bayani, *et al*., 2000	2		Normal
	3		70-103chromosomes,double ring and dmins
	3.5		55-57,XX,-X,del(1)(p22),i(4)(p10), -5,+6,+add(7)(q36), add(9)(p21),-11,-13,-17,add(18)(q23),-19,-19, +13mars,+dmins
	4		46,Xrea(X),?rea(10p),?(14q),add19q,?ass(22q),22q
	6		46,XY,t(6;13)(q25;q14)
Roberts, *et al*., 2001		Cerebral	46,XX, del(2)(p22.2-2p23.1),del(5)(q33q35)/46,idem,del(17)(q21.3)
		Parieto-occipital	der(9;15)(q10;q10)x2,+11,+13,+18,+20,+20, 56-59,Xc,+X,+1,+1,+1,add(1)(p?),add)(1)(q?),+2,del(2)(p24),+7,+8,add(8)(q?)
		Parietal	69~75XX,-X,add10(q42)x2,-4,-4,add(4)(q3?),-10,-11,del(11)(q2?),-13,-16,-18,+7,13mar,dmin(cp7)dmins
Uematsu, *et al*., 2002	7	Insular Cortex	52,XX,+1x2,add(3)(q25),+7x2,add(11)(q25)x2,+21x2
Batanian, *et al*., 2003	<1, F	Occipital-temporal	50,XX,+9,+13,+1q,+18p,complex t(1:11,18)

Between 1988 and 2006, 7 studies have published a total of 12 pineoblastoma karyotypes (Table 1.12). Patient age ranged from 6 weeks to 13 years. Only a single pineoblastoma maintained a normal karyotype. Translocations were identified in 5/12 (41.67%) pineoblastoma karyotypes, with the most common chromosomal alterations involving gains of chromosome 1 (4/12, 33.3%), chromosome 19 (3/12, 25%) and loss involving chromosome 20 (3/12, 25%). 3 pineoblastomas harboured single genetic alterations, specifically, a deletion at 11q13, monosomy 22 and a translocation between chromosomes 16 and 22. This is in contrast to 8 pineoblastomas with vast genetic alterations and aneuploidy. In summary, whereas a third of CNS PNETs contained normal karyotypes, this was not consistent in the pineoblastomas which only rarely had normal karyotypes. Also, whilst CNS PNETs more commonly contained genetic alterations involving chromosomes 7, 11, 13 and 18, pineoblastomas contained alterations involving chromosomes 1, 19 and 20. Both CNS PNETs and pineoblastomas harboured translocations involving chromosome 11, 6/11 (54.5%).

Table 1.12 Pineoblastoma karyotypes from the literature

Authors and year	**Age (Yrs), sex**	**Karyotype**
Griffin, *et al*., 1988	3, F	42-46,XX,add(1)(p36),del(1)(p13p21),inc
	10, M	45-47,XY,add(1)(q44),inc
Sreekantaiah, *et al*., 1989	6wk, M	46,XY,del(11)(q13.1q13)
Agamanolis & Malone, 1995	1, F	Normal
Bigner, *et al*., 1997	1.5, F	46,XX,+14,-22/46,idem,-20+mar
Roberts, *et al*., 2001	U/N, F	45,XX,-22
	U/N, F	63-82,XXX,+X,+2,-3,+4,+5,+7,+9,+11,+12,-14,+15,+16,+17,+18,+20,+21,+22[cp6]
Sawyer, *et al*., 2003	0.5, F	46,XX,t(16;22)(p13.3;q11.2-12)c
Brown, *et al*., 2006	4, F	42,XX,+1,dup(1)(q11q25)x2,-8,der(11)t (11;17)(p11.2;q11),der(13)t(13;?17)(p11;?q11),-16,-17,-18,-19,-20,-21,+2mar[7]/42,idem,add(2)(p21)[3]
	6, F	54-56,XX,t(1;16)(p13q13),+add(1)(p21)x2,-15,+19,+19,del(19)(q13),+21,+21,+2-5mar[cp8]/46,XX[1]
	7, F	80-83<4n>,XXXX,-1,-2,-3,-4,-6,-9,add(12)(p13),-13,-16,-20,-21,+mar[cp6]
	13, F	93-99,XXXX,+9,-13,+14,i(17)(q10),+19,+19,+20,+0~5mar[cp7]/93-99,idem,der(1)t(1)(11)(p36;q14),-6,~+12[cp7]

1.5.2 Comparative genomic hybridisation

Comparative genomic hybridization (CGH) was developed in 1992 by Kallioniemi as a simple one colour in situ hybridisation to identify unknown regions of amplification in tumour cell lines and primary bladder tumours (Kallioniemi, Kallioniemi et al. 1992). While useful in genome-wide screening and in the identification of amplified DNA sequences in tumours, low-level gains (duplication and insertion) and loss (deletion) of DNA were not reliably detected. A two colour strategy was later developed. The principal of CGH is based on the simultaneous competitive hybridisation of two genomic DNA samples (differentially labelled normal and tumour DNA) with the fluorochromes, Rhodamine and FITC, respectively. Labeled DNA is subjected to competitive hybridisation to normal metaphase spreads on a glass slide. The DNA counterstain DAPI is used as a third fluorochrome to visualise metaphase chromosomes. Addition of Cot-1 DNA blocks the hybridisation of repetitive sequences. The ratio of red and green fluorescent signals is measured along each chromosome, with regions involved in deletion appearing green (only reference DNA has hybridised, no tumour DNA) and gain of a region appearing red (more tumour DNA than reference DNA), whereas chromosomal regions equally represented in sample and normal DNA will appear yellow (Figure 1.16). Loci involved in tumourigenic transformation can therefore be established.

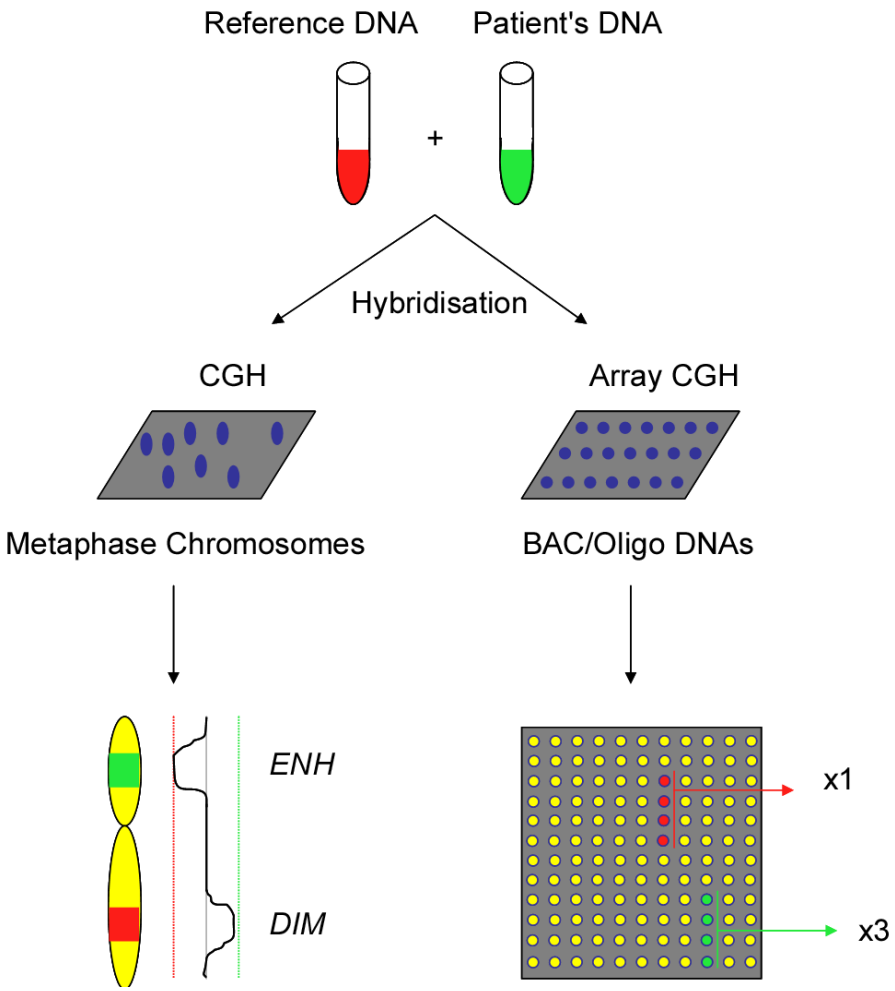

Figure 1.16 Comparison of conventional CGH and array CGH. DNA hybridisation identifies regions of loss (Red) or gain (Green). ENH = enhanced copy number, DIM = diminished copy number. Adapted from www.array-cgh.de

To date, 4 studies have published conventional CGH profiles for 12 CNS PNETs and 1 pineoblastoma (Avet-Loiseau, Venuat et al. 1999; Nicholson, Ross et al. 1999; Rickert, Simon et al. 2001; Inda, Perot et al. 2005). The ability to analyse the CNS PNET genomes at a higher resolution has led to the identification of more accurately assigned, smaller regions of interest. Compilation of the CGH profiles for CNS PNETs show gain of chromosome 1 to be a prominent feature (8/12, 66.7%), in particular the long arm of the chromosome in 6/12 (50%) cases (Table 1.13). Chromosome 2 was gained in 4/12 (33.3%) cases. 5 regions of high level gain were identified within the CNS PNETs and of particular interest were amplicons on 7p11.2-p12 and 8q22.3-q24.22 encompassing genes *EGFR* and *MYC*, respectively (Nicholson, Ross et al. 1999; Inda, Perot et al.

2005). Overexpression of EGFR has been identified in ependymomas, although the mechanism of this overexpression still needs to be elucidated, as amplification is rare (Mendrzyk, Korshunov et al. 2006). Interestingly, amplification of *MYC* is observed in 5-10% of medulloblastomas and has been linked to both large cell and anaplastic variants, in addition to poor patient outcome (Bigner, Friedman et al. 1990; Aldosari, Bigner et al. 2002; Eberhart, Kratz et al. 2004; Lamont, McManamy et al. 2004). The CNS PNETs harboured regions of loss most frequently on chromosomes 3p, 9p and 16p (each 3/12, 25%). Only a single CNS PNET had a balanced genetic profile, which is a lower proportion to that seen in the CNS PNET karyotypes, however, this could be due to the higher resolution of CGH analyses compared to the low resolution of karyotyping. The majority of cases contained complex CGH profiles with many alterations and only 2 CNS PNETs contained a single alteration each.

Table 1.13 CNS PNET CGH results from the literature

Authors and year	**Age (yrs), sex**	**Location**	**CGH gain**	**CGH loss**
Nicholson, *et al*., 1999	1.1	Cerebral	None	None
	2.6	Cerebral	X,1p32pter,1q32qter,2p,7q33qter	3p12p14,3p21.3pter,5pterq33,6,7p12p21.1,9p23 q32.11,14q24qter
	6.4	Cerebral	None	3p13p21.1
	8.3	Cerebral	X,1,7p,9,13,16p,19,20,22**,(7p11.2p12,7q21.3q 22)**	3,4,5,6,8q13qter,10q11q22,10q24.3qter,12p12q2 3,14,15q11q23,16q12q22.1,18q
Avet-Loiseau, *et al*., 1999	4.0	Supratentorial	1q,2,17	None
	4.2	Supratentorial	None	9pterq22,11q23qter
Inda, *et al*., 2005		Supratentorial	1q,5,6,20	16q
		Supratentorial	**1q**	3q21q25,9
		Supratentorial	1q,2,**19q12q13.11**	16p,19p
		Supratentorial	14q12qter	16p,19,22
		Supratentorial	1p13p22,2q21.3q24.2,5p14pter,5q14q23.1,9p, 13q21q22,18q22qter	16p,17,19,22
		Supratentorial	1,2,**8q22.3q24.22**,9p11p22,17q22qter,18	4pterq24,4q32qter,9q,11p13pter,13,17pterq21.32

Profiles in bold indicate areas of high level gain.

To date, a single pineoblastoma CGH profile has been analysed and contained 4 distinct regions of high level gain. Large regions of chromosomes 1q, 6p and 14q were amplified, in addition to a region on chromosome 5p, encompassing a cadherin gene cluster also had high level gain (Table 1.14) (Rickert, Simon et al. 2001). A study by Russo *et al.*, in 1999 analysed a further 6 paediatric CNS PNETs, however, due to the combination of both paediatric and adult CNS PNET samples within the analysis, it was not possible to distinguish between specific genetic aberrations common to the patients under the age of 18 years and therefore the data is not presented in this review of paediatric CNS PNET CGH profiles (Russo, Pellarin et al. 1999).

Table 1.14 Pineoblastoma CGH results from the literature

Authors and Year	**Age (Yrs), Sex**	**Location**	**CGH Gain**	**CGH Loss**
Rickert, *et al*., 2001	1, M	Pineal	**1q12qter,5p13.2p14,6p12pter,14q21qter**	None

Profiles in bold indicate areas of high level gain

A genome-wide, DNA based technique, CGH utilises both fresh frozen and formalin fixed paraffin embedded (FFPE) tissues in a single experiment. Metaphase chromosomes from the patient are not required. The use of control slides hybridised in parallel to sample slides can be used to depict if hybridisation signals in particular regions are inconsistent. The false results identified in controls can therefore be disregarded in the sample slides on analysis. CGH does however have limitations. Relatively large amounts of DNA (450ng) are needed for conventional CGH, and balanced rearrangments cannot be detected. Bayani *et al.*, identified a CNS PNET presenting with a normal CGH profile, in contrast to the cytogenetic findings which revealed a reciprocal translocation between chromosomes 6 and 13 with no net loss or gain of DNA (Bayani, Zielenska et al. 2000). Lastly, karyotypic anomalies which may have central roles in tumour development and progression are not detected, these include ploidy, balanced translocations and genetic inversions.

1.5.3 Array CGH

In comparison to conventional CGH which utilises the hybridisation of DNA to metaphase chromosomes, array CGH uses genomic clones (termed probes) which are spotted onto a glass slide (termed an array) and these are used as the hybridisation target for DNA. Clones can be either bacterial artificial chromosomes (BACs) or P1-derived artificial chromosomes (PACs) and can receive inserts between 50-300 Kbp (Cowell, Matsui et al. 2004). Like conventional CGH, test and reference DNA compete for binding to the probes and the ratio between red and green signals is used to identify differences in copy number between the two samples (Ward, Harding et al. 2001). The initial CGH arrays developed contained on average 6000 BACs, with a resolution of up to 1Mb, however, advances in technology have led to the development of oligonucleotide arrays now capable of analysing 244,000 probes per array with a resolution of 100Kb (Table 1.15). The resolution of CGH arrays is dependent on the number of probes per slide, the size of the probes and also the genomic distince between probes. DNA extracted from both fresh/frozen and FFPE tissues can be analysed using the aCGH platform (Johnson, Hamoudi et al. 2006). The quality of results is dependent on the integrity of the sample DNA and often due to processing; FFPE DNA is frequently degraded, resulting a high background, potentially masking the genetic imbalances.

Table 1.15 Comparison of the resolution of different platforms used in oncogenomics

Technique	**Platform type**	**Number of probes per array**	**Genomic resolution**
Karyotyping	Microscopy	-	5-10Mb
CGH	Fluorescence microscopy	-	1-10Mb
Array CGH (BAC/PAC or Oligo)	Microarray	6000-244,000	1Mb-100Kb
100K SNP array	Microarray	100,000	Mean inter-probe distance 23Kb
500K SNP array	Microarray	500,000	Mean inter-probe distance 5.8Kb
SNP6.0 array	Microarray	1.8 million	Mean inter-probe distance <700 bases

aCGH profiles for CNS PNETs were first published in 2006 (Table.1.16). Kagawa *et al.*, used an array containing 287 target genes of interest in cancer research to analyse 10 medulloblastomas alongside 3 CNS PNETs (Kagawa, Maruno et al. 2006). Of particular interest was gain of 17q detected in 6/10 (60%) of medulloblastomas, however, this was not found in the CNS PNETs of the study. Whole chromosome arm imbalance was identified for a single CNS PNET, with gain of chromosome 7 and loss of chromosome 6q. Interestingly, 1 CNS PNET was found to contain amplification of *MYCN* (2p24.3). Although the author suggests that CNS PNETs have less genomic imbalance than medulloblastomas, it is hard to conclude since only limited numbers of CNS PNETs were analysed.

Table 1.16 CNS PNET aCGH from the literature.

Author and year	**Age (yrs), sex**	**Location**	**aCGH gain**	**aCGH loss**
Kagawa, *et al*., 2006	0.6, M	Midbrain	*MSH2* (2p22.3-p22.1), *ERBB2* (17q11.2-q12), *BCR* (22q11.23)	None
	2.3, F	Parietal Lobe	Chr 7, *MYCN* (2p24.1), *MSH3* (5q11.2-q13.2), *EGFR* (7p12.3-p12.1), *RFC2* (7q11.23), *PTCH* (9q22.3), *DMBT1* (10q25.3-q26.1), *GLI* (12q13.2-q13.3), *ERBB2, TK1* (17q23.2-q25.3), *STK6* (20q13.2-13.3), *BCR*	Chr 6q, *MSH2*
	3, M	Temporal	*MSH2, EGFR, RFC2, DBCCR1* (9q33.2), *CDK2, ERBB3* (12q13), *BRCA1* (17q21), *STK6*	*APC* (5q21-q22), *SNRPN* (15q12), *HRAS* (11p15.5), *GLI*
McCabe, *et al*., 2006		Cerebral	*FIP1L1-CHIC2* (4q12)	13q14.11-qter
		Cerebral	None	*CDKN2A/CDKN2B* (9p21.3)
		Cerebral	None	Chr 13q
		Cerebral	*FOXQ1-FOXF2* (6p25.3), *ALDH8A1-MYB* (6q23.3), *PHACTR2-SF3B5* (6q24.2)	*RASA3* (13q34)
		Cerebral	None	None
		Cerebral	*CACNG8-LILRB5* (19q13.42)	*RASA3*
		Cerebral	None	None
Pfister, *et al*., 2007	1, F	Supratentorial	None	None
	<1.5, M	Supratentorial	*ADAM8* (10q26.3)	None
	2, M	Supratentorial	*UNC5B/CDH23* (10q22.1)	None
	3, F	Supratentorial	*PRDM16* (1p36.32), *CNTNAP2* (7q35), *NOS3* (7q36.1), *URP2* (11q13.1), *DACH1* (13q22), *TNFRSF6B* (20q13.33)	*UNC5C* (4q22.3)
	3, M	Supratentorial	*TNFRSF6B*	*AJAP* (1p36.13), *IGSF21* (1p36.13), *GRM2* (3p21.1), *TAF6L/HRASLS3* (11q13)
	6, M	Supratentorial	*TMEM/MGC33556* (1p34.1), *MM-1* (12q13.13), *NULL* (12q23)	*NULL* (1q31.1), *UNC5C, GPR116*
	7, F	Supratentorial	*RHOB* (2p24.1), *MAP3K7* (6q16), *MM-1, NULL* (12q23), *DACH1*	*AJAP, IGSF21, HRG* (3q27.3), *DOK7* (4p16.2), *DUSP8* (11p15.5), *RHOG* (11p15.4), *JAM3* (11q25)
	7, M	Supratentorial	*CNTNAP2, NOS3*	*GPR116* (6p12.3), *MED4* (13q14.2)
	11, F	Supratentorial	*LMO1/STK33* (11p15.4)	*MGMT* (10q26.3), *DUSP8, RHOG, TAF6L/HRASLS3, GRM5* (11q14.2), *JAM3*
	12, F	Supratentorial	*IGFB2/5* (2q35), *TNFRSF6B, PDGFB* (22q13.1)	*MED4*

In a second study, McCabe *et al* analysed 7 CNS PNETs, (5 primary and 2 recurrences) using aCGH (McCabe, Ichimura et al. 2006). Patient age ranged from 2.7 to 23 years. Five distinct amplifications were identified, one CNS PNET contained an amplicon involving *PDGFRA/KIT* (4q12), one contained 3 separate amplicons on chromosome 6 (one of which encompassed the oncogene *MYB* (6q23.3)) and an amplicon at 19q13.42 was identified in a single CNS PNET. Loss of 9p21.3 encompassing *CDKN2A* and *CDKN2B* was also identified in a single CNS PNET case.

More recently, Pfister *et al.,* identified a genetically balanced CNS PNET and found no high level amplifications using the aCGH platform (Pfister, Remke et al. 2007). Table 1.16 shows DNA copy number alterations of less than 3 Mb, however larger regions of alteration were also noted. Gains of 1q21.3-qter, 6p22.1-pter, 17q21.31-qter and 19p were identified in 2/10 (20%) CNS PNETs and the most frequent loss involved regions 1p12-p34.1, 9p, 16q12.1-qter and 17p11.2-pter also in 2/10 (20%) of cases. In addition to the 10 CNS PNETs analysed by aCGH, an independent set of 11 CNS PNETs were presented for analysis by FISH. In total, *CDKN2A* and *CDKN2B* deletions were found in 7/21 (33.3%) CNS PNETs, 4 of which were homozygous. On evaluation of patient clinical factors and genetic aberrations, a trend was identified between the loss of *CDKN2A* and metastatic disease at diagnosis ($p = 0.07$). FISH analysis was also used to investigate high level gains of *MYCN* (2p24.3) and a single CNS PNET was found to contain this amplification.

Importantly, even using the higher resolution aCGH platform, 3 CNS PNETs were identified which did not contain any copy number imbalance (McCabe, Ichimura et al. 2006; Pfister, Remke et al. 2007). This suggests other mechanisms of tumourigenesis could be involved in this tumour type, including balanced translocations, mutations, alterations in gene expression levels and epigenetic silencing of genes via aberrant methylation. Overall, aCGH analysis of 20 CNS PNETs from 3 studies identified that genes were gained on chromosome 2p22.3-p24.1 in 4/20 (20%); on chromosome 7q 6/20 (30%); on chromosome 12, 7/20 (35%) and on chromosome 17q in 4/20 (20%) cases. Of particular interest were genes identified in the CNS PNET studies which are known to be amplified in other paediatric brain tumours, for example *PDGFRA/KIT* (4q12), which was found amplified in 2 CNS PNETs by CGH and aCGH techniques (Inda, Perot et al. 2005; McCabe, Ichimura et al. 2006). Amplification of this region has previously been identified in GBM and could provide a novel target for kinase

inhibiting treatments (Fleming, Saxena et al. 1992; Hermanson, Funa et al. 1996; Holtkamp, Ziegenhagen et al. 2007). A separate member of the platelet derived growth factor family, *PDGFB* (22q13.1) was gained in a single CNS PNET, of which the expression of the encoded receptor (*PDGFRB*, 5q31-q32) has been found linked with both metastatic disease and poor prognosis in medulloblastoma (Gilbertson and Clifford 2003). *EGFR* (*ERBB1*, 7p12) was gained in 3 CNS PNETs identified by aCGH. This gene has been found amplified in GBM, with an association with poor prognosis (Shinojima, Tada et al. 2003). A novel target for future therapy, *EGFR* tyrosine kinase inhibitors are currently being investigated for activity in GBM (Stea, Falsey et al. 2003; Efferth, Ramirez et al. 2004; Halatsch, Gehrke et al. 2004; Raizer 2005; Halatsch, Schmidt et al. 2006). 2 other members of the *ERBB* family were amplified within the aCGH analyses, *ERBB2* (HER2) in 2 cases and *ERBB3* (*HER3*) in a single CNS PNET. The *ERBB* family induced signalling pathways include PI3-K/AKT, PLC-γ and RAS/RAF/MAPK (Yarden and Sliwkowski 2001), with involvements in cell proliferation, angiogenesis, survival, metastasis, and resistance to therapy (Andersson, Guo et al. 2004). Clearly this family of genes needs to be further investigated in CNS PNET.

An anomaly identified between the CGH and aCGH analyses was the lack of genes amplified on 1q by the aCGH analysis, compared to the high proportion of 1q gains identified by conventional CGH. One explanation for this difference could be the heterogeneous genetics within the different CNS PNET patient populations. In the aCGH analyses, several common regions of loss were identified, particularly genes on chromosome 11 including *HRAS* (which has a regulatory role on cell division), which was lost in 3/20 (15%) cases. Loss of genes on chromosome 13q was a second feature of the aCGH studies. The loss of *CDKN2A* was identified in a single CNS PNET by McCabe *et al.*, in addition to 7/21 in the Pfister study by a combination of aCGH and FISH analyses (McCabe, Ichimura et al. 2006; Pfister, Remke et al. 2007). Understandably the loss at 9p21.3 needs to be further elucidated in CNS PNET, with the loss of tumour suppressors *CDKN2A* and *CDKN2B*, potentially having an important role in the pathogenesis of CNS PNET.

aCGH analyses identified a *MYCN* amplification in a single CNS PNET (Kagawa, Maruno et al. 2006), with the addition of a another CNS PNET also containing the amplification identified by FISH (Pfister, Remke et al. 2007). Amplification of *MYCN*

is a common feature of neuroblastoma, the most common extracranial solid tumour of childhood which is also considered a PNET. Arising from the neural crest of the sympathetic nervous system, this neuroendocrine tumour typically occurs in children under the age of 2 years. A recent SNP array study revealed *MYCN* amplifications in 26% of neuroblastomas and also identified *CDKN2A* deletions in 9 cases (Caren, Erichsen et al. 2008). The current WHO classification of tumours of the CNS has termed a subtype of CNS PNET with neuronal differentiation as 'central' neuroblastoma, thus pathways and genes important in the pathogenesis of neuroblastoma may be similar to those in the tumourigenesis of CNS PNET. As with conventional CGH, array CGH can be used to identify alterations in copy number when there is a change in the net amount of chromosome material, however when there is no overall loss or gain in chromosome material (e.g. balanced translocations), array CGH will not show the genetic alteration. The method of array CGH also lacks the ability to identify regions of uniparental disomy, when loss of heterozygosity (LOH) occurs with no net loss of DNA due to the loss of one allele and subsequent duplication of the remaining allele. Advances in modern technology has recently led to the introduction of a new CGH platform, oligo array CGH. By replacing BAC and PAC clones with short DNA sequences (oligonucleotides) as probes, oligo arrays can be produced rapidly and are less expensive than the former aCGH platform, even with the 30,000 probes needed for a full genome-wide scan (Carvalho, Ouwerkerk et al. 2004). With an increased resolution of 100Kb, the oligo array CGH platform can detect single copy number alterations and is highly informative when compared to aCGH.

1.5.4 SNP arrays

On completion of the human genome project in 2001 (Lander, Linton et al. 2001). Single Nucleotide Polymorphisms (SNPs) and their locations throughout the genome were identified. SNPs are the single nucleotide bases which differ between individuals. DNA between humans is 99.9% identical, with polymorphisms constituting this 0.1% difference. At present there are thought to be 10^6 SNP loci in the human genome comprising the most common type of polymorphism (Dong, Wang et al. 2001). Currently, the market leaders in the production of SNP arrays is Affymetrix and the arrays produced can be utilised to identify both SNP copy numbers and allele genotypes across the entire genome in a single experiment. Therefore, this high resolution

technology is of immense benefit in cancer research where genomic instability, gene copy number alterations and LOH are all common features.

Whereas array CGH and oligo array CGH allow for the identification of regions of loss and gain across the genome, they are not of sufficiently high resolution to identify copy number changes in single bases within genomic material which the ultra high resolution SNP arrays are capable of (Herr, Grutzmann et al. 2005). The high resolution of SNP array analysis can be used to identify minute alterations in DNA copy number and also genotype individual SNPs, thus copy neutral events such as mitotic recombination, gene conversion and uniparental disomy can be detected (Zhao, Li et al. 2004). Affymetrix have produced SNP arrays to examine 10K, 100K, 500K and 1.8 million SNPs at a time (Section 1.5.3, Table 1.15) (Herr, Grutzmann et al. 2005; Hu, Wang et al. 2005; Slater, Bailey et al. 2005; Suzuki, Kato et al. 2008). The genechip mapping sets need only tiny amounts of DNA (250ng per chip), which is particularly attractive for small sample cohorts of precious brain tumour tissue. An important factor of SNP array analysis is the inclusion of a control dataset alongside the tumour cohort. Since, there is significant SNP variation between individuals, it is important to consider the patient's own constitutional SNP content (Iafrate, Feuk et al. 2004; Sebat, Lakshmi et al. 2004). Constitutional blood samples are usually obtainable from brain tumour patients and are essential for validation of tumour-specific events with respect to the patients own constitutional SNP variation. By correcting for the normal polymorphisms present in constitution DNA, regions of interest in the tumour DNA can therefore be identified. If the patient's own blood is not however available, one solution is too use a population based control set for unpaired normalisation. As current literature suggests diversity in both copy number and SNP variation within different populations, a control dataset most likely to represent the patient's own copy number and genotype variation is needed to extract tumour-specific events (Sebat, Lakshmi et al. 2004; Iafrate, Feuk et al. 2004).

The main mapping set used within this thesis is the 100K mapping set. Each array contains over 2.5 million features and consists of more than one million copies of 25bp probes of defined sequence arranged on a glass chip (Figure 1.17, *left*). 40 different probes per SNP are interrogated to provide perfect match and mismatch data. The mismatch probes act as internal controls detecting levels of non-specific hybridisation, hence, this error is corrected. The 100K mapping set consists of 100,000 probes. Single

stranded sample DNA molecules bind to complementary probes (hybridisation) (Figure 1.17, *right*) and data produced on scanning of the fluorescently tagged hybridised probes provides the signal intensities for each SNP. Increased copy number changes are detected by an increase in signal intensity and a loss in copy number is detected upon a decrease in signal intensity when compared to constitutional controls.

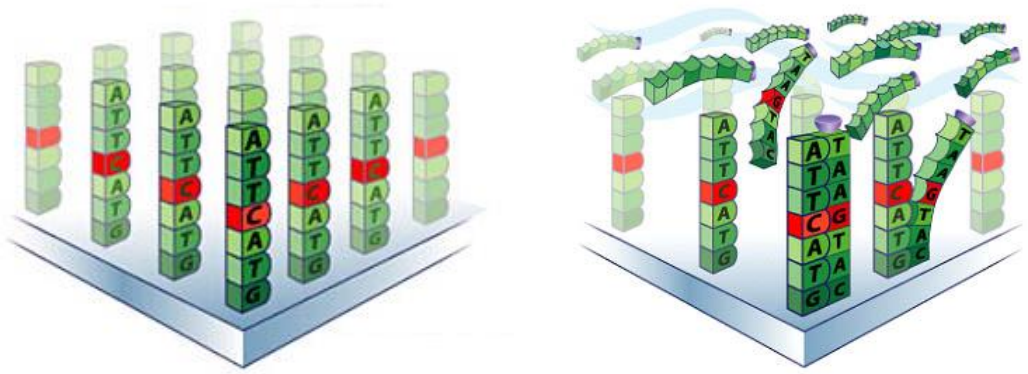

Figure 1.17 Visualisation of probes on the surface of a SNP array. *(left)* Oligonucleotide probes on the surface of the SNP array. *(right)* The sample DNA is washed over the array surface and complementary sequences anneal. www.affymetrix.com

Previously SNP arrays required the use of high quality DNA for the generation of good results with a minimum of background noise; however the newly released SNP6.0 array is capable of producing excellent results using DNA extracted from archival FFPE tissues which is usually of low quality and relatively degraded (Tuefferd, De Bondt et al. 2008). While SNP array technology has significantly increased the resolution of genome-wide analysis, its potential could be hindered by the fact that the technology brings challenges in data analysis. Software for SNP array analysis is currently in its infancy and remains under developed. It is also important to validate SNP array data to confirm reliability and rule out errors within individual arrays, assays or programs used in the analysis. SNP array data published to date, establishes the platform as accurate, reliable and informative when validated by fluorescence in situ hybridisation, real time PCR and immunohistochemical analyses (Hu, Wang et al. 2005; Kotliarov, Steed et al. 2006; Harada, Chelala et al. 2008). One flaw with the design of SNP arrays is that although the arrays provide excellent genome coverage, the vast majority of probes fall

outside gene regions due to selective pressure away from coding regions of the genome. Thus, when analysing SNP arrays it is important to analyse consecutive SNPs of gene regions and to not only consider probes located within the genes themselves, but also to consider the surrounding probes. To date, no high resolution SNP array studies have been undertaken in CNS PNET.

1.5.5 Gene mutation

The mutational status for a number of genes have been analysed in CNS PNET. Mutational screening of *PTEN* (10q23) and *p53* (17p13.1) were analysed in 12 CNS PNETs in addition to screening for LOH at 10q and 17p (Kraus, Felsberg et al. 2002). 1/12 (8%) CNS PNETs harboured a missense mutation in the *p53* gene (C413T), but showed no allelic loss of 17p. In the same case an inactivating mutation in the *PTEN* gene was identified downstream of exon 5 (IVS5 = 5delT) and interestingly this sample had LOH of 10q, therefore the tumour had lost both functional copies of *PTEN*. Also in the study, homozygous loss of *CDKN2A* was investigated; however, none of the 12 CNS PNETs harboured this alteration.

p53 mutations have been found within other CNS PNET studies. On mutational analysis, 2 siblings diagnosed with CNS PNET were found to have missense mutation of the P53 gene in codon 213 (CGA, Arg – TGG, Tyr) (Reifenberger, Janssen et al. 1998). In addition, both had LOH of 17p. In a separate study, a 12 year old female was found to have a *p53* mutation in codon 179 (CAT-ATT) (Postovsky, Ben Arush et al. 2003). In 2005, Eberhart *et al.,* demonstrated that 88% of CNS PNETs were immunopositive for the *p53* protein (Eberhart, Chaudhry et al. 2005). Mutations within *p53* are rare in CNS PNET, suggesting that the aberrant expression was due to a different mechanism other than gene mutation. One recent study used somatic cell gene transfer in mice to investigate the roles of *MYC*, *CTNNB1* and *p53* in CNS PNET formation (Momota, Shih et al. 2008). Although the use of mouse models is useful in cancer research, it is important to consider that the mouse brain is not the same as human, and this was clearly demonstrated by the existence of a large cell CNS PNET variant that developed in the mouse models; since this variant has not been identified in human CNS PNET.

Mismatch repair genes are commonly mutated and deleted in cancer and a study of 4 CNS PNET patients (from 2 consanguineous families), identified mutations of the *PMS2* gene (7p22.1) in each case (De Vos, Hayward et al. 2004). The first family harboured a mutation in exon 14 of *PMS2* (Arg 802 – STOP) whereas the second family harboured a homozygous mutation for a single deletion in exon 6 (543ΔT which caused a protein truncation (Y181 – STOP)). The link between CNS PNET and alterations in mismatch repair genes have previously been noted in patients with Turcots syndrome. Finally, other mutational studies of CNS PNETs have identified single CNS PNETs with mutations in *PTCH* (C2161T) and *CTNNB1* (G34V) (Reifenberger, Wolter et al. 1998; Koch, Waha et al. 2001). Further mutational screening of candidate genes is needed in CNS PNET to elucidate the extent of mutations and their involvements in the development of CNS PNET.

1.5.6 Loss of heterozygosity

LOH analysis has not been performed on pineoblastomas and only in relatively few CNS PNETs. Kraus *et al.,* revealed LOH of 17p not to be a feature of the 12 CNS PNETs in the study, which was in contrast to previous studies performed on medulloblastoma (Kraus, Felsberg et al. 2002). Burnett *et al.,* identified 37% of the 35 medulloblastomas studied for LOH of 17p harboured loss, whereas 8 CNS PNETs did not feature the loss of this region (Burnett, White et al. 1997). Only one additional LOH result has been published for CNS PNETs with a case report of a 5 year old male CNS PNET patient recurring with a tumour indicative of GBM at the age of 7 years. LOH analysis of the primary tumour revealed regions of LOH at 2q36 and 13q21 (Kuhn, Hanisch et al. 2007).

1.5.7 Gene expression

Genome-wide gene expression analyses have not presently been performed for pineoblastomas. Investigations into the underlying genetics of CNS PNET have identified this tumour type to encompass tumours with many different genomic imbalances and rearrangements, in addition to identifying a number of genetically balanced CNS PNETs. Evaluating whether the genetic alterations in the DNA give rise to altered levels of gene expression has currently not been studied in CNS PNET. The gene expression profiles of balanced tumours identified within the literature have not

been explored. To date, a single study has investigated the expression profiles of a small cohort of CNS PNETs. In 2002, the expression profiles of 42 patient samples, including 10 medulloblastomas, 5 ATRTs, 5 non-CNS rhabdoid tumours, 8 CNS PNETs, 10 malignant gliomas and 4 normal cerebellar samples were analysed (Pomeroy, Tamayo et al. 2002). Hierarchical clustering of samples by variation in expression led to the identification of clear tumour groups. 8/10 (80%) medulloblastomas grouped together, as did 9/10 (90%) malignant gliomas and 9/10 (90%) of the ATRT/rhabdoid tumours. Thus, the majority of tumours grouped depending on tumour classification (Figure 1.18). Moreover, the 4 normal cerebellar samples grouped separately to the tumour samples. Most strikingly, was the fact that the 8 CNS PNETs did not form a distinct cluster group, identifying the CNS PNETs to have unique and individual expression profiles, which were dissimilar to each other. This result could however be due to histological misinterpretation, highlighting the difficulties in diagnosing and differentiating between WHO grade IV brain tumours.

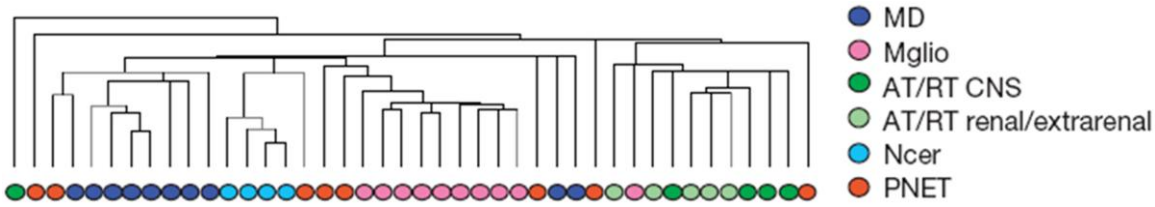

Figure 1.18 Hierarchical clustering of tumours based on expression variation. Whereas the majority of medulloblastomas, gliomas, ATRT/ rhabdoid tumours and normal cerebellar samples clustered depending on tumour type, the CNS PNETs did not form a distinct cluster group and clustered separately to one another. MD = medulloblastoma, Mglio = malignant glioma, Ncer = normal cerebullum, PNET = supratentorial PNET. Reproduced from (Pomeroy, Tamayo et al. 2002).

On comparison of gene expression profiles for each tumour type, genes with particularly high or low expression corresponding to a particular tumour type were established (Figure 1.19). The expression of granule-cell-specific transcription factors, *NSCL1* (1q23.2) and *ZIC* (3q24) were significantly higher in medulloblastoma than CNS PNET, highlighting that whereas medulloblastomas may originate from cerebellar granule cell precursors, this is not the case for CNS PNET, and provides further evidence that medulloblastoma and CNS PNETs do not share the same cell of origin. Two CNS PNETs (column 3 and 7 of the CNS PNET group) showed similar patterns of

upregulation which could indicate these 2 CNS PNETs share common underlying genetic defects which are different to the other tumours of the CNS PNET group. Although this is a limited dataset of only 8 CNS PNETs, the results show that there is a high degree of genetic heterogeneity within the group of tumours classified as CNS PNETs. Analysing the expression profiles of a larger sample set of CNS PNETs is needed to further define whether subgroups of CNS PNETs exist depending on expression signatures.

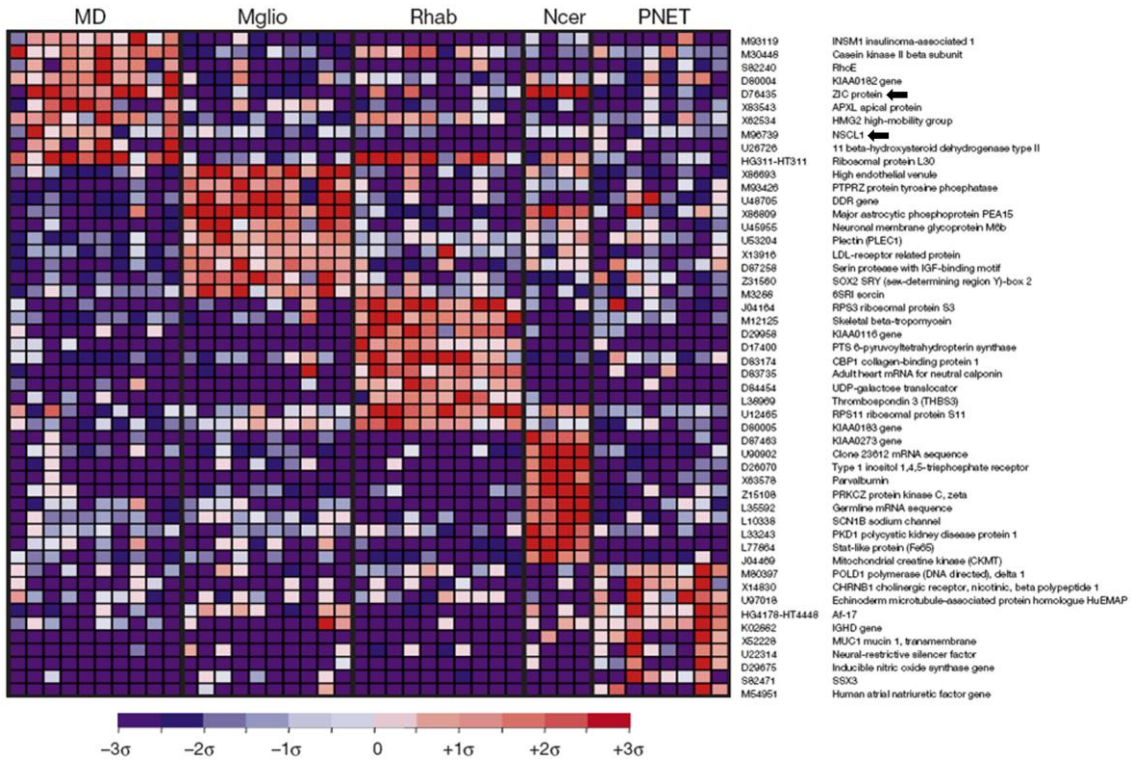

Figure 1.19 Variations in the gene expression profiles of embryonal brain tumours. The gene expression signatures shows higher expression of *ZIC* and *NSCL1* (arrowed) in medulloblastoma than in CNS PNET samples. MD = medulloblastoma, Mglio = malignant glioma, Ncer = normal cerebullum, PNET = supratentorial PNET. Reproduced from (Pomeroy, Tamayo et al. 2002).

Additional studies into individual gene expressions involved in the pathogenesis of CNS PNETs have been performed. Increased mRNA expression levels of genes involved in normal brain development have been identified in CNS PNET. In 1998, a study by Reifenberger *et al*., found 4/4 (100%) CNS PNETs with high expression of *PTCH* (9q22.3) and *SMOH* (7q31-q32), in addition to 2/4 (50%) CNS PNETs with high levels of *GLI* expression (Reifenberger, Wolter et al. 1998). In a separate study, the expression

levels of *NOTCH1* (9q34.3), Notch2 (1p13-p11) and *HES1* (3q28-q29) was analysed in 12 CNS PNETs, showing high levels of expression in the CNS PNET samples compared to medulloblastoma and normal brain samples (Fan, Mikolaenko et al. 2004). The results of these studies highlight that deregulation of normal developmental pathways (including SHH, Notch and Gli pathways) are involved in CNS PNET and further investigation into the expression profiles of a larger sample cohort are now needed to help elucidate the pathways and genes contributing to CNS PNET pathogenesis.

1.5.8 Epigenetics

Presently no methylation studies have included pineoblastomas. Methylation studies involving CNS PNETs have identified a number of genes with aberrant methylation. *RASSF1A* (3p21.3) is methylated in 80% of medulloblastomas (Harada, Toyooka et al. 2002; Lusher, Lindsey et al. 2002; Zuzak, Steinhoff et al. 2002). RASSF1A has roles in the regulation of the cell cycle and the promotion of cell death (Shivakumar, Minna et al. 2002; Rong, Jin et al. 2004; Matallanas, Romano et al. 2007). Subsequently researchers have questioned whether *RASSF1A* is methylated in the histologically similar CNS PNET. In 2006, Muhlisch *et al.*, studied the methylation status of paediatric brain tumours identifying 15/20 (75%) CNS PNETs and 4/6 (66.7%) ATRTs with a methylated *RASSF1A* promoter region, compared to 5 normal cortical controls which showed no methylation (Muhlisch, Schwering et al. 2006). In addition, a separate study found *RASSF1A* was methylated in 25/25 (100%) primary medulloblastoma, 6/9 (66.7%) CNS PNETs and 5 PNET cell lines in comparison to 7 normal brain tissue specimens which showed the *RASSF1A* gene to be unmethylated (Chang, Pang et al. 2005). Cell lines deficient in *RASSF1A* expression were subsequently treated with a demethylating agent, which restored expression, demonstrating the loss in expression was due to aberrant hypermethylation. Further studies have subsequently identified the methylation of *RASSF1A* in 19/21 (90.5%) medulloblastomas and 5/6 (83.3%) CNS PNETs, however, this study contained tumours from both paediatric and adult patients (Inda and Castresana 2007).

CASP8 (2q33-q34) is a known tumour suppressor with central roles in apoptotic pathways. Muhlisch *et al.,* identified that whereas *CASP8* was methylated in the medulloblastomas, the gene was unmethylated in the CNS PNETs and ATRTs

(Muhlisch, Schwering et al. 2006). This difference in the methylation status of *CASP8* highlights yet another distinction in the genetic/epigenetic signatures of CNS PNET and medulloblastoma. The methylation status of other tumour suppressor genes have also been investigated. The fragile histidine triad gene (*FHIT*, 3p14.2), which is lost in many cancers was found aberrantly methylated in 2/9 (22.2%) CNS PNETs. Secereted frizzled receptor protein 1 (*SFRP1*, 8p11.21), is a modulator in WNT signalling and regulates cell growth and differentiation. *SFRP1* was aberrantly methylated in 1/9 (11.1%) CNS PNETs (Chang, Pang et al. 2005). In 2006, Inda *et al.*, analysed 23 medulloblastomas and 9 CNS PNETs alongside 3 medulloblastoma and 1 CNS PNET cell line for homozygous deletion of *CDKN2A* and promoter hypermethylation of both splice variants of the expressed genes (*P16INK4A* and *P14ARF*) (Inda, Munoz et al. 2006). No homozygous deletions were identified, however *P16INK4A* methylation was observed in 1/6 (16.7%) primary CNS PNETs and 1/23 (4.3%) medulloblastomas and p14 in 3/6 (50%) and 3/23 (13%), respectively. Although not statistically significant in this small study, promoter region methylation of *P14ARF* and *P16INK4A* is higher in CNS PNET than medulloblastoma. A separate study analysed the methylation status of *P16INK4A, P14ARF, TIMP3, CDH1, P15INK4B, DAPK1* and *DUTT1* in 5 CNS PNETs (Muhlisch, Bajanowski et al. 2007). Interestingly, only *TIMP3* and *CDH1* were methylated in 1/5 (20%) and 3/5 (60%) CNS PNETs, respectively. DLC1 methylation has been investigated in 9 CNS PNETs and 2 cell lines (Pang, Chang et al. 2005), identifying 1 primary tumour with hypermethylation. Named deleted in liver cancer (*DLC1*, 8p21.3-22) (Yuan, Miller et al. 1998), cell lines deficient for this gene showed reduced growth and an induction of apoptosis upon re-expression (Ng, Liang et al. 2000; Yuan, Zhou et al. 2003; Yuan, Jefferson et al. 2004; Zhou, Thorgeirsson et al. 2004). Methylation analysis of *MCJ* (13q14.1), a methylation controlled J protein which is associated with chemoresistance in ovarian cancer, has been carried out in both CNS PNET samples and cell lines (Shridhar, Bible et al. 2001; Lindsey, Lusher et al. 2006). 3/10 primary CNS PNETs and 2/2 (100%) CNS PNET cell lines were found to be methylated. Interestingly in the CNS PNET cell line, PFSK1, *MCJ's* expression was absent in a methylation dependent manner and on treatment with 5-aza-2'-deoxycytidine, the expression of *MCJ* was restored.

Additional studies analysing the aberrant methylation profiles of CNS PNETs are needed and with the advent of genome-wide methylation profiling arrays, another level of analysis identifying alterations in the CNS PNET genome will be uncovered.

Currently, Illumina are the market leaders in the production of methylation arrays in the UK. In cancer, the hypermethylation of CpG islands in the promoter regions of tumour suppressor genes has been identified as the most common mechanism for gene inactivation (Esteller 2002; Herman and Baylin 2003). When utilised, the arrays developed by Illumina will undoubtedly generate valuable information in the identification of aberrantly methylated genes in paediatric brain tumours. The Illumina GoldenGate® platform contains probes to interrogate >1,500 CpG loci whilst the newer Illumina Infinium® platform is genome-wide and contains 27,000 probes. Interestingly, the methylation profile of the normal brain has recently been investigated. 76 brain samples (35 cerebral cortex, 34 cerebellar and 7 pons) were analysed (Ladd-Acosta, Pevsner et al. 2007). Upon unsupervised hierarchical clustering, the brain samples clustered into groups dependent on brain region signifying separate methylation profiles for each distinct region of the brain. The use of this platform on brain tumour samples would be interesting to analyse whether the methylation profiles of CNS PNETs and pineoblastomas were independent and clustered separately or if cluster groups emerged relating to other clinically relevant factors, for example by patient age.

1.6 Genetic alterations of medulloblastoma

Prior to the advances in genetic technology it was presumed all intracranial PNETs originated from a common cell of origin, independent of anatomical tumour location (Rorke 1983). This assumption was due to the similar cellular morphologies of CNS PNETs and medulloblastomas (both containing 'small round blue cells'), in addition to the poor prognosis facing patients diagnosed with a PNET. More recently it has been shown that the underlying genetic alterations in medulloblastoma are distinct to those observed in CNS PNET. A recent study analysed the genomes of 22 medulloblastomas using aCGH. The most common events identified were gains on chromosome 7 in 8/22 (36.4%), gain of chromosome 9 in 6/22 (27.3%) and gains on chromosomes 8 and 18 in 5/22 (22.7%) medulloblastomas (Lo, Rossi et al. 2007). Losses involved chromosome 11 in 8/22 (36.4%) cases and chromosome arms 8 and 10 in 7/22 (31.8%). The most frequent genetic alteration observed in medulloblastoma is the i17q found in 30-40% cases (Bigner, Mark et al. 1988; Griffin, Hawkins et al. 1988). The loss of chromosome 6 is also a common feature of medulloblastoma and has been associated with the incidence of WNT pathway activation due to mutation of β-catenin (*CTNNB1*) and/or β-catenin nuclear stabilisation (Clifford, Lusher et al. 2006; Thompson, Fuller et al. 2006).

Genetic analyses in medulloblastoma have identified *MYC* and *MYCN* amplification to be an event in 5-10% of cases and correlated with poor prognosis (Badiali, Pession et al. 1991; Eberhart, Kratz et al. 2004; Mendrzyk, Radlwimmer et al. 2005).

1.7 Direct comparisons of the genetics of CNS PNET and medulloblastoma

To date, three separate studies have directly compared the genetic profiles of CNS PNET and medulloblastoma. Firstly in 2005, Inda *et al.,* analysed a small series of 14 medulloblastomas and 6 CNS PNETs using conventional CGH (Inda, Perot et al. 2005). Although not achieving statistical significance with such a small sample set, the study showed that gain of 17q and loss of chromosome 10 were more commonly identified in medulloblastoma than CNS PNET. Also, whilst 4/14 (29%) medulloblastomas harboured isochromosome 17q; none of the CNS PNETs showed this chromosomal alteration. In comparison, the CNS PNETs contained more losses of 16p and 19p than the medulloblastomas. Interestingly, 3 regions of amplification were identified within the medulloblastomas, 2 cases contained amplification of *MYCN* (2p24.3) and a single amplification of *MYC* (8q24) was identified. Amplification of these genes have previously been associated with a poor outcome in medulloblastoma (Aldosari, Bigner et al. 2002; Michiels, Weiss et al. 2002). Additionally, 2 medulloblastomas contained amplification of the *PDGFRA/KIT* locus at 4q12. This amplification has been identified in only a minority of CNS PNETs (Inda, Perot et al. 2005; McCabe, Ichimura et al. 2006).

Secondly, in 2006, a study by McCabe *et al.,* compared the genetic profiles of 34 medulloblastomas and 7 CNS PNETs analysed by aCGH. Of the CNS PNETs in the study, 5 were primary tumour samples and 2 were recurrent samples. CNS PNET patient age ranged between 2.7-23 years. One CNS PNET showed a homozygous deletion at 9p21.3 encompassing *CDKN2A* and *CDKN2B*. 10/34 (29.4%) medulloblastomas contained an isochromosome 17q although this was not identified in any CNS PNET of the study (McCabe, Ichimura et al. 2006). On direct comparison of the medulloblastoma and CNS PNET genetics from the aCGH data 3 statistically significant differences were identified. Firstly gain of 17q was associated with medulloblastomas (20/34, 58.8%) compared to (0/7) CNS PNETs, ($p = 0.00862$).

Secondly the loss of the telomeric end of 13q was more frequently associated with CNS PNETs (4/7, 57%) compared to 1/34 (3%) medulloblastomas, ($p = 0.00162$). This genetic difference between the CNS PNETs and medulloblastomas could denote the loss of tumour suppressor genes located on 13q have an involvement in the pathogenesis of CNS PNET but not the histologically similar medulloblastoma. Finally, the CNS PNETs of the study contained significantly more amplification than the medulloblastomas (3/7, 43% and 2/34, 6%, respectively), $p = 0.02782$. Unfortunately, the article was written in such a way that individual patient clinical characteristics could not be determined. Ideally, in future studies of CNS PNET, sample cohorts should include either individual clinical information for each patient or limit the study to only include paediatric or adult cases. It should also be possible to distinguish between primary and recurrent tumours and separately report by tumour location, either CNS PNET or pineoblastoma.

Lastly in 2007, Pfister *et al.*, compared 10 CNS PNETs analysed by aCGH with a compilation of 47 medulloblastomas previously analysed on the same platform (Mendrzyk, Radlwimmer et al. 2005; Pfister, Remke et al. 2007). Three statistically significant differences between the underlying genetics of the two tumour types were identified. Loss of *CDKN2A* (9p21.3) was associated with CNS PNETs ($p<0.001$), as was gain of chromosome arm 19p ($p = 0.02$), whilst gain of 17q was more frequently observed in medulloblastoma ($p = 0.02$). Interestingly, no high level amplifications were identified in any CNS PNET of the study.

The 3 studies comparing the genetic profiles of medulloblastomas and CNS PNETs were restricted to using only CNS PNETs and not pineoblastoma. This could however have been due to the overall rarity of pineal based tumours and their successful resection. Hence, more genetic research is required on PNETs of differing locations before specific treatment strategies can be applied accordingly based on tumour biology and genetics. Although only few studies have analysed both CNS PNETs and medulloblastomas jointly, the available evidence suggests that the two tumours are genetically distinct; however, more evidence is needed to address this.

1.8 Altered pathway activity and telomere dysfunction in intracranial PNETs

The investigation of normal developmental pathways provides an invaluable background to better understand the genetic and biological dysfunctions leading to paediatric cancers (see Section 1.1.2). Probing defects within the normal developmental pathways could provide clues into how brain tumours arise and the cell/s from which they originate. At present, pathways involved in the tumourigenesis of CNS PNET are unknown. Evidence for pathways involved in the development of medulloblastoma have emerged identifying Hedgehog, Wnt and Notch pathways as having potential involvements in medulloblastoma tumourigenesis. Gene mutations of *PTCH* and *SMO* in the Hedgehog signalling pathway, *APC* and *CTNNB1* in the APC/WNT pathway and *NOTCH1* and *NOTCH2* in the NOTCH signalling pathway causing pathway deregulation have previously been identified (Pietsch, Waha et al. 1997; Raffel, Jenkins et al. 1997; Reifenberger, Wolter et al. 1998; Zurawel, Chiappa et al. 1998; Zurawel, Allen et al. 2000; Fan, Mikolaenko et al. 2004). Research into the histologically similar medulloblastoma has suggested the Shh-Gli pathway might not only be important in normal cerebellar development, but may also control the development of the cerebral cortex growth (Dahmane, Sanchez et al. 2001). This implies a potential role for deregulation of the Shh-Gli pathway in the tumourigenesis of CNS PNET.

1.8.1 The Shh-Gli pathway

Sonic hedgehog (SHH) is an important molecule involved in the formation of embryonic structures, including the brain. The Shh-Gli signalling pathway is involved in the promotion of cell cycle progression. Signalling is activated by the binding of SHH to a membrane associated protein (PTCH, patched) which contains 12 transmembrane domains (Figure 1.20). PTCH negatively regulates signalling by SMO (smoothened) in the absence of SHH ligand (Pelengaris 2007). SMO activation allows GLI (glioma-associated oncogene homologue) transcription factors to translocate to the nucleus and promote the expression of genes involved in SHH mediated proliferation. SUFU (suppressor of fused) negatively regulates GLI1 activity resulting in silencing of GLI mediated gene transcription (Pelengaris 2007). Recently, small molecule inhibitors targeting the SHH pathway have been used demonstrating the regression of

medulloblastoma in a transgenic mouse model. Romer *et al.*, questioned whether the suppression of overactive Shh signalling in medulloblastoma could cause tumour regression. The small molecular inhibitor HhAntag-691 was used to suppress SHH signalling within the brain of mice (Romer, Kimura et al. 2004). As well as a reduction in the expression of overactive genes in the Shh pathway, a decrease in proliferation was noted, in addition to an increase in apoptosis. These findings provide evidence for the important role played by the SHH pathway in the tumourigenesis of medulloblastoma and shows the potential for this molecule as a targeted therapy. Other genes involved in the SHH-GLI pathway have also been implicated in the pathogenesis of medulloblastoma. Dahmane *et al.*, identified downstream effectors of Shh signaling (Gli1-3) in the ventricular and subventricular zone of perinatal murine cerebral cortex and midbrain (Dahmane, Sanchez et al. 2001). The results suggested that the SHH-GLI pathway (in addition to its involvement in cerebellar development), could also control the development of other parts of the brain, more specifically the cerebral cortex and CNS PNET could develop from inappropriate activation or maintainence of the SHH-GLI pathway. Several small studies have shown increased expression of *PTCH* (Patched 1), *SMO*, *GLI1* and *MYCN* mRNA (MYCN is also a downstream target of SHH signaling), all indicating a likely pathogenic role in a subset of CNS PNETs (Vorechovsky, Tingby et al. 1997; Wolter, Reifenberger et al. 1997; Dahmane, Sanchez et al. 2001).

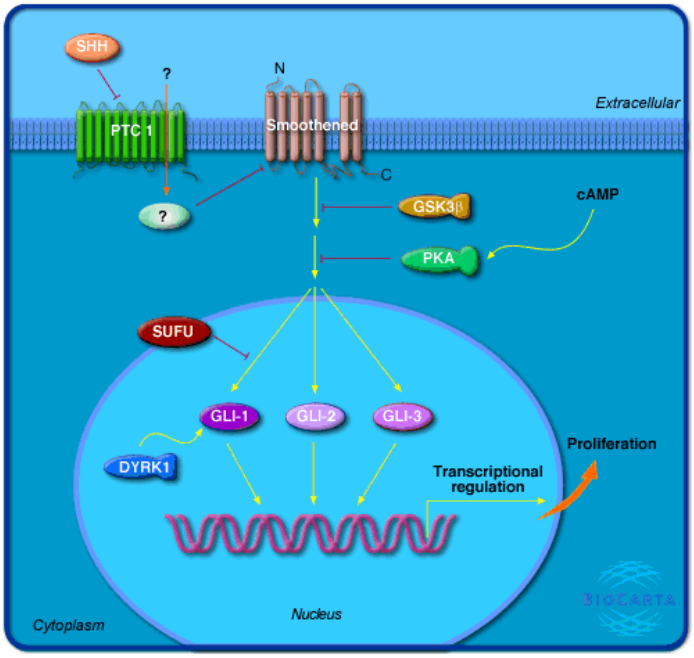

Figure 1.20 The SHH/GLI pathway. Sonic hedgehog (SHH) binds to its receptor patched1 (PTCH1) and relieves the inhibition of smoothened (SMO). SMO activates the GLI transcription factors which accumulate in the nucleus. This promotes the transcription of hedgehog target genes. Reproduced from www.biocarta.com

1.8.2 The WNT pathway

WNT signaling regulates many developmental processes including differentiation, proliferation and migration, all of which can potentially lead to cancer formation if uncontrolled. Upregulation of the WNT signaling pathway has previously been reported in medulloblastoma (Koch, Waha et al. 2001). The WNT signaling cascade blocks degradation of β-catenin (β-Cat) in the cytoplasm by binding to Frizzled (Fz, a 7 transmembrane receptor) (Figure 1.22). Frizzled promotes phosphorylation of the 'dishelved' (Dvl) protein and binding to a complex (containing β-catenin, CK1, Axin, APC and GSK-3β) takes place. β-catenin is released and translocates to the nucleus to act with TCF transcription factors to activate the transcription of WNT responsive genes, some of which are involved in tumourigenesis, such as *MYC*. Mutations in β-catenin, thus preventing degradation, have been reported to be common in up to 15% of medulloblastomas (Zurawel, Chiappa et al. 1998). Interestingly, mutations involving β-catenin have been reported in one CNS PNET study, with 1/4 (25%) CNS PNETs affected, suggesting a role not only in medulloblastoma but also the development of CNS PNET (Koch, Waha et al. 2001).

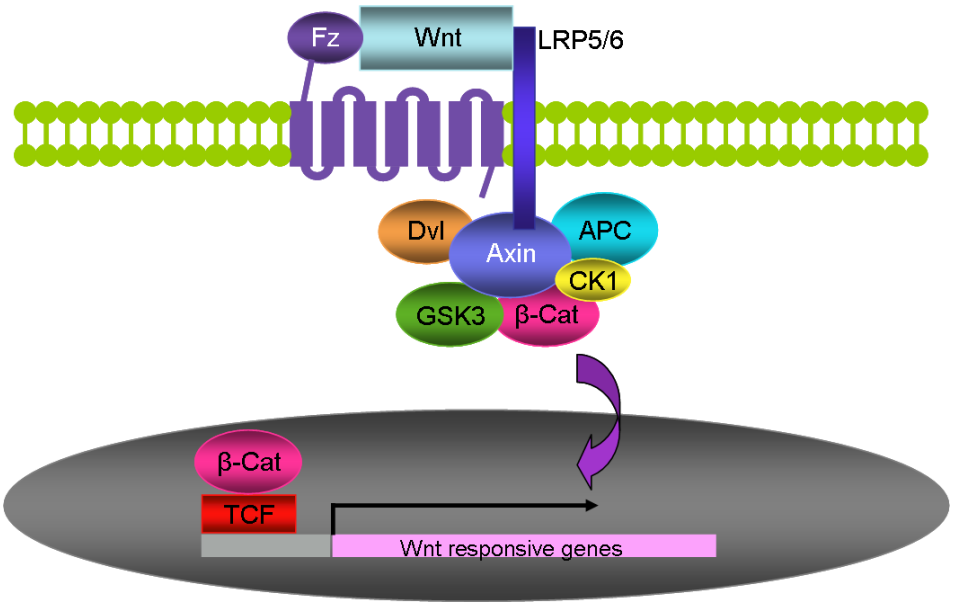

Figure 1.22 The WNT pathway. When the pathway is inactive, β-catenin is bound in the cytoplasm to a complex containing APC, Axin1 and GSK-3β, whilst in its active state, β-catenin is released from the cytoplasmic complex and translocates to the nucleus where it co-activates the transcription of target genes. Adapted from www.ped.wustl.edu.

1.8.3 The NOTCH-HES pathway

NOTCH signaling regulates both cellular proliferation and differentiation. Membrane bound ligands (JAGGED/DELTA) bind to the notch receptor of neighbouring cells causing cleavage and release of intracellular fragments of notch. These translocate to the nucleus, heterodimerise with the transcription factor CBF1 and activate genes of the HES family (reviewed in depth by Li MH *et al*), (Li, Bouffet et al. 2005). HES1 has been shown to negatively regulate HASH1, a neurogenic transcription activator (Sriuranpong, Borges et al. 2002). *HASH* and *NEUROD* are both family members of genes responsible for the regulation of neurogenesis. High expression of *HES1* in the developing brain has previously been reported and the prevention of neural differentiation by *HES1* misexpression has been observed (Ishibashi, Moriyoshi et al. 1994). In a separate study, *HASH1* expression was observed in 3/5 (60%) CNS PNETs and 0/12 (0%) medulloblastomas (Rostomily, Bermingham-McDonogh et al. 1997). These observations correspond with the largely undifferentiated, primitive cells of CNS PNET and further investigation is needed.

1.8.4 Telomeric alteration

Unlimited cell division is essential for tumour growth. Controlling this increase in cell division is an important anti-cancer mechanism. Telomeres are repetitive regions of DNA at the end of a chromosome which are enzymatically added to by DNA repeats. In humans the telomeric repeat is made up of 6 bases (TTAGGG). Telomere maintainence is observed in 90% of cancers. In non-cancerous cells, telomeres are shortened upon every cell division, however in cancer, the enzyme responsible for telomeric binding (with the catalytic subunit hTERT) is reactivated, thus cells bypass apoptosis and are immortalised. These cells may also have other hallmarks of cancer, such as fused chromosomes and chromosomal rearrangements. Amplification of *hTERT* has previously been identified in paediatric brain tumours. In one study, *hTERT* was found amplified in 4/8 (50%) CNS PNETs (Fan, Wang et al. 2003). In 2004, a study by Didiano *et al.*, investigated *hTERT* mRNA expression levels in a sample cohort containing both medulloblastomas and CNS PNETs. The primary PNET samples contained ≥5 fold upregulation of *hTERT* mRNA expression when compared to normal cerebellum (Didiano, Shalaby et al. 2004). Thus, combating the uncontrolled

lengthening of telomeres within cancer cells is one potential targeted therapy for the treatment of brain tumours and warrants further investigation.

1.9 High resolution genetic analysis of CNS PNET and pineoblastoma

1.9.1 Project objectives

Patients with CNS PNET and pineoblastoma have a very poor prognosis. Understanding the fundamental biology and genetics leading to the development and progression of CNS PNET and pineoblastoma is essential to improve existing treatment strategies and lead to the identification of novel targets for therapy. The aim of this thesis was to undertake a high resolution genetic analysis of a large cohort of CNS PNETs and pineoblastomas, link genetic alterations with clinical attributes and to provide further evidence that the genetics of CNS PNETs and medulloblastomas are distinct. The hypotheses of the study were:-

- PNETs occurring in different anatomical locations within the brain (CNS PNET vs. pineoblastoma) harbour different genetic aberrations

- CNS PNETs and pineoblastomas occurring in patients of different ages will harbour different genetic alterations due to variation in the spatial and temporal expression of genes involved in normal brain development

- The study of relapsed CNS PNETs will identify genes involved in tumour progression and biologically adverse behaviour linked to tumour recurrence

- The study of CNS PNETs and pineoblastomas with metastasis will identify genes involved in the development of metastatic disease

- CNS PNETs and medulloblastomas are distinct entities at the genetic level

- Pathways involved in the tumourigenesis of CNS PNET and pineoblastoma will be identified providing novel targets for therapy

CHAPTER 2

MATERIALS AND METHODS

2.1 Clinical samples entered into the SNP array analysis

46 tumour samples where available for analysis using the Affymetrix™ SNP arrays. 32 primary CNS PNETs, 6 recurrent CNS PNETs, 6 primary pineoblastomas and 2 recurrent pineoblastomas were analysed. Included within the primary CNS PNETs was a commercially available CNS PNET cell line, PFSK1 (CRL-2060, ATCC). 5 of the primary CNS PNETs were paired with a relapsed tumour sample, whilst for the 3 remaining recurrent samples; a primary tumour sample was unobtainable. CNS PNET and pineoblastoma samples were collected from 7 Children's Cancer and Leukaemia Group (CCLG) registered centres in the UK, in addition to the Cooperative Human Tissue Network (CHTN) in America. The 7 CCLG centres supporting the study were Birmingham's Children's Hospital, Queen's Medical Centre in Nottingham, Newcastle General Hospital, Great Ormond Street Hospital in London, Southampton General Hospital, Addenbrook's Hospital in Cambridge, and Liverpool Children's Hospital. Tumours were histologically reviewed at each centre according to the WHO criteria of the time, in addition to a central review by 2 histopathologists (Prof James Lowe and Dr Keith Robson) at the Queen's Medical Centre (Louis, Ohgaki et al. 2007).

2.2 Sample preparation – 'tumour' assessment

Consideration of viable tumour cells within the tumour samples was essential to select for tissue areas containing representative tumour cells when sampling for DNA extraction. Samples containing >10% of contaminating 'normal' brain and/or necrosis could thus be excluded. The tumour viability of frozen samples was reviewed by cutting a small Section parallel to the piece used for DNA extraction. The tissue (stored in vials at -80ºC) was cut in a recirculating laminar flow preparation station (Labcaire PCR hood 8) which had been sterilised using ethanol (Fisher Scientific, UK). Following 30 minutes of UV (to minimise contaminants), the tumour tissue was cut in a petri dish (Corning, USA) on top of a small polystyrene box filled with dry ice to keep the tissue frozen, maintaining the integrity of the tumour sample. The tissue was cut using a scalpel which had been washed in ethanol. The tissue was smeared between 2 glass slides (VWR, USA) and stained with Harris haematoxylin (Surgipath UK) and 1% (w/v) eosin (ProSciTech AU). Acetic acid alcohol (Fisher Scientific UK) fixed smeared tissue to the glass slides. Slides were stained in Harris haematoxylin for 30 seconds,

washed in water, placed in saturated lithium carbonate (Sigma UK) for 10 seconds, again washed and finally stained in 2% eosin for 20 seconds. Following a third wash in water, slides were dehydrated for 10 seconds each in 95% (v/v) ethanol, 100% (v/v) ethanol and xylene (Fisher Scientific UK). Slides were mounted using coverslips (SLS UK) and DPX mountant (Surgipath UK). Under neuropathological review, only viable tumour samples with PNET histology were included in the study (Figure 2.1).

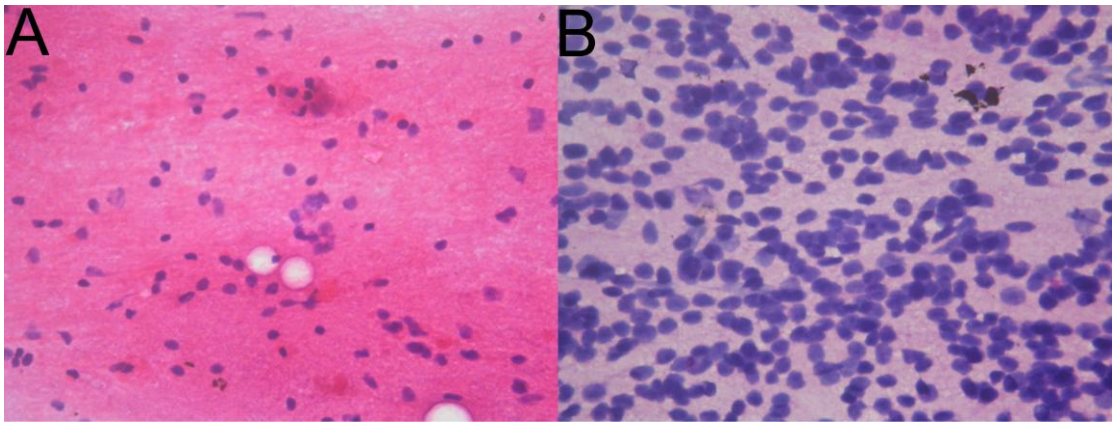

Figure 2.1 Smears of normal brain cells (A) and CNS PNET cells (B). Classic representation of CNS PNET exhibits a vast amount of small blue round cells depicting many haematoxylin stained nuclei, in a small area with scant cytoplasm. DNA was only extracted from tissue containing viable tumour cells. Magnification x40.

2.3 DNA extraction

2.3.1 DNA extraction from fresh/frozen tumour tissue

10mg of tumour tissue was homogenised in vials containing 0.5ml DNA lysis buffer (1M Tris, (Sigma, UK), 0.5M EDTA (BDH, UK), 5M NaCl (Fisher Scientific, UK), 10% (w/v) SDS (Sigma, UK) and H_2O) and 0.1ml 20mg/ml proteinase K (Sigma, UK). Vials were kept on dry ice to prevent nucleic acid degradation. After homogenisation (Powergen 125, Fisher Scientific), samples were incubated overnight at 37ºC at 10xg in a thermomixer (Eppendorf®, UK). Following incubation, phase lock gel tubes (PLG) (Eppendorf®, UK) were spun at 12,000g in a microcentrifuge (Sigma, UK) for 30 seconds. 0.7ml of sample was added directly to pre-spun PLG tubes with the addition of an equal amount of phenol/chloroform isoamyl alcohol (Sigma, UK). Contents of each tube were mixed until a transiently homogenous suspension formed.

Microcentrifugation at 16,000g for 5 minutes separated the phases. PLG forms a barrier between aqueous and organic phases and the upper phase containing the nucleic acid was subsequently transferred to a fresh 1.5ml vial (Eppendorf®, UK). DNA was precipitated by the addition of an equal volume of ice-cold isopropanol (Fisher Scientific, UK). DNA pellets were formed by microcentrifugation at 12,000g for 5 minutes. Following the removal of supernatant, pellets were twice washed in 0.5ml of 70% (v/v) ethanol and air dried for 20 minutes. DNA was subsequently resuspended with the addition of up to 0.2ml of ddH_2O. DNA quantification was performed using a spectrophotometer (Nanodrop, UK) and DNA was visualised by electrophoresis on a 1% (w/v) agarose gel to check for degradation and/or contamination. A 1% (w/v) agarose gel was made by adding 0.5g agar (Sigma, UK) to 50ml of 1x TAE buffer. For 50x TAE stock, 242g Tris (Sigma, UK) was dissolved in 500ml H_2O, 10ml 0.5M Na_2EDTA (pH8, BDH, UK) and 57.1ml glacial acetic acid (Fisher, UK) was added. The volume was adjusted to 1L with the addition of H_2O. 1x TAE buffer was made from 1ml of the 50x stock and 50ml of H_2O. After heating in a microwave (Proline, SM18, 750W) for 2 minutes on full power, the agar had dissolved. Following cooling, 0.5µl of ethidium bromide (Sigma, UK) was added and mixed. The mixture was poured into a gel mould and allowed to set. The gel was added to a gel tank (Flowgen, UK) which was filled with TAE buffer and finally, 1µl of DNA (with 4µl of gel loading solution, Sigma, UK) was added to wells adjacent to a well containing 5µl of 10kb hyperladder (Bioline, UK). The gel was electrophoresed at 120V for 20 minutes. On the spectrophotometer reading a 260nm/280nm ratio of >1.8 and a 260nm/230nm ratio of >2.0 signifies intact DNA with no contamination. DNA was then stored at -80ºC.

2.3.2 DNA extraction from blood

Blood samples were available from 10 CNS PNET patients for the 100K SNP array assay and 33 for the 500K SNP array assay, whom also had tumour tissue available for the study. Inclusion of constitutional DNA (analysed using the Affymetrix SNP array platform) highlighted tumour specific events and were used to account for normal copy number variation found within the CNS PNET study population. DNA was extracted from lymphocytes by the transfer of 1ml of anticoagulated blood to a 15ml falcon tube (Greiner, UK). 14ml of distilled water was added and the mixture incubated on ice for 5 minutes. Red cells were lysed by osmosis whilst the lymphocytes remained intact.

Tubes were spun in a microcentrifuge for 5 minutes at 660g. Supernatant was discarded leaving a pellet. The protocol continues from the addition of lysis buffer as stated in Section 2.3.1 'DNA extraction from fresh/frozen tumour tissue'**.**

2.3.3 DNA extraction from cell line pellets

PFSK1 was purchased from American Type Culture Collection (ATCC, Middlesex, UK), and grown using the manufacturer's protocol. Cells were frozen to form a DNA pellet and homogenised in DNA lysis buffer and proteinase K. Section 2.3.1 'DNA extraction from fresh/frozen tumour tissue' was subsequently followed.

2.3.4 DNA extraction - clean up and precipitation of DNA

DNA samples with phenol or ethanol contamination (low 260nm/230nm ratios) or with a lower concentration than that needed for the SNP array analysis (<50ng/ul) were precipitated (and washed). 3M sodium acetate (for 1L stock, 408.3g of sodium acetate (Sigma, UK) was added to 800ml H_2O, the pH was adjusted to 5.2 with glacial acetic acid and the volume adjusted to 1L with H_2O) was added to the DNA, (1/10 volume of DNA was needed). 2 volumes of absolute ethanol were then added to the DNA. Following incubation at -80ºC for 1 hour, DNA was centrifuged at 16,000g for 20 minutes. Removal of supernatant and addition of 70% (v/v) ethanol washed the DNA pellet. After centrifugation for 5 minutes at 16,000g and removal of supernatant, pellets were resuspended in ddH_2O.

2.4 100K and 500K Affymetrix SNP array protocol

2.4.1 100K and 500K SNP array protocol overview

The Affymetrix genechip mapping assay, in conjunction with the genechip human mapping 100K/500K set, is designed to detect > 100,000/500,000 single nucleotide polymorphisms (SNPs) in samples of genomic DNA. The mapping 100K/500K set is comprised of two arrays and two assay kits. To achieve maximum genomic coverage 2 separate assays are performed using DNA digested by either XbaI or HindIII for the 100K assay or NspI or StyI for the 500K assay. Each array and its corresponding assay

kit are processed independently from the second enzyme. The protocol starts with 250ng of genomic DNA per array and will generate SNP genotype calls for more than 50,000/250,000 SNPs for each array of the two array set (Figure 2.2). For each array type, a human reference genomic 103 positive control DNA is run in conjunction with every 10 chips processed to serve as a control for the entire process and helps in troubleshooting. The genomic 103 DNA is made from 9 independent replicates and the genotype is provided. A concordance check can be made between sample and genomic 103 DNA run on the arrays. Every array contains a number of internal controls. Certain SNP IDs within each array contain control genotype calls which are the same irrespective of the DNA being analysed on the array (sample or control). If (however) these control genotype calls are different, the array results are discarded. Arrays also contain in-built controls to cross-check for consistency. 31 SNPs on the 50K XbaI and HindIII arrays and 50 on the 250K NspI and StyI arrays serve as controls to cross-check genotypes from the same sample. This is to allow easy verification if patient samples are confused. The 5 day protocol consists of 10 main steps (Figure 2.3). Firstly DNA is digested using enzymes specifically chosen by Affymetrix to provide the maximum genome coverage for the assay. End linkers are ligated to the digested DNA which are targeted for PCR. Following PCR, fragmentation reduces the size of the PCR products, which are subsequently labeled in preparation for hybridisation onto the array. Following hybridisation, unbound DNA fragments are washed away, leaving only hybridised DNA bound to the array. Upon scanning, the raw signal intensity data generated is analysed using a number of computational programs which implement algorithms for both copy number and genotype results for each probe on the array.

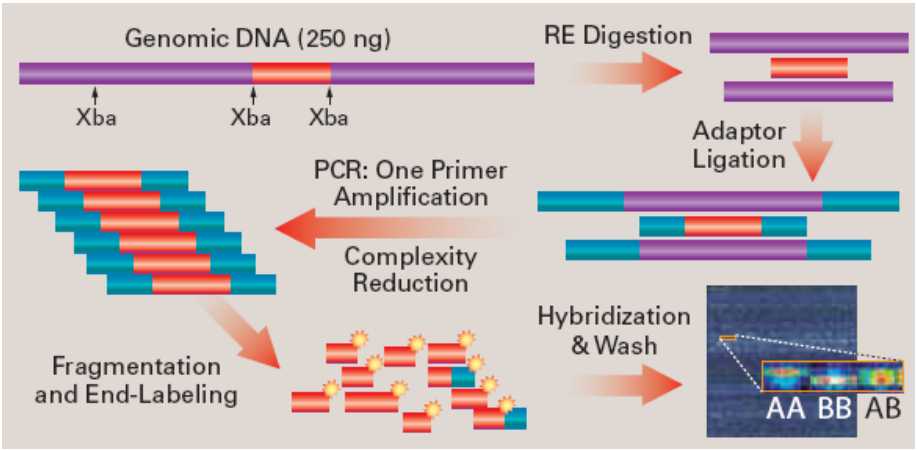

Figure 2.2 Diagramatic representation of the Affymetrix 50K XbaI SNP assay. 250ng of sample DNA is digested; end linkers are ligated onto digested DNA and subsequently amplified by PCR. Following purification of the PCR product, the sample is fragmented and labeled. The sample is hybridised overnight on the genechip, washed, stained and finally scanned. As a result data is directly stored electronically. Reproduced from 'Genechip® Human Mapping 100K Set' (Affymetrix).

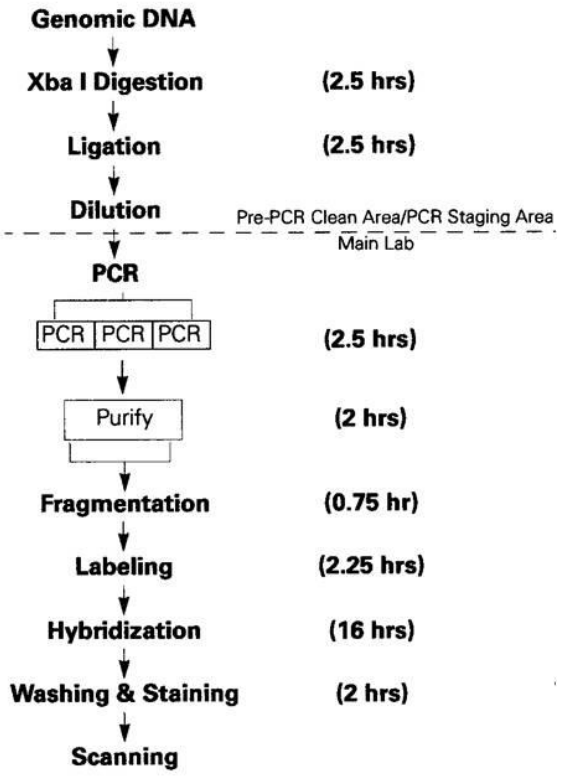

Figure 2.3 An overview of the time taken for the 10 main steps of the Affymetrix SNP array protocol. Reproduced from 'Genechip® Mapping 100K Assay Protocol' (Affymetrix).

2.4.2 Room set up

Reagents necessary for restriction digestion, ligation and PCR steps were stored in a pre-PCR room which is free of PCR products to minimize cross contamination between samples. To avoid multiple freeze-thaws, aliquots of each reagent (apart from enzymes) were prepared and stored at -20ºC. Arrays from different enzyme fractions were not processed on the same day to avoid contamination and error.

NB Unless otherwise stated, all reagents within the tables of section 2.4 were manufactured by Affymetrix™ UK.

2.4.3 DNA digestion

Digestion mastermix (Table 2.1a or 2.1b) was prepared which included the preparation of a 10% excess. A negative control reaction (water replacing DNA) was also set up

alongside samples to check for contaminants present which could give a false positive results. All mastermixes and PCR reactions were prepared in a recirculating laminar flow preparation station (Labcaire PCR hood 8) which had been sterilised using ethanol and had been irradiated with UV for 30 minutes.

Table 2.1a 100K digestion mastermix

Reagent stock	**1 sample (µl)**
H_2O	10.5
10X NE buffer 2 (New england biolabs-NEB, UK)	2
BSA (10X (1mg/ml, NEB, UK)	2
XbaI OR HindIII (20U/µl, NEB, UK)	0.5

Table 2.1b 500K digestion mastermix

Reagent stock	**1 sample (µl)**
H_2O	11.55
NE buffer 2 (10X)	2
BSA (100X (10mg/ml)	0.2
NspI OR StyI (10U/ul, NEB, UK)	1

Two different enzymes were used for each assay. Cutting the genome at different regions produced an increased SNP coverage (Figures 2.4a and 2.4b). XbaI/HindIII and NspI/StyI were chosen by Affymetrix to be used in the 100K/500K mapping assays after in silico digests with a number of restriction enzymes. Results found that these enzymes cut DNA frequently and produced fragment sizes containing SNPs that were readily amplifiable.

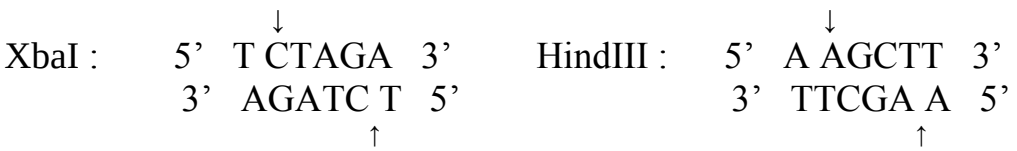

Figure 2.4a XbaI and HindIII recognition sites for digestion

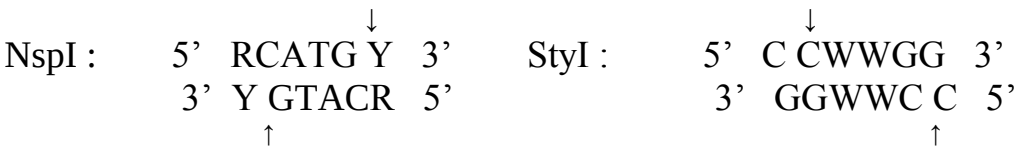

Figure 2.4b NspI and StyI recognition sites for digestion. Where R = A or G, Y = C or T and W = A or T.

In the PCR staging area (separate to the pre-PCR area) 5µl of 50ng/µl genomic DNA (250ng) was added to 200µl thin walled PCR tubes (MJ Research USA). The total amount of genomic DNA was 250ng for each restriction enzyme. For the 100K assay, 15µl of digestion mastermix was added to each tube containing genomic DNA whereas in the 500K assay 14.75µl was added. Following vortexing (Fisherbrand UK) and centrifugation at 290g for 1 minute, the tubes were placed in a thermal cycler (DNA Engine Tetrad, MJ Research USA). Samples were incubated at 37°C for 2 hours, (the optimal temperate for all 4 restriction enzymes to work). Inactivation of the enzymes of the 100K assay was performed by incubation at 70°C for 20 minutes and the 500K assay, 65°C for 20 minutes. Samples were kept at 4°C until ready for use or stored at -20°C if not being used immediately.

2.4.4 DNA ligation

The digested genomic DNA was ligated to adaptors that recognize the cohesive 4 base pair overhangs. All fragments resulting from the restriction enzyme digestion, regardless of size, were substrates for adaptor ligation. Depending on the restriction enzyme used, the following ligation mastermix was prepared (Tables 2.2a and 2.2b).

Table 2.2a 100K ligation mastermix

Reagent	**1 sample (µl)**
Adaptor XbaI or HindIII	1.25
T4 DNA ligase buffer (10X, NEB,UK)	2.5
T4 DNA ligase (NEB,UK)	0.625
H_2O	0.625
Total	5

Table 2.2b 500K ligation mastermix

Reagent	**1 sample (µl)**
Adaptor NspI or StyI (50µM)	0.75
T4 DNA ligase buffer (10X)	2.5
T4 DNA ligase (40U/µl)	2
Total	5.25

In the PCR staging area, ligation mastermix was added to each digested DNA sample (5µl for the 100K assay and 5.25µl for the 500K assay). After vortexing at medium speed for 2 seconds and centrifugation at 290g for 1 minute, tubes were run on the thermal cycler. For the 100K assay tubes were run for 2 hours at 16°C, whilst for the 500K assay, tubes were run for 3 hours at 16°C, (the optimal temperate for T4 DNA Ligase to ligate). Following this an inactivation step at 70°C for 20 minutes was performed and tubes were held at 4°C. Each sample of DNA ligate was diluted with water prior to polymerase chain reaction (PCR) by adding 75µl of molecular biology grade water (Cambrex UK), making the total volume 100µl. Samples were stored at -20°C if not proceeding to the next step within 60 minutes.

2.4.5 Polymerase chain reaction

Polymerase chain reaction (PCR) was used to amplify the ligated DNA. This step also reduces the complexity of the DNA resulting in only 200-2000bp length chains of DNA for the 100K assay and 250-1100bp for the 500K assay being taken on to the next step. Although this is a whole genome array, there are limitations in the coverage of the genome. PCR mastermix was prepared on ice (Tables 2.3a and 2.3b). 3 x PCR reactions, each containing 10µl ligated DNA, produced sufficient product for hybridisation to one array.

Table 2.3a 100K PCR mastermix

Stock reagent	**3 PCR (µl)**
H_2O	132
Pfx amplification buffer (10X, Invitrogen, UK)	30
PCR enhancer (10X, Invirtogen, UK)	30
MgSO4 (50mM, Invitrogen, UK)	6
dNTP (2.5mM each, Fisher, UK)	36
PCR primer (10µM)	30
Pfx polymerase (2.5 U/µl, Invitrogen. UK)	6
Total	270

Table 2.3b 500K PCR mastermix

Stock reagent	**3 PCR (µl)**
H^2O	118.5
TITANIUM *Taq* PCR buffer (10X, Clontech, USA)	30
GC - Melt (5M, Clontech, USA)	60
dNTP (2.5µM each)	42
PCR primer 002 (100µM)	13.5
TITANIUM Taq DNA polymerase (50X, Clontech, USA)	6
Total	270

In a recirculating laminar flow preparation station (Labcaire PCR hood 8), 10µl of each diluted ligated DNA was transferred into the corresponding 3 PCR tubes. 90µl of PCR mastermix was added to each tube. After vortexing at high speed for 3 seconds and centrifugation at 290g for 1 minute the samples were transferred to the thermal cycler (DNA Engine Tetrad, MJ Research USA). Samples were denatured at 94°C for 3 minutes. For the 100K assay, 30 cycles of denaturation at 94°C for 15 seconds, primer annealing at 60°C for 30 seconds and primer extension at 68°C for 60 seconds was performed. For the 500K assay, 30 cycles of denaturation at 94°C for 30 seconds, primer annealing at 60°C for 30 seconds and extension at 68°C for 15 seconds was performed. Both assays had a final primer extension at 68°C for 7 minutes and samples were subsequently held at 4°C. To avoid cross-contamination of PCR products, the digestion and ligation step was performed in one block of the tetrad, and the PCR step performed in a separate block. For quality control 3µl of each PCR product, mixed with 3µl of 2 X gel loading dye (G2526, Sigma UK), were electrophoresed on a 2% (w/v) agarose gel (BMA USA) at 120V for 1 hour (Figure 2.5). The PCR products were stored at -20°C if not proceeding onto the next step within 1 hour. For fragmentation, 40µg of PCR product was needed for the 100K assay and 90 µg for the 500K assay. If the yield was lower than this, further PCR product was amplified. 2 negative controls were included. The first negative control (Figure 2.5, lane 14) had water and not DNA added at the DNA digestion, ligation and PCR steps, and the second negative control (Figure 2.5, lane 15) was an internal negative control to determine the presence of contamination during the PCR set up.

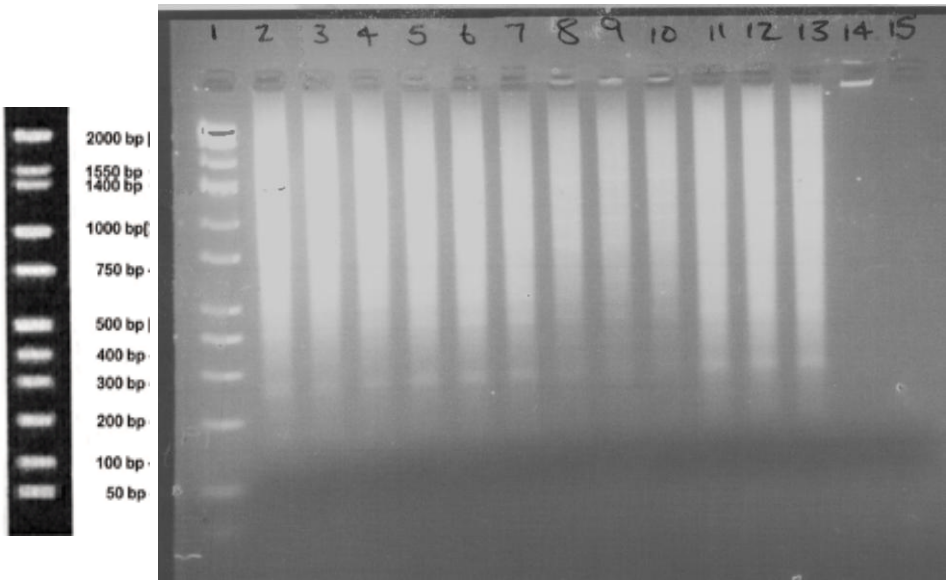

Figure 2.5 PCR products from the 100K SNP array assay analysed on a 2% (w/v) agarose gel electrophoresed for 20 minutes at 120V. The average size of PCR product should be between 250 – 2000bp. Lane 1 = hyperladder (Bionexus), lanes 2-4 = sample 1, lanes 5-7 = sample 2, lanes 8-10 = sample 3, lanes 11-13 = sample 4, lane 14 = process negative which should give a band at the well due to ligation artefacts and lane 15 = PCR negative (PCR mastermix + water) which shows no contamination. If the gel was satisfactory, purification was performed. For the 500K assay products should be between 250-1100bp.

2.4.6 PCR purification and elution

Following PCR, a washing and vacuum drying step was used to purify PCR products. A vacuum manifold (Qiagen UK) was set at 800mbar for the 100K assay and 600mbar for the 500K assay. The PCR purification plate (Qiagen UK) was placed on top of the manifold and wells not being used were covered with a foil lid (Beckmann UK). The 3 or more PCR reactions were consolidated for each sample into one well of the MinElute plate (Qiagen UK). The vacuum was maintained until wells were completely dry. Washing of PCR products was performed by adding 50µl of molecular biology grade water followed by drying of the wells. This was repeated 2 additional times. Once dried, the vacuum was switched off. Following removal from the vacuum manifold, 40µl of elution buffer ((EB), Qiagen UK)) was added to each well for the 100K assay and 45µl for the 500K assay. The wells were covered by PCR plate cover film (Beckmann UK) and the plate moderately shaken on a plate shaker (Boekel scientific USA) for 5 minutes at room temperature. Purified PCR products were recovered by pipetting the eluate from each well.

2.4.7 Quantification of purified PCR product

Quantification of purified PCR product was performed on a nanodrop spectrophotometer (Thermo Scientific UK) using 1.5µl of each sample. Purified PCR products needed to be at least 900ng/µl for fragmentation for the 100K assay and 2000ng/µl for the 500K assay. If not achieved, PCR amplification was repeated with ligated DNA. Conversely, if the PCR product concentration was higher than needed, it was adjusted by the addition of EB.

2.4.8 Fragmentation and end labeling

Upon successful quantification of the purified PCR products, 5µl of 10X fragmentation buffer (Affymetrix, Santa Clara, CA) was added to each sample and vortexed at 5970g for 2 seconds in thin walled tubes. 5µl of diluted fragmentation reagent (Affymetrix, Santa Clara, CA), (0.04U/µl for the 100K assay and 0.05U/µl for the 500K assay), was added to the fragmentation mix and thoroughly mixed. Tubes were tightly sealed; vortexed for 2 seconds and spun at a medium speed for 1 minute at room temperature for the 100K assay and at 4°C at 5970g for 30 seconds for the 500K assay. Tubes were placed in a heat block (Grant UK) preheated to 37°C. A separate pre-heated heat block was set at 95°C (Grant UK). The samples were heated to 37°C for 35 minutes (the optimal temperature for the fragmentation reagent to work). Following this the samples were heated to 95°C for 15 minutes to inactivate the enzyme and subsequently held at 4°C. Fragmented PCR products were electrophoresed on a 4% (w/v) agarose gel (BMA USA) at 120V for 1 hour, to assess successful fragmentation (~180bp products) (Figure 2.6).

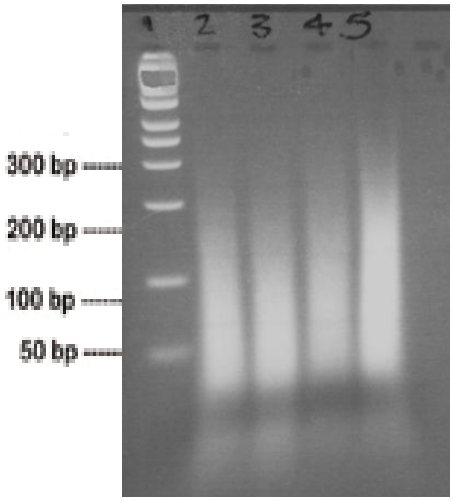

Figure 2.6 A 4% (w/v) agarose gel of successfully fragmented PCR products. Lane 1 = hyperladder (G2526, Sigma, UK), Lane 2-5 = patient samples. Average fragmented DNA length = ~180bp. 4 µl of product and 4 µl of gel loading dye was added to each well.

Labeling mastermix was prepared on ice and vortexed at medium speed for 2 seconds (Table 2.4). Efficient end labeling required aliquoting 19.5µl of mastermix into the tubes containing fragmented DNA. After vortexing for 2 seconds and spinning for 1 minute at 290g, samples were heated (in heat blocks), firstly for 2 hours at 37°C for the 100K assay and 4 hours for the 500K assay (for the labelling reagent to work optimally) and secondly for 15 minutes at 95°C to inactivate the reagent. Samples were held at 4°C. If not proceeding to the next step samples were stored at -20°C.

Table 2.4 Labelling mastermix

Reagent	**1X (µl)**	**Final conc. in sample**
5X TdT buffer	14	1X
Genechip DNA labeling reagent (7.5mM for 100K and 30mM for 500K)	2	0.214mM
TdT (30U/µl)	3.5	1.5U/µl
Total	19.5	

2.4.9 Hybridisation

190µl of hybridisation cocktail was added to 70µl of labeled DNA (Table 2.5).

Table 2.5 Hybridisation mastermix

Reagent	**1 X (µl)**	**Final conc. in sample**
MES (12X; 1.22M, Sigma, UK)	12	0.056M
DMSO (100%, (v/v), Sigma, UK)	13	5.00%
Denhardt's soultion (50X, Sigma, UK)	13	2.50X
EDTA (0.5M, Ambion, UK)	3	5.77mM
HSDNA (10mg/ml, Promega, UK)	3	0.115mg/ml
OCR, 0100	2	1X
Human Cot1 (1mg/ml, Invitrogen, UK)	3	11.5µg/ml
Tween20 (3% (v/v), Pierce, UK)	1	0.0115%2.69M
TMACL (5M, Sigma, UK)	140	2.69M
Total	190	

Samples were heated to 95°C for 10 minutes to denature the hybridisation mix. Following cooling for 10 seconds on ice, samples were briefly spun in a microcentrifuge at 290g for 1 minute. After heating (in a heat block) to 48°C for the 100K assay and 49°C for the 500K assay (optimal hybridisation temperature), 200µl of the denatured hybridisation mix was directly pipetted into the appropriate array (XbaI or HindIII for the 100K assay and either StyI or NspI for the 500K assay). Arrays had been previously stored at room temperature to equilibrate, to prevent leakage from chips and septa cracking. Samples were washed over the array at 0.32g for 16 hours in the hybridiser (Affymetrix Hybridisation Oven 450) at the optimal hybridization temperature of 48ºC. Following 16 hours of hybridisation the arrays were removed from the hybridisation station. All hybridisation cocktail was removed from the probe array and stored in vials at -80°C. The array was finally filled completely with 250µl array holding buffer for the 100K assay and 27µl for the 500K assay (for 100µl mix 8.3ml of 12X MES Stock buffer, 18.5ml of 5M NaCl, 0.1ml of 10% (v/v) tween-20 and 73.1ml of water, wrapped in foil to shield from the light).

2.4.10 Array washing and staining

Before the washing and staining of each array in the fluidics station, samples were registered on a computer connected to the fluidics station and scanner (Genechip scanner 3000) using GCOS (GeneChip Operating Software, Affymetrix). Library files (containing probe information) for the mapping 50K HindIII/XbaI and 250K NspI/StyI arrays were uploaded into GCOS from the Affymetrix website (www.affymetrix.com). Following this, the fluidics station was primed to ensure no air bubbles in the tubes which could hinder array scanning. Tubes from the fluidics station were directed into the appropriate bottles (tube 1 in non-stringent wash buffer A, tube 2 in stringent wash buffer B and tube 3 in distilled sterile water), (Figure 2.8). For 1000ml of wash A, 300ml of 20X SSPE (Cambrex UK) was added to 1ml of 10% (v/v) tween-20 (Pierce chemical, UK), 699ml of water and filtered through a 0.2µm filter (Millipore UK). For 1000ml of wash B, 30ml of 20X SSPE was added to 1ml of 10% (v/v) tween-20, 969ml of water and filtered through a 0.2µm filter, with a final pH of 8. After priming, arrays were loaded into the appropriate cartridge and sample information was entered into the GCOS software. For the array wash and stain, the following reagents were prepared (Tables 2.6-2.8).

Table 2.6 Stain buffer

Components	**1X (µl) 100K**	**1X (µl) 500K**	**Final conc.**
H_2O	666.7	800.04	
SSPE (20X)	333	360	6X
Tween-20 (3%, v/v)	3.3	3.96	0.01%
Denhardt's (50X)	20	24	1X
Subtotal	990	1188	
Subtotal/2	495	594	

Table 2.7 SAPE solution mix

Components	**Volume (µl) 100K**	**Volume (µl) 500K**	**Final conc.**
Stain buffer	495	594	1X
1mg/ml streptavidin phycoerythin (SAPE, Molecular probes, USA)	5	6	10µg/ml
Total	500	600	

Table 2.8 Antibody stain solution

Components	**Volume (µl) 100K**	**Volume (µl) 500K**	**Final conc.**
Stain buffer	495	594	1X
0.5mg/ml biotinyated antibody, Vector Labs, UK)	5	6	5µg/ml
Total	500	600	

The reagents were added to the fluidics station into each array position. Vials containing SAPE (streptavidin phycoerythin) stain solution (placed in vial position 1), vials containing antibody stain solution (in vial position 2) and vials containing array holding buffer (in vial position 3, 800µl for 100K assay and 820µl for 500K assay) were added, (Figure 2.7).

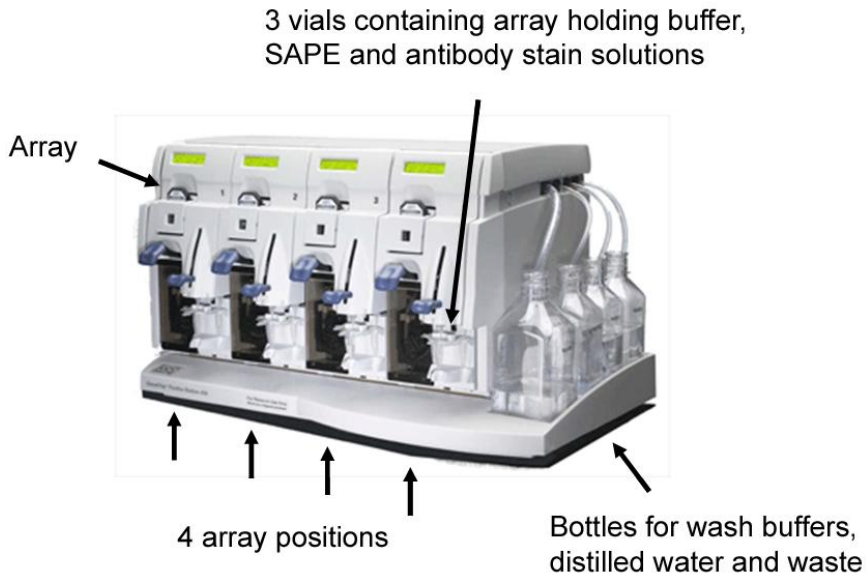

Figure 2.7 Fluidics station set up (www.affymetrix.com).

The fluidics station was run using the GCOS software. The Affymetrix mapping100Kv1_450 or the mapping500Kv1_450 protocol was selected, which directed the wash and stain protocol (Table 2.9a and 2.9b).

Table 2.9a Wash and stain protocol for the Affymetrix fluidics station 450 for the 100K assay

Post hyb wash #1	6 cycles of 5 mixes/cycle with wash buffer A (stringent) at 25°C
Post hyb wash #2	6 cycles of 5 mixes/cycle with wash buffer B (non stringent) at 45°C
Stain	Stain the probe array for 10 minutes in SAPE solution at 25°C
Post stain wash	6 cycles of 5 mixes/cycle with wash buffer A at 25°C
2nd stain	Stain the probe array for 10 minutes in antibody solution at 25°C
3rd stain	Stain the probe array for 10 minutes in SAPE solution at 25°C
Final wash	10 cycles of 6 mixes/cycles with wash buffer A at 30°C. The final holding temperature is 25°C
Filling array	Fill the array with array holding buffer

Table 2.9b Wash and stain protocol for the Affymetrix fluidics station 450 for the 500K assay

Post hyb wash #1	6 cycles of 5 mixes/cycle with wash buffer A (stringent) at 25°C
Post hyb wash #2	24 cycles of 5 mixes/cycle with wash buffer B (non stringent) at 45°C
Stain	Stain the probe array for 10 minutes in SAPE solution at 25°C
Post stain wash	6 cycles of 5 mixes/cycle with wash buffer A at 25°C
2nd stain	Stain the probe array for 10 minutes in antibody solution at 25°C
3rd stain	Stain the probe array for 10 minutes in SAPE solution at 25°C
Final wash	10 cycles of 6 mixes/cycles with wash buffer A at 30°C. The final holding temperature is 25°C
Filling array	Fill the array with array holding buffer

Once complete the probe arrays were ejected and checked for large air bubbles. If present, array holding buffer was manually pipetted into arrays. The arrays were stored at 4°C in the dark if not immediately scanned. Scans were performed within 24 hours. A weekly bleach protocol of the fluidics station decreased the risk of contamination (Affymetrix 100K mapping assay manual).

2.4.11 Scanning and interpretation of results

The Affymetrix genechip scanner 3000 was controlled by the GCOS software with patch 5. Arrays were automatically scanned upon loading into the scanner. On

completion, a DAT file displayed the fluoresent intensity of probes on the arrays. Inspection of the DAT file is an important quality control measure (Figure 2.9). Hybridisation of the B2 oligo, a component of the Oligonucleotide Control Reagent (spiked into each hybridisation cocktail) is highlighted in the top right corner and middle of each array. Additionally, arrays with artifacts present need to be omitted at this stage.

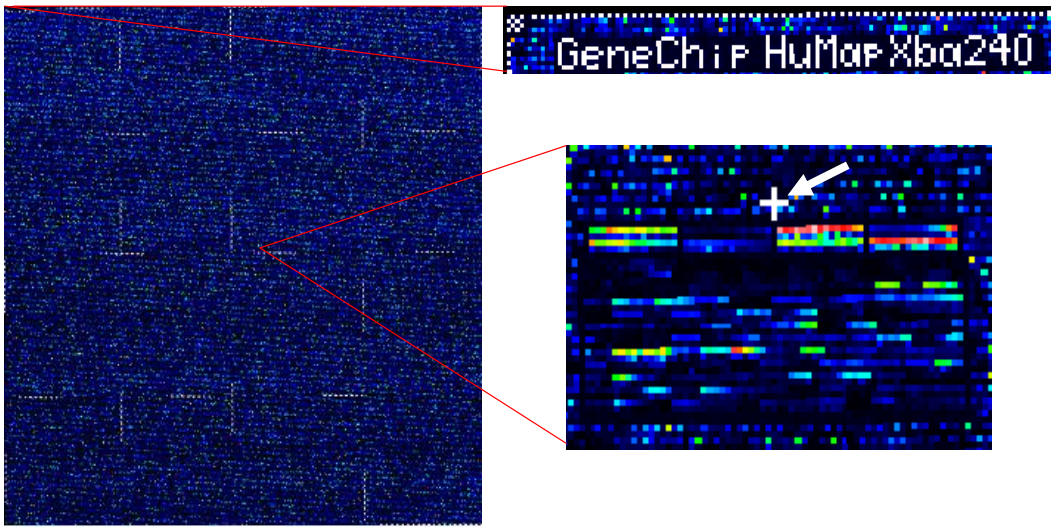

Figure 2.9 DAT. file with quality control measures. The top right hand corner of each image displays an internal control fluoresing the type of array used. Alignment of probes was checked using a grid and successful arrays displayed an internal control cross in the middle (arrow).

2.4.12 SNP array analysis – GTYPE

Following scanning, each probe on the array was given a fluorescent signal value. CEL and CHP files were generated in GTYPE (GeneChip Genotyping Analysis Software) to evaluate the SNP call rate and genotype calls for each array (Figure 2.9). CEL files are in a binary form and are only readable by Affymetrix softwares. CEL files store the results of the intensity calculations of the pixel values of the DAT file. CHP files contain the results of the experiment, including the average signal measures for each probe set and information for which probes are called as present, absent or marginal and the p values for these calls. The SNP call rate is defined as the percentage of SNPs with a reliable genotype call compared to the total number of SNPs on the array. SNP call rates of 93% or above were deemed successful, however with the mass of abnormalities in tumour DNA, lower rates were also excepted. If too low (<85%), the array was not

included in the study due to the unreliability of results. To generate a report for each sample, batch analysis (comparing the results of each tumour to the normal constitutional sample/s) was performed in GTYPE. There are 31 quality control SNPs on the 50K arrays and 50 QC SNPs on the 250K arrays to help identify sample mismatch.

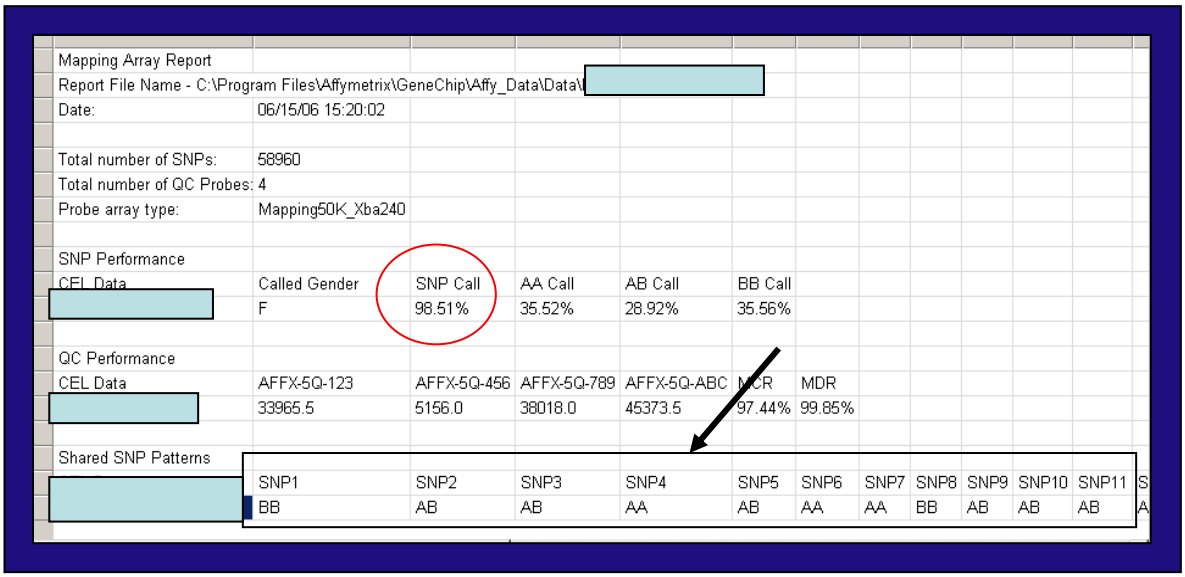

Figure 2.9 GTYPE batch analysis. Results of a CNS PNET sample highlighting the SNP call rate (red circle) and genotype calls for each of the QC SNPs (arrow).

2.4.13 SNP array analysis - CNAG

CEL and CHP files were imported into CNAG (Copy Number Analyser for Genechip) where data was extracted (Nannya, Sanada et al. 2005). An overview of the SNP array data analysis is shown in Figure 2.10. The CNAG program is used to normalise tumour data against reference data, to transform fluoresent signal intensities to copy numbers using the hidden markov model and to visualise normalised tumour data in a chromosome ideogram. Firstly individual CHP files generated from CNS PNET samples which had matching paired constitutional (blood) CHP files were analysed in a 'paired' test, whilst CNS PNET samples without matching paired CHP files were analysed in an 'unpaired' test using the data from all 10 constitutional CHP files (for the 100K analysis) or 33 constitutional CHP files (for the 500K analysis), many of which were available from a separate study within the Children's Brain Tumour Research Centre. This was performed in the 'extract data' function in CNAG which analyses the

CHP data generating CFH files which were deposited into the 'array data' folder. Secondly using the 'sample manager' function, results were generated from the CFH files using either allele specific or non-allele specific reference files. CFS files were generated for paired self referenced data and CFN files were generated for non-self referenced data. Data was stored in the 'results files' folder. Thirdly using the 'display samples' function within CNAG, data from the 2 arrays of a mapping set were combined, each sample was visualised, a txt file for each sample was generated and stored in the 'array output' folder. CNAG implements the use of the hidden markov model whereby the fluorescent signal values are normalised against references and given a copy number in the range of 0 to 6, with a copy number of 2 demonstrating a normal allele copy number.

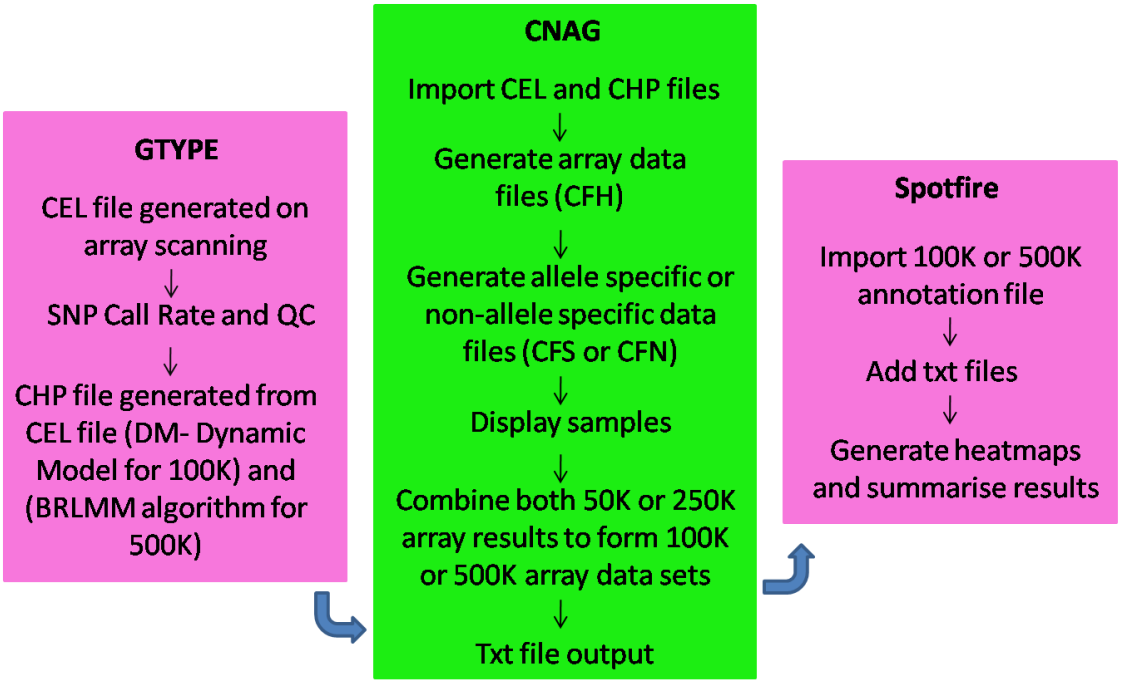

Figure 2.10 SNP array analysis overview using GTYPE, CNAG and Spotfire® programs.

2.4.14 SNP array analysis – Spotfire®

46 CNS PNET txt files generated in CNAG were imported into the data handling program, Spotfire® Decision Site, with the addition of either the 100K or 500K annotation files (Appendix). The Spotfire program is used to visualise large datasets and summarise results to identify both chromosome arm and gene copy number alterations,

in addition to LOH and aUPD. Files were annotated with information for each probe on the array including information on probe set ID, probe number in genomic order, physical position on each chromosome, actual physical position within the genome, location to the nearest gene, gene name, gene role, locus and normal copy number variation. Txt files were shown as a Table in Spotfire® in which the probe copy numbers of all or clinically relevant groups could be added together for each of the 100,000 or 500,000 data points. Visual respresentations of 100K and 500K SNP array data were generated in Spotfire® separately and joined together a chromosome at a time in adobe photoshop. Chromosomal arm aberrations were clearly identified in the heatmaps, however, for an unbiased approach, the data was also analysed using excel 2007 (Microsoft) where the sum of probes with aberrant copy numbers along each chromosomal arm were identified. For a chromosome arm to be aberrant, at least 80% of the probes on the arm had a loss or gain in copy number. If the arm contained 80% probes with a copy number of either 0 or 1, this constituted a loss (homozygous and ehmizygous, respectively), whereas copy numbers of 3-6 signified a gain. 5 consectutive probes with a copy number of 0 were candidate regions of homozygous deletion, whilst 5 consectutive probes with a copy number of 6 were candidate regions of amplification. The X chromosome was not analysed due to the use of both genders within the reference sets. Chromosome arm 21p was discounted due to the small number of probes characterising the arm. Unsupervised hierarchical clustering was performed in Spotfire® for the copy numbers of ~800 cytobands in 25 primary CNS PNETs and pineoblastomas. The cytobands of each chromosome have previously been identified by Geisma staining (Shaffer, Slovak et al 2009) and a ‘cytoband’ column was produced in Spotfire by concatenating the ‘chromosome’ and ‘locus’ columns within the Affymetrix SNP array annotation files. The average copy number of probes in each cytoband was calculated in Excel 2007 (Microsoft) and these values were used in the clustering analysis performed in Spotfire®. Both UPGMA (unweighted average) and euclidean distance settings were applied. Hierarchical clustering of the aberrant cytoband copy numbers in the CNS PNETs was used to identify which tumours contained common genetic alterations. A second method of clustering was used to verify the tumour groups identified from the unsupervised hierarchical clustering. Principle component analysis was performed for the cytoband imbalance detected in 25 primary CNS PNETs and pineoblastoma (as identified in the 100K SNP array analyses). A 3D plot was generated in Spotfire® using 3 principle components. Gene lists were generated in Excel 2007 (Microsoft) for the most commonly gained and lost probes

within all 46 CNS PNETs as a whole and also in clinically relevant groups. Annotated SNP copy number data was ordered by frequencies of loss and gain for each SNP probe within the tumours identifying genes with the most frequently aberrant copy numbers. To identify true results, at least 5 consecutive SNP probes needed to be aberrant for the gene to be included in the gene list. To identify regions of maintained and acquired copy number imbalance in 5 primary and recurrent CNS PNET pairs, a Spotfire® heatmap of each pair was generated. In addition, gene lists of the most common regions of maintained and acquired copy number alteration in all 5 primary and recurrent CNS PNET pairs were generated using Excel 2007 (Microsoft). SNP copy number data was ordered by frequencies of maintained or acquired, loss or gain for each SNP probe and at least 5 consecutive SNP probes needed to be aberrant for the gene to be included in the gene list.

2.4.15 SNPview

The SNPview program was made by Dr Alain Pitiot and Francois Morvillier at the Brain and Body Centre, University of Nottingham, UK in collaboration with the Children's Brain Tumour Research Centre. To visualize both the 100K and 500K SNP array data together as one SNPview chromosome ideogram, separate ideograms were firstly made for the 100K and 500K datasets and the visualisations were joined in adobe photoshop. For the analysis of 5 primary and recurrent CNS PNET pairs analysed using the 100K SNP array platform, chromosome ideograms were made in SNPview. Initially in Excel 2007 (Microsoft) the probe copy numbers of each primary and recurrent CNS PNET pair were used to generate the values of new columns which demonstrated whether candidate regions of maintained and acquired, gain or loss was present for each probe. The new columns generated were imported into SNPview as .txt files and the annotated data visualised as chromosome ideograms.

2.4.16 aUPD analysis

In addition to the generation of a SNP copy number, the SNP array data also includes a genotype for each SNP probe. In the CNAG data analysis, the comparison of a tumours' genotype with its paired blood genotype can be used to identify regions of LOH in the tumours' genome. Moreover, the combination of probe copy number and LOH results can be used to identify regions of copy number neutral LOH (aUPD). Columns of

genotyping data produced from the CNAG output included the genotype of the paired reference (blood) and the genotype of the test (tumour). In CNAG, a number of states can be observed, 0 = No call, 1 = AA (homozygous), 2 = AB (heterozygous) and 3 = BB (homozygous). To identify aUPD in tumour samples, the CNAG output file was opened in Excel (Microsoft), where values of 3 in the test and reference columns were converted to 1 and values of 2 were converted to 0. An LOH column was therefore produced using the formula:-

=IF(test>blood,"1","0")

3 possible combinations were present;-

Tumour (Test)	Blood (Reference)	Formula results
1	1	= 0 (no LOH)
1	0	= 1 (LOH)
0	1	= 0 (no LOH)

To identify regions of aUPD the LOH column and copy number columns were incorporated into the following formula:-

=IF(AND(CN=2,LOH=,"1","0"))

The aUPD columns of paired tumours were uploaded into Spotfire® for both visualisation and the generation of a heatmap. The most common regions of aUPD from the 100K SNP array data was summarised and ordered by frequency in Excel 2007 (Microsoft).

2.5 Validation of SNP array results – real time PCR

2.5.1 Primer design

For real time PCR (qPCR) a gene with a known normal copy number of 2 in all tumour samples is required to be compared to the test gene. *ARHGAP10* was used as the gene with a normal copy number in all CNS PNETs analysed on the 100K and 500K SNP arrays. Control DNA with a normal copy number of 2 in the test gene is also needed to normalise fluorescent signals in the qPCR analysis. Genomic sequences from candidate genes were imported into the web-based program, Primer3 (http://frodo.wi.mit.edu/)

which identified forward and reverse primers to specifically amplify exons. An optimal product length between 100-150bp and GC content of 40-60% was selected. Forward and reverse primers for candidate exons within genes were subsequently analysed using a blast search (http://www.ensembl.org/Multi/blastview) to identify other hits within the genome which could result in an incorrect product being amplified (Figure 2.11). All primers were ordered from Operon.

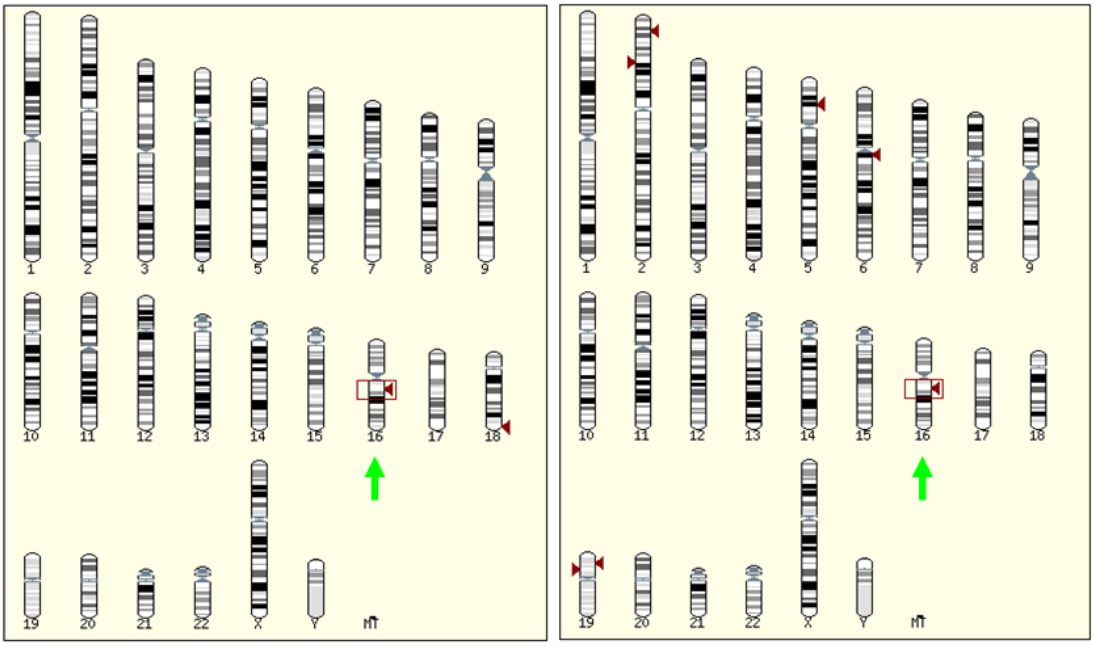

Figure 2.11 Blast search results for the gene *SALL1*. Left: Forward primer has 2 hits (red arrows), Right: Reverse primer has 7 hits (red arrows). Only one product (*SALL1* on chromosome 16) will be produced. No other hits are close enough to each other to produce a product in a standard PCR reaction. Primers for genes of interest are shown in Table 2.10. www.ncbi.nlm.nih.gov/BLAST/.

Table 2.10 Primer sequences for 9 genes of interest identified by the SNP array analysis, in addition to the control gene *ARHGAP10*.

Gene name	Locus	Exon	Product size	Forward	Reverse
ARHGAP10	4q31.23	1	123	GGAGTTCAGCGACTGCTACC	ATGAGGTTCTTCCCGTCCTT
CADPS	3p21.1	2	113	TGAGCGAGAAGGAGAAGGAA	ATTAAAGGGGTAGGCGATGC
CDKN2A	9p21.3	2	132	TCAGGTAGCGCTTCGATTCT	GGCTCCTCATTCCTCTTCCT
CDKN2B	9p21.3	2	105	GCGGATTTCCAGGGATATTT	CACCAGGTCCAGTCAAGGAT
FAM129A	1q25.3	15	130	CCACCACAGGTGAAGGAAGT	AGGAGCCACTTGGAGAGACA
MYCN	2p24.3	2	103	CGCTACAGCCCTGCTTCTAC	GGCAGCAGCTCAAACTTCTT
OR4C12	11p11.12	1	125	GGCTCAAGCCTATGCAGAAC	GGCTGTGGCTCATAATGGTT
PCDHGA3	5q31.3	1	136	TAAAATGCCTGGGAAAATCG	AAGACCTGGTCCATCCTGTG
PDGFRA	4q12	4	111	AGTCAGGGGAAACGATTGTG	AGCCATTGCACGTTTTGAG
SALL1	16q12.1	3	132	CCAACGAGATCTCCGTCATT	GAGCATTGGGCTCTGAGTTC

2.5.2 Primer optimisation

Optimal annealing temperatures for all qPCR primers were established using a temperature gradient (on a thermal cycler) (Techne TC-512). Control DNA (Promega, UK) was amplified using a range of annealing temperatures. PCR reactions were set up (Table 2.11) and a temperature gradient program was run including annealing temperatures 56 ºC, 58 ºC, 60 ºC and 62ºC (Table 2.12).

Table 2.11 PCR mastermix set up

Reagent	**Volume (µl)**
Brilliant SYBR green qPCR mastermix (Stratagene, UK)	12.5
Forward primer (1µM, Operon, UK)	2.5
Reverse primer (1µM, Operon, UK)	2.5
H_2O	6.125
DNA (10ng)	1
Reference dye (ROX, 1:500, Stratagene, UK)	0.385

Table 2.12 Temperature gradient program for *ARHGAP10*

No. of cycles	**Duration**	**Temperature (°C)**
1	10 min	95
40	30 sec	95
	1 min	56-62
	1 min	72

PCR products electrophoresed on a 2% (w/v) agarose gel (1g agar, 50ml TAE buffer and 0.5µl ethidium bromide, refer to gel production on page 81) led to the identification that 58°C was the optimal annealing temperature for the majority of primers used to validate the SNP array results, apart from *PDGFRA* and *FAM129A* which achieved optimal production at 57ºC.

2.5.3 Primer efficiencies

Due to the use of 2 sets of primers, (to amplify reference and test genes) the efficiencies of all primers are required before quantitative analysis can take place. In real time PCR,

the more commonly used ΔΔCt equation does not take into account the difference in primer efficiences (the rate at which the PCR reaction takes place and the amount of product which is made following a given number of cycles), therefore in this analysis of quantification of copy number, the Pfaffl equation was used to dispel differences in primer efficiencies (Pfaffl 2001). Serial dilutions of all primers to be analysed were set up (using decreasing amounts of control DNA (Table 2.13)). Reactions using the Stratagene Mx4000 machine were performed in triplicate and the average taken to limit pipetting error. Tubes were set up as in Table 2.11 and reaction conditions are shown in Table 2.12. On each round of PCR, the newly synthesised product incorporated SYBR green, thus, the fluorescent signal was used to calculate the amount of product made (Figure 2.12). A dissociation curve was also generated for each reaction (for all 10 primer sets) to show a melting curve for each product which confirmed product specificity (one example is shown in Figure 2.13). Since the control DNA has a copy number of 2 for both the reference and test genes, and the test sample (for example) has a copy number of 2 for the reference gene, incorporation of the SYBR green fluorescence signals measured for each reaction into the Pfaffl equation lead to the calculation of the unknown value (the copy number of the test gene in the test sample).

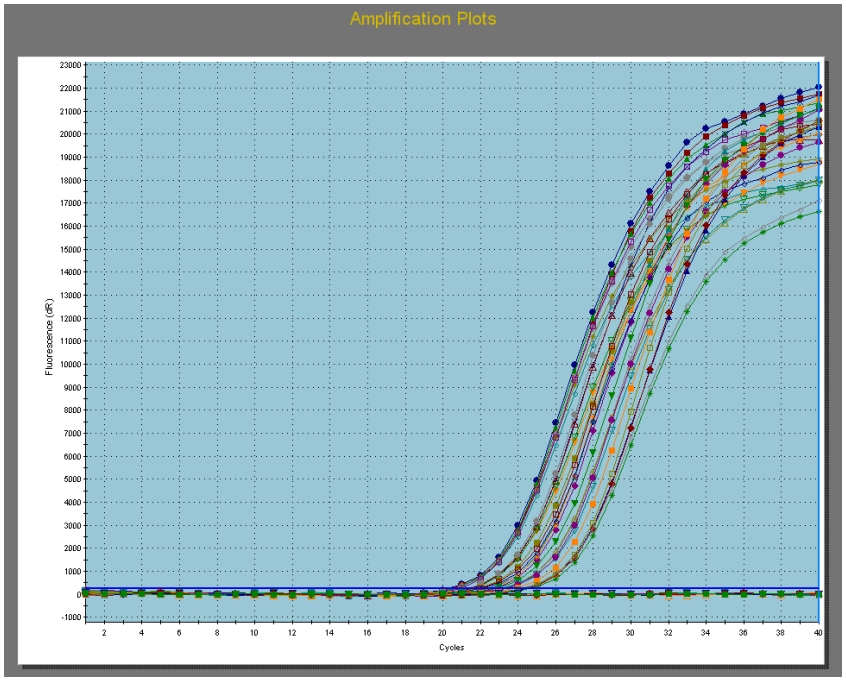

Figure 2.12 An example of an amplification plot for the evaluation of primer efficiencies. The threshold intensity for SYBR green was set to a subtracted baseline fluorescence reading of 250dR (blue horizontal line). Each curve is the amount of SBYR green fluorescence per PCR cycle and represents the amount of PCR product made from each sample DNA. Figure produced using MxPro software (Stratagene 2006).

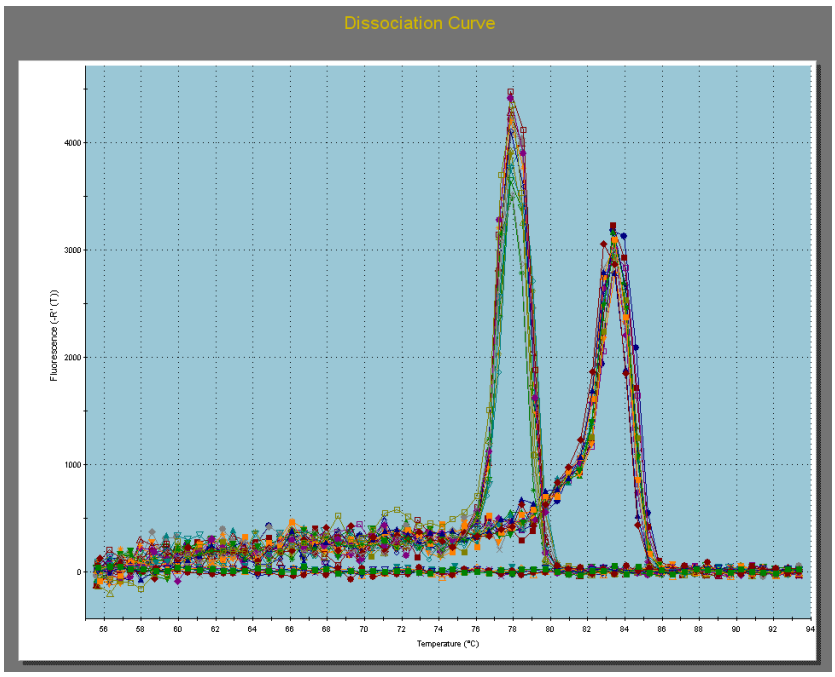

Figure 2.13 Dissociation curves of for *CDKN2B* and *ARHGAP10*. The first curve shows the dissociation of *CDKN2B* whilst the second shows *ARHGAP10*. This data was used to test for contamination and find errors in the plate set up. Figure produced using MxPro software (Stratagene 2006).

Results for each primer set were plotted in excel as a graph (log DNA vs Ct) to produce a gradient of the slope to identify primer efficiencies (examples are shown in Table 2.13 and Figures 2.14a and 2.14b). Primer efficiencies were subsequently applied in the Pfaffl equation for copy number results.

Table 2.13 The SYBR green fluorescence of *ARHGAP10* and *CDKN2B* with differing starting amounts of DNA. A threshold fluorescence of 250dR was used.

DNA (ng)	**Log DNA**	***ARHGAP10* average Ct (dR)**	***CDKN2B* average Ct (dR)**
10	1	20.54	20.65
5	0.7	21.3	21.49
2.5	0.4	22.34	22.21
1.25	0.1	23.32	23.3
0.625	-0.2	24.31	24.4

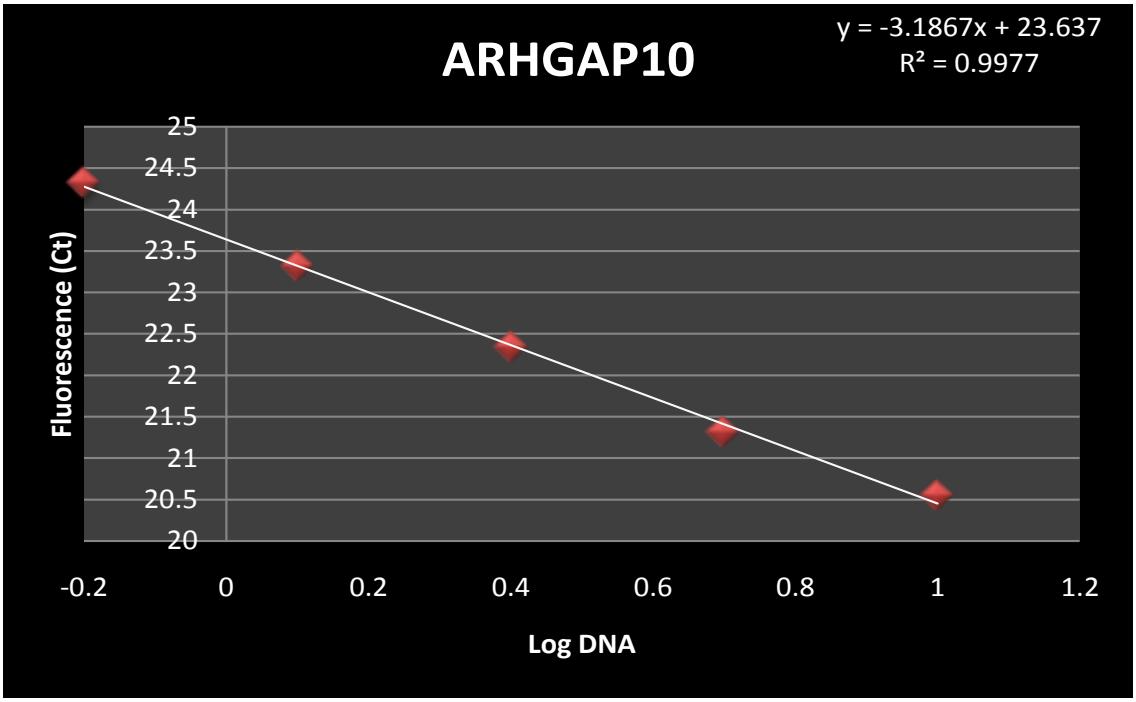

Figure 2.14a Concentration gradient for *ARHGAP10* primers to calculate PCR efficiency. The log of the starting amount of DNA was plotted against SYBR green fluorescence for *ARHGAP10* primers. Y=mx+c where m is the gradient of the slope.

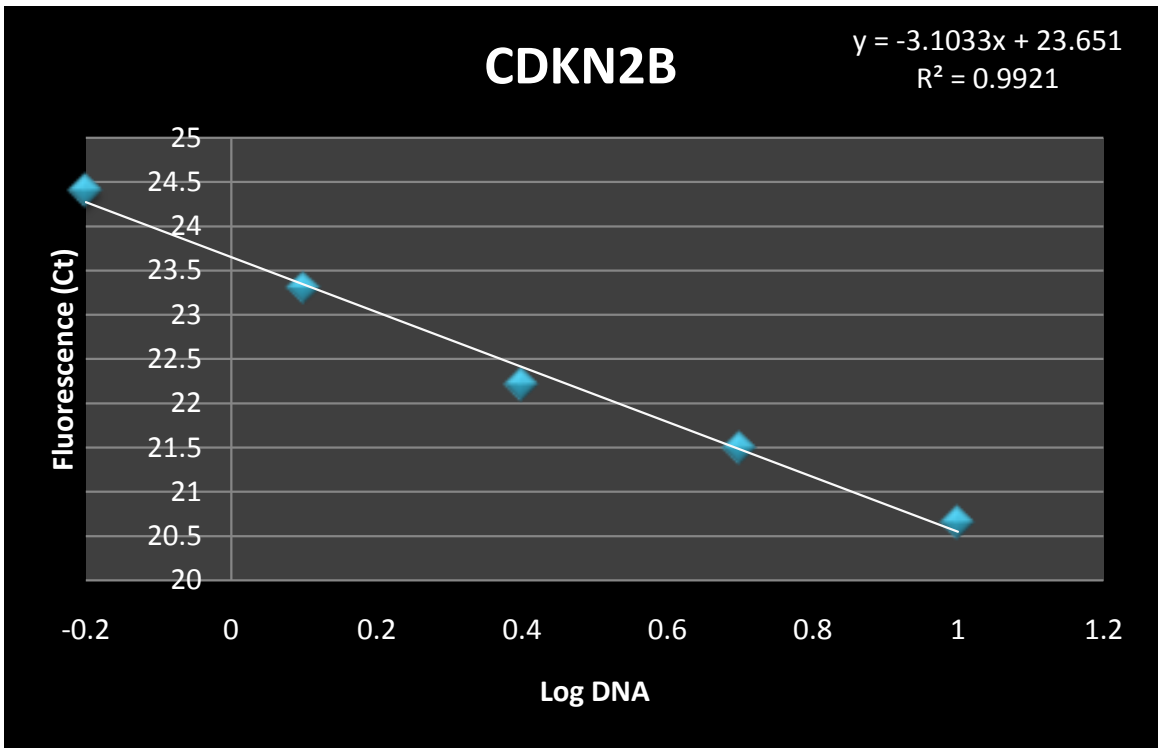

Figure 2.14b Concentration gradient for *CDKN2B* primers to calculate PCR efficiency. The log of the starting amount of DNA was plotted against SYBR green fluorescence for *CDKN2B* primers. Y=mx+c where m is the gradient of the slope.

Primer efficiencies were thus identified:-

Primer efficiency	**E = 10 (-1/Slope) -1**	
ARHGAP10	E = 10 (-1/-3.1867) -1	E = 1.01 or 101% efficient
CDKN2B	E = 10 (-1/-3.1033) -1	E = 1.04 or 104% efficient

To convert the primer efficiencies for use in the Pfaffl equation add 1.

ARHGAP10 = 2.01

CDKN2B = 2.04

All 10 primer sets (shown in Table 2.10) produced specific PCR products and were of high enough efficiency to be used in the Pfaffl equation.

2.5.4 Quantification of copy number

Using CNS PNET and control (constitutional) DNAs, the fluorescent threshold (250dR) for both test and control genes were identified and used in the Pfaffl equation alongside the primer efficiencies to identify the copy number ratios (r).

The Pfaffl equation

$$r = \frac{E_{target}^{\Delta Ct\,(Ct\ target\ gene\ blood - Ct\ target\ gene\ tumour)}}{E_{control}^{\Delta Ct\,(Ct\ \textit{ARHGAP10}\ blood - Ct\ \textit{ARHGAP10}\ tumour)}}$$

Where r is the ratio of fluorescent signal between the target gene in the blood sample and the tumour sample when compared to the control gene. Therefore if r = 1, the blood sample has a copy number of 2, as would the tumour sample. As a normal copy number is 2, to calculate the copy number for the tumour sample, double the r value identified. The criteria used to call loss and gain for the real time qPCR derived gene copy numbers were:- $0 < 0.5$ = homozygous loss, $\geq 0.5 < 1.5$ = hemizygous loss, $\geq 1.5 < 2.5$ = normal (diploid), $\geq 2.5 < 6$ = gain and ≥ 6 = amplification. These were subsequently

compared to the (CNAG) SNP array derived copy numbers for validation of copy number in genes of interest.

2.6 Immunohistochemistry

Spotting of formalin fixed paraffin embedded (FFPE) CNS PNET tissue blocks was performed by a neuropathologist (either Prof James Lowe or Dr Ian Scott) to pick respresentative tumour areas for cores to be taken from. The tissue microarrays (TMAs) were produced by coring (using a microarrayer, Beecher, USA) triplicate cores (0.6mM in diameter) taken from 52 CNS PNET FFPE blocks. The TMA was kindly produced by Mr Lee Ridley (CBTRC). Immunohistochemistry (IHC) was performed for the proteins encoded by *CDKN2B* (9p21.3) and *INI1* (22q11.23) (p15INK4B and BAF47, respectively), to investigate if the loss in gene copy number had affected protein expression levels. The Dako Chemate Envision Detection kit was used alongside antibodies raised against each protein. For the p15INK4B antibody (ab4068, Abcam), optimal conditions were an antibody dilution of 1:50, used overnight at 4ºC. The positive control showing nuclear staining was colon carcinoma. BAF47 (Cat no. 612110, BD Biosciences) was optimised with an antibody dilution of 1:200 with an overnight incubation at 4ºC and a positive control of tonsil. Negative controls consisted of antibody diluent only (Dako UK). Slides were deparaffinised in xylene for 15 minutes, placed in absolute ethanol for 5 minutes, 95% (v/v) ethanol for 4 minutes, then washed in running water. For antigen retrieval, sodium citrate (pH 6.0) was heated in a pressure cooker (Kern China) until boiling, slides were then added and the lid closed. On the pressure cooker gaining full pressure, slides were treated for 1 minute. Remaining in the pressure cooker, slides were cooled in water for 20 minutes. At this stage peroxidase blocking solution (Dako UK) was applied to the slides for 5 minutes to block the non specific endogenous peroxidase found within human tissue. Slides were washed in PBS (5 PBS Tablets in 500ml H_2O, (Oxoid UK) for 5 minutes and incubated overnight at 4ºC with 100µl primary antibody. Following incubation, slides were washed in PBS and 3 drops of secondary antibody was applied for 30 minutes. After washing in PBS for 5 minutes, 100µl of 3-3'-diaminobenzidine (DAB) (20µl DAB and chromogen in 1ml substrate, (Dako UK)) was added for 5 minutes. Slides were washed in PBS for 5 minutes then counterstained in haematoxylin (Surgipath) for 10 seconds. After washing in running water the slides were placed in lithium carbonate (Sigma UK) and the wash in water was repeated. Finally slides were washed in absolute ethanol,

95% (v/v) ethanol and xylene. Slides were mounted with coverslips using DPX mountant and visualised with an Olympus BX41 light microscope. As part of a separate project a FFPE tissue Section of CNS PNET17 was analysed for MYCN protein expression and the result is shown as part of this thesis. The MYCN antibody was optimised at a dilution of 1:500 with the above experimental procedure and conditions (OP13, Calbiochem). Scoring for INI1 consisted of either positive or negative staining whereas for p15INK4B, both percentage of positive cells and staining intensity were considered. Tumours were scored as negative, weak, moderate or strongly staining for p15INK4B. Weak staining constituted <50% cells with low intensity staining, moderate staining was considered if >50% cells had low intensity staining and strong staining denoted >50% cells with intense staining.

2.7 Sequencing

2.7.1 Primer optimisation

PCR primers were designed for exons 5 and 9 of the *INI1* gene (Table 2.14). The optimal annealing temperature for each was identified using a temperature gradient on a thermal cycler (Techne TC - 512). PCR mastermix and conditions used are shown in Tables 2.15a and 2.15b.

Table 2.14 Primer sequences for *INI1* production

Gene name	Locus	Exon	Product size	Forward	Reverse
INI1	22q11.23	5	340	TGTGCAGAGAGAGAGGCTGA	CAAAACTATGCCCCGATGTC
INI1	22q11.23	9	587	CTCTGTTCCCACCCCTACAC	TGTGCCAACCTTGTTCACAT

Table 2.15a PCR mastermix for *INI1*

Reagent	Volume (µl)
Biomix red (Bioline, UK)	5
H^2O	2
Forward primer (10µM, Operon, UK)	1
Reverse primer (10µM, Operon, UK)	1
DNA (50ng)	1

Table 2.15b PCR conditions for *INI1*

No. of cycles	Duration	Temperature (°C)
1	12 min	95
35	45 sec	95
	30 sec	56 – 62
	30 sec	72
1	10 min	72

A 2% (w/v) agarose gel (1g agar, 0.5ml TAE buffer, 0.5µl ethidium bromide, refer to gel production, page 81) was electrophoresed and used to identify the optimal annealing temperatures of both exons 5 and 9 to be 62ºC. PCR of all available CNS PNET tumour and blood DNAs was performed as above and if a product was visualised on the gel, the sample was taken on to the next stage.

2.7.2 PCR clean up – exoSAP

Purification of PCR products was required to remove remaining reagents in the PCR mix. 0.3µl SAP (1U/µl, Promega UK), 0.15µl ExoI (10U/µl, NEB)) and 1.55µl H_2O was added to each PCR product. Products were incubated at 37°C for 8 minutes followed by 15 minutes at 72°C.

2.7.3 Big dye sequencing reaction

Big dye (ABI UK) was used in the sequencing reaction, which was set up as shown in Tables 2.16a and 2.16b. The sequencing reaction was performed using a thermal cycler (Techne TC – 512).

Table 2.16a Big dye sequencing reaction mix

Reagent	Volume (µl)
PCR product	1
Big dye	0.5
Forward primer (1µM, Operon, UK)	1.5
Better buffer (ABI, UK)	3.5
Water	3.5
Total	10

Table 2.16b PCR cycle for Big dye sequencing

Temperature (°C)	Time (seconds)	No. of cycles
96	30	25
50	15	
60	240	
28	60	1

2.7.4 Precipitation

10µl of each sequencing reaction was transferred to a 96 well plate. 64µl of precipitation mix was added to each well (Table 2.17). The plate was sealed, vortexed and incubated at room temperature for 15 minutes. Following centrifugation at 4°C for 30 minutes at 2000g, the seal was removed from the plate and the plate was centrifuged upside down on a paper tissue at 4°C for 1 minute at 185g to remove the supernatant. 70µl of 70% (v/v) ethanol was added to each well to wash the DNA and the plate was spun at 4°C for 15 minutes at 1650g. For the second time the plate had the seal removed and was centrifuged at 4°C at 185g for 1 minute. Pellets were air dried with open lids at 50°C for 10 minutes.

Table 2.17 Sequencing precipitation mix

Reagent	per well (µl)	96 well plate (µl)
125mM EDTA (BDH UK)	2	200
3M NaAc (Sigma UK)	2	200
100% (v/v) Ethanol (Fisher UK)	50	5000
Water	10	1000
Total	64	6400

2.7.5 Sequencing scan

Pellets in the 96 well plate were resuspended in 10µl formamide and the plate was placed into the ABI 3130 sequencer. The capillary electrophoresis was set to 20KV and the laser induced fluorescence reading performed. The sequence scan was run using the Foundation Data Collection Software v3 and analysed using Sequence Analysis Software v5.2. At this stage the baseline fluorescence for each base was accounted for. The peak detection and base calling was visualised from the output ABI files (ab1 and seq files). Mutational analysis was subsequently performed using Chromaslite v2.01 where a comparison of the normal sequence and the test sequence was made.

2.8 Statistics

Statistical analysis was performed using SPSSv16 (Statistical Package for the Social Sciences, Version 16, Chicago, USA).

2.8.1 Associations in two-way frequency Tables – Fisher's exact test

Clinical information for CNS PNET and pineoblastoma patients were entered into SPSSv16, including tumour location, whether the tumour was a primary or recurrence, whether the patient had metastatic disease at presentation, length of patient survival and whether the patient was presently alive or deceased (patient status). Alongside this, genetic information identified from the SNP array analysis and immunohistochemical staining was added. This included chromosomal arm aberrations, copy number imbalance at the gene level and immunohistochemical results. For reliable statistics at least 4 patients were required in each group. Following the analysis of the association between all combinations of variables, a 2 sided, significance value was given. A p value of <0.05 indicated a statistically significant result, whilst due to the small numbers of samples within the analysis; a p value > 0.05 and < 0.1 emphasized a possible trend in variables.

2.8.2 Associations with age – independent samples t-test

With age a continuous variable, independent samples t-tests were performed to identify associations firstly between clinical groups and age and secondly with chromosome arm alteration, gene copy number imbalance, immunohistochemical staining and patient age.

2.8.3 Survival analysis – Kaplan-Meier

Univariate survival curves were constructed using the Kaplan-Meier method and univariate comparisons made by the log-rank test to assess whether clinical factors and genetic or immunohistochemical data was linked to patient survival. A p value of <0.05 was a significant result, whilst a p value of. 0.05 – 0.10 was marginally significant.

2.8.4 Extent of chromosome arm imbalance in patients of different ages with CNS PNET and pineoblastoma

To test whether the extent of chromosome arm imbalance was significantly different in patients with tumours arising in separate brain locations (CNS PNET or pineoblastoma) or in CNS PNET patients of different age groups, a Mann-Whitney test was used.

2.8.5 Real time PCR vs SNP array results – Spearman's rank correlation coefficient

To test if the SNP array copy number results were confirmed by real time PCR, Spearman's rank correlation coefficient (SRCC) analysis was applied to demonstrate an overall correlation between the results of the two independent methods. Copy number results of both the CNAG derived SNP array and real time PCR analyses of 9 genes were incorporated into SPSSv16. A SRCC value (r) of 0 indicated no correlation whilst a value of 1 signified excellent correlation.

2.8.6 Power statistics

Power statistics were performed using PS Power and sample size calculations version 3.0 (2009) available at http://biostat.mc.vanderbilt.edu/PowerSamplesSize (Dupont, Plummer et al 1990). A significance criterion of 0.05 and power of 0.8 were tested for.

CHAPTER 3

CLINICAL ASPECTS OF CNS PNET AND PINEOBLASTOMA

3.1 Introduction

Current treatment strategies for CNS PNET and pineoblastoma are not optimal and a detailed knowledge of the genetic and biological components leading to tumour development and progression is needed to provide novel targets for therapy. Two recent genetic studies undertaken in CNS PNET highlighted the rarity of tumour tissue, with only 7 and 21 CNS PNET samples available for analysis (McCabe, Ichimura et al. 2006; Pfister, Remke et al. 2007). At present, no pineoblastomas have been studied at a higher resolution than conventional CGH. One important aim was to draw together a sufficiently large sample cohort to identify genetic aberrations common to CNS PNET, thus the compilation of the largest cohort of CNS PNETs and pineoblastomas was performed. The clinical data was also collected alongside tissue samples so that associations between clinical factors could be identified.

3.2 CNS PNET and pineoblastoma patient clinical overview

In total, the tumours of 60 patients were included in the study. Samples were used in either SNP array, real time PCR, immunohistochemical or sequencing analyses. Clinical information was collected for 48 CNS PNET and 12 pineoblastoma patients and is shown in Table 3.1. Of the CNS PNET patients, 24/48 (50%) were male and 24/48 (50%) female, with no sex predominance. CNS PNET patient age ranged from 0.8 – 15.8 years, with mean and median ages of 6 and 5.1 years, respectively. Of the information available, 18/31 (58%) CNS PNET patients underwent incomplete tumour resections and 13/31 (42%) had complete resections. 18 CNS PNET patients had tumour relapse, with a mean time to relapse 1.1 years post diagnosis (range 0.1 – 5.6 years). 12/41 (29%) CNS PNET patients had metastatic disease at presentation, whilst 29/41 (71%) had no metastasis present at diagnosis (Chang 1969). To date, from the information available, 34/44 (77%) CNS PNET patients are deceased and 10/44 (23%) are still presently alive. Of the pineoblastoma patients, 8/12 (67%) were male and 4/12 (33%) female, with a 2:1 male predominance. Pineoblastoma patient age ranged from 0.4 – 15.3 years, with mean and median ages of 4.9 and 2 years, respectively. 5 pineoblastoma patients underwent incomplete tumour resctions and 1 had a complete resection. 6 pineoblastoma patients had tumour relapse, with a mean time to relapse 1.43 years (range 0.6 – 4.3 years). 7/8 (87.5%) pineoblastoma patients had metastatic disease at diagnosis, whilst 1/8 (12.5%) had no evidence of metastases at presentation.

To date, 7/8 (87.5%) pineoblastoma patients are deceased and 1/8 (12.5%) is still presently alive.

Table 3.1 Clinical demographics of 48 CNS PNETs and 12 pineoblastomas

ID	Sex	Location	Resection	Treatment	Age (Yr)	Time to Relapse (Yr)	Censor	Survival (Yr)	Metastatic status
42	Female	Pineal	Incomplete	Chemotherapy	0.4	1	U	1.2	M2
1	Female	Pineal	Incomplete	Chemotherapy	0.5	0.6	U	0.8	M3
3	Male	Pineal	-	-	1	-	-	-	-
4	Female	Pineal	Incomplete	Chemotherapy	1.1	-	U	0.8	M3
5	Male	Pineal	Incomplete	Chemotherapy	1.3	0.7	U	1.6	M3
11	Male	Pineal	Complete	Radiotherapy & chemotherapy	2	-	C	14.9	M0
12	Male	Pineal	-	Chemotherapy	2	-	-	-	-
46	Male	Pineal	-	Chemotherapy	2.4	1.2	U	1.3	M2
52	Male	Pineal	-	Radiotherapy & chemotherapy	8.2	4.3	U	4.9	M3
23	Male	Pineal	-	-	11	-	-	-	-
27	Female	Pineal	-	-	14	-	-	-	-
59	Male	Pineal	Incomplete	Radiotherapy & chemotherapy	15.3	0.8	U	3.1	M3
2	Female	Cerebral	Incomplete	None	0.8	0.5	U	3.4	M2
43	Male	Cerebral	Incomplete	Chemotherapy	0.5	-	.	-	-
44	Male	Cerebral	-	Chemotherapy	1	0.4	U	0.7	M3
29	Female	Cerebral	Complete	Radiotherapy	1.2	-	C	2	M1
6	Female	Cerebral	Incomplete	Radiotherapy	1.6	-	U	0.3	M3
7	Male	Cerebral	Incomplete	Radiotherapy & chemotherapy	1.6	0.7	U	0.9	M3
8	Male	Cerebral	Incomplete	Chemotherapy	1.7	1.7	U	1.7	M0
9	Female	Cerebral	Incomplete	None	1.7	-	U	0	M0
41	Male	Cerebral	-	-	1.8	-	.	-	-
30	Female	Cerebral	-	Chemotherapy	1.9	-	U	0.6	M0
10	Female	Cerebral	Complete	Chemotherapy	2	-	U	0.3	M0
31	Female	Cerebral	-	Chemotherapy	2.2	-	U	0.3	M0
45	Male	Cerebral	-	None	2.3	-	U	3.2	M0
47	Male	Cerebral	-	Radiotherapy & chemotherapy	2.5	-	U	0.5	M0
13	Male	Cerebral	-	None	2.7	-	-	-	-
32	Female	Cerebral	-	Radiotherapy & chemotherapy	3	-	U	1.3	M0
14	Male	Cerebral	Complete	Radiotherapy & chemotherapy	3.1	0.3	U	0.5	M4
48	Female	Cerebral	Incomplete	Radiotherapy	3.2	0.9	U	1.3	M0
49	Female	Cerebral	-	None	3.8	-	U	0.9	M0
15	Female	Cerebral	Complete	Radiotherapy & chemotherapy	4.3	-	U	2	M0
16	Female	Cerebral	Incomplete	Chemotherapy	4.4	0.4	C	1.8	M0
17	Male	Cerebral	Incomplete	Radiotherapy & chemotherapy	4.9	0.6	U	0.8	M2
18	Male	Cerebral	Incomplete	Chemotherapy	5.1	1.1	U	1.8	M0

33	Male	Cerebral	-	Chemotherapy	5.1	-	U	0.2	M0
50	Male	Cerebral	Incomplete	Chemotherapy	5.2	-	U	3.2	M0
19	Female	Cerebral	Incomplete	Radiotherapy	5.9	-	U	0.4	M0
34	Male	Cerebral	-	Radiotherapy & chemotherapy	6.4	-	U	1.4	M0
35	Male	Cerebral	Complete	Radiotherapy & chemotherapy	7	0.5	U	1.6	M1
20	Female	Cerebral	Complete	Radiotherapy & chemotherapy	7.1	-	C	6.9	M0
51	Female	Cerebral	-	Radiotherapy & chemotherapy	7.3	0.5	U	0.8	M0
36	Female	Cerebral	Complete	Radiotherapy & chemotherapy	7.6	-	C	2.6	M1
53	Female	Cerebral	-	Radiotherapy & chemotherapy	8.3	-	U	0.7	M0
54	Female	Cerebral	-	None	8.4	0.1	C	9	-
21	Male	Cerebral	Complete	Radiotherapy	8.9	5.6	U	5.9	M2
22	Male	Cerebral	Incomplete	Radiotherapy & chemotherapy	10.2	-	C	4.3	M0
55	Male	Cerebral	Incomplete	Radiotherapy & chemotherapy	10.3	-	U	1.3	M0
56	Female	Cerebral	Incomplete	-	10.5	-	U	0	M0
37	Male	Cerebral	-	Radiotherapy & chemotherapy	10.6	-	C	0.4	M0
24	Male	Cerebral	Complete	Radiotherapy	11.8	1.1	U	2.5	M3
25	Male	Cerebral	Incomplete	.	11.8	-	U	0	M0
57	Female	Cerebral	Complete	Radiotherapy & chemotherapy	11.8	2.2	U	4.8	M4
38	Female	Cerebral	Incomplete	Radiotherapy & chemotherapy	12	-	C	0.3	M0
26	Female	Cerebral	Complete	Radiotherapy & chemotherapy	12.3	2.3	U	3	-
58	Male	Cerebral	Complete	Radiotherapy	12.4	0.4	U	3.3	M0
60	Male	Cerebral	Complete	Radiotherapy & chemotherapy	15.5	-	C	18.3	M0
39	Female	Cerebral	Incomplete	Radiotherapy & chemotherapy	15.8	0.5	C	0.5	M0
28	Male	Cerebral	-	-	<16	-	-	-	-
40	Female	Cerebral	-	-	<16	-	U	-	-

Patients were firstly ordered by tumour location and secondly by age. U = uncensored (patient deceased), C = censored (patient alive to date), - information unavailable. M0 – M4 metastatic status based on Chang's staging system (Chang 1969).

Statistical analysis was performed in SPSS to identify links between specific patient clinical attributes, including tumour location, resection, and metastatic status (as defined in chapter 2, Section 2.8.1), in addition to patient age (detailed in chapter 2, Section 2.8.2). 1 statistically significant association was identified; when compared to the CNS PNETs, pineoblastomas more commonly had metastatic disease at diagnosis ($p = 0.0035$, Fisher's exact test, 2 tailed).

3.3 Discussion

Utilizing the clinical information collected for 60 CNS PNET and pineoblastoma patients, clinical variables were tested to investigate if statistical associations were present within the cohort. An important part of the study was to pull together a patient cohort which well represented the clinical spectrum of CNS PNETs and pineoblastomas. This was achieved by the collection of a relatively large cohort of tumours. Notably, 12/60 (20%) patients had pineoblastomas, a similar Figure to those entered into previous studies (Dirks, Harris et al. 1996; Timmermann, Kortmann et al. 2002; Pizer, Weston et al. 2006; Fangusaro, Finlay et al. 2008; Johnston, Keene et al. 2008). The mean age at diagnosis for the CNS PNET cohort (6 years) was consistent with the current edition of the WHO of tumours of the CNS, which states a mean age at diagnosis for CNS PNET patients of 5.5 years (Louis, 2007). Also, whereas previous reports have identified metastatic disease at presentation in 16% - 78% of CNS PNET patients, the present CNS PNET cohort harboured metastatic disease at presentation in 29% CNS PNET patients (Timmermann, Kortmann et al. 2002; Pizer, Weston et al. 2006; Fangusaro, Finlay et al. 2008; Gilheeney, Saad et al. 2008; Johnston, Keene et al. 2008). Overall this retrospective cohort reflected the clinical CNS PNET spectrum and provided a meaningful group to undertake statistical comparison of clinical variables.

Patient age was an important area to study, with previous reports showing a correlation between young patient age and poor prognosis, however, this analysis was not performed due to the tumours being respectively collected and not having had the same treatment (Geyer, Zeltzer et al. 1994; Albright, Wisoff et al. 1995; Cohen, Zeltzer et al. 1995; Dirks, Harris et al. 1996; Fangusaro, Finlay et al. 2008; Johnston, Keene et al. 2008). Previously reports of CNS PNETs have shown a younger patient age is linked to poorer prognosis (Albright, Wisoff et al. 1995; Dirks, Harris et al. 1996). This correlation has also previously been identified in other paediatric brain tumours, especially medulloblastoma and ependymoma (Stiller and Bunch 1992; Duffner, Horowitz et al. 1993; Ater, van Eys et al. 1997; Mason, Grovas et al. 1998; Duffner, Horowitz et al. 1999; Walter, Mulhern et al. 1999; Geyer, Sposto et al. 2005; Johnston, Keene et al. 2009; Merchant, Li et al. 2009).

Relating patient prognosis to anatomical location in the brain is still a controversial issue. Although it is now recognised that patients diagnosed with medulloblastoma have

better outcomes than those diagnosed with a CNS PNET or pineoblastoma, it still remains unclear whether there is a difference in the prognoses between CNS PNETs and pineoblastoma (Geyer, Sposto et al. 2005; Timmermann, Kortmann et al. 2006). Previous reports have provided conflicting observations. Whereas a number of studies reported patients with CNS PNETs had a better prognosis than pineoblastoma patients (Cohen, Zeltzer et al. 1995; Jakacki, Zeltzer et al. 1995; Pizer, Weston et al. 2006; Fangusaro, Finlay et al. 2008), an earlier study identified that patients with pineoblastoma achieved a better outcomes than those with CNS PNETs (Cohen, et al. 1995). The difference in results emphasizes the need for specific treatments tailored to tumour location, although these differences could be due to the seperate treatment protocols used in the studies and the variation in patient cohorts. Interestingly, 2 previous studies concluded that CNS PNET patients harbouring metastatic disease had a poorer prognosis than those without metastatic disease (Reddy, Janss et al. 2000; Hong, Mehta et al. 2004). Further investigation is needed to test whether the metastatic status in CNS PNETs can potentially be used as a prognostic indicator. Only upon the collection and comparison of a larger CNS PNET clinical dataset will this potentially be elucidated.

In the present study, pineoblastoma patients more commonly had metastatic disease at presentation when compared to CNS PNET patients. This association corroborates the findings of a recent study by Johnston *et al.*, which found a higher incidence of metastasis in patients with pineoblastoma, (with 33.3% of patients having metastasis at diagnosis compared to 26% of CNS PNET patients) (Johnston, Keene et al. 2008).

Statistical associations now need to be confirmed in a larger series of CNS PNETs and pineoblastomas which are treated in uniformly as part of a clinical trial. Increased understanding of the underlying genetics and biology driving CNS PNET and pineoblastoma development, especially within the different age groups and PNETs of different locations of the brain (CNS PNET and pineoblastoma) will undoubtedly lead to novel therapeutic targets enhancing patient prognosis.

CHAPTER 4

GENOME WIDE APPROACH TO CHARACTERISING CNS PNET AND PINEOBLASTOMA

4.1 Introduction

Revolutionizing the capabilities within the scientific community, the human genome project (completed in 2001), has led to a wealth of scientific research increasing the understanding of many complex diseases (The International Human Genome Sequencing Consortium). The project enabled the identification and location of single nucleotide polymorphisms (SNPs) throughout the human genome to be established. SNPs are single nucleotide bases (either an A, T, G or C) which can differ between individuals. DNA in humans is 99.9% identical; with the 0.1% difference between individuals constituted by polymorphisms, of which the SNP is the most common form. Exploiting this new level of genetic information, Affymetrix have designed high resolution SNP arrays to interrogate SNP alleles across the genome. Firstly used in the identification of complex traits and population genetics, more recently the technology has been applied to the area of cancer research. Variation in polymorphic sequences has been identified which contribute to the susceptibility of many diseases, including alzheimer's disease and breast cancer (Corder, Saunders et al. 1993; Easton, Pooley et al. 2007).

In addition to SNP allele calls, SNP arrays can be used to identify SNP copy number alteration across the entire genome in a single experiment, hence, this technology is of immense benefit in cancer research where genomic instability, gene copy number alteration and LOH are all common features. In the research of cancer, SNP arrays have previously been used to identify consecutive SNPs harbouring copy number imbalance and LOH to discover regions of interest. At present, SNP arrays can be used to examine 10,000, 100,000, 500,000 and 1.8 million SNPs (Table 4.1) (Herr, Grutzmann et al. 2005; Hu, Wang et al. 2005; Slater, Bailey et al. 2005; Kotliarov, Steed et al. 2006; Harada, Chelala et al. 2008; Suzuki, Kato et al. 2008; Tuefferd, De Bondt et al. 2008).

Table 4.1 Comparison of the resolution of different techniques used in oncogenomics

Genetic platform	Resolution
Conventional CGH	10-20 Mb
Array CGH	100 Kb
10K SNP array	113 Kb
100K SNP array	25 Kb
500K SNP array	2.5 Kb
SNP6 (1.8 million probes)	700 b

The market leaders of SNP array production, Affymetrix, have developed genechip mapping sets which use only tiny amounts of DNA (250ng per chip), which were especially attractive for use in the present study in the analysis of small brain tumour tissue samples. The inclusion of a control dataset was also an important factor in the identification of tumour specific alterations, therefore eliminating aberrations and SNP variation already present in the patient's germline. Constitutional blood samples were available for many CNS PNET patients of the study. The main mapping set used in this study was the 100K mapping set, providing allele calls and copy numbers for over 100,000 SNPs. 40 different probes per SNP were interrogated to provide both perfect match and mismatch data. Single stranded sample DNA molecules bind to complementary probes (hybridisation) and the data produced upon scanning of the fluorescently tagged hybridised probes provided signal intensities for each SNP. Whilst a gain in copy number was detected by increased signal intensity when compared to the constitutional control, a loss in copy number was detected by a decrease in signal intensity. These signal values can then be given an inferred copy number (a whole number) by implementation of a hidden markov model in CNAG.

Presently, no high resolution SNP array studies have been undertaken in CNS PNET, with previous genetic analyses using the lower resolution techniques available at the time. Previous genetic studies in CNS PNET are shown earlier in this thesis (Chapter 1, Section 1.5). Our ability to achieve significant advances in the diagnosis, prognosis and therapy of CNS PNETs relies on gaining a better understanding of the underlying genetics through high resolution molecular characterisation of these tumours. We hypothesise that genetic aberrations relating to clinical characteristics will provide

markers of prognosis and whereas previous studies have included only small sample sets and limited clinical information, this study includes the largest cohort of CNS PNETs for genetic analysis to date, with the addition of clinical information.

4 2 Materials and methods

4.2.1 100K and 500K SNP array analysis of 46 CNS PNETs and pineoblastomas

In total, 50 CNS PNETs and pineoblastomas were analysed using the Affymetrix 100K and 500K platforms (Table 4.2). DNA was extracted as described in Chapter 2, Section 2.3 and the SNP arrays processed as described in chapter 2, Section 2.4). 25 CNS PNETs and 8 pineoblastoma were analysed using the 100K mapping set whilst a further set of 17 were analysed using the higher resolution 500K mapping set. Of these, 4 tumours were analysed using both the 100K and 500K platforms. Constitutional bloods were analysed for 10 CNS PNET/pineoblastoma patients on the 100K mapping set and 33 brain tumours on the 500K mapping set. These were used as a reference set to normalise the tumour data therefore only tumour specific events were identified. The SNP array data was analysed as shown in Chapter 2, Section 2.4.11 – 2.4.14.

Table 4.2 Clinical demographics of 46 CNS PNETs and pineoblastomas analysed using Affymetrix SNP arrays

ID	Sex	Location	Primary/ Recurrence	Resection	Treatment	Age (Yr)	Time to Relapse (Yr)	Censor	Survival (Yr)	Metastatic status	SNP array
1	Female	Pineal	Primary	Incomplete	Chemotherapy	0.5	0.6	U	0.8	M3	100K
3	Male	Pineal	Primary	-	-	1	-	-	-	-	100K
4	Female	Pineal	Primary	Incomplete	Chemotherapy	1.1	-	U	0.8	M3	100K
5	Male	Pineal	Recurrence	Incomplete	Chemotherapy	1.3	0.7	U	1.6	M3	100K
11	Male	Pineal	Primary	Complete	Radiotherapy & chemotherapy	2	-	C	14.9	M0	100K
12	Male	Pineal	Recurrence	-	Chemotherapy	2	-	-	-	-	100K
23	Male	Pineal	Primary	-	-	11	-	-	-	-	100K
27	Female	Pineal	Primary	-	-	14	-	-	-	-	100K
2P	Female	Cerebral	Primary	Incomplete	None	0.8	0.5	U	3.4	M2	100K
2R	Female	Cerebral	Recurrence	Complete	None	0.8	-	U	3.4	M2	100K and 500K
29	Female	Cerebral	Primary	Complete	Radiotherapy	1.2	-	C	2	M1	500K

6	Female	Cerebral	Primary	Incomplete	Radiotherapy	1.6	-	U	0.3	M3	100K and 500K
7	Male	Cerebral	Primary	Incomplete	Radiotherapy & chemotherapy	1.6	0.7	U	0.9	M3	100K
8P	Male	Cerebral	Primary	Incomplete	Chemotherapy	1.7	1.7	U	1.7	M0	100K
8R	Male	Cerebral	Recurrence	Incomplete	Chemotherapy	1.7	-	U	1.7	M0	100K
9	Female	Cerebral	Primary	Incomplete	None	1.7	-	U	0	M0	100K and 500K
30	Female	Cerebral	Primary	-	Chemotherapy	1.9	-	U	0.6	M0	500K
10	Female	Cerebral	Primary	Complete	Chemotherapy	2	-	U	0.3	M0	100K
31	Female	Cerebral	Primary	-	Chemotherapy	2.2	-	U	0.3	M0	500K
13	Male	Cerebral	Primary	-	None	2.7	-	-	-	-	100K
32	Female	Cerebral	Primary	-	Radiotherapy & chemotherapy	3	-	U	1.3	M0	500K
14	Male	Cerebral	Primary	Complete	Radiotherapy & chemotherapy	3.1	0.3	U	0.5	M4	100K
15	Female	Cerebral	Primary	Complete	Radiotherapy & chemotherapy	4.3	-	U	2	M0	100K and 500K
16	Female	Cerebral	Primary	Incomplete	Chemotherapy	4.4	0.4	C	1.8	M0	100K
17	Male	Cerebral	Primary	Incomplete	Radiotherapy & chemotherapy	4.9	0.6	U	0.8	M2	100K
18	Male	Cerebral	Primary	Incomplete	Chemotherapy	5.1	1.1	U	1.8	M0	100K
33	Male	Cerebral	Primary	-	Chemotherapy	5.1	-	U	0.2	M0	500K
19	Female	Cerebral	Primary	Incomplete	Radiotherapy	5.9	-	U	0.4	M0	100K
34	Male	Cerebral	Primary	-	Radiotherapy & chemotherapy	6.4	-	U	1.4	M0	500K
35	Male	Cerebral	Primary	Complete	Radiotherapy & chemotherapy	7	0.5	U	1.6	M1	500K
20	Female	Cerebral	Primary	Complete	Radiotherapy & chemotherapy	7.1	-	C	6.9	M0	100K
36	Female	Cerebral	Primary	Complete	Radiotherapy & chemotherapy	7.6	-	C	2.6	M1	500K
21P	Male	Cerebral	Primary	Complete	Radiotherapy	8.9	5.6	U	5.9	M2	100K
21R	Male	Cerebral	Recurrence	Incomplete	Chemotherapy	8.9	-	U	5.9	M2	100K
22P	Male	Cerebral	Primary	Incomplete	Radiotherapy & chemotherapy	10.2	-	C	4.3	M0	100K
22R	Male	Cerebral	Recurrence	Incomplete	Radiotherapy & chemotherapy	10.2	-	C	4.3	M0	100K
37	Male	Cerebral	Primary	-	Radiotherapy & chemotherapy	10.6	-	C	0.4	M0	500K
24P	Male	Cerebral	Primary	Complete	Radiotherapy	11.8	1.1	U	2.5	M3	100K
24R	Male	Cerebral	Recurrence	-	Chemotherapy	11.8	-	U	2.5	M3	100K
25	Male	Cerebral	Primary	Incomplete	-	11.8	-	U	0	M0	100K
38	Female	Cerebral	Primary	Incomplete	Radiotherapy & chemotherapy	12	-	C	0.3	M0	500K
26	Female	Cerebral	Recurrence	Complete	Radiotherapy & chemotherapy	12.3	2.3	U	3	-	100K
39	Female	Cerebral	Primary	Incomplete	Radiotherapy & chemotherapy	15.8	0.5	C	0.5	M0	500K
28	Male	Cerebral	Primary	-	-	<16	-	-	-	-	100K
40	Female	Cerebral	Primary	-	-	<16	-	U	-	-	500K
41	Male	Cerebral	Cell line from Primary	-	-	1.8	-	.	-	-	500K

Patients were firstly ordered by tumour location and secondly by age at original diagnosis. U = uncensored (patient deceased), C = censored (patient alive to date), - information unavailable. M0 – M4 metastatic status based on Chang's staging system (Chang 1967). SNP array = single nucleotide polymorphism arrays with either 100K (100,000 probes) or 500K (500,000) probes.

4.2.2 SNP array call rates

SNP call rates indicate the quality of the SNP array results and were given as a percentage signifying the number of reliable probes on the array for each experiment. For the 100K SNP array platform, a SNP call rate of >96% was preferred for the generation of high quality data, whilst for the 500K SNP array platform, a SNP call rate of >94% was deemed accepTable. Due to the nature of highly aberrant tumour DNA however, lower SNP call rates were common when analysing tumour samples. The SNP call rate results for the CNS PNETs and constitutional bloods analysed were of a high quality and are shown in Tables 4.3 – 4.6.

Table 4.3 SNP call rates for 33 CNS PNETs and pineoblastomas analysed using Affymetrix 100K SNP arrays

ID	XbaI 50K array (%)	HindIII 50K array (%)	Average (%)
1	98.74	96.07	97.41
2P	93.39	97.74	95.57
2R	96.49	97.07	96.78
3	97.49	93.47	95.48
4	98.63	89.43	94.03
5	98.41	88.66	93.54
6	98.25	98.43	98.34
7	97.96	97.55	97.76
8P	98.84	89.18	94.01
8R	96.86	96.62	96.74
9	84.9	85.45	85.18
10	97.3	93.59	95.45
11	97.53	92.22	94.88
12	98.99	99.12	99.06
13	98.11	96.5	97.31
14	95.94	95.67	95.81
15	99.73	96.25	97.99
16	96.15	94.29	95.22
17	91.59	93.41	92.5
18	98.91	95.48	97.2
19	99.13	88.92	94.03
20	96.58	90.36	93.47
21P	98.34	97.18	97.76
21R	99.25	93.57	96.41
22P	83.93	99.29	91.61

22R	96.96	94.6	95.78
23	99.56	97.95	98.76
24P	98.72	98.74	98.73
24R	96.06	91.64	93.85
25	98.31	96.17	97.24
26	97.32	90.18	93.75
27	98.34	91.01	94.68
28	98	76.01	87.01

The Affymetrix XbaI 50K array results for CNS PNET and pineoblastoma DNA had a mean SNP call rate of 96.81% (±0.63%), a median of 98% and a range of 83.93% – 99.73%. The Affymetrix HindIII 50K arrays had a mean SNP call rate of 93.69% (±0.83%), a median of 94.6% and a range of 76.01% – 99.29%. P, primary; R, recurrence.

Table 4.4 SNP call rates for 10 constitutional bloods of CNS PNET patients analysed using Affymetrix 100K SNP arrays

ID	XbaI 50K array (%)	HindIII 50K array (%)	Average (%)
Blood1	98.88	96.86	97.87
Blood2	98.58	86.45	92.505
Blood3	98.51	96.22	97.365
Blood4	88.49	90.97	88.73
Blood5	98.35	98.99	98.67
Blood6	99.59	91.65	95.62
Blood7	96.75	92.85	94.8
Blood8	99.51	96.73	98.12
Blood9	98.88	92.3	95.59
Blood10	99.39	99.45	99.42

ID	NspI 250K array (%)	StyI 250K array (%)	Average (%)
29	94.26	98.53	96.395
30	98.48	97.66	98.07
31	98.2	98.7	98.45
32	98.76	87.48	93.12
33	99.3	99.47	99.385
34	94.8	98.28	96.54
35	93.25	98.26	95.755
36	93.85	97	95.425
37	96.24	78.73	87.485
38	94.24	98.41	96.325

The

Affymetrix XbaI 50K array results for the constitutional blood DNA had a mean SNP call rate of 97.29% (±1.25%), a median of 98.695% and a range of 86.49% – 99.59%. The Affymetrix HindIII 50K arrays had a mean SNP call rate of 94.25% (±1.29%), a median of 94.535% and a range of 86.45% – 99.45%.

Table 4.5 SNP call rates for 17 CNS PNETs analysed using Affymetrix 500K SNP arrays

39	96.63	87.52	92.075
40	94.27	97.19	95.73
41	96.07	95.5	95.785
2R	93.5	88.68	91.09
6	91.97	93.43	92.7
9	95.09	96.04	95.565
15	82.5	82.16	82.33

The Affymetrix NspI 250K array results for the CNS PNET DNA had a mean SNP call rate of 94.79% (±0.93%), a median of 94.8% and a range of 82.5% – 99.3%. The Affymetrix StyI 250K arrays had a mean SNP call rate of 93.71% (±1.55%), a median of 97% and a range of 78.73% – 99.47%. P, primary; R, recurrence.

Table 4.6 SNP call rates for 33 constitutional bloods of brain tumour patients analysed using Affymetrix 500K SNP arrays

ID	NspI 250K array (%)	StyI 250K array (%)	Average (%)
Blood11	90.39	94.45	92.42
Blood12	92.9	86.99	89.945
Blood13	98.26	87.64	92.95
Blood14	98.89	90.16	94.525
Blood15	90.13	87.03	88.58
Blood16	98.75	94.5	96.625
Blood17	98.47	94.43	96.45
Blood18	87.51	83.5	85.505
Blood19	98.69	93.99	96.34
Blood20	98.14	93.92	96.03
Blood21	97.78	92.62	95.2
Blood22	98.93	94.45	96.69
Blood23	98.49	94.95	96.72
Blood24	87.09	88.85	87.97
Blood25	88.19	88.76	88.475
Blood26	81.49	92.71	87.1
Blood27	88.63	90.22	89.425
Blood28	94.98	92.82	93.9
Blood29	93.01	91.55	92.28
Blood30	94.73	91.11	92.92
Blood31	86.05	91.36	88.705
Blood32	85.57	91.39	88.48
Blood33	86.12	92.75	89.435
Blood34	94.5	92.5	93.5
Blood35	98.66	93.67	96.165
Blood36	98.53	93.69	96.11
Blood37	84.49	87.63	86.06
Blood38	95.94	92.57	94.255
Blood39	92.28	90.61	91.445
Blood40	97.4	96.74	97.07
Blood41	98.31	74.07	86.19
Blood42	92.19	97.46	94.825
Blood43	93.08	95.41	94.245

The Affymetrix NspI 250K array results for the constitutional blood DNA had a mean SNP call rate of 93.29% (±0.91%), a median of 94.5% and a range of 81.49% – 98.93%. The Affymetrix StyI 250K arrays had a mean SNP call rate of 91.35% (±0.76%), a median of 92.57% and a range of 74.07% – 97.46%.

The identification of chromosome arm copy number imbalance and generation of Spotfire® heatmaps are described in chapter 2, Section 2.4.14, whilst the generation of

a SNPview ideogram is detailed in chapter 2, Section 2.4.15. Gene lists were generated as described in chapter 2, Section 2.4.14. Unsupervised hierarchical clustering and principle component analysis of cytoband copy numbers was performed as stated in chapter 2, Section 2.4.14. To identify associations between broad copy number imbalances and patient clinical characteristics, statistical analyses were applied (detailed in chapter 2, Section 2.8).

4.3 Results

4.3.1 Chromosomal arm imbalance in 46 CNS PNETs and pineoblastomas

To assess for chromosome arm alterations, copy number heatmaps were generated in both Spotfire® and SNPview for 46 CNS PNET and pineoblastoma samples analysed using the SNP microarray platform (Figures 4.1 – 4.3). A summary of the chromosome arm alterations identified for each patient are shown in Table 4.6 and the most common alterations overall are shown in Figure 4.4 and Tables 4.8a and 4.8b (in order of frequency). Overall, genetic gain was a more common event than loss. Many whole chromosome imbalances were identified, 39 whole chromosomes were gained and 2 whole chromosomes lost. Gain of chromosomes 12 and 20 were found in 4/46 (8.7%) CNS PNETs and pineoblastomas. At the chromosome arm level 108 chromosome arms were gained whilst 16 were lost. Gain of the long arm of chromosome 1 (1q) was the most common imbalance throughout the cohort, identified in 10/46 (21.7%) tumours. Gains of 2p and 21q were found in 7/46 (15.2%) cases whilst gains of 2q and 20q were identified in 6/46 (13%) cases. Other common gains identified in more than 10% of tumours analysed included 7p, 12p and 19p occurring in 5/46 (10.9%) cases. Interestingly, 3 CNS PNET patients harboured high level chromosome arm gains. CNS PNET20 harboured high level gain of 1q, whilst CNS PNET14 had high level gain of 13q and CNS PNET34 contained high level gain of 21q.

Chromosome arm loss was a relatively infrequent event, with loss of 16q the most common finding in 5/46 (10.9%) tumours. Loss of 9p was identified in 2/46 (4.3%) CNS PNETs. Interestingly one tumour (CNS PNET13) harboured a gain of chromosome 2p alongside the loss of 2q indicative of an isochromosome.

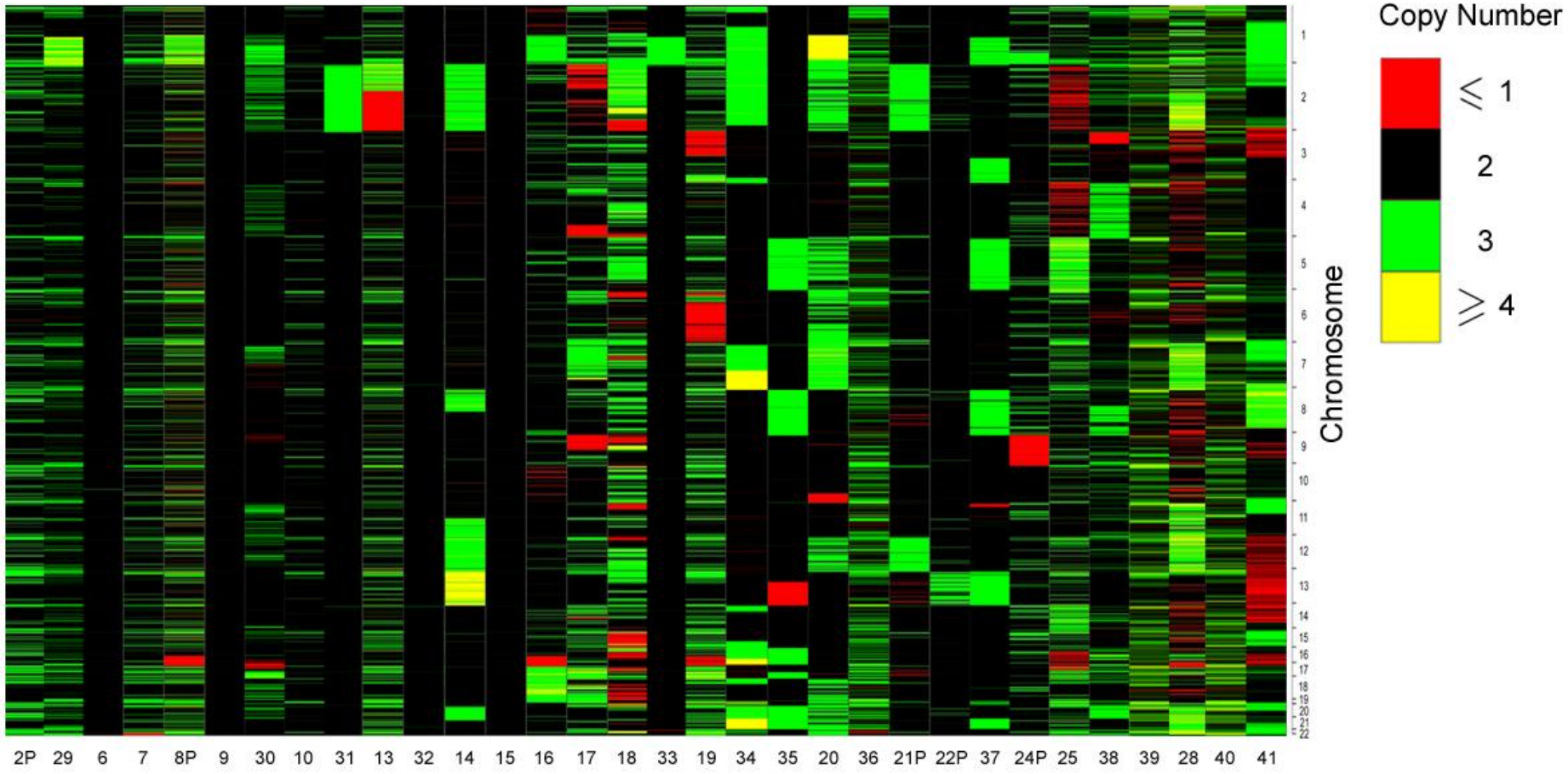

Figure 4.1 Spotfire heatmap visualisation of the genome wide copy number results for 32 primary CNS PNETs. 19 primary CNS PNETs were analysed using the 100K SNP arrays whilst 13 primary CNS PNETs were analysed using the 500K SNP arrays. P, primary.

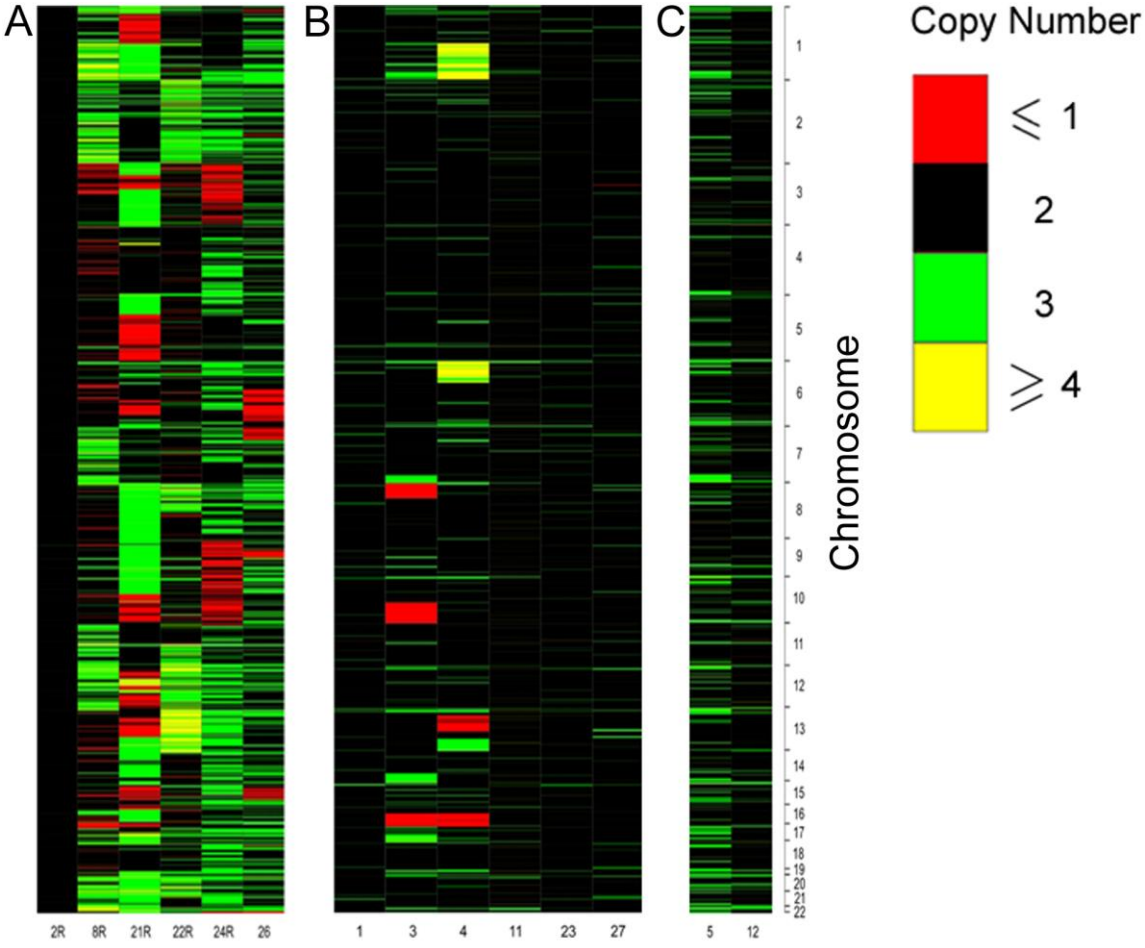

Figure 4.2A-C Spotfire heatmap visualisation of the genome wide copy number results for recurrent CNS PNETs and primary and recurrent pineoblastomas analysed using the 100K Affymetrix SNP arrays. Copy number results for 6 recurrent CNS PNETs (A), 6 primary pineoblastoma (B) and 2 recurrent pineoblastoma (C). R, recurrence.

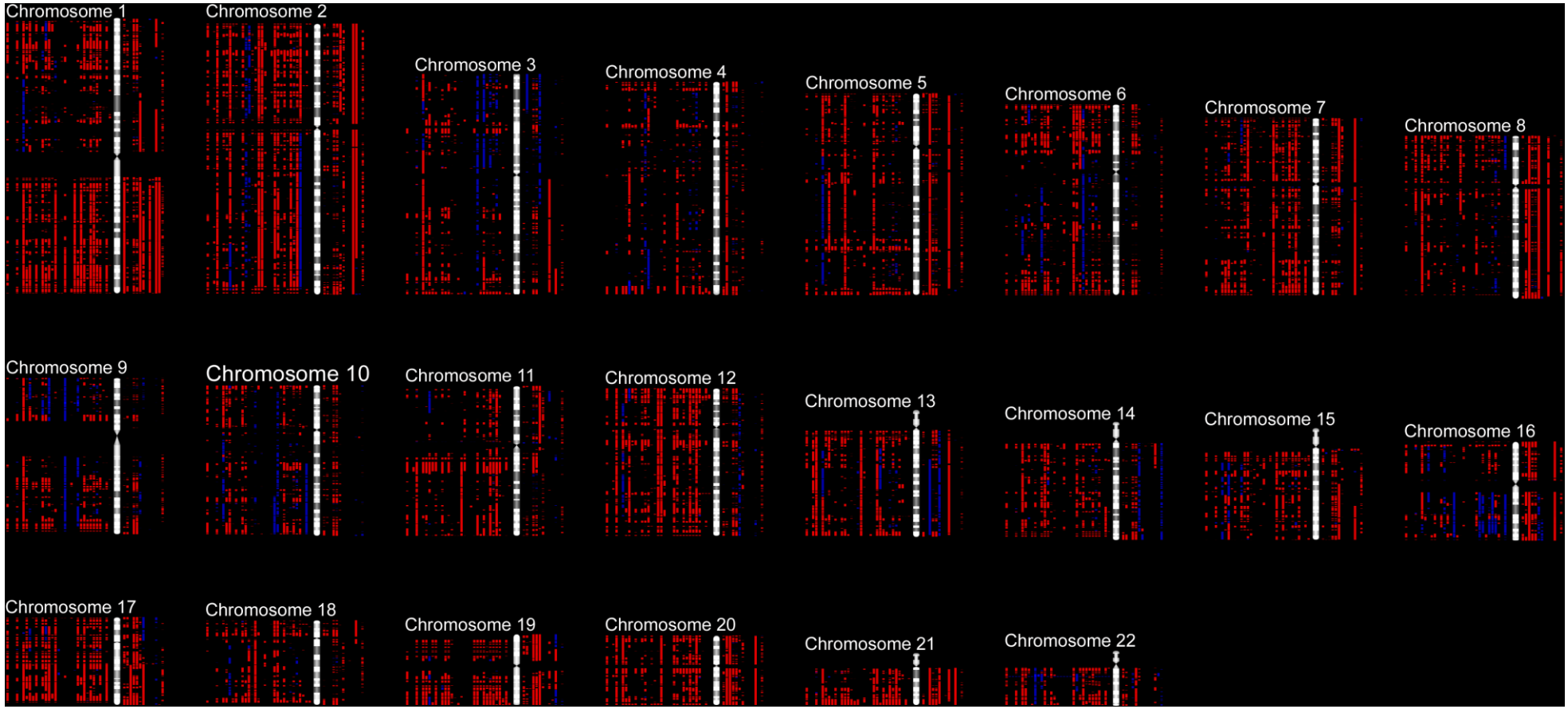

Figure 4.3 Chromosome ideogram of the 100K and 500K SNP array data visualised in SNPview. 100K data is left of the chromosome and 500K data is on the right. Red signifies gain in copy number and blue shows loss in copy number.

Table 4.7 CNS PNET and pineoblastoma chromosome arm copy number alterations identified using both 100K and 500K SNP array data.

ID	Gains	Losses
1	-	-
2P	-	-
2R	-	-
3	-	8p, 16q
4	1q, 6p	16q
5	-	-
6	-	-
7	-	22q
8P	1q, 19p	16q
8R	1q, 2q, 12p, 20q	-
9	-	-
10	-	-
11	-	-
12	-	-
13	2p**	2q**
14	2p, 2q, 8p, 11q, 12p, 12q, 13q*, 20p, 20q	-
15	-	-
16	1q, 17p, 17q, 18p, 18q	16q
17	7p, 17q	9p
18	2p	-
19	17p, 22q	3p, 6q, 16q, 17q
20	1q*, 2q, 7p, 7q, 18p, 19p, 21q, 22q	-
21P	2p, 2q, 12p, 12q	-
21R	1q, 3q, 5p, 8p, 8q, 9p, 9q, 10p, 16p, 17q, 19p, 19q, 20p, 20q, 21q, 22q	5q
22P	-	-
22R	12p, 12q, 13q, 20q	-
23	-	-
24P	-	9p, 9q
24R	17p, 18p, 21q	-
25	5p, 5q, 19p, 19q	-
26	17p	-
27	-	-
28	2q, 7p, 7q, 11p, 11q, 12p, 12q, 20p, 20q, 21q	-
29	-	-
30	-	17p
31	2p, 2q	-
32	-	-
33	1q	-
34	1q, 2p, 7p, 7q, 16p, 16q, 18p, 20p, 20q, 21q*	-
35	-	-
36	-	-
37	1q, 3q, 5p, 5q, 8p, 8q, 13q, 21q	-
38	-	-
39	-	-
40	-	-
41	1q, 2p, 7p, 8p, 8q, 11p, 19p, 19q, 21q	-

* High level gain (copy number ≥ 4), ** Isochromosome. P = primary, R = recurrence. Pineoblastomas ID's underlined.

Figure 4.4 Frequency plot of chromosome arm gains and loss in 46 CNS PNETs and pineoblastomas

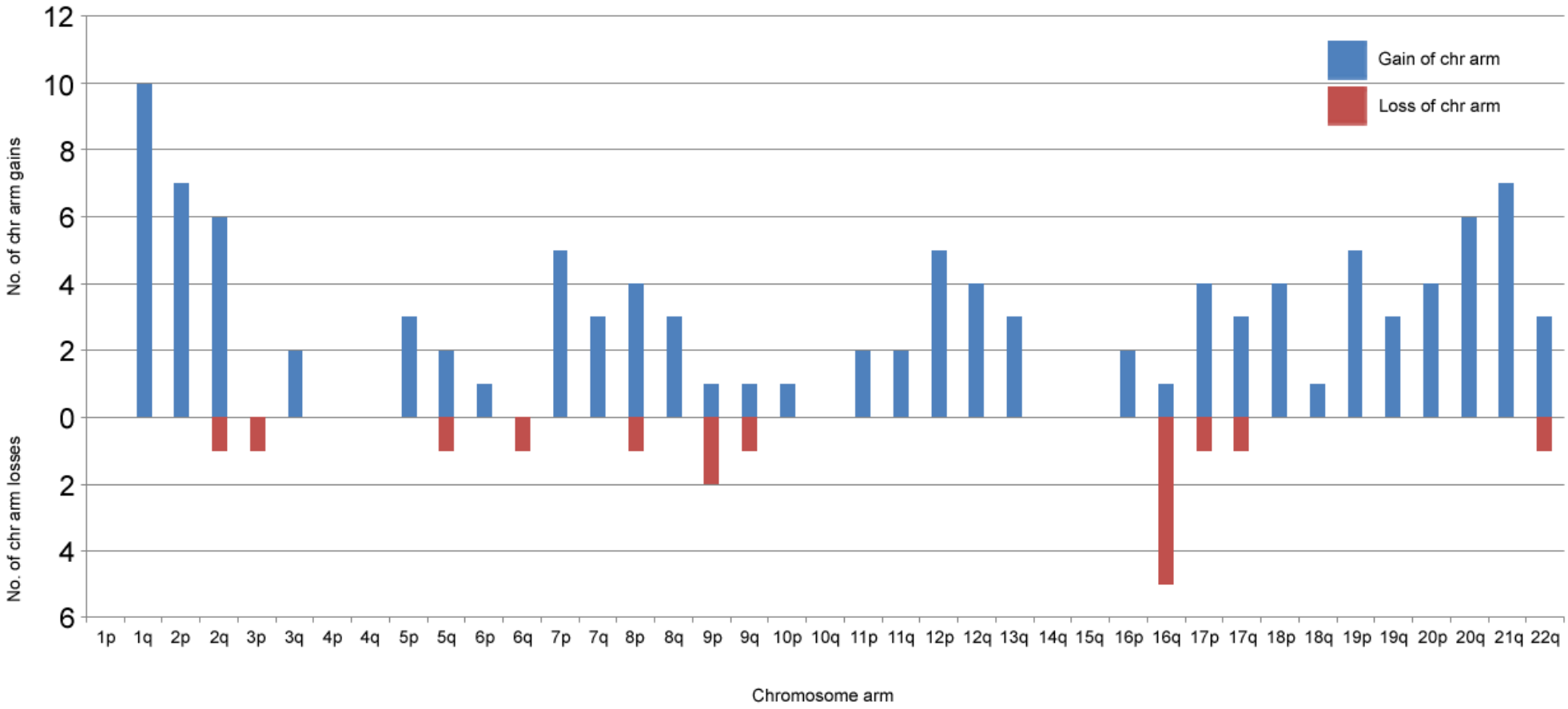

Tables 4.8a and 4.8b Chromosome arm alterations in 46 CNS PNETs and pineoblastomas in order of frequency

A. Chromosome arm gain

Chromosome arm	Number of CNS PNETs with imbalance
1q	10
2p	7
21q	7
2q	6
20q	6
7p	5
12p	5
19p	5
8p	4
12q	4
17p	4
18p	4
20p	4
5p	3
7q	3
8q	3
13q	3
17q	3
19q	3
22q	3
3q	2
5q	2
11p	2
11q	2
16p	2
6p	1
9p	1
9q	1
10p	1
16q	1
18q	1

B. Chromosome arm loss

Chromosome arm	Number of CNS PNETs with imbalance
16q	5
9p	2
2q	1
8p	1
17p	1
17q	1
22q	1
5q	1
9q	1
3p	1
6q	1

Separating the chromosome arm data by tumour locations (CNS PNET or pineoblastoma) and whether tumours were primary or recurrent samples led to the identification of chromosome arm alterations within specific clinical groups (Tables 4.9 - 4.11 and Figures 4.4 – 4.6).

Tables 4.9a and 4.9b Chromosome arm alterations in 32 primary CNS PNETs in order of frequency

A. Chromosome arm gain

Chromosome arm	Number of CNS PNETs with imbalance
1q	7
2p	7
2q	5
7p	5
21q	5
19p	4
7q	3
8p	3
12p	3
12q	3
18p	3
20p	3
20q	3
5p	2
5q	2
8q	2
11p	2
11q	2
13q	2
17p	2
17q	2
19q	2
22q	2
3q	1
16p	1
16q	1
18q	1

B. Chromosome arm loss

Chromosome arm	Number of CNS PNETs with imbalance
16q	3
9p	2
2q	1
3p	1
6q	1
9q	1
17p	1
17q	1
22q	1

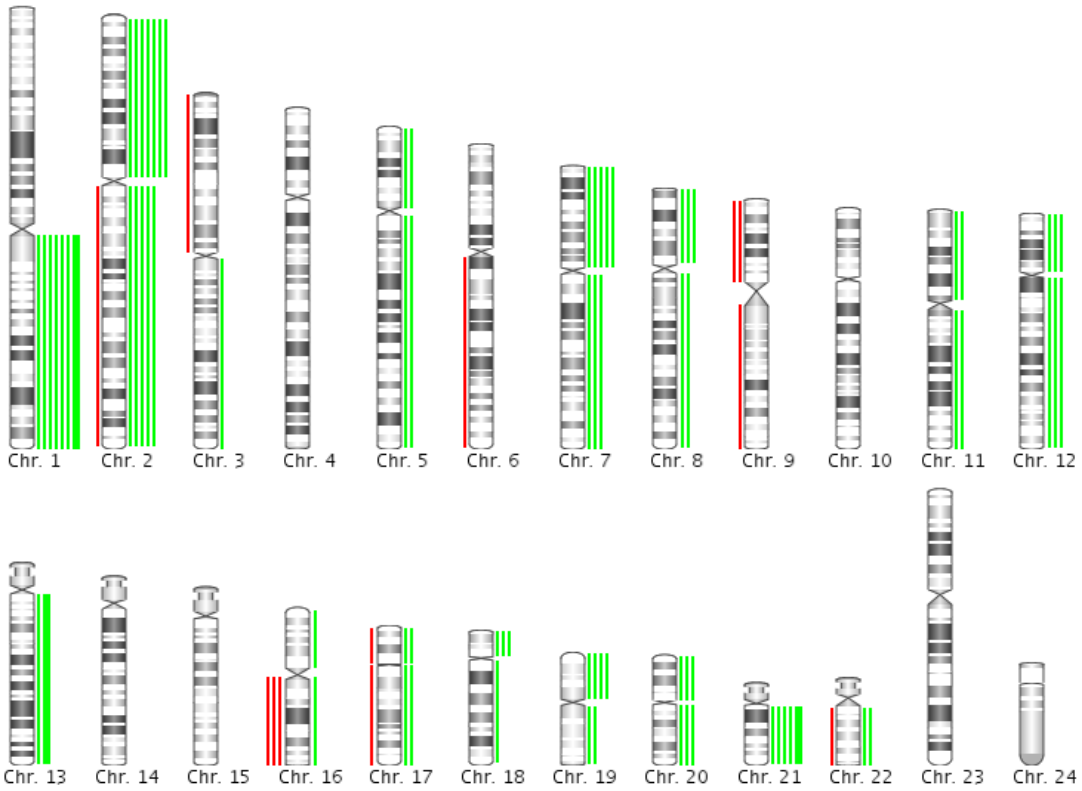

Figure 4.5 Schematic representation of chromosome arm alterations found in 32 primary CNS PNETs analysed using SNP arrays. Thick lines represent high level chromosome arm copy number alteration. Green = gain in copy number, red = loss in copy number.

Table 4.10a and 4.10b Chromosome arm alterations in 6 recurrent CNS PNETs in order of frequency

A. Chromosome arm gain

Chromosome arm	Number of CNS PNETs with imbalance
20q	3
1q	2
12p	2
17p	2
21q	2
2q	1

B. Chromosome arm loss

Chromosome arm	Number of CNS PNETs with imbalance
5q	1

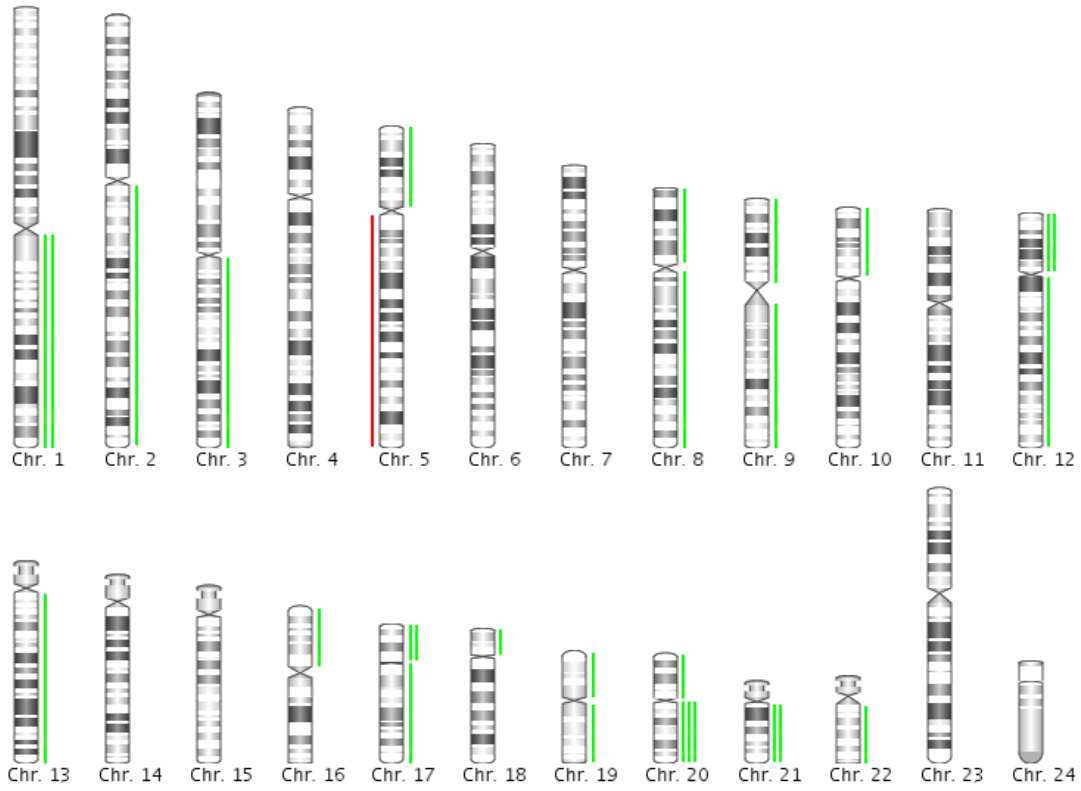

Figure 4.6 Schematic representation of chromosome arm alterations found in 6 recurrent CNS PNETs analysed using SNP arrays. Green = gain in copy number, red = loss in copy number.

Table 4.11a and 4.11b Chromosome arm alterations in 6 primary pineoblastomas in order of frequency

A. Chromosome arm gain

Chromosome arm	**Number of pineoblastomas with imbalance**
1q	1
6p	1

B. Chromosome arm loss

Chromosome arm	**Number of pineoblastomas with imbalance**
16q	2
8p	1

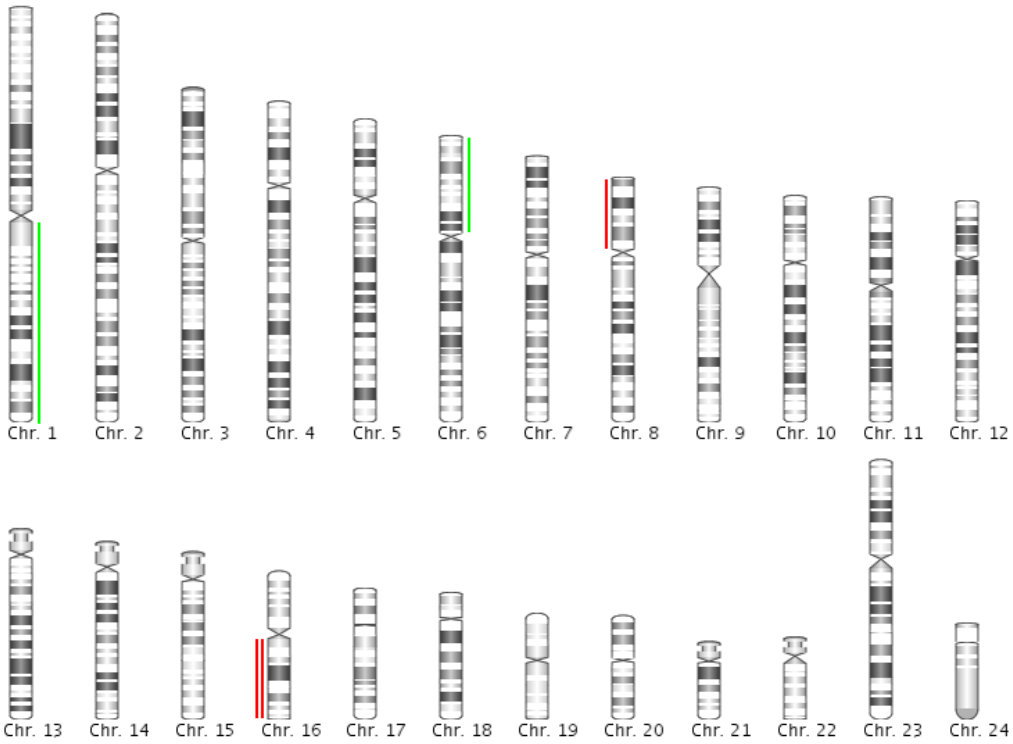

Figure 4.7 Schematic representation of chromosome arm alterations found in 6 primary pineoblastomas analysed using SNP arrays. Green = gain in copy number, red = loss in copy number.

No chromosome arm alteration was identified in the 2 recurrent pineoblastomas.

Statistical analysis was performed to test whether specific chromosome arm alterations were significantly associated with a clinically relevant group. Due to the relatively small CNS PNET and pineoblastoma cohort, no statistically significant results were identified linking specific chromosome arm alterations with clinical characteristics. Although no statistically significant associations were identified, we were able to make a number of observations. Tumours with gain of 2p, 2q or 21q were all CNS PNETs, not pineoblastoma. CNS PNETs with gain of 20q were found to be from male patients. Interestingly, all of the CNS PNETs with gain of 21q were over the age of 6 years. Finally, CNS PNETs with loss of 16q had a very poor outcome, with an overall survival of less than 2 years. This result is however only suggestive as the tumour samples used within this analysis were not uniformly treated as part of a clinical trial.

An interesting observation was the level of chromosome arm imbalance in primary PNETs arising in separate regions of the brain (CNS PNET or pineoblastoma). The CNS PNETs contained over 18 times the frequency of genomic imbalance than those

arising in the pineal region (pineoblastoma), (90 chromosome arm alterations vs 5, respectively). When compared by age, it was also noted that CNS PNET patients over the age of 3 years at diagnosis had 4 times more chromosome arm imbalance in the tumour than those under the age of 3 years (72 chromosome arm alterations vs 18, respectively). On statistical analysis however, the extent of chromosome arm imbalance was not significantly different in patients with tumours arising in separate locations (cerebral vs pineal) or in CNS PNET patients of different age groups (Mann-Whitney test, $p = 0.2301$ (2-tailed) and $p = 0.303$ (2-tailed), respectively.

On comparison of the patients with no copy number imbalance (termed 'balanced') and the clinical information an interesting result was identified. Although not statistically significant, all patients with balanced tumours were under the age of 5 years. 4 CNS PNETs analysed firstly using the 100K SNP arrays were found to be genetically balanced across the entire genome and were therefore analysed using the 5 times higher resolution 500K SNP array to identify smaller regions of copy number alteration, however none were identified (CNS PNET2R, 6, 9 and 15). Additionally a further CNS PNET analysed only using the 500K SNP arrays was identified with a balanced genome (CNS PNET32), thus a total of 5/46 (10.9%) copy number neutral CNS PNETs and pineoblastomas were identified.

4.3.2 Unsupervised hierarchical clustering of cytoband copy numbers for 25 primary CNS PNETs and pineoblastomas

To test whether genetically distinct subsets of tumours were present within the CNS PNET and pineoblastoma cohort, unsupervised hierarchical clustering and principal component analyses (PCA) were performed as an unbiased approach to analyse the cytoband imbalances of 25 primary CNS PNETs and pineoblastomas (analysed using the 100K SNP arrays) (Figure 4.8A-C). The average copy number of probes in each cytoband was calculated in Excel 2007 (Microsoft) and these values were used in the clustering analysis performed in Spotfire®. Utilizing the clinical information collected alongside CNS PNET and pineoblastoma samples, an investigation was made into whether the tumours clustered depending on specific clinical attributes and thus tumours of a common clinical group contained similar genetic signatures. Four cluster groups were identified containing similarly aberrant genomes (Figure 4.8A). The first group contained CNS PNETs with numerous whole chromosome arm aberrations

whereas the second group contained CNS PNETs with many small regions of loss and gain spanning the genome. The third group harboured pineoblastomas with only few whole chromosome arm copy number imbalances (Figure 4.8B). The fourth group contained 3 genetically balanced CNS PNETs. PCA of the cytoband copy number imbalance in 25 primary CNS PNETs and pineoblastomas revealed 4 cluster groups which were representative of the groups identified from the hierarchical cluster analysis, with the primary pineoblastomas of group 3 clustering separately to the majority of primary CNS PNETs. CNS PNETs 14 and 21P (of cluster group 3) clustered separately to the other tumours potentially warranting the addition of a further tumour subgroup.

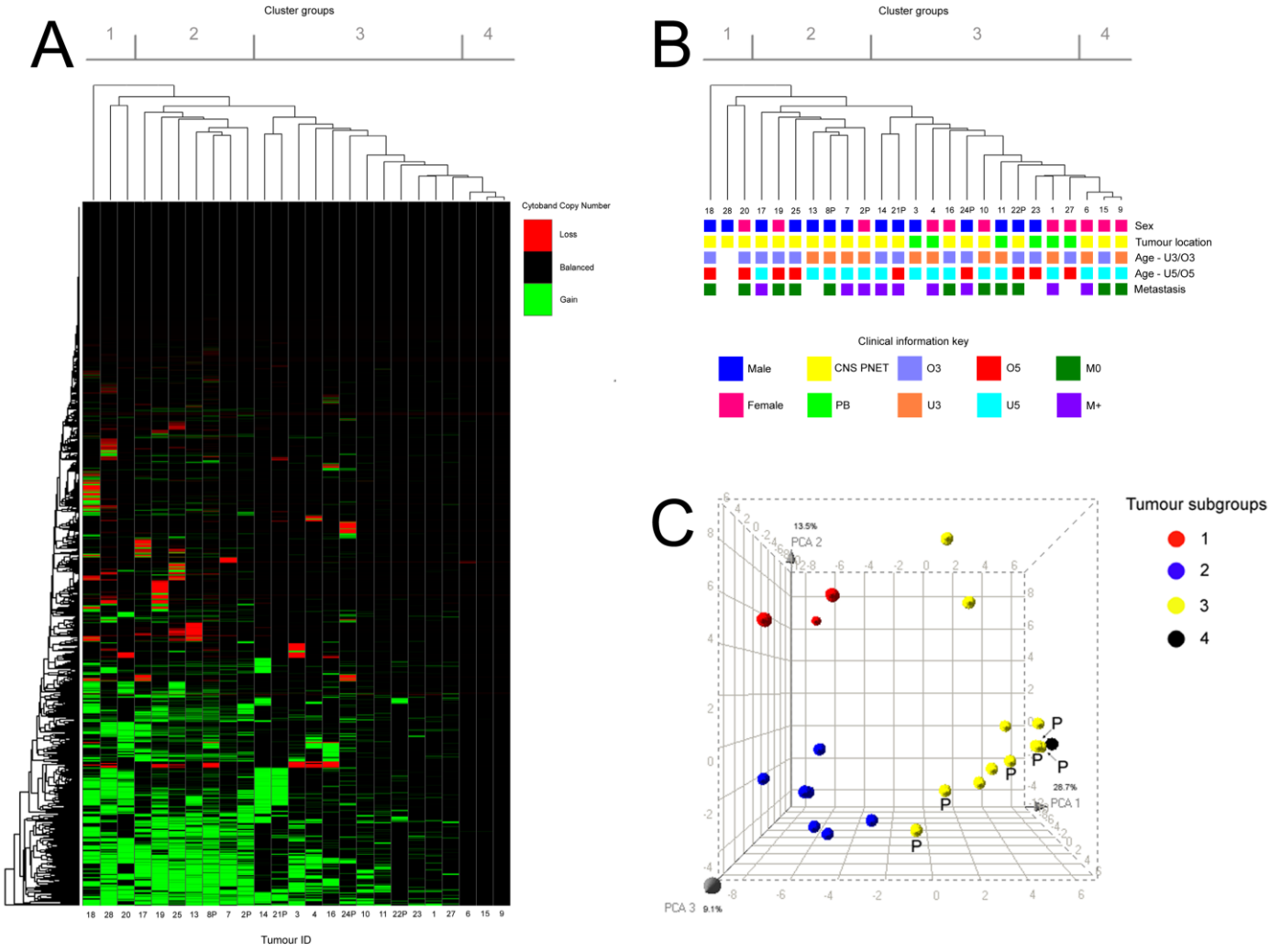

Figure 4.8 (A) Unsupervised hierarchical clustering of cytoband loss and gain for 25 primary CNS PNETs and pineoblastomas analysed using the Affymetrix 100K SNP arrays. Clustering was performed in Spotfire®. Group (1) consists of samples harbouring mainly whole arm aberrations, group (2) consists of samples with many small imbalances, group (3) consists of samples with few imbalances which are mainly whole chromosomal arm aberrations and group (4) comprises of samples with balanced genomes. Loss of cytoband copy number is shown in red whereas gain of cytoband is shown in green. P, primary; R, recurrence. **(B)** Clinical information plotted alongside the 4 cluster groups. All 6 primary pineoblastomas clustered into group 3. PB, pineoblastoma; O, over; U, under; M, metastasis. **(C)** Principal component analysis (PCA) of cytoband gain and loss in 25 primary CNS PNETs and pineoblastomas analysed using 100K SNP arrays. The clusters identified using PCA well represented the groups identified from the hierarchical cluster analysis, with the primary pineoblastomas of group 3 clustering separately to the majority of primary CNS PNETs. Cluster group 1 (with the highest amount of cytoband imbalance) clustered farthest away from the 3 'balanced' tumours of cluster group 4. CNS PNETs 14 and 21P (of cluster group 3) clustered separately to the other tumours. P, Pineoblastoma. Percentage variance of each principal component are also shown.

Statistical analysis was performed to test if the tumours containing similar genetic profiles within each cluster group shared specific clinical characteristics. The Fisher's exact test was used to compare the tumours of the 4 cluster groups with patient clinical information (including patient sex, tumour location, patient age and metastatic disease status). A single significant result was identified whereby the pineoblastomas clustered within group 3, separately from the majority of CNS PNETs clustering in groups 1, 2 and 4, ($p = 0.005$). Survival analysis was performed to test if patients with tumours clustering to a specific cluster group had a better or worse survival than those of other cluster groups, however, in this non-uniformly treated set of retrospectively collected tumours, no association with survival was identified.

4.4 Discussion

This high resolution SNP array analysis of the largest cohort of CNS PNETs and pineoblastomas to date has led to the identification of the most common chromosome arm copy number alterations. Previous studies have analysed only limited numbers of CNS PNETs and pineoblastomas using lower resolution karyotyping and CGH techniques, with the majority of studies concentrating on the genetic alterations of CNS PNETs, rather than pineoblastomas. The present study however, is the first to analyse a large cohort of 38 CNS PNETs and 8 pineoblastomas at the genetic level, using the high resolution SNP array platform. The use of a constitutional reference set to normalise tumour data was an important part of the study to exclusively identify tumour-specific alterations and exclude genetic alteration already present in the germline. The excellent SNP call rates of the arrays demonstrated the data generated was of high-quality. Current literature on the genetics of CNS PNETs demonstrates the complex genomic alterations occurring in these tumours (Avet-Loiseau, Venuat et al. 1999; Nicholson, Ross et al. 1999; Inda, Perot et al. 2005; Kagawa, Maruno et al. 2006; McCabe, Ichimura et al. 2006; Pfister, Remke et al. 2007). We identified copy number gain to be a more prominent feature than loss, possibly signifying oncogene activation as a more frequent event than tumour suppressor gene inactivation in CNS PNET and pineoblastoma pathogenesis.

Of the 46 CNS PNETs and pineoblastomas analysed, 1q gain was the most common event in 10/46 (21.7%) tumours. Gain of 1q has previously been identified in CNS PNET (Avet-Loiseau, Venuat et al. 1999; Nicholson, Ross et al. 1999; Rickert and

Paulus 2004; Inda, Perot et al. 2005; Pfister, Remke et al. 2007), in addition to other brain tumours including ependymoma, astrocytoma and medulloblastoma (Rickert, Simon et al. 2001; Ward, Harding et al. 2001; Dyer, Prebble et al. 2002; Mendrzyk, Korshunov et al. 2006; Lo, Rossi et al. 2007). Gain of 1q has been observed in the CNS PNETs of other studies. A report by Pfister *et al.*, found 5/21 (23.8%) CNS PNETs contained gain of 1q and those had a longer median survival than patients with tumours not containing gain of 1q (Pfister, Remke et al. 2007). On comparison of 1q gain and patient survival in our primary CNS PNET cases, we also found patients with 1q gain to have increased mean and median survivals (2.4 years and 1.7 years, respectively) compared to those without 1q gain (1.42 years and 0.8 years, respectively) however, this small difference was not tested statistically in these non-uniformly treated tumours. A previous study by Pfister *et al*., found 1q to be associated with a better mean survival in CNS PNETs whereas the study of other paediatric brain tumours has shown a correlation of 1q gain and poor prognosis. In 2006, Mendrzyk *et al.*, identified gain at 1q25 to be associated with a poor prognosis in ependymoma patients, with poor recurrence free and overall survivals of $p < 0.001$ and $p = 0.003$, respectively (Mendrzyk, Korshunov et al. 2006). Whilst in 2007, Lo *et al.*, identified the presence of 1q gain to be a negative prognostic marker in the survival of medulloblastoma patients, ($p < 0.0001$) (Lo, Rossi et al. 2007). Additionally, gain of 1q has been associated with an unfavourable outcome in Wilm's tumour, neuroblastoma and ewing's sarcoma, suggesting genes located on 1q could harbour putative roles in many paediatric cancers (Hirai, Yoshida et al. 1999; Hing, Lu et al. 2001; Ozaki, Paulussen et al. 2001). The research of larger CNS PNET and pineoblastoma cohorts is needed to better define the frequency of 1q gain, identify its role in the pathogenesis of CNS PNET and pineoblastoma, and to evaluate whether 1q gain can be used to predict the prognosis of CNS PNET patients. Validation of the gain of 1q needs to be performed in the present study, with fluorescence in situ hybridisation (FISH) one proposed method for this.

Gain of chromosome 2 was a common finding in the CNS PNET cohort of the present study, (2p in 7/32, 21.9% and 2q in 5/32, 15.6% primary CNS PNETs), and has previously been observed in 4/8 (50%) CNS PNETs from 2 CGH studies (Avet-Loiseau, Venuat et al. 1999; Inda, Perot et al. 2005). Improved characterisation of the involvement of chromosome 2 and the genes implicated in the pathogenesis of CNS PNET needs further elucidation. A novel finding in our dataset was a candidate isochromosome 2p. The loss of the q arm and gain of the p arm in the formation of an

isochromsome has been identified in many cancers (Mertens, Johansson et al. 1994). Interestingly, isochromosome 2p has been found in a subset of neuroblastomas giving rise to the over-representation of the *MYCN* gene (Valent, Le Roux et al. 2002). To date, no other CNS PNET in the literature has been identified with an isochromosome; however, karyotyping or FISH confirmation is still needed to validate this result.

There is currently conflicting evidence for the involvement of chromosome 19p in the pathogenesis of CNS PNET. Whilst our study identified gain of 19p in 4/32 (12.5%) CNS PNETs and a seperate study by Pfister *et al.*, identified 19p gain in 3/10 (30%) CNS PNETs by aCGH, this is in contrast to a study of 6 CNS PNETs by Inda *et al.*, which identified loss of 19p in 50% of cases (Inda, Perot et al. 2005; Pfister, Remke et al. 2007). Compilation of a larger sample set of CNS PNETs needs to be performed and be genetically analysed at high resolution to provide further evidence for the involvement of genes located on 19p in CNS PNET.

Three high level chromosome arm gains were identified by the SNP array analysis involving 1q, 13q and 21q. The high level gain of 4 copies of chromosome 1q in CNS PNET20 was validated using the FISH result from a separate Children's Brain Tumour Research Centre study and is shown in Figure 4.9. Although high level chromosome arm gain was a rare event in the CNS PNETs in this cohort, their involvement in the pathogenesis of individual CNS PNETs will be an interesting area of future work.

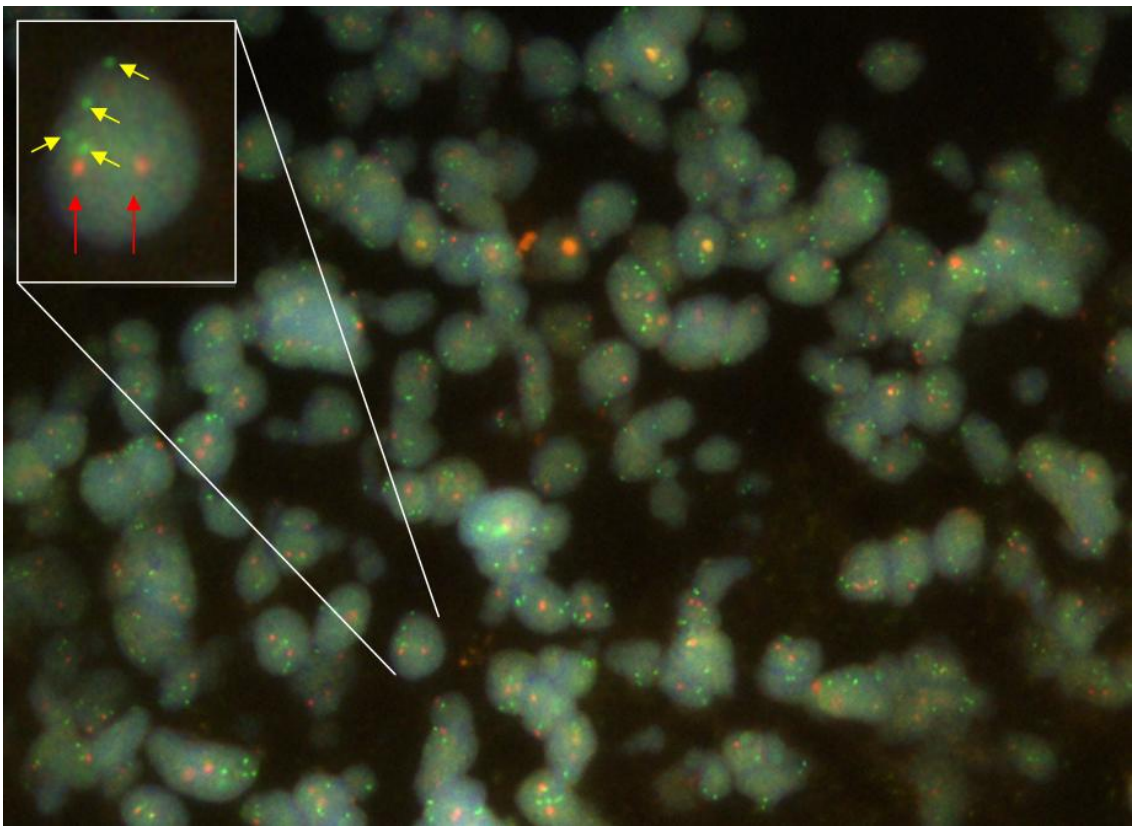

Figure 4.9 FISH validation of a high level gain of chromosome arm 1q in CNS PNET20. The SNP array data was used to identify 4 copies of 1q which was subsequently validated by FISH. The LSI 1p36/ LSI 1q25 dual colour probes were used, 1p36 (red probe) and 1q25 (green probe), (Abbott Molecular, Berkshire, UK). Top left diagram shows a cell with 4 copies of 1q25 (yellow arrows) whilst 1p36 (red arrows) has a normal copy number of 2. The FISH result and Figure was produced by J. Barrow of the Children's Brain Tumour Research Centre.

Despite the association between retinoblastoma and pineoblastoma, so called trilateral retinoblastoma (De Potter, et al. 1994; Amoaku, et al. 1996), our study did not reveal loss at the *RB1* locus (13q14) in the 8 pineoblastomas studied, however, the loss of 13q in CNS PNETs has previously been identified in other studies (Russo, Pellarin et al. 1999; Inda, Perot et al. 2005; McCabe, Ichimura et al. 2006; Pfister, Remke et al. 2007). More recently a homozygous deletion involving 13q14.2 was reported and we also identified 4 CNS PNETs with loss of this region (Lee 2008).

16q was the most frequently lost chromosome arm in 5/46 (10.9%) CNS PNETs and pineoblastomas. 16q loss has been reported in 2 previous CNS PNET studies involving 3/16 (18.75%) tumours (Inda, Perot et al. 2005; Pfister, Remke et al. 2007). Loss of 16q has also been observed in CGH studies of medulloblastoma involving 8/56 (14.3%) tumours (Kagawa, Maruno et al. 2006; Rossi, Conroy et al. 2006; Lo, Rossi et

al. 2007). CGH analyses by Inda *et al.,* in 2005, identified the loss of the short arm of chromosome 16 in 3/6 (50%) CNS PNETs, however this was not observed in the 46 CNS PNETs and pineoblastomas analysed in the present study (Inda, Perot et al. 2005).

Although no statistical associations were found when chromosome arm alterations were correlated to clinical attributes, a number of factors were observed. All 7 tumours with gain of 2p and 6 tumours with gain of 2q were CNS PNETs, not pineoblastomas, as were all 7 tumours with a gain involving 21q. This result could indicate specific alterations common to CNS PNET not found in pineoblastoma; however, larger studies are needed to confirm these findings. Of the 7 CNS PNETs with gain of 21q, 6 had information collected regarding patient age and 5 were over the age of 6 years. The relationship between gain of 21q in patients with CNS PNET and in older patients needs further elucidation. Firstly, the gain of 21q could be linked to the aberrant genetics specific to the cell or origin in CNS PNET or secondly the gain of 21q could be related to the older age of children suggesting differences in the tumourogenic mechanisms and pathways involved in CNS PNETs in children of different age groups. Interestingly, the 6 tumours with gain of 20q were male and had CNS PNETs, which could signify important differences in the genetic alterations in tumours arising in the different genders and different anatomical locations. 4/5 (80%) of the tumours with 16q loss had a very poor survival of less than 2 years following original diagnosis. Although the tumour cohort was too small for significant correlations linking the loss of 16q and poor survival, the result does suggest the loss of important tumour suppressor genes located on 16q to be involved with CNS PNET and pineoblastoma and poor outcome. This is however, only suggestive as the tumours studied in the present study were not treated uniformly as part of a clinical trial.

On comparison of the frequency of chromosome arm imbalance in PNETs arising in separate regions of the brain, the CNS PNETs harboured over 18 times the amount of imbalance than pineoblastomas (90 chromosome arm alterations vs 5, respectively). Also when compared by age, it was noted that CNS PNET patients over the age of 3 years at diagnosis harboured over 3 times more chromosome arm imbalance than those under the age of 3 years (72 chromosome arm alterations vs 23, respectively). This result reflects a previous study of pilocytic astrocytomas, which showed a tendency for an increased chromosome copy number change with age (Jones, Ichimura et al. 2006). Taken together, these results suggest fewer genetic changes are needed for

tumourigenic transformation in younger children and in tumours of the pineal region (pineoblastoma), thus highlighting distinct genetic alterations in brain tumours which are dependent on age and where the tumour arises.

Unsupervised hierarchical clustering was performed to identify if subsets of CNS PNETs and pineoblastomas containing similar genetic profiles were present in the tumour cohort. Clustering was performed for the cytoband copy numbers of 25 primary CNS PNETs and pineoblastomas analysed using the 100K arrays. Due to computational limitations in the programs available for cluster analysis, it was not possible to cluster the SNP array data using all 100,000 SNPs; therefore the data was simplified to contain averaged copy number data for ~800 cytobands. Unsupervised hierarchical clustering and PCA revealed 4 distinct groups of tumours: group 1 was characterised by many whole chromosome arm imbalances; group 2 by many small regions of loss and gain, group 3 by few whole chromosome arm imbalances; (all pineoblastomas residing in this group) and group 4 with 'copy number balanced' CNS PNET genomes. These groupings are reminiscent of those identified in ependymoma (Dyer, Prebble et al. 2002), but unlike ependymoma there are as of yet no clear clinical correlations within these genetic groups of CNS PNET. This may however, reflect the relatively small sample size of CNS PNETs available to study, as found initially for childhood ependymoma, warranting the study of a larger CNS PNET and pineoblastoma cohorts.

Cluster group 3 contained all 6 primary pineoblastomas (Fishers exact, 2 tailed, $p = 0.005$). This showed not only that the pineoblastomas shared similarities in genetic profiles, but also a genetic signature which differed from the majority of CNS PNETs. This result suggests that CNS PNET and pineoblastoma contain different genetic profiles which are potentially dependent on their (potentially site-specific) cell of origin. Distinct genetic profiles for the glial tumour astrocytoma, have previously been reported to be dependent on the brain region origin (Sharma, Mansur et al. 2007). The assumption that CNS PNET and pineoblastoma arise from different cells of origin is not yet proven and further investigation into the cells of origin are required. The link between genetics and anatomical location of CNS PNETs and pineoblastomas needs to be further tested in a larger cohort of tumours to confirm firstly the validity of this result and secondly to better define the genetic alterations which differ between these small round blue cell tumours. Primary tumours clustering into the cluster group 4

contained 3 CNS PNETs with copy number balanced genomes. 4 CNS PNETs (3 primary and 1 recurrence) with balanced genomes analysed on the 100K array were further analysed using the 500K array platform confirming that the tumours did not contain alteration in copy number at this higher resolution. A further CNS PNET analysed using the 500K array platform also contained a copy number balanced genome, with a total number of 5/38 (13.2%) copy number balanced CNS PNETs. To further confirm the neutral copy number status of these CNS PNETs, analysis using the even higher resolution SNP6 array, containing 1.8 million probes will be one option for future analysis. One concern was that the DNA analysed contained normal brain tissue which could be providing the normal DNA copy number, however this is unlikely as tumour content was careful checked. On comparison of the balanced CNS PNETs and patient clinical details, it was identified that all 5 CNS PNET samples were from CNS PNET patients under the age of 5 years. This suggests mechanisms other than aberrant DNA copy number could be important in the tumourigenesis of this subset of CNS PNETs. Other series have also reported a minority of CNS PNETs with balanced profiles (Pfister, Remke et al. 2007) (Lee 2008). Other paediatric brain tumours including 2 ependymomas and 24 astrocytomas have been identified with copy neutral profiles (Jones, Ichimura et al. 2006; Mendrzyk, Korshunov et al. 2006). There are several mechanisms which could potentially play important roles in the pathogenesis of copy number balanced paediatric brain tumours, for example regions of copy neutral LOH (aUPD), balanced chromosomal rearrangements, point mutations, alterations in gene expression levels and lastly epigenetic silencing are all mechanisms by which tumourigenesis can arise. Whether any of these are responsible requires further investigation.

Importantly, one CNS PNET in the present study had previously been analysed by both karyotyping and aCGH. A balanced translocation between chromosomes 15q and 19p was identified, however, this was not detected using the higher resolution SNP array analysis (Figure 4.10) (Dyer 2007). This highlights a limitation of using the SNP array platform and shows that balanced translocations may arise in CNS PNETs and needs further investigation. Although karyotyping is now deemed a relatively low resolution cytogenetic technique which has been overtaken by higher resolution technologies, this result shows the importance of karyotyping in brain tumour research and that karyotyping still has a role in uncovering novel translocations in CNS PNET, although

karyotyping can be a time consuming and laborious technique when brain tumour cells are often hard to grow in culture.

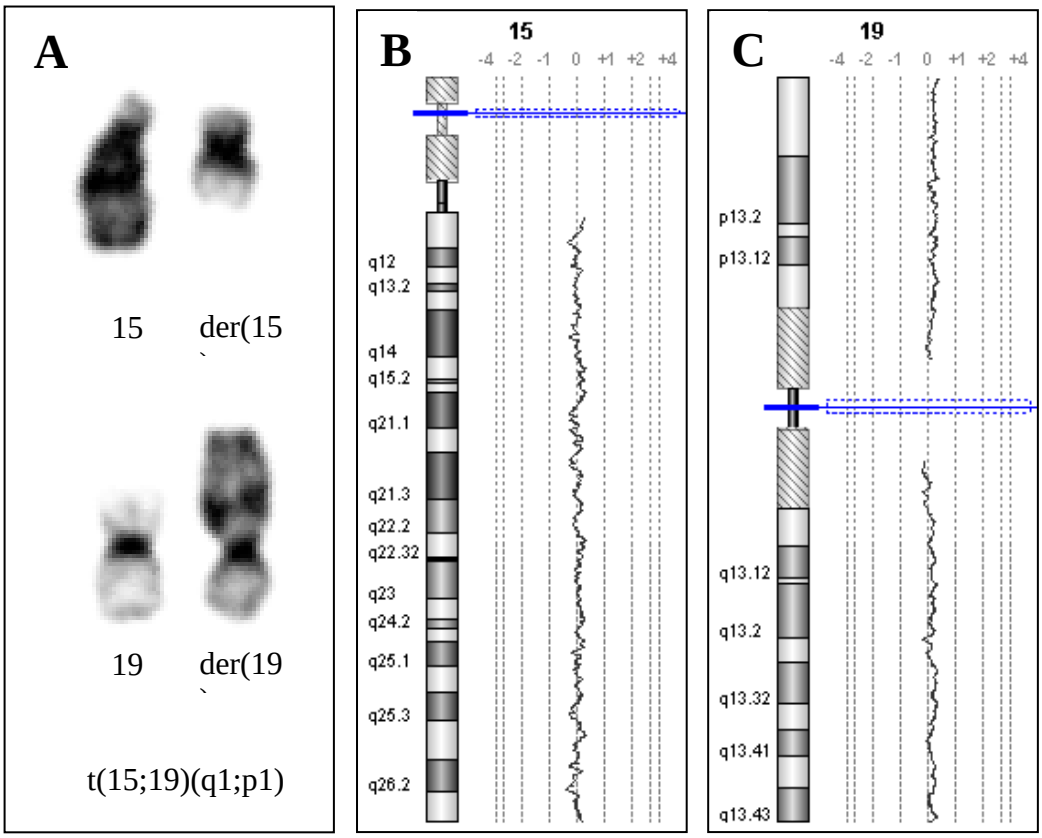

Figure 4.10 Cytogenetic and aCGH results from a genetically balanced tumour (CNS PNET9) showing a balanced translocation between chromosomes 15q and 19p. a) Normal and derived chromosomes 15 and 19; b) Chromosome view output from CGH Analytics 3.3.4 software for chromosome 15, showing a balanced profile, in particular there is no imbalance at translocation breakpoint (15q1); c) Chromosome view output from CGH Analytics 3.3.4 software for chromosome 19, showing a balanced profile, in particular there is no imbalance at translocation breakpoint (19p1). Reproduced from (Dyer 2007).

The complex and diverse genomic alterations in the majority of CNS PNETs was reflective of a study by Pomeroy *et al.*, who reported the cluster analysis of gene expression profiles for 42 paediatric brain tumours which included 8 CNS PNETs (Pomeroy, Tamayo et al. 2002). Interestingly, the 8 CNS PNETs studied by this group did not cluster together and remained separate. This report, in addition to our data, suggests the possibility of a number of CNS PNET subgroups which are genetically distinct to one another. These results also highlight the heterogeneity within tumours currently termed 'CNS PNET'. Even though the cytoband copy number clustering

analysis of the present study separated the data into 4 distinct genetic groups, the tumours within these groups did not share many of the same alterations and clustered on the amount of copy number alteration rather than specific alterations common to a cluster group. Increasing the CNS PNET cohort could potentially help to identify genetic groups within CNS PNETs sharing specific alterations, which could also link both genetic alterations and clinical characteristics with patient prognosis. Further investigation is now needed in a larger cohort of CNS PNETs.

CHAPTER 5

MAINTAINED AND ACQUIRED ALTERATIONS IN PRIMARY AND RECURRENT CNS PNET PAIRS

5.1 Introduction

Few studies have investigated the genetic basis of tumour progression and relapse in paediatric brain tumours. Currently, no studies have been performed to identify the genetics of progression in CNS PNET and pineoblastoma, perhaps due to the lack of recurrent tumour tissue available to research. As part of this thesis, a large dataset of clinical information was collected for the 48 CNS PNET and 12 pineoblastoma patients, including information on tumour relapse (chapter 3, Table 3.1). Of the clinical information available, 18/48 (37.5%) CNS PNET patients had relapse. The time taken to relapse was between 3.6 and 67 months, with mean and median times to relapse, 13.2 months and 6.6 months, respectively. 6/12 (50%) pineoblastoma patients had tumour relapse. The time taken for the tumour to relapse was between 7.2 – 51.6 months, with mean and median time to relapse 17.2 and 10.8 months, respectively. This information highlights that over a third of CNS PNET patients and half of pineoblastoma patients have tumours which relapse and the tumours recur in a short space of time. Following tumour relapse, the prognosis for CNS PNET and pineoblastoma patients is poor due to the lack of effective salvage therapies, thus the genetic characterisation of alterations involved in CNS PNET and pineoblastoma relapse need to be elucidated to better understand the tumourigenic pathways involved.

Regions of alteration identified in the primary tumours which are maintained at relapse, potentially encompass genes involved in sustaining tumourigenesis whilst regions of alteration acquired at relapse potentially encompass genes involved in aggressive tumour behaviour, tumourigenic transformation and consequently recurrence. 2 recent studies have investigated the genetic basis of tumour relapse in paediatric medulloblastoma and ependymoma. An article by Korshunov *et al.*, identified aberrations associated with relapse in medulloblastoma (Korshunov, Benner et al. 2008). FISH was performed for 28 paired primary and recurrent samples. 5 regions of interest were tested, *MYC, MYCN*, 6q, 17p and 17q. Both maintained and acquired alterations at relapse were identified. 11 cases had maintained i17q at relapse, 2 cases had maintained the amplification of *MYC*, i17q and gain of 6q, whilst 1 case had maintained amplification of *MYCN* and gain 17q. Finally a single primary and recurrent medulloblastoma pair had maintained gain of chromosome 17. Of the acquired alterations identified at relapse, 7 primary tumours with balanced genomes had acquired genetic alterations at the time of recurrence 5 had gained 17q (one of which

was part of an isochromosome 17q), two of which had also gained chromosome 6q. Two cases had *MYCN* amplification at relapse, not present in the primary sample and also had different histological features at relapse when compared to first presentation of the primary tumour (Figure 5.1). Both were diagnosed as classic medulloblastomas at presentation, whereas the recurrent samples were diagnosed as the large cell/anaplastic variant conferring a poorer prognosis.

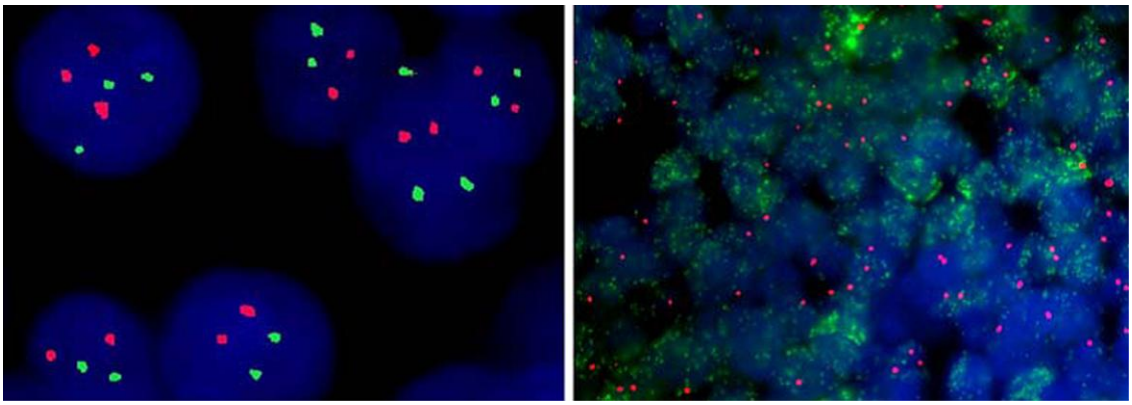

Figure 5.1 *MYCN* amplification in medulloblastomas analysed using FISH. *(left)* Primary tumour: balanced for *MYCN* at 2p24 (green) and the 2p11-q11 control (red) with 2 copies of each probe. *(right)* Recurrent tumour: *MYCN* amplification with numerous green signals and signal clusters. Reproduced from (Korshunov, Benner et al. 2008).

The accumulation of genetic alterations at relapse, not observed in the primary samples, holds invaluable information on the genes driving tumour growth and progression in tumour cells which are treatment resistant. The study showed that oncogenes located on 17q were of particular interest as the region was gained in the 5 recurrent tumours which were genetically balanced in the primary samples of the corresponding patients. The hypotheses questioned within the study by Korshunov *et al.*, need to be applied to CNS PNET and pineoblastoma to provide evidence of the underlying genetics driving tumour recurrence.

In 2009, Puget *et al*, investigated genetic alterations implicated in the progression of paediatric ependymoma and identified candidate genes on chromosome 9q33-34 (Puget, Grill et al. 2009). The study concentrated on the acquired alterations at relapse. Using 1Mb CGH BAC-microarrays they found a greater incidence of 9q34 gain, 1q gain and loss of 6q at relapse (54% vs 21%, 12% vs 0% and 27% vs 6%, respectively). Additionally, upon supervised hierarchical clustering they identified that gains of 9q33

and 9q34 were associated with tumour recurrence ($p = 0.03$ and $p = 0.009$, respectively).

These studies have increased our knowledge of the genetic alterations leading to medulloblastoma and ependymoma relapse. The strategies used within these studies now need to be utilized in the investigation of the genetic alterations leading to tumour relapse in CNS PNET and pineoblastoma. In chapter 6, a group-wise analysis for primary and recurrent CNS PNETs and pineoblastomas is performed; however, the analysis of 5 paired primary and recurrent CNS PNETs of this chapter will show more specifically similarities and differences of the genetic alterations involved in individual CNS PNET pairs.

5.2 Materials and methods

The inclusion of primary and recurrent tumour pairs from 5 CNS PNET patients enabled a comparison of the tumour genetics identified (using 100K SNP array analysis) at both presentation and relapse. No primary and recurrent pineoblastoma pairs were available for the study. Matching regions of gain and loss identified in both the primary and recurrent tumours from the same patient were termed 'maintained' alterations, whilst regions of gain and loss identified at relapse which was a normal copy number in the primary tumour were termed 'aquired' alterations. Visualisations of the genome-wide copy number alterations in the each of the 5 primary and recurrent CNS PNET pairs was generated in Spotfire (detailed in chapter 2, Section 2.4.14). To visualise the maintained and aquired copy number alterations in the 5 primary and recurrent pairs, an in house tool 'SNPview' was used (described in chapter 2, Section 2.4.15). Gene lists were also created in Spotfire® for the most common regions of maintained and acquired copy number alteration, and ordered by frequency (as detailed in chapter 2, Section 2.4.14).

5.3 Results

5.3.1 Chromosome arm imbalance identified in 5 primary and recurrent CNS PNET pairs

With the exclusion of recurrent tumour CNS PNET2R (with a copy number balanced genome), the remaining 4 recurrent CNS PNETs (CNS PNET8R, 21R, 22R and 24R) contained a greater frequency of copy number alteration (Figure 5.2). Chromosome arm alterations were not identified in the primary and recurrent tumours of patient 2. For patient 8, both the primary and recurrent tumours (CNS PNET8P and 8R), harboured gain of 1q. Although the primary CNS PNET contained gain of 19p and loss of 16q, these alterations were not maintained at relapse. New alterations only found at relapse were found within the recurrent tumour of patient 8; gain of 2q, 12p, 12q and 20q. The genomic imbalance identified in the primary and recurrent tumours of patient 21 differed dramatically. Whilst CNS PNET21P harboured gain of chromosomes 2 and 12, not present at relapse, the recurrent tumour contained the gain of 16 different chromosome arms not observed in the primary sample. Loss of 5q was also identified in CNS PNET21R which was not present in the primary sample (CNS PNET21P). Only few gains were identified for CNS PNET22P, with a large proportion of chromosome 13q gained. This gain in copy number was subsequently identified at relapse, however, with a further increase in copy number. Chromosomes 12 and 20q were gained CNS PNET22R, but were not present in the primary tumour (CNS PNET22P). Hemizygous loss of chromosome arms 9p and 9q were identified in the primary tumour of patient 24, with large regions of loss on chromosome 9 also present at relapse. The recurrent tumour (CNS PNET24R) had acquired many copy number alterations, including large regions of gain involving many chromosomes, apart from chromosome 1 with a balanced copy number and large regions of chromosomes 3, 9 and 10 which were deleted.

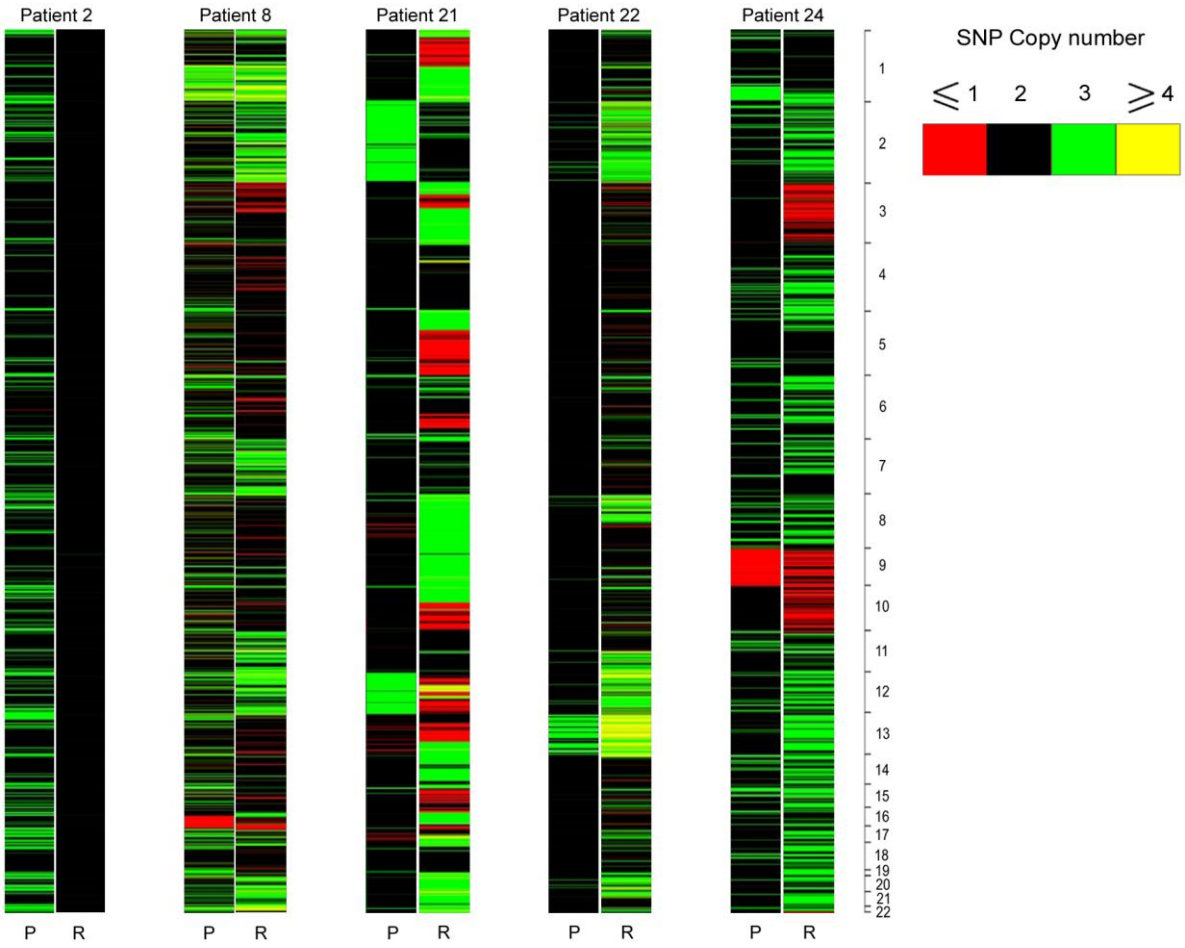

Figure 5.2 Spotfire heatmap visualisation of 5 paired primary and recurrent CNS PNETs analysed using 100K SNP arrays. P = primary tumour, R = paired recurrent tumour. Increasing chromosome number from top to bottom.

5.3.2 Common regions of maintained copy number alteration in 5 primary and recurrent CNS PNET pairs

Using 100K SNP arrays, genome wide copy number analysis of 5 paired primary and recurrent CNS PNETs was performed to identifying regions of maintained copy number gain and loss (visualised in Figure 5.3). To identify the most common focal regions of maintained copy number gain and loss, the most frequently altered regions shared between the 5 tumour pairs were identified from the 100K SNP array analyses and ordered by frequency (Tables 5.1 and 5.2).

Table 5.1 Most common regions of maintained copy number gain in 5 primary and recurrent CNS PNET pairs

Cytoband	Start (bp)	End (bp)	Gene symbol	No. of tumour pairs with gain maintained
2p21	43818511	44611058	*PLEKHH2 (i) - C2orf34 (i)*	4
2p21	42391499	43803761	*EML4 (i) - PLEKHH2 (i)*	3
2p12	75644173	75748577	*TMEM166 (i) - MRPL19 (i)*	3
2q33.1	197195870	197207681	*HECW2 (u)*	3
2q37.1	231320474	233166697	*CAB39 (i) - EIF4E2 (d)*	3
2q37.2	235439780	236072455	*SH3BP4 (u) - CENTG2 (i)*	3
4q35.1	184043457	184086599	*DCTD (u-d)*	3
8p23.2	4561747	4744792	*NULL (d)*	3
8q11.22	52217779	52463524	*PXDNL (i-d)*	3
11q13.4	72701001	76262809	*ARHGEF17 (i) PHCA (i)*	3
21q22.3	41737239	44369022	*MX1 (i) - PWP2 (CDS)*	3

bp, base pair; No., number; d, downstream; i, intronic; u, upstream; CDS, coding region; NULL, no gene symbol.

Regions of maintained gain were observed more frequently than loss. The most commonly maintained regions of alteration involved focal gains on chromosome 2, particularly at 2p21 (in 4/5, 80% CNS PNET pairs). This region of chromosome 2 encompasses 2 genes encoding ATP-binding cassette (ABC) transporters, *ABCG5* and *ABCG8* (Figure 5.4).

Figure 5.3 Chromosome ideogram of the maintained copy number imbalances in 5 paired primary and recurrent CNS PNETs analysed using Affymetrix 100K SNP arrays. Visualisation created in SNPview. Maintained loss at relapse is shown to the left of each chromosome (blue) and maintained gain is the right (red).

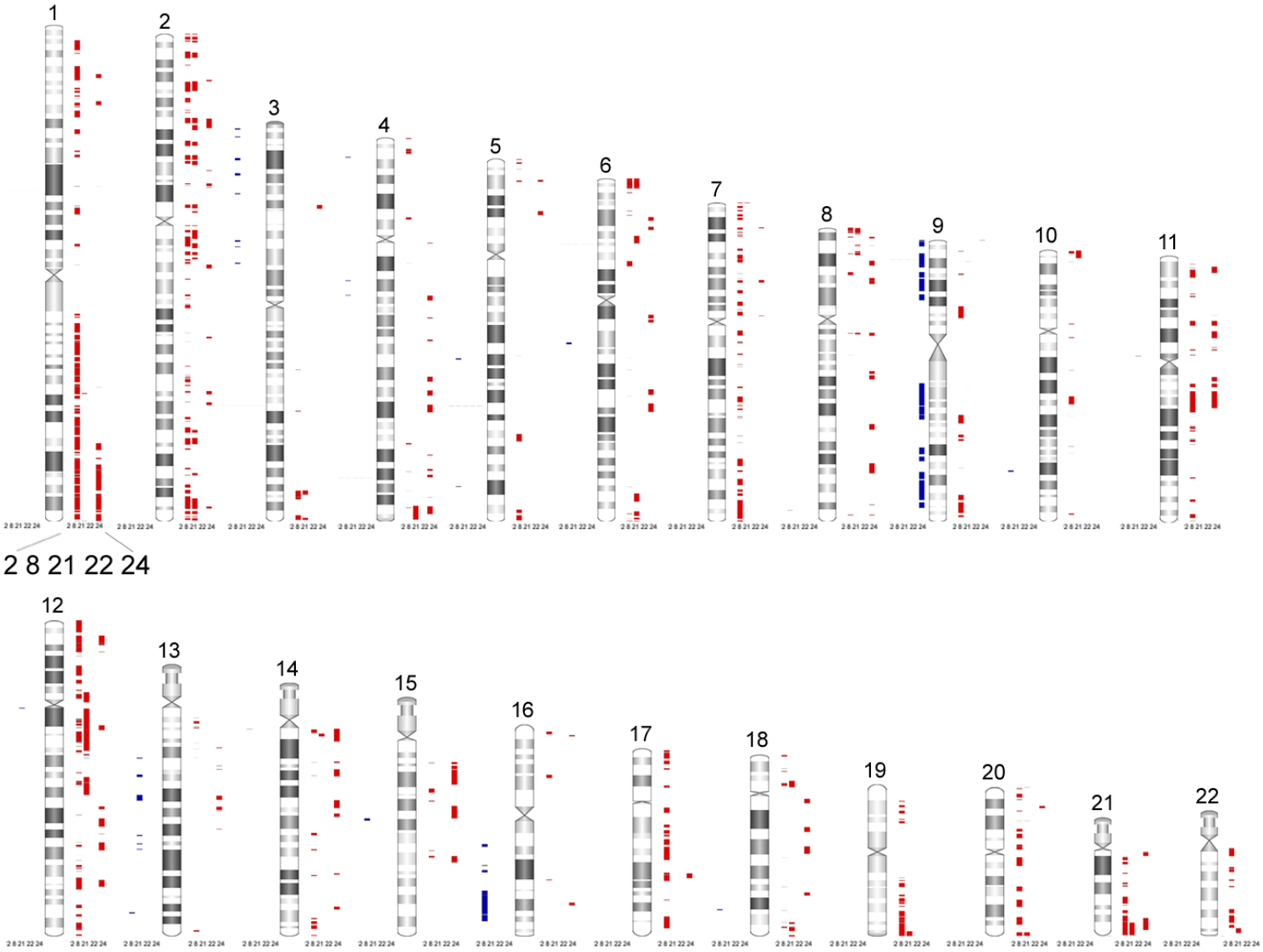

Figure 5.4 Genes located on chromosome 2 between 43818511 – 44611058bp. www.ensembl.org

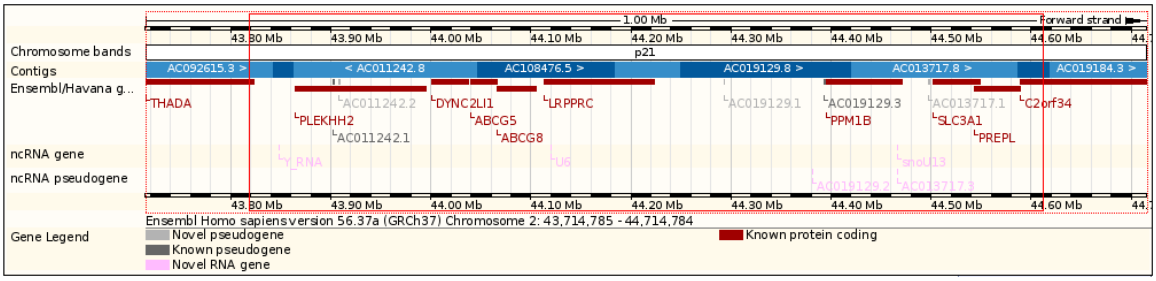

Table 5.2 Most common regions of maintained copy number loss in 5 primary and recurrent CNS PNET pairs

Cytoband	Start (bp)	End (bp)	Gene symbol	No. of tumour pairs with loss maintained
3p26.2	3833692	4303811	*LRRN1 (i) - NULL (i)*	1
3p26.1	7711246	7980785	*GRM7 (d)*	1
3p24.3	18544296	19589049	*SATB1 (u) - EFHB (d)*	1
3p24.2 - p24.1	25964778	27217157	*OXSM (d) - NEK10 (i)*	1
3p22.3	36031184	36346505	*STAC (u)*	1
3p14.2	59414093	60016727	*FHIT (i-d)*	1
3p14.2	62456915	62651525	*CADPS (i)*	1
3p14.1	70507951	70922442	*MITF (d) - NULL (u)*	1
4p16.1	9761976	9949584	*WDR1 (u) - KIAA1729 (d)*	1
4q13.3	71067652	71252668	*C4orf40 (d) - C4orf35 (d)*	1
4q21.1	78358184	78551611	*CXCL13 (u)*	1
5q21.1	99560705	99996277	*TMEM157 (u-d)*	1
5q34	163038000	163226607	*MAT2B (d) - NULL (u)*	1
6q14.1	81656549	82365338	*BCKDHB (d) - NULL (u)*	1
8q24.3	140603245	140739149	*KCNK9 (i-d)*	1
9p24.3	239391	508675	*C9orf66 (u) - ANKRD15 (i)*	1
9p24.3 - p24.2	894078	3267834	*DMRT1 (i) - RFX3 (i)*	1
9p24.1 - p23	6759229	13460926	*JMJD2C (i) - MPDZ (u)*	1
9p22.3 - p22.1	15909694	18520255	*C9orf93 (i) - ADAMTSL1 (i)*	1
9p22.1 - p21.3	19438473	25389371	*ASAH3L (i) - TUSC1 (d)*	1
9p21.2 - p21.1	27141645	30030317	*TEK (i) - LINGO2 (u)*	1
9q21.11 - p21.31	71401145	82445304	*APBA1 (i) - NULL (u)*	1
9q21.31 - p21.33	82781305	87024911	*TLE1 (d) - NTRK2 (d)*	1
9q21.33	87204305	89183421	*NULL (d) - FLJ45537 (d)*	1
9q31.1	103306774	106516009	*NULL (i) OR13D1 (d)*	1
9q31.2	107721067	109912128	*TMEM38B (d) - NULL (u)*	1
9q32 - p33.1	115341270	118967331	*RGS3 (i) - ASTN2 (i)*	1
9q33.1 - q34.13	119502074	133054549	*ASTN2 (u) - NUP214 (i)*	1

10q25.1	109899733	110441328	*NULL (d)*	1
11p11.12	50396846	51230448	*OR4C12/OR4A5 (d)*	1
12q12	36588164	36830367	*NULL (u-d)*	1
13q13.3 - q14.11	39388685	39616680	*NULL (u)*	1
13q14.2	46240774	47326516	*LRCH1 (d) - SUCLA2 (d)*	1
13q21.1	55025447	57344531	*NULL (u) - PCDH17 (d)*	1
13q21.33	71648649	71972490	*NULL (u)*	1
13q22.2	75393452	75633401	*NULL (d) - KCTD12 (d)*	1
13q22.3 - q31.1	77591733	77889154	*NULL (d) - POU4F1 (d)*	1
13q33.2	104273019	104635900	*SLC10A2 (u) - DAOA (u)*	1
14q11.2	19574026	19631920	*OR4K13 (u) - OR4K17 (u)*	1
15q21.2	50919088	51740487	*WDR72 (i-d)*	1
16q12.1 - q12.2	50191797	51373170	*SALL1 (u) - CHD9 (u)*	1
16q21	58937971	59436112	*NULL (d)*	1
16q21	61108982	62116021	*CDH11 (d)*	1
16q22.2 - q23.2	69587667	79509800	*NULL (i) - CDYL2 (u)*	1
16q23.2 - q23.3	79787842	82569605	*PKD1L2 (i) - EFCBP2 (CDS)*	1
18q22.1 - q22.2	64751059	65165094	*CCDC102B (i) - DOK6 (u)*	1

bp, base pair; No., number; d, downstream; i, intronic; u, upstream; CDS, coding region; NULL, no gene symbol.

The most common regions of maintained copy number loss involved chromosomes 3p, 9p (encompassing *CDKN2A/B*), 9q and 13q (in 1/4, 20% CNS PNET pairs).

5.3.3 Common regions of acquired copy number alteration in 5 primary and recurrent CNS PNET pairs.

An overview of the acquired copy number gain and loss in 5 primary and recurrent CNS PNET pairs is shown in Figure 5.5. To identify the most common regions of acquired copy number gain and loss, the most frequently altered regions found at recurrence (not observed in the paired primary) were identified from the 100K SNP array analyses and ordered by frequency (Tables 5.3 and 5.4, respectively). The most common regions of acquired copy number gain at relapse involved focal gains of 1p36.11 – p35.3, 6p21.1, 11q23.3, 16p13.3, 17q25.1 and 21q21.1 in 4/5 (80%) CNS PNET pairs. Broader regions of acquired gain at relapse were identified between 19q13.2 – 13.33, 20p13 – 11.21 and 20q11.22 – 13.2, in 4/5 (80%) CNS PNET pairs. The acquired gain identified at 1p35.3

Figure 5.5 Chromosome ideogram of the acquired copy number imbalances in 5 paired primary and recurrent CNS PNETs analysed using Affymetrix 100K SNP arrays. Visualisation created in SNPview. Acquired loss at relapse is shown to the left of each chromosome (blue) and acquired gain is the right (red).

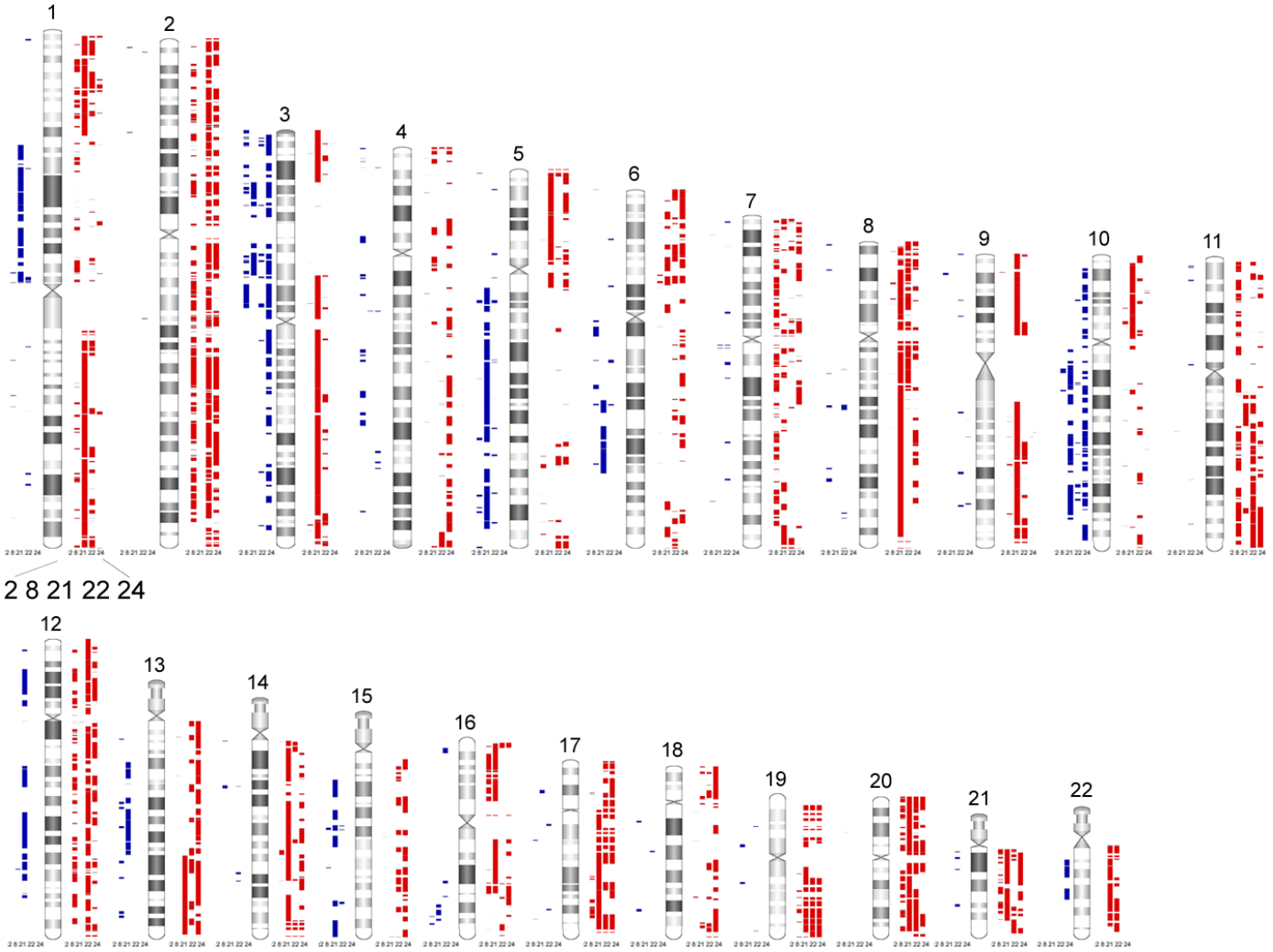

Table 5.3 Most common regions of acquired copy number gain in 5 recurrent CNS PNETs when compared to paired primary tumour

Cytoband	Start (bp)	End (bp)	Gene symbol	No. of paired recurrences with gain acquired
1p36.11 - p35.3	27744311	29631044	*AHDC1 (i) - PTPRU (d)*	4
6p21.1	43761383	44426050	*MRPS18A (i) - SPATS1 (i)*	4
11q23.3	116255283	117435638	*KIAA0999 (i) - NULL (u)*	4
11q23.3	117687870	118510298	*CD3E (i) - MIZF (CDS)*	4
16p13.3	4094852	4223830	*ADCY9 (i) - NULL (i)*	4
17q25.1	68935600	70324574	*SDK2 (i) - TMEM104 (i)*	4
19q13.2	45796700	46260460	*LTBP4 (i) - CYP2A13 (u)*	4
19q13.31	49522732	49659554	*ZNF228 (3UTR) - ZNF229 (u)*	4
19q13.32	51308749	53202202	*IGFL3 (d) - ELSPBP1 (i)*	4
19q13.33	57024188	57117898	*ZNF577 (d) - ZNF649 (u)*	4
20p13	86460	546278	*DEFB127 (i) - TCF15 (u)*	4
20p13	867023	2543515	*RSPO4 (d) - TMC2 (i)*	4
20p13	4237066	4871286	*PRNP (u) - SLC23A2 (i)*	4
20p12.3	5086590	5148227	*CDS2 (i-d)*	4
20p12.3	5376300	5921189	*NULL (u) - MCM8 (i)*	4
20p12.1	13539596	13990478	*TASP1 (i) - MACROD2 (i)*	4
20p11.22 - p11.21	21514717	24122028	*NKX2-2 (u) - NULL (d)*	4
20q11.22	32970124	33549562	*ACSS2 (i) - CEP250 (i)*	4
20q13.2	52149491	52200214	*CYP24A1 (d) - BCAS1 (u)*	4
20q13.2	52317793	53764130	*DOK5 (u) - CBLN4 (d)*	4
21q21.1	17034406	17067648	*NULL (u-d)*	4

bp, base pair; No., number; d, downstream; i, intronic; u, upstream; CDS, coding region; 3'UTR, 3'untranslated region; NULL, no gene symbol.

in 4/5 (80%) CNS PNET pairs, encompasses *PTPRU*, encoding for a protein tyrosine phosphatise receptor. Acquired gain of SNPs upstream of *BCAS1* (20q13.2), in 4/5 (80%) CNS PNET pairs, encodes for the breast carcinoma amplified sequence 1 gene.

Table 5.4 Most common regions of acquired copy number loss in 5 recurrent CNS PNETs when compared to paired primary tumour

Cytoband	Start (bp)	End (bp)	Gene symbol	No. of tumours with loss acquired
3p14.2	60064326	60265103	*FHIT (i)*	4
3p14.2	62672251	63050307	*CADPS (u-i)*	4
3p26.3	48603	170962	*CHL1 (u)*	3
3p26.1	6808535	7698179	*GRM7 (u-i)*	3
3p24.2	25816202	25922324	*LRRC3B (u) - OXSM (d)*	3
3p24.1	27271826	28762307	*NEK10 (i) - RBMS3 (u)*	3
3p24.1	29367167	30693536	*RBMS3 (i) - TGFBR2 (i)*	3
3p22.3	35962610	36236321	*ARPP-21 (d)*	3
3p14.2	59239357	60016727	*FLJ42117 (u) - FHIT (i)*	3
3p14.2	60285416	60898214	*FHIT (i) - NULL (u)*	3
3p14.2	62389174	62651525	*CADPS (i)*	3
3p14.2	63095602	63549171	*SYNPR (u-i)*	3
3p14.1	67394681	68764105	*SUCLG2 (d) - FAM19A4 (d)*	3
3p12.2 - p12.1	83008414	84564348	*GBE1 (u) - CADM2 (u)*	3
5q12.1 - q12.3	62799515	63949443	*NULL (u) - RGS7BP (d)*	3
6q16.3	102132218	102765994	*GRIK2 (i-d)*	3
10q21.1	53916144	54712286	*DKK1 (d) - NULL (u)*	3
10q23.1	87036546	87285785	*KIAA1128 (d)*	3
10q23.31	92305795	92456069	*NULL (u) - HTR7 (d)*	3
10q25.1	106413736	107318185	*SORCS3 (i) - SORCS1 (d)*	3
10q25.1	109789992	110457665	*NULL (d)*	3
10q25.2	113018607	113744337	*ADRA2A (d)*	3
15q21.3	52518427	52901811	*NULL (i) - C15orf15 (d)*	3

bp, base pair; No., number; d, downstream; i, intronic; u, upstream; NULL, no gene symbol.

The most common regions of acquired copy number loss identified at relapse involved intronic SNPs within the fragile histidine triad gene, *FHIT* (3p14.2) and SNPs upstream and intronic of the calcium dependent secretion activator 1 gene, *CADPS* (also 3p14.2) in 4/5 (80%) CNS PNET pairs. Broader regions of acquired copy number loss were identified at 3p26.3 – 3p12.1 and 10q21.1 – 10q25.2, in 3/5 (60%) CNS PNET pairs.

5.4 Discussion

The comparison of copy number imbalance in 5 primary and recurrent CNS PNET pairs showed there to be a greater frequency of copy number alteration at relapse in the majority of cases, especially copy number gain. This result potentially demonstrates that

oncogene activation is more prevalent than tumour suppressor gene inactivation in the progression of CNS PNET, however, an increase in genomic instability caused by therapy could be masking the driving alterations of tumour recurrence. Although primary tumour CNS PNET2P contained focal regions of copy number gain, the paired recurrent tumour (CNS PNET2R) did not contain copy number imbalance. This result highlights that in a subset of CNS PNETs, mechanisms other than copy number alteration are potentially responsible for tumour relapse, and these include alterations at the gene expression level potentially caused by altered levels of methylation or miRNA expression.

Chromosome 2p was frequently gained in the SNP array analysis (detailed in chapter 4), which suggested potential oncogenes involved in both initiating and sustaining CNS PNET pathogenesis are located on this chromosome arm warranting further investigation. The comparison of 5 paired primary and recurrent CNS PNETs identified the most frequent region of maintained gain involved genes on 2p21 in 4/5 (80%) CNS PNETs. This genomic region encompasses 2 ATP-binding cassette (ABC) transporters (*ABCG5* and *ABCG8*). ABC transporters have previously been proposed to be involved in the multidrug resistance of brain tumours (Ling 1997). Interestingly, one recent study has identified a link between ABCG5-positivity and poor prognosis in colorectal cancer patients (Hostettler, Zlobec et al. 2010). Thus, validation of *ABCG5* now needs to be performed to confirm the copy number results within the 4 CNS PNET primary and recurrent pairs. If confirmed with maintained gain, function analyses using CNS PNET cell lines will be an important area of future work. Regions of maintained loss were not commonly shared between the 5 CNS PNET pairs and was identified in 1/5 (20%) CNS PNETs pairs involving broad regions of chromosome 3p, 9, 13q and 16q.

Upon analysing the aquired alterations at relapse, gain in copy number was identified more frequently than loss. When analysing the acquired alterations found at relapse, it was difficult to distinguish between true ‘driving’ alterations linked to tumour progression and recurrence with those arising due to an increase in genomic instability caused by therapy (passenger alterations). Thus, following validation of gene copy number results, functional analyses of candidate genes identified will enable the distinction between aberrant genes which possess a tumourigenic role and those which do not. Broad regions of acquired copy number were identified involving chromosome arms 19q, 20p and 20q, whilst focal regions of acquired gain were identified at 1p36.11

– 35.3, 6q21.1, 11q23.3, 16p13.3, 17q25.1 and 21q21.1 (each in 4/5, 80% CNS PNET pairs). *PTPRU* (1p35.3), was found have acquired copy number gain at relapse (4/5, 80% CNS PNET pairs). The encoded protein is a protein tyrosine phosphate which regulates many cellular processes included cell growth, differentiation and mitotic cycle and oncogenic transformation. *PTPRU* would therefore be an interesting candidate oncogene worthy of validation and if confirmed, could be worthy to take forward for functional work. Aquired loss of copy number was most frequently identified at 3p14.2, encompassing *FHIT* and *CADPS* (4/5, 80% CNS PNET pairs). Broader regions of acquired loss was identified at 3p26.3 – 12.2 and 10q21.1 – 25.2. In summary, candidate maintained and acquired gene gain and loss now needs to be validated using either real time qPCR or FISH analyses. Future studies incorporating larger sample sets of paired primary and recurrent tumours are now required to further this initial work.

CHAPTER 6

REGIONS ENCOMPASSING CANDIDATE GENES POTENTIALLY INVOLVED IN THE PATHOGENESIS OF CNS PNET AND PINEOBLASTOMA

6.1 Introduction

Until recently, aCGH was the highest resolution technology available to interrogate tumour genomes for copy number alterations, however; recent advances in technology have led to the ability to provide information at the SNP level. Although conventional and array CGH technologies are of immense benefit to cancer research, the SNP array platform allows for a more precise detection of the boundaries of copy number alteration, thus refining between regions of normal and altered copy number. In addition to providing a higher resolution, SNP array analysis generates information regarding a SNPs copy number and also genotypes each SNP allele. Therefore, SNP arrays can be used to identify areas of LOH and aUPD previously undetecTable by other methodologies. Thus, for a given SNP, if a patient's constitutional blood has a heterozygous SNP allele call (A/B) and the corresponding patient's tumour SNP allele call is homozygous (A/A or B/B), the loss in heterozygosity can be identified. SNP arrays are the first high resolution platform able to provide genome-wide information for LOH. The ability to generate both copy number and LOH information for each SNP also provides the opportunity to analyse each tumour genome for regions of acquired uniparental disomy (aUPD). aUPD is a somatic event whereby one allele is lost and the remaining copy is duplicated resulting in homozygosity. If an allele is lost and the remaining copy is mutant, duplication of the mutant allele by aUPD can give rise to a pathogenetic mutation. Interestingly, recent reports have shown regions of aUPD to be associated with the prognosis of patients with lymphoma (O'Shea, O'Riain et al. 2009). Identifying regions of aUPD (also known as copy neutral LOH) will be essential in the identification of mutational gene targets in CNS PNET and pineoblastoma.

We have therefore analysed a large cohort of 46 CNS PNETs and pineoblastomas at the highest resolution available to date, to identify (i) common genes/genetic regions with copy number imbalance in primary and recurrent, CNS PNETs and pineoblastomas, (ii) genes/genetic regions of amplification and homozygous deletion and (iii) genes/regions acquiring UPD. In addition using the clinical information collected for each patient, gene copy number alterations were then compared to patient clinical variables and statistical associations investigated. In 'chapter 4, Section 4.3.1', the analysis of 46 CNS PNETs and pineoblastomas using the Affymetrix 100K and 500K SNP arrays led to the identification of the most common chromosome arm alterations, firstly overall and secondly in clinically related patient groups. The analysis identified gain of

chromosome 1q and loss of 16q to be common events in the pathogenesis of CNS PNET and pineoblastoma, hence, candidate genes identified within these chromosome arms will be of particular interest. Thus, candidate genes/genetic regions involved in the development and progression of CNS PNET and pineoblastoma will be elucidated and verified to identify aberrant pathways involved in the pathogenesis of CNS PNET and pineoblastoma, potentially providing novel targets/pathways for therapeutic intervention.

6.2 Materials and methods

CNS PNET and pineoblastoma samples analysed using the 100K and 500K SNP arrays are documented in chapter 4, Table 4.2. Copy number gene lists were generated as described in chapter 2, Section 2.4.14 for 46 CNS PNETs and pineoblastomas. The aUPD analysis was performed as described in chapter 2, Section 2.4.16.

6.3 Results

6.3.1 Gene copy number imbalance in CNS PNET and pineoblastoma

6.3.1.1 Genomic regions encompassing candidate gene gain in primary CNS PNETs analysed using 100K SNP arrays

The most frequent copy number gains (involving 5 consectutive SNPs) in primary CNS PNETs analysed using the 100K SNP array were identified and ordered by frequency (Table 6.1, Figure 6.1). Of the 19 primary CNS PNETs analysed, regions of copy number gain (with 5 or more consectutive SNPs) most commonly involved 12p13.33, 12q22 and 21q22 (each in 14/19, 73.7% primary CNS PNETs). Broad regions of gain were identified along chromosomes 1q25.3 – 1q42, 12p13.2 – 12p13.33 and 12q13.11 – 12q24.33. Gain at 5q31.3 was a common event (identified in 13/19, 68.4% primary CNS PNETs) encompassing a protocadherin gene cluster.

Table 6.1 Regions of increased copy number in 19 primary CNS PNETs analysed using the 100K SNP array platform

Cytoband	Start (bp)	End (bp)	Gene symbol	Total	CN 3 or 4	CN 5 or 6
12p13.33	93683	546804	*IQSEC3(i) - NINJ2(i)*	14	13	1
12q22	94205728	94797422	*VEZT(CDS) - CCDC38(i)*	14	14	0
21q22.3	43759285	44369022	*HSF2BP(d) - PWP2(CDS)*	14	13	1
1q25.3	180623022	180696351	*GLUL(CDS) - RGSL2(i)*	13	10	3
1q42.3	234362639	234362983	*GPR137B(u)*	13	11	2
5q31.2 - 31.3	137861990	139156866	*ETF1(d) - PSD2(i)*	13	12	1
5q31.3	139225946	139985396	*NRG2(i) - CD14(d)*	13	13	0
5q31.3	140027784	140371106	*WDR55(i) - PCDHA2(3'UTR)*	13	12	1
5q31.3	140594436	140679241	*NULL(5'UTR)*	13	10	3
5q31.3	140697923	140799142	*PCDHGA1(d) - PCDHGA3(i)*	13	9	4
7p21.3	12487750	12502468	*NULL(u) - SCIN(u)*	13	13	0
7p21.3	12615495	12681102	*SCIN(i) - ARL4A(u)*	13	12	1
7p14.1	39576702	39628793	*C7orf36(CDS) - RALA(u)*	13	8	5
12p13.33	661471	1471285	*WNK1(u) - ERC1(3'UTR)*	13	12	1
12p13.33	1732419	1926624	*ADIPOR2(i) - DCP1B(i)*	13	12	1
12p13.31	6450843	8787981	*MRPL51(d) - FAM80B(i)*	13	12	1
12p13.31	8986493	9312096	*M6PR(i) - NULL(u)*	13	12	1
12p13.31	9384549	9986108	*NULL(d) - FLJ46363(d)*	13	13	0
12q13.11 - 13.2	46880781	48178418	*DKFZP779L1853(3'UTR) - SPATS2(i)*	13	12	1
12q13.13	50200322	50434904	*GALNT6(u) - SCN8A(i)*	13	12	1
12q13.13	50462502	50469752	*SCN8A(i)*	13	11	2
12q13.13	50935536	50960976	*NULL(i) - KRT81(d)*	13	9	4
12q23.1	94903058	95164036	*HAL(i) - ELK3(i)*	13	13	0
12q24.11 - 24.13	108935070	111296665	*ANKRD13A(i) - RPL6(d)*	13	12	1
20q13.33	61366365	62376958	*NULL(i) - PCMTD2(3'UTR)*	13	12	1
21q22.3	41737239	42462999	*MX1(i) - UMODL1(d)*	13	12	1
21q22.3	42865011	43558435	*SLC37A1(i) - CRYAA(d)*	13	12	1
21q22.3	44740755	46924583	*KRTAP10-8(u) - PRMT2(d)*	13	12	1
1p34.3	39020861	39323829	*RRAGC(d) - MACF1(i)*	12	12	0
1q25.3	180759210	180845658	*RGSL1(i) - RGS8(d)*	12	11	1
1q25.3	180879332	181099214	*NULL(i) - DHX9(i)*	12	12	0
1q25.3	183180625	183219736	*FAM129A(u-i)*	12	9	3
1q32.1	198909108	198971377	*DDX59(u)*	12	8	4
1q32.1	199014490	199415656	*CAMSAP1L1(i) - TMEM9(u)*	12	9	3
1q42.2	229804452	232334433	*NULL(i) - SLC35F3(i)*	12	12	0
1q42.2 - 42.3	232415025	232783216	*SLC35F3(i) - TARBP1(u)*	12	11	1
1q42.3	233084260	234352185	*NULL(u) - GPR137B(u)*	12	12	0
1q42.3 - 43	234376647	235219020	*GPR137B(i) - NULL(d)*	12	12	0
1q43	239266618	240425395	*RGS7(i) - PLD5(i)*	12	12	0
2p25.3	53452	672363	*SH3YL1(d) - TMEM18(u)*	12	11	1
2p25.1	8704019	9066695	*C2orf46(u) - MBOAT2(u)*	12	11	1
2p25.1	9812469	9968504	*TAF1B(u-i)*	12	11	1

2p25.1	10029352	10265469	*GRHL1(i) - C2orf48(i)*	12	10	2
2p21	43818511	44580233	*PLEKHH2(i) - C2orf34(i)*	12	12	0
2p16.1	55301236	55766465	*FLJ31438(i) - PNPT1(i)*	12	9	3
5q31.2	137378377	137733367	*C5orf5(i) - JMJD1B(i)*	12	11	1
7p21.3	12475419	12481007	*NULL(u)*	12	12	0
7p11.2	54669673	54865896	*NULL(d) - SEC61G(u)*	12	11	1
8p23.3	180568	2150810	*ZNF596(i) - MYOM2(d)*	12	12	0
10q26.3	135125348	135189835	*NULL(i) - SYCE1(d)*	12	9	3
11q13.1	64130080	64310154	*SLC22A12(d) - SF1(u)*	12	8	4
11q13.1 - 13.2	64642021	68216480	*ZNHIT2(u) - MTL5(d)*	12	11	1
11q13.4	72701001	73761415	*ARHGEF17(i) - PGM2L1(i)*	12	11	1
11q13.4 - 13.5	73935137	76262809	*NULL(d) - PHCA(i)*	12	12	0
12p13.32	3638603	3730037	*EFCAB4B(i)*	12	12	0
12p13.32	3737732	3953126	*PARP11(u-d)*	12	11	1
12p13.32	4028445	4364055	*PARP11(u) - FGF6(d)*	12	12	0
12p13.2	10023132	10203229	*CLEC12A(i) - OLR1(3'UTR)*	12	12	0
12q13.12 - 13.13	48364391	49957396	*FMNL3(i) - LOC57228(u)*	12	11	1
12q15	67955713	68283401	*CPSF6(d) - LRRC10(d)*	12	12	0
12q23.2	100614130	100647352	*MYBPC1(d) - SYCP3(i)*	12	9	3
12q24.11	108051728	108600642	*NULL(i) - C12orf34(u)*	12	11	1
12q24.31	119395013	123492096	*SFRS9(u) - NCOR2(i)*	12	11	1
12q24.33	130772542	132194394	*SFRS8(i) - ZNF140(d)*	12	12	0
13q12.11	22169909	22177254	*NULL(u)*	12	6	6
13q12.12	22234562	22245061	*NULL(u)*	12	7	5
13q12.12	22601270	22616744	*NULL(u-d)*	12	9	3
13q12.12	22630199	23434660	*SGCG(u) - FLJ46358(u)*	12	11	1
13q12.12 - 12.13	23996413	24518426	*PARP4(u) - PABPC3(u)*	12	12	0
15q13.1	27327709	27378426	*NDNL2(u-d)*	12	11	1
15q13.1	27381829	27534051	*NDNL2(u)*	12	12	0
15q13.1 - 13.3	27717103	29817989	*TJP1(d) - OTUD7A(u)*	12	12	0
18q23	72322501	76068963	*NULL(i) - PARD6G(i)*	12	12	0
20q13.33	60877329	61061785	*NTSR1)d) - C20orf59(i)*	12	11	1
21q22.3	41468687	41636158	*BACE2(i) - FAM3B (i)*	12	11	1
21q22.3	42531275	42800012	*ABCG1(i) - RSPH1(u)*	12	11	1

Genes in blue were validated by RT-qPCR. bp = base pair, Total = number of samples with alteration, CN = copy number, d = downstream, i = intronic, u = upstream, 3'UTR = 3' untranslated region, 5'UTR = 5' untranlated region, CDS = coding region, NULL = no gene name.

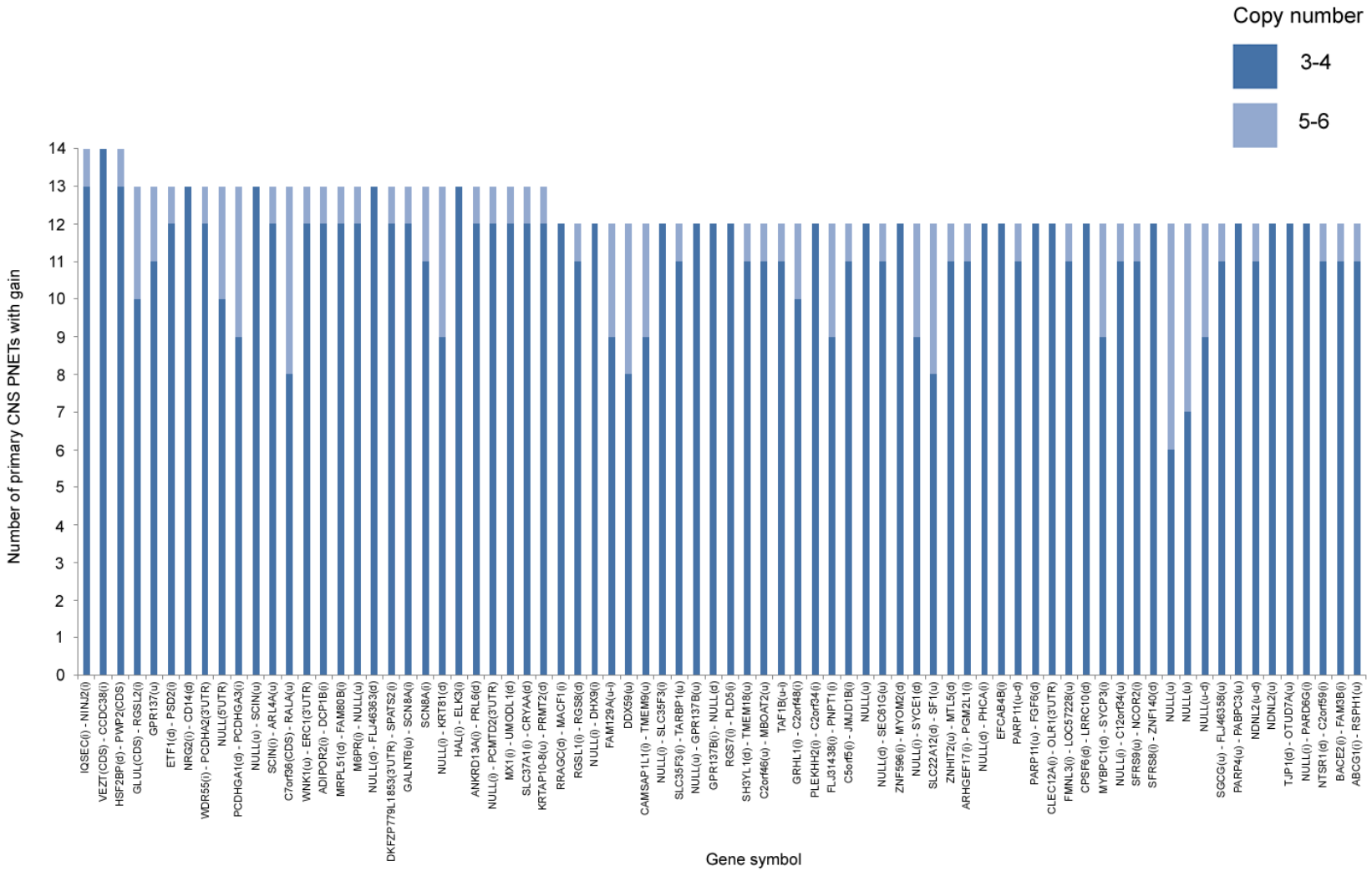

Figure 6.1 Graphical representation of increased gene copy numbers identified in 19 primary CNS PNETs analysed using the 100K SNP array platform. d = downstream, i = intronic, u = upstream, 3'UTR = 3' untranslated region, 5'UTR = 5' untranslated region, CDS = coding region, NULL = no gene name.

6.3.1.2 Genomic regions encompassing candidate gene loss in primary CNS PNETs analysed using 100K SNP arrays

The most frequent regions of SNP copy number loss of 19 primary CNS PNETs analysed using the 100K SNP arrays were identified and ordered by frequency (Table 6.2, Figure 6.2). The most common region of copy number loss was identified at 11p11.12, downstream of an olfactory receptor gene (*OR4C12*), in 10/19 (52.6%) primary CNS PNETs. Candidate regions of copy number loss on 4q21.1 were also identified involving 2 genes, one encoding a chemokine ligand (*CXCL13*), lost in 9/19 (47.4%) primary CNS PNETs and one encoding a negative regulator of the cell cycle, cyclin G2 (*CCNG2*), in 8/19 (42.1%) primary CNS PNETs. Other genes commonly found with copy number loss included the calcium dependent secretion activator, *CADPS* (3p14.2), in 6/19 (31.6%) primary CNS PNETs and 11 genes located between 16q21.1 and 16q23.2 in 5/19 (26.3%) primary CNS PNETs. The 11 candidate genes with copy number loss included the transcriptional repressor *SALL1* (sal-like 1), cadherin genes (*CDH8* and *CDH11*), with important roles in cell-cell adhesion. Also identified with copy number loss was an M phase phosphoprotein (*MPHOSPH6*) and the oxidoreductase gene *WWOX*, an essential mediator of TNFα induced apoptosis.

Table 6.2 Regions of decreased copy number in 19 primary CNS PNETs analysed using the 100K SNP array platform

Cytoband	Start (bp)	End (bp)	Gene symbol	Total	CN1	CN 0
11p11.12	50396846	51230448	*OR4C12/OR4A5(d)*	10	10	0
4q21.1	78358184	78433089	*CXCL13(u)*	9	8	1
11p11.12	51285867	51383437	*OR4C12/OR4A5(u) - OR4C46(d)*	9	9	0
4q21.1	78317830	78349245	*NULL(i) - CXCL13(u)*	8	7	1
4q21.1	78452089	78554270	*CCNG2(d)*	8	8	0
4p16.1	9761976	9949584	*WDR1(u) - KIAA1729(d)*	7	7	0
3p22.3	36106544	36226719	*ARPP-21(d)*	6	6	0
3p14.2	62456915	62651525	*CADPS(i)*	6	6	0
4q31.23	150087415	150570172	*NULL(u-d)*	6	6	0
7q11.21	61714398	63477770	*NULL(u) - ZNF680(d)*	6	6	0
9p24.1	7087123	7106020	*JMJD2C(i)*	6	6	0
12q24.21	112975442	113101937	*TBX5(d)*	6	6	0
3p14.2	62672251	62688091	*CADPS(i)*	5	5	0
9p24.1	6967233	7069643	*JMJD2C(i)*	5	5	0
9p24.1	7127500	8221617	*JMJD2C(i) - C9orf(u)*	5	5	0
9p22.2	17680387	18208437	*SH3GL2(i) - ADAMTSL1(u)*	5	5	0
16q12.1 - 12.2	49603589	51469110	*SALL1(d) - CHD9(u)*	5	5	0
16q12.2	52942909	54326141	*IRX3(u)- SLC6A2(d)*	5	5	0
16q21	59340771	60500332	*NULL(d) - CDH8 (i)*	5	5	0
16q21	64309638	64583654	*CDH11(u)*	5	5	0
16q23.1	74542425	74948793	*NULL(u) - CNTNAP4(i)*	5	5	0
16q23.1 - 23.2	77192727	78872807	*WWOX(i) - MAF(u)*	5	5	0
16q23.3	80779108	82441847	*MPHOSPH6(u) - HSBP1(d)*	5	5	0
17q11.2 - 12	28551621	29335160	*ACCN1(i)*	5	5	0

Genes in blue were validated by RT-PCR. bp = base pair, Total = number of samples with alteration, CN = copy number, d = downstream, u = upstream, i = intronic, NULL = no gene name.

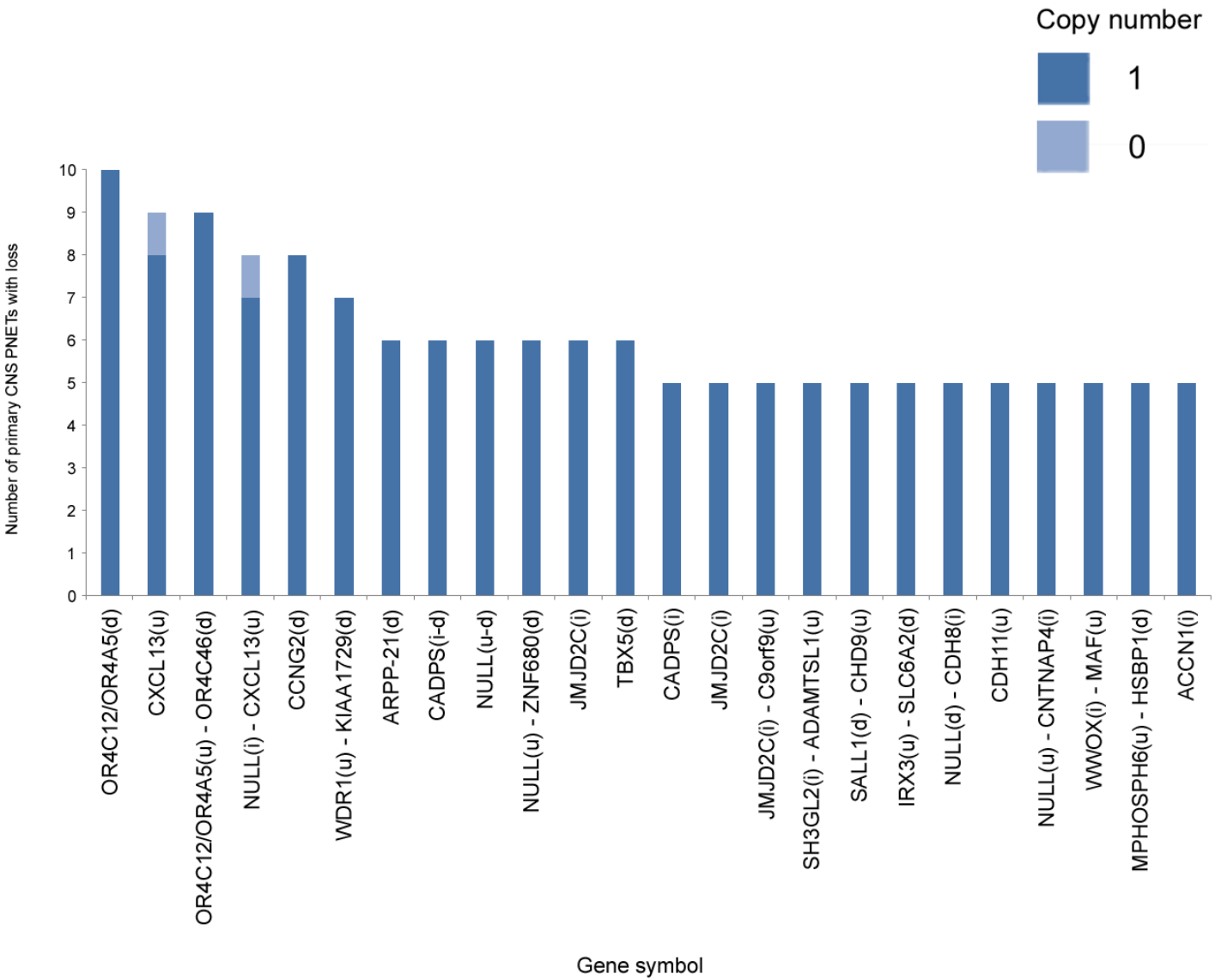

Figure 6.2 Graphical representation of decreased gene copy numbers identified in 19 primary CNS PNETs analysed using the 100K SNP platform. d = downstream, u = upstream, i = intronic, NULL = no gene name.

6.3.1.3 Genomic regions encompassing candidate gene gain in primary CNS PNETs analysed using 500K SNP arrays

During this study, Affymetrix developed and released a higher resolution array, the 500K SNP chip. This was subsequently used to analyse 13 newly collected primary CNS PNET cases. Gain in copy number was a more frequent event than loss for the CNS PNETs analysed using the 500K array set, in agreement with data from the 100K array set. Ordered by the frequency of increased SNP copy numbers, gain of genes on chromosome 1q was again the most prominent feature identified in the primary CNS PNETs analysed using the 500K arrays (Table 6.3). More specifically, gene gain was a common event at 1q32.1, 1q42.13 and also 2p24.1 in 10/13 (76.9%) primary CNS PNETs. Candidate regions of copy number gain located at 1q32.1 encompassed the adenosine receptor encoding gene, *ADORA1,* and the phosphoinositol 3-phosphate-binding encoding gene, *PLEKHA6*. Also gained at this region was the neurofascin gene, *NFASC,* which has roles in axon targeting and synapse formation in neural development. *GALNT2,* a known GalNAc transferase located on 1q42.13 was also observed with copy number gain.

A region located on 2p24.1 was identified as a frequent area of copy number gain in 10/13 (76.9%) primary CNS PNETs and resided 7.4Mb downstream of the oncogene, *MYCN*. Copy number gain was a common feature between 1q21.1–1q44, in at least 9/13 (69.2%) of the primary CNS PNETs analysed using the 500K arrays. Exploring current literature for the names and functions of candidate genes gained on chromosome 1q (identified in Table 6.3) led to 8 genes potentially of interest due to their possible roles in tumourigenesis, (i) gain of *CHD1L* which encodes a DNA helicase and has roles in chromatin remodelling and the promotion of cell proliferation and inhibiting apoptosis, (ii) *LHX4* (LIM homeobox 4) which is involved in the regulation of transcription, the control of cell differentiation and the control of the development of certain brain regions, (iii) *IER5* which encodes an immediate early response protein with potential roles in mediating the cellular response to mitogenic signals, (iv) *RNF2* which is involved in cell proliferation in early development, (v) *NAV1* which is a neuron navigator expressed predominantly in the nervous system, (vi) *PARP1* which is a poly (ADP-ribose) polymerase modifying nuclear proteins involved in the regulation of cell differentiation, proliferation and tumour transformation. Interestingly, the encoded protein of this gene also has roles in regulating the molecular

events in the recovery of a cell following DNA damage. (vii) *AKT3* which functions as an AKT kinase, regulating cell proliferation, survival, differentiation, apoptosis and tumorigenesis and lastly, (viii) *SYMD3*, a histone methyltransferase was identified with frequent gain in copy number in the primary CNS PNETs. Intriguingly, contrary to its supposed tumour suppressor status, *SFRP1* (8p11.21) was gained in 8/13 (61.5%) primary CNS PNETs analysed using the 500K SNP array platform. Of particular interest was gain of *FAM129A* (1q25.3) which was found with frequent copy number gain in both the 100K and 500K datasets, totalling 21/32 (65.6%) primary CNS PNETs.

Table 6.3 Regions of increased copy number in 13 primary CNS PNETs analysed using the 500K SNP array platform

Cytoband	Start (bp)	End (bp)	Gene Symbol	Total	CN 3 or 4	CN 5 or 6
1q32.1	201397908	201475471	*ADORA1 (i) - CHIT1 (u)*	10	10	0
1q32.1	202511509	202636498	*PLEKHA6 (u-i)*	10	10	0
1q32.1	203074793	203213010	*ENST00000367173 (i) - NFASC (i)*	10	10	0
1q42.13	228483917	228632249	*GALNT2 (3'UTR) - COG2 (u)*	10	10	0
2p24.1	23448857	23507416	*ENST00000388128 (d) - ENST00000288548 (i)*	10	10	0
1q21.1	144995145	145014814	*ENST00000386162 (u) - ENST00000302098 (d)*	9	7	2
1q21.1	145154537	145191032	*FMO5 (i) - CHD1L (i)*	9	9	0
1q25.2	177918599	177947819	*TDRD5 (i-d)*	9	9	0
1q25.2	177983204	178467807	*C1orf76 (i) - LHX4 (i)*	9	9	0
1q25.2	178489463	178599310	*LHX4 (i) - ACBD6 (i)*	9	9	0
1q25.3	178708470	179249680	*ACBD6 (i) - STX6 (i)*	9	9	0
1q25.3	179255259	179380064	*STX6 (i) - IER5 (d)*	9	9	0
1q25.3	183204350	183274586	*FAM129A (i) - RNF2 (u)*	9	9	0
1q32.1	198928801	199031936	*DDX59 (u) – CAMSAP1L1 (i)*	9	9	0
1q32.1	199455362	199546021	*DKFZp434B1231 (i) - PKP1 (i)*	9	9	0
1q32.1	199626320	199769978	*LAD1 (i) - NAV1 (u)*	9	9	0
1q32.1	199779619	199895613	*NAV1 (u-i)*	9	9	0
1q32.1	201272866	201377927	*PPFIA4 (i) - ADORA1 (i)*	9	9	0
1q32.1	201503095	201581983	*CHIT1 (u) - FMOD (i)*	9	9	0
1q42.12	223855543	224023506	*ENAH (i) - SRP9 (u)*	9	9	0
1q42.12	224055441	224587815	*TMEM63A (d) – PARP1 (d)*	9	9	0
1q42.12	224606373	224840632	*PARP1 (d) - C1orf95 (i)*	9	9	0
1q42.13	227401354	228469247	*ENST00000385399 (u) - GALNT2 (i)*	9	9	0
1q42.2	229048446	229434563	*C1orf198 (i) - C1orf131 (i)*	9	9	0
1q42.2	231495450	231536777	*ENST00000366656 (i) - KIAA1804 (i)*	9	9	0
1q42.3	232702522	232880099	*TARBP1 (u) - IRF2BP2 (u)*	9	9	0
1q44	241702098	241788349	*SDCCAG8 (i) - AKT3 (i)*	9	9	0
1q44	241847840	244352979	*AKT3 (i) - SMYD3 (i)*	9	9	0
2p24.1	20451446	20688172	*PUM2 (u) - HS1BP3 (u)*	8	0	8
2p24.1	23627453	23838496	*ENST00000288548 (u) - ENST00000238789 (i)*	8	0	8
2q35	218370272	218577787	*TNP1 (i) - RUFY4 (i)*	8	0	8
8p23.1	6775512	6814575	*DEFA4 (u-d)*	8	0	8
8p11.21	41221594	41395128	*SFRP1 (i)*	8	0	8
8q24.3	141052273	141257873	*NIBP (u-d)*	8	0	8
17q21.31	41587072	41610271	*KIAA1267 (i)*	8	0	8
17q24.2	62282771	63224948	*CACNG5 (u) - BPTF (u)*	8	0	8
17q25.3	75396320	75513529	*CBX8 (u) - CBX4 (u)*	8	0	8
19q13.31	48704720	49158203	*ETHE1 (i) - ZNF221 (i)*	8	0	8
19q13.31	49204464	49305501	*ZNF230 (i) - ZNF225 (i)*	8	0	8
21q22.2	38867699	38875356	*ERG (i)*	8	0	8

Genes in blue were validated by RT-PCR. bp = base pair, Total = number of samples with alteration, CN = copy number, i = intronic, u = upstream, 3'UTR = 3'untranslated region, d = downstream.

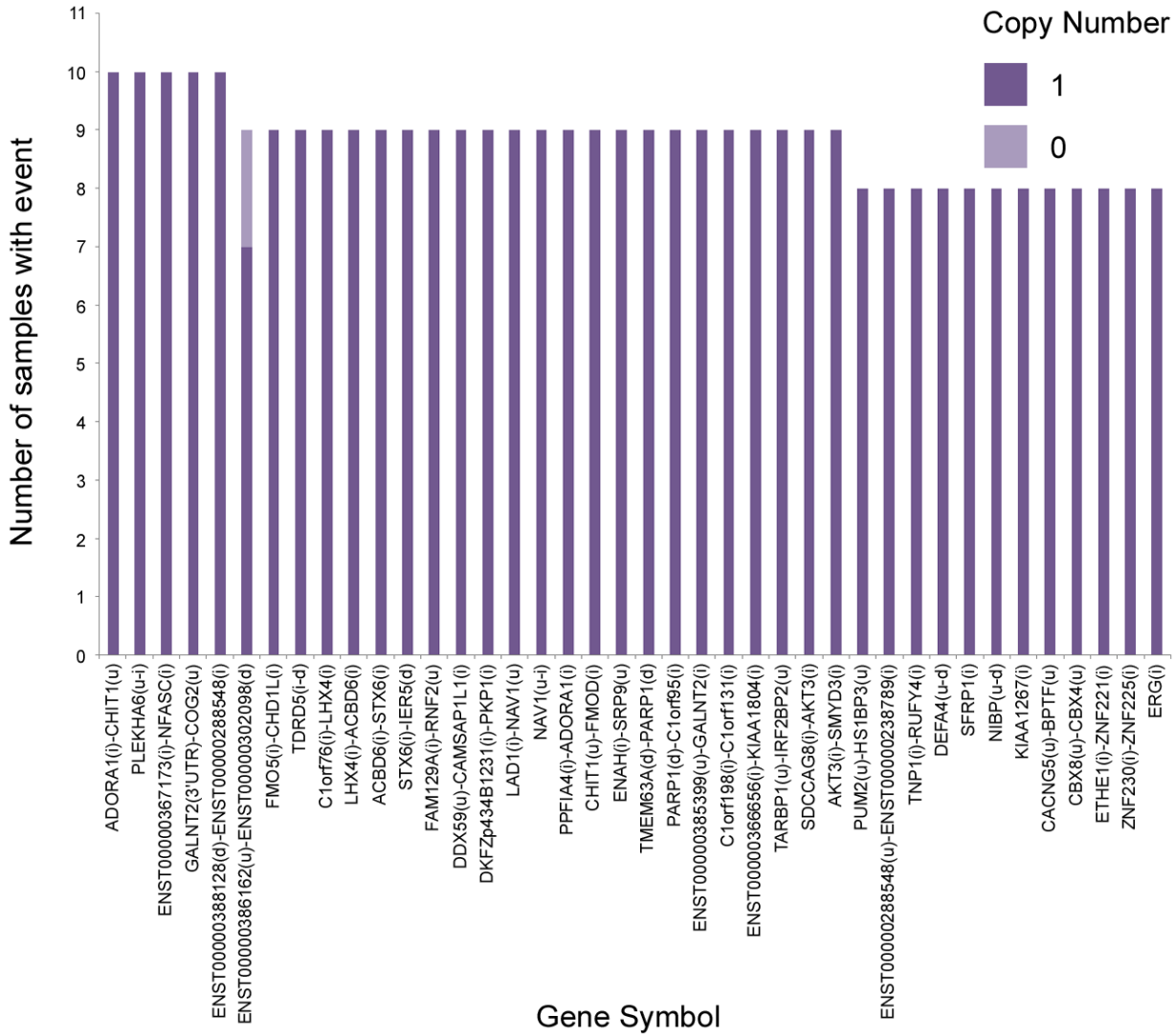

Figure 6.3 Graphical representation of increased gene copy numbers identified in 13 primary CNS PNETs analysed using the 500K SNP array platform. i = intronic, u = upstream, 3'UTR = 3'untranslated region, d = downstream.

6.3.1.4 Genomic regions encompassing candidate gene loss in primary CNS PNETs analysed using 500K SNP arrays

Common regions of copy number loss in the 13 primary CNS PNETs were identified using the 500K SNP array platform (Table 6.4, Figure 6.4). The most common region of loss involved 3p12.3-3p26.3, in 5/13 (38.5%) primary CNS PNETs, where the genes, *STAC* and *ARPP-21* are located. Additionally, a number of genes located at 19q12 were found with copy number loss, in 5/13 (38.5%) primary CNS PNETs. Other genomic regions of copy number loss encompassed 3p14.1-3p26.3 in 4/13 (30.8%) and 12q12-12q24.23 and 14q11.2-14q32.13, each identified in 3/13 (23.1%) primary CNS PNETs. The genes identified with copy number loss from the CNS PNETs analysed using the 500K SNP array platform were similar to those found in the previous set of CNS PNETs analysed using the 100K SNP arrays. Gene copy number loss was again identified as a common event, involving *STAC* and *ARPP-21* located at 3p22.3 in 5/13 (38.5%) primary CNS PNETs. Additionally, SNP copy number loss located upstream of *MAF* at 16q23.2 was identified in 4/13 (30.8%) CNS PNETs. Loss of *CXCL13* and *CCNG2* at 4q21.1 in 3/13 (23.1%) CNS PNETs, SNP copy number loss downstream of *BCKDHB* at 6q14.1 and loss of *MPHOSPH6* were all similarly identified on comparison of the 100K and 500K SNP datasets. Interestingly, *OR4A5/OR4C12* was lost in 3/13 (23.1%) of primary CNS PNETs analysed on the 500K SNP array platform, as was the tumour suppressor, *FHIT* (3p14.2) which is similar to the results identified from the 100K SNP array data. In summary, a number of candidate genes potentially involved in CNS PNET pathogenesis have arisen in both the 100K and 500K analyses which warrant further investigation.

Table 6.4 Regions of decreased gene copy number in 13 primary CNS PNETs analysed using the 500K SNP array platform

Cytoband	Start (bp)	End (bp)	Gene Symbol	Total	CN 1	CN 0
3p22.3	36034756	36099145	*STAC (u)*	5	5	0
3p22.3	36186347	36258534	*ARPP-21 (d)*	5	5	0
19q12	32651846	32764651	*ZNF254 (d)*	5	5	0
19q12	32833529	32948190	*ENST00000357319 (u) - ENST00000379373 (u)*	5	5	0
3p26.3	1336323	1383344	*CNTN6 (i)*	4	4	0
3p24.3	19267508	19614854	*KCNH8 (i) - EFHB (d)*	4	4	0
3p14.1	67345718	67422715	*SUCLG2 (d) - KBTBD8 (d)*	4	4	0
3p14.1	68174569	68455776	*FAM19A1 (i)*	4	4	0
3q12.1	100302676	100590752	*COL8A1 (u)*	4	4	0
3q13.11	105899251	105995908	*ENST00000388649 (d)*	4	4	0
3q13.31	116478304	116760529	*ZBTB20 (u) - GAP43 (u)*	4	4	0
6q14.1	78270742	78311369	*HTR1B (u)*	4	4	0
7q11.21	61269841	62076716	*ENST00000380888 (u) - ENST00000384712 (d)*	4	3	1
9q33.1	120004820	120138861	*DBC1 (d)*	4	4	0
14q12	25401719	25596847	*ENST00000323440 (u) - ENST00000384946 (d)*	4	4	0
16q23.2	78610467	78761825	*MAF (u)*	4	4	0
2q22.1	139468995	139686340	*ENST00000363563 (u) - ENST00000384174 (u)*	3	3	0
3p26.1	7595382	7728230	*GRM7 (CDS-d)*	3	3	0
3p25.3	9592634	9711741	*MTMR14 (u-i)*	3	3	0
3p24.3	18558769	18864489	*SATB1 (u)*	3	3	0
3p24.3	21743250	21960421	*ZNF659 (u-i)*	3	3	0
3p24.1	30158532	30359069	*RBMS3 (d) - TGFBR2 (u)*	3	3	0
3p23	30828255	30890909	*GADL1 (i) - STT3B (u)*	3	3	0
3p14.2	59420738	59738912	*FHIT (i-d)*	3	3	0
3p13	72946194	73071309	*SHQ1 (i) - ENST00000389617 (i)*	3	3	0
3p12.3	74541208	74731875	*CNTN3 (u-i)*	3	3	0
4p15.31	22755985	22910607	*GBA3 (d) - PPARGC1A (d)*	3	3	0
4q21.1	78376846	78420051	*CXCL13 (u) - CCNG2 (d)*	3	3	0
4q35.2	189999425	190015453	*ENST00000321235 (d) - ENST00000378771 (d)*	3	3	0
5q21.3	108235413	108570425	*FER (i-d)*	3	3	0
5q23.1	121013969	121185837	*FTMT (u)*	3	3	0
6p22.3	18807196	18880846	*ENST00000364653 (u) - ENST00000385041 (d)*	3	3	0
6p21.2	40022680	40195492	*MOCS1 (u) - FLJ41649 (d)*	3	3	0
6p12.2	51589630	51807363	*PKHD1 (3'UTR-i)*	3	3	0
6q14.1	82093483	82768560	*BCKDHB (d) - IBTK (d)*	3	3	0
8q11.1	47667951	47702135	*ENST00000388124 (d)*	3	3	0
8q11.1	47717099	47915603	*ENST00000388119 (u) - ENST00000388177 (d)*	3	3	0
8q23.1	109621322	109757932	*TMEM74 (d) - TTC35 (d)*	3	3	0
9p23	9228714	9385912	*ENST00000360531 (d) - ENST00000363183 (u)*	3	3	0

9q33.1	119565323	119640521	*TLR4 (d)*	3	3	0
10q21.1	54553366	54607500	*ENST00000387222 (u)*	3	3	0
11p11.12	50301567	51084702	*OR4C12/OR4A5 (d)*	3	3	0
12p11.22	28541832	28556975	*CCDC91 (i)*	3	3	0
12q12	39900866	40126477	*ENST00000380795 (i) - PDZRN4 (i)*	3	3	0
12q12	41567838	41813990	*PRICKLE1 (u)*	3	3	0
12q14.1	60060452	60075246	*FAM19A2 (d)*	3	2	1
12q21.33	89908752	90315412	*EPYC (i) - BTG1 (d)*	3	3	0
12q22	91357737	91397437	*CLLU1 (d) - CLLU1OS (u)*	3	3	0
12q24.21	113112523	113143493	*TBX5 (d) - RBM19 (u)*	3	3	0
12q24.23	117813170	117883568	*KIAA1853 (u)*	3	3	0
13q21.33	71519394	71792838	*ENST00000363167 (d) - ENST00000362412 (u)*	3	3	0
13q31.1	78187844	78263140	*RBM26 (d)*	3	3	0
13q31.3	93138384	93386359	*GPC6 (i)*	3	3	0
14q11.2	19272965	19489991	*OR4Q3 (u) - OR4K15 (u)*	3	2	1
14q13.1	33082593	33116762	*NPAS3 (i)*	3	3	0
14q24.3	77803297	78060635	*ENST00000330071 (i)*	3	3	0
14q31.1	79473616	79688928	*NRXN3 (d) - DIO2 (d)*	3	3	0
14q32.13	95282468	95350903	*TCL1A (u) - C14orf132 (u)*	3	3	0
16q12.1	50638445	50780605	*ENST00000219746 (d) - ENST00000388816 (d)*	3	3	0
16q23.2	78766944	78804411	*DYNLRB2 (u)*	3	3	0
16q23.3	80661587	80710211	*HSD17B2 (i-d)*	3	3	0
16q23.3	80722907	80765783	*MPHOSPH6 (u -d)*	3	3	0
18q12.2	34315960	34494317	*BRUNOL4 (u)*	3	3	0
19q13.42	60227101	60229274	*GP6 (i)*	3	3	0

Genes in blue were validated by RT-PCR. bp = base pair, Total = number of samples with alteration, CN = copy number, u = upstream, d = downstream, I = intronic, 3'UTR = 3' untranslated region.

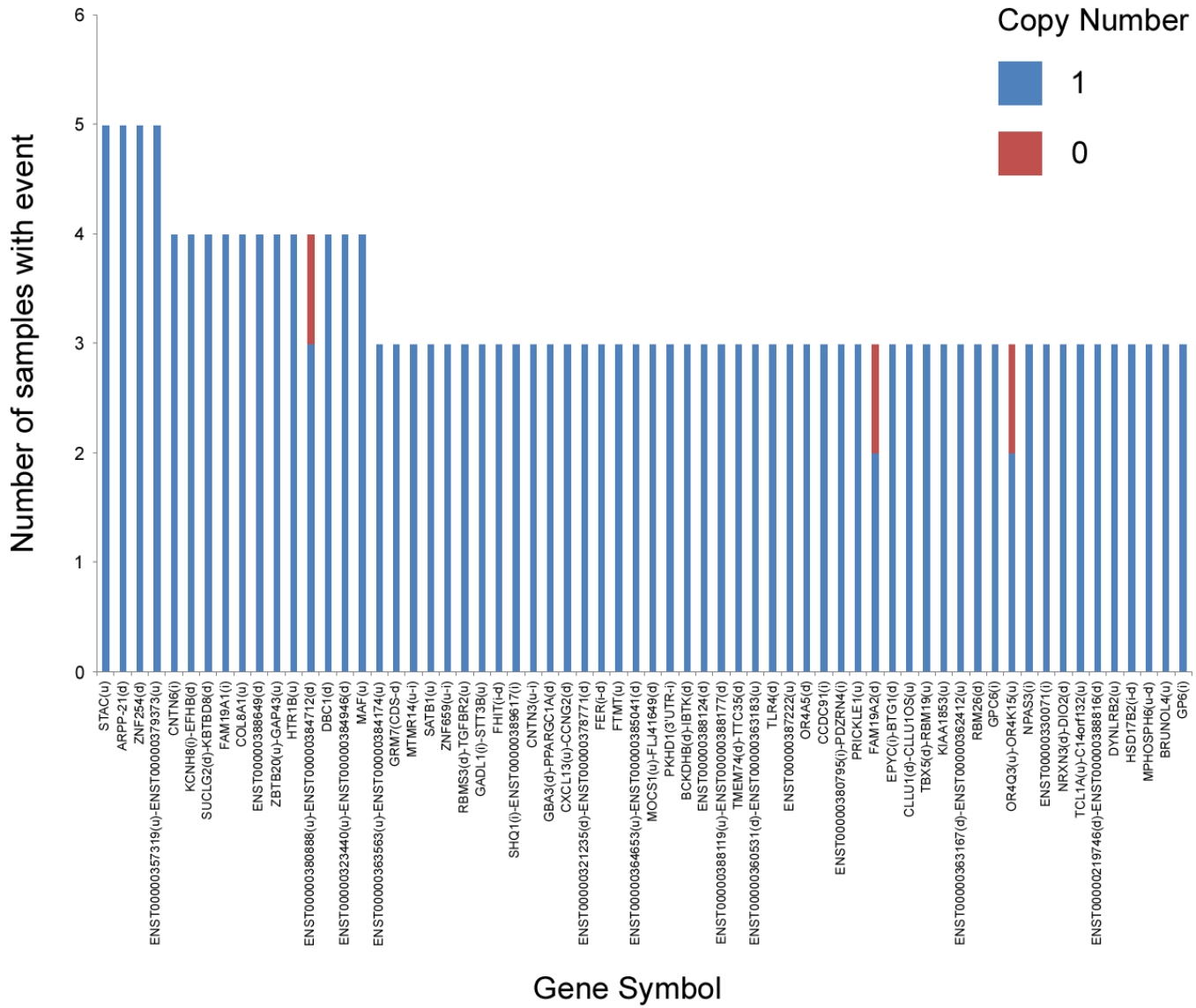

Figure 6.4 Graphical representation of decreased gene copy numbers identified in 13 primary CNS PNETs analysed using the 500K SNP array platform. u = upstream, d = downstream, I = intronic, 3'UTR = 3' untranslated region, NULL = no gene name.

6.3.1.5 Genomic regions encompassing candidate gene gain in recurrent CNS PNETs analysed using 100K SNP arrays

Of the 6 recurrent CNS PNETs analysed using the 100K SNP array platform, 5/6 (83.3%) had candidate regions of copy number gain involving genes located on chromosomes 1q, 2, 8p, 12q, 17q, 20p, 20q and 21q (Table 6.5 and Figure 6.5). In common with the primary CNS PNETs analysed on the 100K SNP arrays, the recurrent CNS PNETs also showed copy number gain of SNPs upstream of *FAM129A* in 5/6 (83.3%) CNS PNETs.

Table 6.5 Regions of increased copy number in 6 recurrent CNS PNETs analysed using the 100K SNP array platform

Cytoband	Start (bp)	End (bp)	Gene symbol	Total	CN 3 or 4	CN 5 or 6
1q25.3	182250203	182282330	*GLT25D2(u-i)*	5	3	2
1q25.3	182338873	183219736	*C1orf19(d) - FAM129A(u)*	5	5	0
1q32.3	209711705	211398026	*RD3(d) - RPS6KC1(i)*	5	5	0
1q41	219129420	219142492	*HLX(d)*	5	4	1
1q42.12	223810960	224667758	*ENAH(i) - PARP1(u)*	5	4	1
1q42.12 - 42.13	224985742	225130294	*ITPKB (i) - PSEN2(i)*	5	4	1
1q42.13	225136360	226688970	*PSEN2(CDS) - HIST3H2A(d)*	5	5	0
1q42.2	228869903	229449796	*COG2(i) - GNPAT(i)*	5	5	0
1q42.2	229467827	229627653	*GNPAT(i) - NULL(i)*	5	4	1
1q42.2	229804452	230650737	*NULL(i) - SIPA1L2(i)*	5	5	0
1q42.3	234361448	234376647	*GPR137B(u-i)*	5	4	1
1q43 – 44	241483148	246591306	*CEP170(i) - OR2T4(u)*	5	5	0
2p25.3	53452	2986979	*SH3YL1(d) - TSSC1(d)*	5	5	0
2p25.3	3606258	4242738	*RPS7(i) - NULL(d)*	5	5	0
2p25.1	9464256	11909579	*ITGB1BP1(3'UTR) - LPIN1(d)*	5	5	0
2p24.1 - 23.2	23782141	28365054	*NULL(i) - BRE(i)*	5	5	0
2p21	42316677	44611058	*EML4(i) - C2orf34(i)*	5	5	0
2p21	45584043	46849708	*SRBD1(i) - MCFD2(d)*	5	5	0
2p21	46967456	47260043	*MCFD2(d) - CALM1(u)*	5	4	1
2p21 - 16.3	47349113	47997913	*CALM1(u) - FBXO11(u)*	5	5	0
2p16.2 - 16.1	53797200	55801434	*ASB3(i) - EFEMP1(d)*	5	5	0
2p16.1 – 14	60935046	64633013	*REL(u) - AFTPH(CDS)*	5	5	0
2p14	64650321	64652930	*AFTPH(i)*	5	4	1
2p14	64666995	65278518	*AFTPH(i) - NULL(u)*	5	5	0
2p11.2	85193570	88935268	*KCMF1(d) - RPIA(d)*	5	5	0
2q11.1 - 11.2	95226463	102017436	*ZNF2(d) - IL1R2(d)*	5	5	0
2q12.1 - 12.2	104312274	106625908	*TMEM182(d) - ST6GAL2(d)*	5	5	0

2q13	112112005	112183171	*ANAPC1(d)*	5	5	0
2q33.1	197195870	197200521	*HECW2(u)*	5	4	1
2q33.1	197207681	198373765	*HECW2(u) - PLCL1(u)*	5	5	0
2q33.1	201059199	201071327	*LOC26010(d) - KCTD18(i)*	5	5	0
2q33.1	201108930	201183402	*SGOL2(i) - AOX1(i)*	5	4	1
2q33.1	201474481	203247311	*NIF3L1(i) - ALS2CR13(i)*	5	5	0
2q35	218613890	219132608	*TNS1(u) - USP37(i)*	5	5	0
2q35	219139535	219757631	*USP37(i) - ZFAND2B(u)*	5	4	1
2q37.1	234432673	234714614	*DKFZp762E1312(u) - SPP2(d)*	5	5	0
2q37.2 - 37.3	235603429	241730891	*SH3BP4(i) - PASK(i)*	5	5	0
4p16.3	103115	459347	*ZNF595(d) - PIGG(u)*	5	5	0
4q35.1	184043457	184086599	*DCTD(u-d)*	5	4	1
6p25.3 - 25.1	99536	4956722	*FLJ43763(u) - RPP40(u)*	5	5	0
6p21.1	41376510	43438734	*TREM1(u) - ZNF318(i)*	5	4	1
7p11.2	54669673	56161603	*NULL(d)*	5	5	0
8p23.3	180568	1303293	*ZNF596(i) - DLGAP2(u)*	5	5	0
8p23.3	1981169	2096739	*MYOM2(i) - CSMD1(d)*	5	5	0
8p23.2	4592774	4993234	*NULL(u-d)*	5	2	3
8p23.1	6557762	6559917	*AGPAT5(i)*	5	4	1
8p22	12869264	12995396	*C8orf79(i) - DLC1(i)*	5	5	0
8p22	13465689	13472133	*DLC1(u) - SGCZ(d)*	5	4	1
8p21.3 - 21.2	21922030	23476947	*NPM2(u) - SLC25A37(i)*	5	4	1
8p21.2 - 21.1	27236982	27646494	*PTK2B(u) - CCDC25(d)*	5	5	0
8q11.22	52308591	52463524	*PXDNL(i-d)*	5	1	4
11q13.1 - 14.1	64130080	78320494	*SLC22A12(d) - NULL(i)*	5	4	1
11q23.3	116255283	117435638	*KIAA0999(i) - NULL(u)*	5	5	0
11q23.3	117687870	118082207	*CD3E(i) - NULL(d)*	5	5	0
12q12	40876491	41293794	*YAF2(i) - PRICKLE1(u)*	5	5	0
12q12	41447887	41898954	*PRICKLE1(u)*	5	5	0
12q12	41902912	42688707	*PRICKLE1(u) - TMEM117(i)*	5	5	0
12q13.11	46021178	47134988	*AMIGO2(u) - ANP32D(u)*	5	5	0
12q13.11 - 13.13	47203274	50434904	*OR8S1(u) - SCN8A(i)*	5	4	1
12q13.13	50462502	50977591	*SCN8A(i) - KRT81(u)*	5	2	3
12q13.13	51005520	52474449	*KRT83(u) - CALCOCO1(u)*	5	3	2
12q13.13 - 13.2	52618170	53146448	*HOXC13(u) - FAM112B(i)*	5	3	2
12q15	67295983	68931659	*RAP1B(i) - CNOT2(i)*	5	5	0
13q34	111660805	112225916	*NULL(u) - TUBGCP3(i)*	5	3	2
14q11.2	19872155	21207935	*CCNB1IP1(u) - NULL(i)*	5	5	0
14q23.2 - 23.3	63175155	64031232	*NULL(d) - ZBTB25(i)*	5	5	0
14q31.1	80689322	81220884	*TSHR(d) - SEL1L(u)*	5	5	0
14q32.2 - 32.33	99018338	106312036	*CCNK(i) - NULL(d)*	5	5	0
16p13.3	3165870	4223830	*NULL(u-i)*	5	5	0
16q21 - 22.1	65160772	65400864	*CMTM1(i) - APPBP1(i)*	5	4	1
17q11.2	25122345	25955997	*SSH2(i) - LRRC37B2(i)*	5	5	0
17q12 - 21.1	32062557	35542587	*MRM1(d) - NULL(i)*	5	5	0
17q21.2	36095188	36264327	*KRT222P(u) - KRT10(u)*	5	5	0
17q21.2 - 21.31	36439324	39463877	*KRTAP1-5(u) - LSM12(d)*	5	5	0

17q21.31 - 21.33	41406176	46295421	*MAPT(i) - TOB1(CDS)*	5	5	0
17q22 - 23.1	54624210	55387230	*PRR11(i) - LOC51136(i)*	5	5	0
17q23.1	55495402	55523104	*HEATR6(u-i)*	5	4	1
17q25.1 - 25.3	68676887	73524449	*SSTR2(i) - TNRC6C(u)*	5	5	0
18p11.21	12085950	13178836	*NULL(i) - C18orf1(u)*	5	5	0
18q22.3	70266527	70548882	*C18orf51(i) - ZNF407(i)*	5	3	2
18q23	72120525	72424285	*LOC284274(u) - FLJ44881(u)*	5	5	0
19q13.11	39302438	39368822	*LSM14A(u-i)*	5	4	1
19q13.12 - 13.2	40489756	43726908	*MAG(i) - RYR1(i)*	5	5	0
19q13.32 - 13.42	52292281	61021559	*NULL(i) - NLRP11(i)*	5	5	0
19q13.42 - 13.43	61207687	63458980	*NLRP5(i) - ZNF544(i)*	5	5	0
20p13 - 12.3	2388652	5148227	*SNRPB(d) - CDS2(d)*	5	5	0
20p12.3	5226869	5240086	*PROKR2(i-d)*	5	4	1
20p12.3	5490092	5921189	*RP5-1022P6.2(i) - MCM8(i)*	5	5	0
20p11.23	19566037	19674798	*SLC24A3(i-d)*	5	4	1
20p11.23 - 11.22	19906303	21329121	*RIN2(i) - NULL(u)*	5	5	0
20p11.21 - 11.1	24309679	26148028	*C20orf39(u) - NULL(d)*	5	5	0
20q11.1 - 11.22	28084896	33549562	*NULL(d) - CEP250(i)*	5	5	0
20q13.31	55526741	55806890	*CTCFL(i) - TMEPAI(u)*	5	5	0
20q13.31 - 13.32	55873063	57657015	*TMEPAI(u) - PHACTR3(i)*	5	5	0
20q13.33	61366365	62376958	*NULL(i) - PCMTD2(3'UTR)*	5	5	0
21q21.1	15907719	17067648	*NULL(u)*	5	5	0
21q21.1	17719812	18275335	*NULL(u) - C21orf91(u)*	5	5	0
21q22.13	37014570	37975732	*SIM2(i) - KCNJ6(i)*	5	5	0
21q22.2	39019706	39720425	*ERG(u) - C21orf13(i)*	5	5	0
21q22.2 - 22.3	41357397	46924583	*NULL(d) - PRMT2(d)*	5	5	0

Genes in blue were validated by RT-PCR. bp = base pair, Total = number of samples with alteration, CN = copy number, u = upstream, d = downstream, i = intronic, 3'UTR = 3' untranslated region, CDS = coding region, NULL = no gene name.

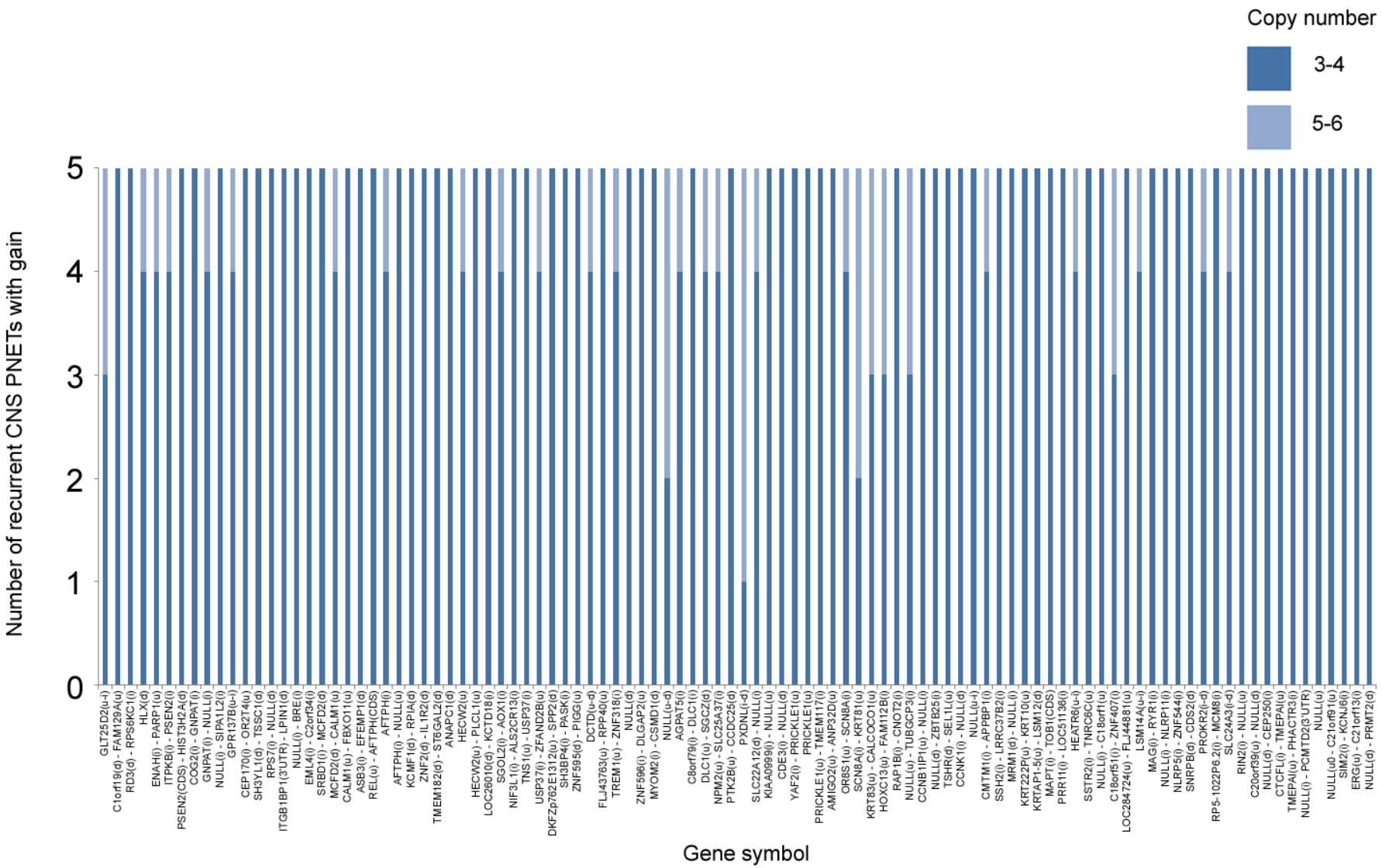

Figure 6.5 Graphical representation of increased gene copy numbers identified in 6 recurrent CNS PNETs analysed using the 100K SNP array platform. u = upstream, d = downstream, i = intronic, 3'UTR = 3' untranslated region, NULL = no gene name.

6.3.1.6 Genomic regions encompassing candidate gene loss in recurrent CNS PNETs analysed using 100K SNP arrays

Regions of SNP copy number loss was identified in 6 recurrent CNS PNETs analysed using the 100K SNP arrays (Table 6.6, Figure 6.6). The most common region of loss identified involved SNPs downstream of an unnamed gene on chromosome 10q25.1 in 5/6 (83.3%) recurrent CNS PNETs. Similarly to the primary CNS PNET cohort, regions of chromosome 3p were lost in 4/6 (66.7%) recurrent CNS PNETs, involving STAC (encoding a protein with roles in neuron-specific signal transduction), *ARPP-21* (encoding a cyclic AMP-regulated phosphoprotein), *FHIT* (a member of the fragile histidine triad gene family) and *CADPS* (encoding a calcium-dependent secretion activator). SNP's upstream and within the tumour suppressors, *CDKN2A* and *CDKN2B* (9p21.3) were lost in 3/6 (50%) recurrent CNS PNETs.

Table 6.6 Regions of decreased copy number in 6 recurrent CNS PNETs analysed using the 100K SNP array platform

Cytoband	Start (bp)	End (bp)	Gene symbol	Total	CN 1	CN 0
10q25.1	109899733	110013826	*NULL(d)*	5	5	0
3p22.3	36031184	36236321	*STAC(u) - ARPP-21(d)*	4	4	0
3p14.2	59414093	60265103	*FHIT(i-d)*	4	4	0
3p14.2	62456915	63050307	*CADPS(u-i)*	4	4	0
3p12.2 – 12.1	83694096	84564348	*GBE1(u) - CADM2(u)*	4	4	0
4q21.1	78358184	78433089	*CXCL13(u)*	4	4	0
6q16.3	102132218	102765994	*GRIK2(i-d)*	4	4	0
10q25.1	109803462	109830861	*NULL(d)*	4	4	0
10q25.1	110029605	110441328	*NULL(d)*	4	4	0
15q21.2 - 21.3	50927337	51173545	*WDR72(d)*	4	4	0
15q21.3	52518427	52901811	*NULL(i) - C15orf15(d)*	4	4	0
3p26.3	48603	170962	*CHL1(u)*	3	3	0
3p26.2	3861180	4236042	*LRRN1(5'UTR) - NULL(i)*	3	3	0
3p26.1	6808535	7558058	*GRM7(u-i)*	3	3	0
3p26.1	7614708	7980785	*GRM7(i-d)*	3	3	0
3p24.2 – 24.1	25816202	28762307	*LRRC3B(u) - RBMS3(u)*	3	3	0
3p24.1	29367167	30693536	*RBMS3(i) - TGFBR2(i)*	3	3	0
3p22.3	36272792	36346505	*STAC(u)*	3	3	0
3p14.2	59239357	59392226	*FLJ42117(u)*	3	3	0
3p14.2	60285416	60898214	*FHIT(i) - NULL(u)*	3	3	0
3p14.2	63095602	63549171	*SYNPR(u-i)*	3	3	0
3p14.1	67394681	68764105	*SUCLG2(d) - FAM19A4(d)*	3	3	0
3p14.1	70345508	70724500	*MITF(d)*	3	3	0
3p12.2	83008414	83598684	*GBE1(u)*	3	3	0
4p16.1	9858849	9949584	*WDR1(u) - KIAA1729(d)*	3	3	0
5q12.1 – 12.3	62799515	63949443	*NULL(u) - RGS7BP(d)*	3	3	0
6q14.1	81224213	82365338	*BCKDHB(d) - NULL(u)*	3	3	0
6q16.3	102010156	102925307	*GRIK2(i-d)*	3	3	0
6q23.1	130409486	130936295	*L3MBTL3(i) - KIAA1913(d)*	3	3	0
7q11.21	61714398	63477770	*NULL(u) - ZNF680(d)*	3	3	0
9p21.3	21844199	22268100	*MTAP(i) - CDKN2B(u)*	3	3	0
9p21.1	29463445	29781410	*LINGO2(u)*	3	3	0
10q21.1	53916144	54712286	*DKK1(d) - NULL(u)*	3	3	0
10q23.1	87036546	87285785	*KIAA1128(d)*	3	3	0
10q23.31	92305795	92456069	*NULL(u) - HTR7(d)*	3	3	0
10q25.1	106413736	107318185	*SORCS3(i) - SORCS1(d)*	3	3	0
10q25.2	113018607	113744337	*ADRA2A(d)*	3	3	0
11p11.12	50396846	51383437	*OR4C12/OR4A5(d) - OR4C46(d)*	3	3	0
15q21.3	51212732	52472755	*ONECUT1(u) - NULL(i)*	3	3	0
15q21.3	52908228	52930076	*C15orf15(d)*	3	3	0
19q13.2	44776627	44996274	*LGALS13(u) - CLC(u)*	3	3	0

Genes in blue were validated by RT-PCR. bp = base pair, Total = number of samples with alteration, CN = copy number, d = downstream, u = upstream, i = intronic, 5'UTR = 5' untranslated region, NULL = no gene name.

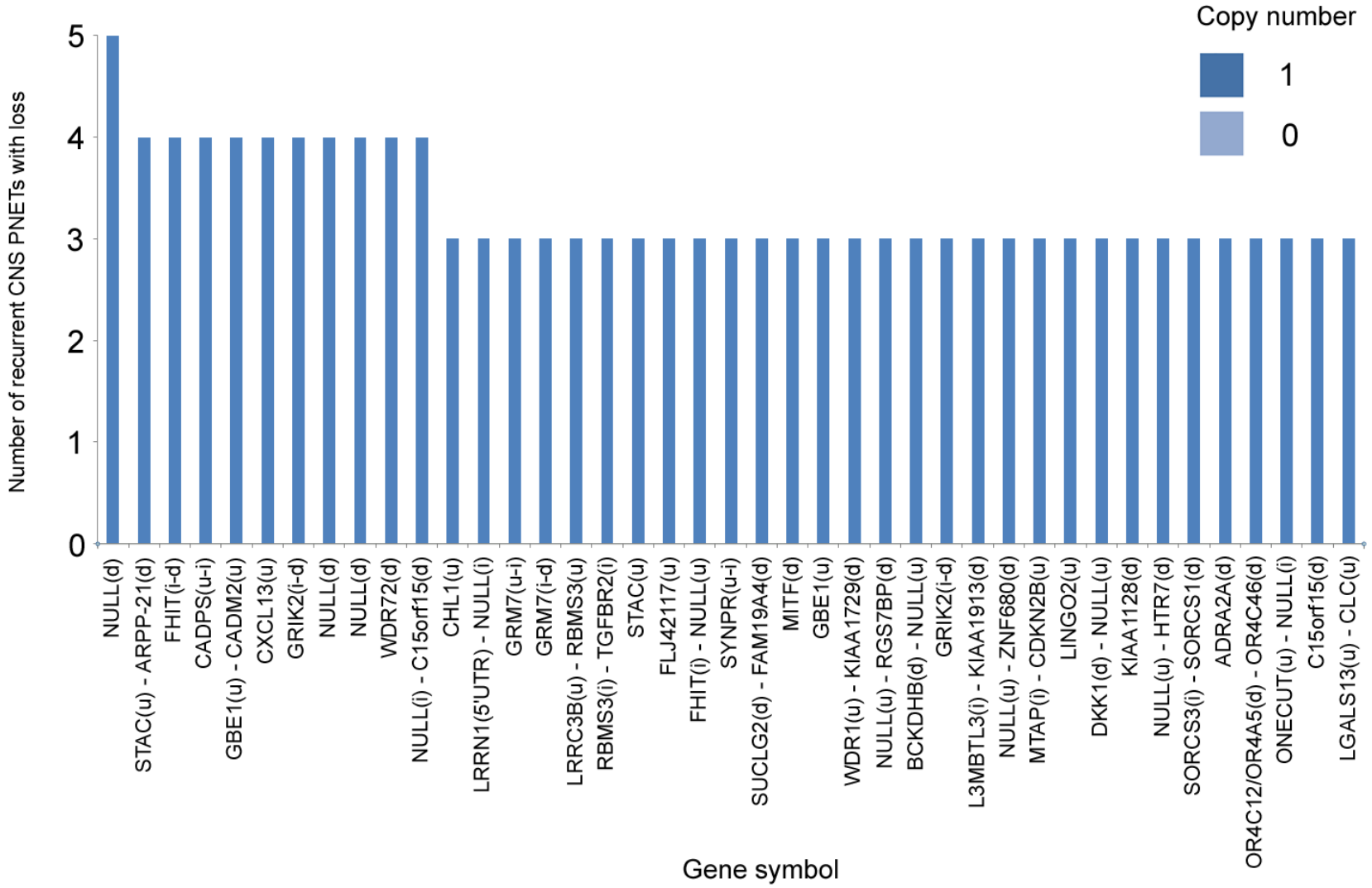

Figure 6.6 Graphical representation of decreased gene copy numbers identified in 6 recurrent CNS PNETs analysed using the 100K SNP array platform, d = downstream, u = upstream, i = intronic, 5'UTR = 5' untranslated region, NULL = no gene name.

6.3.1.7 Genomic regions encompassing candidate gene gain in primary pineoblastomas analysed using 100K SNP arrays

Copy number gain was frequently identified on chromosomes 2q, 5q, 6p and 13q in the primary pineoblastomas analysed using the 100K SNP array platform (Table 6.7 and Figure 6.7). SNPs within the protocadherin gene, *PCDHGA3,* were gained in 6/6 (100%) primary pineoblastomas. SNPs within the introns of 3 genes (*WRNIP1, RIPK1* and *BPHL*) on 6p25.2 were identified with copy number gain in 5/6 (83.3%) primary pineoblastomas. Other regions on 6p25.3 – 25.2 had SNP copy number gain (in 4/6, 66.7% primary pineoblastomas) encompassing genes which including *DUSP22, EXOC2* and *PRPF4B.* Candidate regions of gain were also identified at 13q12.11 – 12.13 in 4/6 (66.7%) primary pineoblastomas encompassing genes *PSPC1, GJB6* and the cyclin dependent kinase, *CDK8*.

Table 6.7 Regions of increased copy number in 6 primary pineoblastomas identified using the 100K SNP array platform

Cytoband	Start (bp)	End (bp)	Gene symbol	Total	CN 3 or 4	CN 5 or 6
5q31.3	140594436	140799142	*NULL(5'UTR) - PCDHGA3(i)*	6	6	0
13q12.11	22169909	22177254	*NULL(u)*	6	4	2
2q11.2	96814079	98195669	*CNNM4(i) - VWA3B(i)*	5	5	0
5q31.3	139985294	140446005	*TMCO6(u) - PCDHB1(d)*	5	5	0
5q35.3	179232737	180607628	*TBC1D9B(CDS) - TRIM52(d)*	5	5	0
6p25.2	2713210	3049695	*WRNIP1(i) - RIPK1(i)*	5	4	1
6p25.2	3095349	3097443	*BPHL(i)*	5	5	0
6q27	168874854	170746883	*THBS2(d) - PDCD2(u)*	5	5	0
10q26.3	135125348	135189835	*NULL(i) - SYCE1(d)*	5	4	1
12p13.31	8695839	9312096	*MFAP5(i) - NULL(u)*	5	5	0
1q21.1	143619946	145161045	*PDE4DIP(i) - FMO5(i)*	4	4	0
1q41	221968168	222086254	*CAPN2(i) - TP53BP2(i)*	4	3	1
2p23.3	24253890	24584351	*FLJ30851(i) - NULL(d)*	4	3	1
2q11.1 - 11.2	95226463	95743980	*ZNF2(d) - NULL(d)*	4	4	0
2q11.2	98333686	98692359	*VWA3B(d) - MGAT4A(i)*	4	4	0
3q29	198322883	198699627	*DLG1(u-i)*	4	4	0
5q35.3	177544899	178537071	*NOLA2(u) - ADAMTS2(i)*	4	4	0
6p25.3	99536	197145	*FLJ43763(u) - DUSP22(u)*	4	4	0
6p25.3	508013	627543	*EXOC2(i)*	4	4	0
6p25.3 - 25.2	1263711	2669836	*FOXQ1(d) - RP11-145H9.1(i)*	4	4	0
6p25.2	3149678	4002232	*TUBB2B(d) - PRPF4B(i)*	4	4	0
6p25.2	4013108	4042314	*PECI(d) - C6orf201(i)*	4	3	1
6q27	166806486	168850158	*RPS6KA2(i) - THBS2(d)*	4	4	0
7p21.1	16784298	16805668	*TSPAN13(i) - AGR2(i)*	4	3	1
12p13.31	6706312	8202643	*COPS7A(i) - CLEC4A(d)*	4	4	0
13q11 - 12.11	18321079	19211924	*NULL(u) - PSPC1(i)*	4	4	0
13q12.11	19870553	20445317	*GJB6(u) - LATS2(3'UTR)*	4	4	0
13q12.12	22234562	22245061	*NULL(u)*	4	4	0
13q12.12	22518343	22601577	*NULL(u-d)*	4	3	1
13q12.13	25502482	25740230	*ATP8A2(d) - CDK8(i)*	4	4	0
15q13.1 – 13.2	27061851	28115352	*APBA2(i) - TJP1(u)*	4	4	0
16p13.3	2681813	3864938	*KCTD5(i) - CREBBP(i)*	4	4	0
17p13.3	450509	457940	*VPS53(i)*	4	3	1
18p11.31	3203337	3529135	*MYOM1(i) - DLGAP1(i)*	4	4	0
22q11.1	15268577	16033955	*OR11H1(u) - CECR1(d)*	4	4	0

Genes in blue were validated by RT-PCR. bp = base pair, Total = number of samples with alteration, CN = copy number, u = upstream, d = downstream, i = intronic, 5'UTR = 5' untranslated region, 3'UTR = 3' untranslated region.

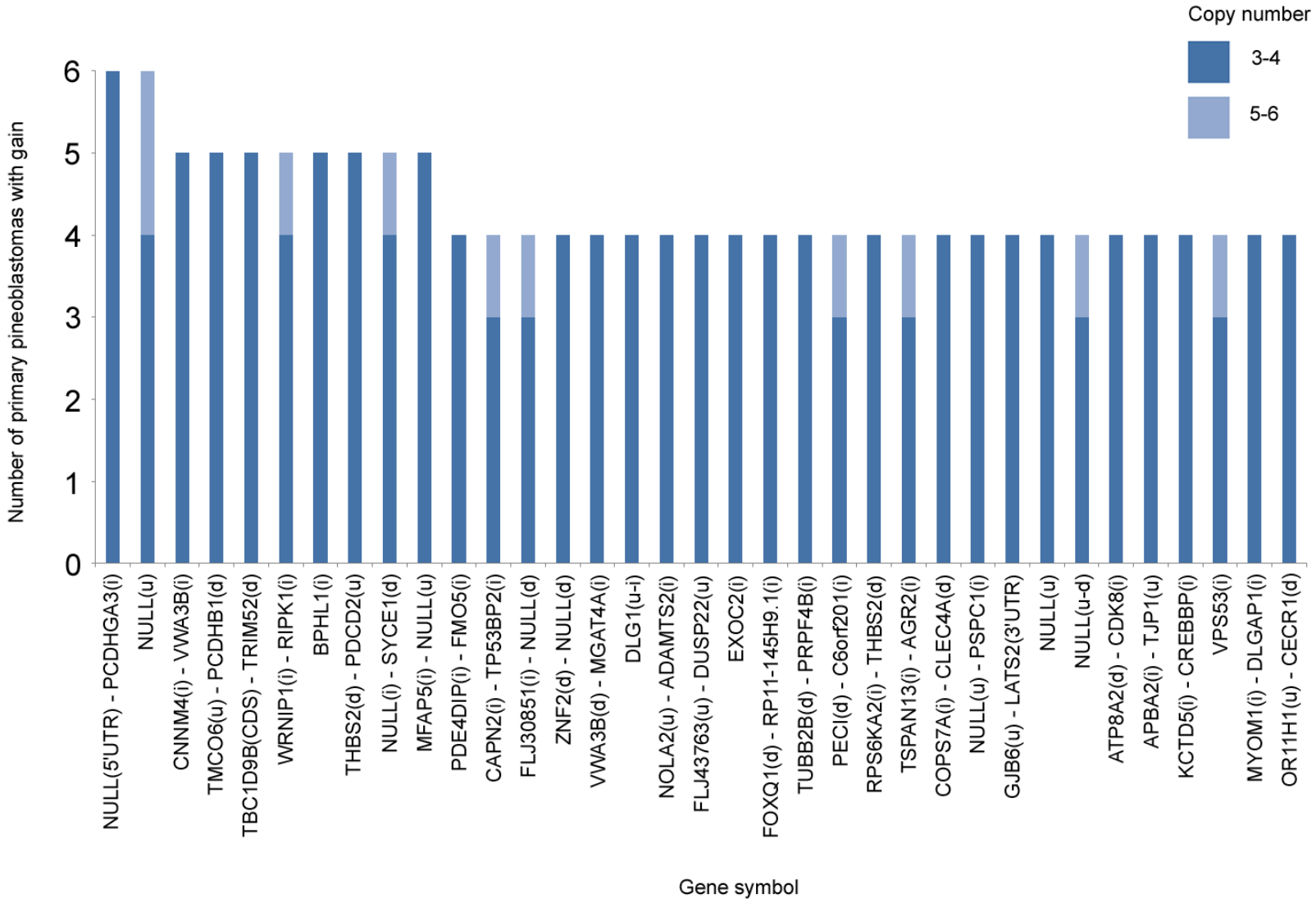

Figure 6.7 Graphical representation of increased gene copy numbers identified in 6 primary pineoblastomas using the 100K SNP array platform. u = upstream, d = downstream, i = intronic, 3'UTR = 3' untranslated region, 5'UTR = 5' untranslated region, CDS = coding region, NULL = no gene name.

6.3.1.8 Genomic regions encompassing candidate gene loss in primary pineoblastomas analysed using 100K SNP arrays

SNP copy number loss was identified on chromosomes 3p, 8p, 13q, 10q, 11p, 13q, 16q and 19p for at least 1/6 (16.7%) primary pineoblastomas (Table 6.8, Figure 6.8). The most frequent candidate region of loss involved SNPs downstream of *OR4C12* in 3/6 (50%) primary pineoblastomas. A broad region of loss (over 20Mb) was identified at 16q12.1 – 22.1 in 2/6 (33.3%) primary pineoblastomas, encompassing the transcriptional repressor, *SALL1*.

Table 6.8 Regions of decreased copy number in 6 primary pineoblastomas identified using the 100K SNP array platform

Cytoband	Start (bp)	End (bp)	Gene symbol	Total	CN1	CN0
11p11.12	50585971	51230448	*OR4C12/OR4A5(d)*	3	2	1
11p11.12	50396846	51383437	*OR4C12/OR4A5(d) - OR4C46(d)*	2	2	0
16q12.1 - 22.1	47282398	67420442	*NULL(d) - CDH1(i), including SALL1*	2	2	0
16q22.3 - 23.2	70523226	79509800	*NULL(i) - CDYL2(u)*	2	2	0
16q23.3 - 24.1	80532566	83804696	*PLCG2(i) - FAM92B(u)*	2	2	0
16q24.2 - 24.3	85631136	88368209	*FOXL1(d) - FANCA(i)*	2	2	0
3p22.3 - 22.2	36491330	36609993	*STAC(i-d)*	1	1	0
3p14.2	62466087	62825850	*CADPS(i)*	1	1	0
8p23.3 - 23.1	180568	11755937	*ZNF596(i) - CTSB(i)*	1	1	0
8p23.1 – 12	12651557	30588991	*C8orf79(u) - GTF2E2(i)*	1	1	0
10q21.3 - 26.3	70340702	134291559	*DDX50(i) - INPP5A(i)*	1	1	0
13q13.2 - 14.11	34503692	39966065	*NBEA(i) - FOXO1(d)*	1	1	0
13q14.11 - 14.12	41755280	45088338	*AKAP11(i) - SPERT(u)*	1	1	0
13q14.12 - 14.2	45759488	47235256	*RP11-139H14.4(d) - SUCLA2(d)*	1	1	0
13q14.3 - 21.33	49731408	71278847	*NULL(d) - DACH1(i)*	1	1	0
16q11.2 - 12.1	45293764	47221947	*MLCK(d) - N4BP1(u)*	1	1	0
16q22.1 - 22.3	67514126	70461679	*NULL(i) - LOC55565(i)*	1	1	0
16q23.2	79570845	80286482	*C16orf61(i) - CMIP(i)*	1	1	0
16q24.1	84264952	85485936	*KIAA0182(3'UTR) - FOXL1(d)*	1	1	0
19p13.3	2705548	4367411	*SLC39A3(u) - CHAF1A(i)*	1	1	0

Genes in blue were validated by RT-PCR. bp = base pair, Total = number of samples with alteration, CN = copy number, u = upstream, d = downstream, i = intronic.

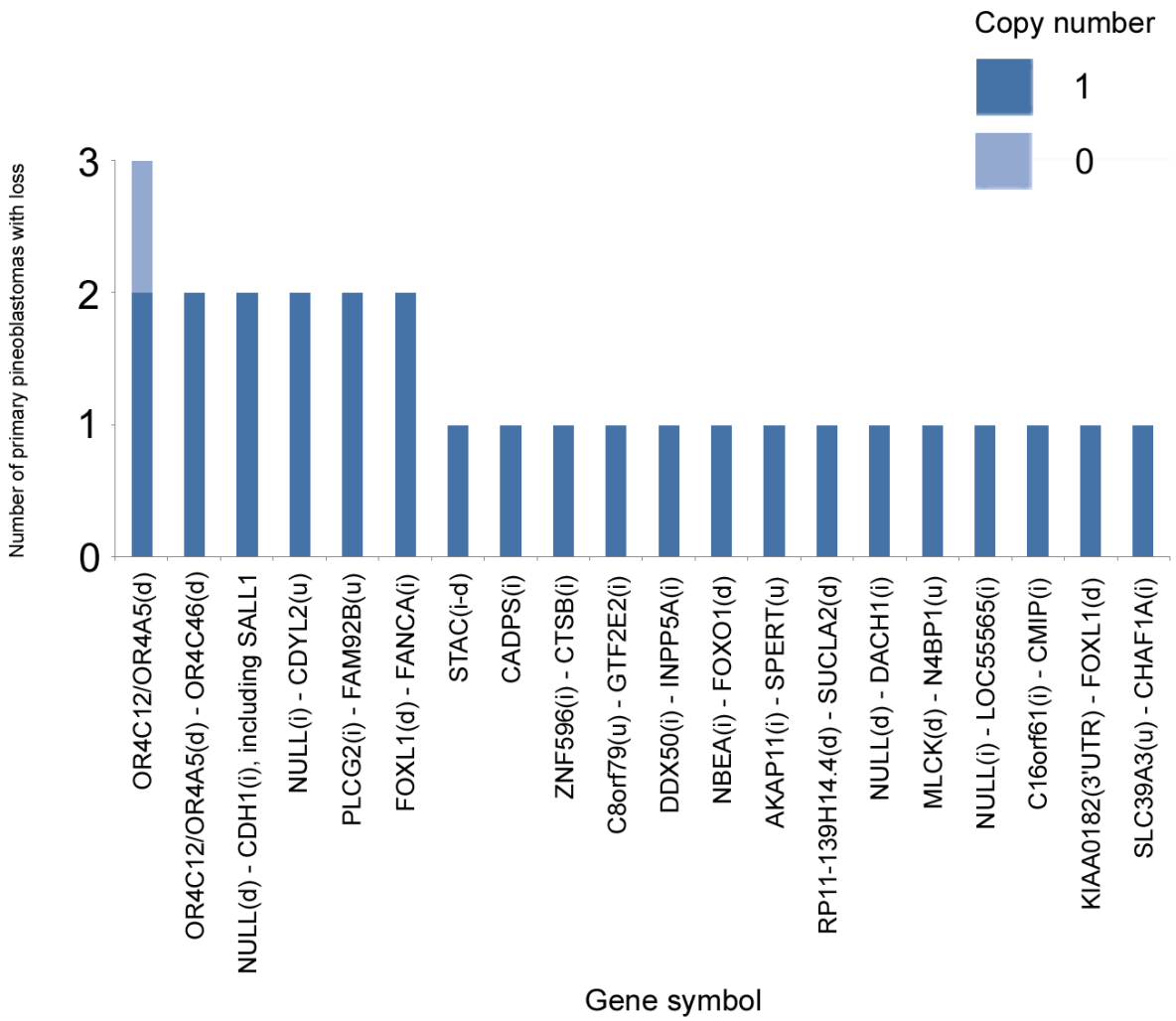

Figure 6.8 Graphical representation of decreased gene copy numbers identified in 6 primary pineoblastomas using the 100K SNP array platform. u = upstream, d = downstream, i = intronic, NULL = no gene name.

6.3.1.9 Genomic regions encompassing candidate gene gain in recurrent pineoblastomas analysed using 100K SNP arrays

SNP copy number gain was identified in 2 recurrent pineoblastomas and showed many focal regions of gain across the genome (Table 6.9). Regions on 1q42.13 – 42.3 were found gained in 2/2 (100%) recurrent pineoblastomas. This region encompasses a member of the WNT gene family (*WNT9A)*, which encodes a ligand implicated in the WNT signalling pathway. Alongside various other candidate regions of gain in the recurrent pineoblastomas, gain of *EGFR* (7p11.2) was identified in 2/2 (100%) recurrent pineoblastomas.

Table 6.9 Regions of increased copy number in 2 recurrent pineoblastomas identified using the 100K SNP array platform

Cytoband	Start (bp)	End (bp)	Gene symbol	Total	CN 3 or 4	CN 5 or 6
1p36.23	7683588	8732928	*CAMTA1(i) - RERE(i)*	2	2	0
1p36.12 - 36.11	23324479	27511370	*NULL(i) - WDTC1(d)*	2	2	0
1p34.3	38893245	39487971	*RRAGC(d) - MACF1(i)*	2	2	0
1p34.2	40635984	40826701	*SMAP1L(i) - ZNF684(d)*	2	1	1
1p34.2 - 34.1	42439233	45759257	*FOXJ3(i) - PRDX1(i)*	2	2	0
1q21.1	143619946	145119652	*PDE4DIP(i) - FMO5(d)*	2	2	0
1q21.3 -22	151487340	154294174	*LOR(u) - MAPBPIP(i)*	2	2	0
1q42.13	226216439	226929148	*WNT9A(i) - RHOU(u)*	2	2	0
1q42.2	229069837	229985464	*C1orf198(i) - DISC(i)*	2	2	0
1q42.2 - 42.3	232699691	234362983	*TARBP1(u) - GPR137B(u)*	2	2	0
2p25.1	9066695	10906039	*MBOAT2(u) - ATP6V1C2(d)*	2	2	0
2p23.3	24155750	27449260	*TP53I3(i) - SNX17(i)*	2	1	1
2p22.3	32368902	33972928	*YIPF4(i) - NULL(u)*	2	1	1
2q11.1 - 11.2	95226463	98195669	*ZNF2(d) - VWA3B (i)*	2	2	0
2q14.2 - 14.3	121954999	122117368	*CLASP1(i)*	2	2	0
2q37.3	239983692	241530315	*HDAC4(i) - MTERFD2(d)*	2	2	0
3p25.3	11397319	11409465	*ATG7(i)*	2	1	1
3p21.31 - 21.1	46512754	54168568	*RTP3(u) - CACA2D3(i)*	2	2	0
3q27.1 - 27.3	184342095	188232996	*LAMP3(i) ST6GAL1(i)*	2	2	0
3q29	194970765	198699627	*HES1(u) - DLG1(u)*	2	2	0
4p16.1	5932934	7855165	*CRMP1(i) - AFAP1(i)*	2	1	1
4p14 - 13	37802206	41017646	*TBC1D1(i) - LIMCH1(u)*	2	2	0
4q35.1	183454790	184086599	*NULL(u) - DCTD(u)*	2	2	0
5p15.33	208367	845362	*KIAA1909(i) - ZDHHC11(d)*	2	2	0

5p15.31	6574837	6844907	*NSUN2(d) - POLS(d)*	2	2	0
5p15.2	11140711	11512318	*CTNND2(i)*	2	2	0
5p15.2	14190691	14922709	*DNAH5(u) - ANKH(i)*	2	2	0
5q13.2	70825622	70893950	*BDP1(i-CDS)*	2	2	0
5q31.1	131309963	131727568	*NULL(i) - FLJ44796(u)*	2	2	0
5q31.3	140594436	140879968	*NULL(5'UTR) - DIAPH1(i)*	2	2	0
5q35.3	177544899	180003855	*NOLA2(u) - FLT4(i)*	2	1	1
6p25.3 - 25.1	99536	4194645	*FLJ43763(u) - NULL(u)*	2	2	0
6p25.1	6889547	6904105	*RREB1(u)*	2	1	1
6p22.1 - 21.32	29756485	32328375	*NULL(i) - NOTCH4(u)*	2	2	0
6p21.32 - 21.31	33166930	33628042	*HLA-DPB1(d) - BAK1(d)*	2	2	0
6p21.1	41278472	41563034	*TREML2(u) - FOXP4(u)*	2	2	0
6q25.1	150324856	150512956	*ULBP2(d) - PPP1R14C(i)*	2	2	0
6q25.1	150953062	151820627	*IYD(d) - C6orf211(i)*	2	2	0
6q25.3 - 26	157055118	162302724	*ARID1B(u) - PARK2(i)*	2	2	0
6q27	166638426	170746883	*PRR18(d) - PCDC2(u)*	2	1	1
7p21.1	16787522	16789400	*TSPAN13(i)*	2	1	1
7p13	43931371	44654924	*URG4(u) - OGDH(i)*	2	1	1
7p11.2	54676967	56161603	*NULL(d) including EGFR*	2	2	0
7q32.1 - 32.2	127647399	129323939	*LEP(u) - UBE2H(i)*	2	2	0
7q34	138372408	141123331	*ZC3HAV1L(u) - TAS2R3(d)*	2	1	1
7q36.1 - 36.3	150491179	157958216	*ASB10(d) - PTPRN2(i)*	2	2	0
8p23.3	180568	604843	*ZNF596(i) - ERICH1(i)*	2	2	0
8p23.1	6360995	6368340	*ANGPT2(i)*	2	2	0
8p23.1	6642801	6709792	*XKR5(d) - DEFB1(d)*	2	1	1
8p21.3 - 21.2	21762020	23453622	*GFRA2(u) - SLC25A37(i)*	2	2	0
8q11.22	52308591	52488349	*PXDNL(u-d)*	2	2	0
8q22.1	98641072	98761399	*NULL(d) - MTDH(i)*	2	2	0
9q22.32 - 22.33	96802976	99910889	*C9orf3(i) - TRIM14(i)*	2	1	1
10p15.3 - 15.2	2419307	3254644	*PFKP(u) - PITRM1(i)*	2	2	0
10p13	12973261	12990205	*CCDC3(i-d)*	2	1	1
10p11.21	34936751	35499982	*PARD3(i) - CREM(i)*	2	2	0
10q22.1 - 22.2	73570575	76100549	*ASCC1(i) - ADK(i)*	2	2	0
10q24.2	101069378	101071375	*CNNM1(u) - HPSE2(u)*	2	1	1
10q26.13	123386796	124907864	*ATE1(d) - BUB3(i)*	2	2	0
10q26.13 - 26.3	126428009	135189835	*FAM53B(u) - SYCE1(d)*	2	2	0
11q13.1	65679165	67096525	*PACS1(i) - GSTP1(u)*	2	2	0
11q13.4 - 14.1	71766454	77825022	*CLPB(i) - NARS2(3'UTR)*	2	2	0
12p13.33 - 13.32	331859	3811676	*JARID1A(i) - PARP11(i)*	2	2	0
12p13.31	6755337	7157242	*LAG3(i) - C1RL(u)*	2	1	1
12q13.13	50605518	51215637	*ACVR1B(i) - KRT5(u)*	2	1	1
12q23.2	100614130	100674112	*MYBPC1(d) - GNPTAB(i)*	2	1	1
13q12.12 - 12.13	24008514	24518426	*PARP4(u) - PABPC3(u)*	2	2	0
13q12.13 - 12.2	26637093	26865841	*USP12(i) - NULL(d)*	2	2	0
13q12.3	29575163	29939595	*KATNAL1(d) - NULL(i)*	2	2	0
13q12.3	30380194	30925764	*C13orf33(i) - RXFP2(u)*	2	1	1

13q34	109333777	113208152	*IRS2(u) - TMCO3(i)*	2	2	0
14q11.2	20156883	20223628	*OR6S1(d) - RNASE4(i)*	2	1	1
14q32.2 - 32.33	98716319	106312036	*BCL11B(i) - NULL(d)*	2	1	1
15q11.2 - 13.2	19208413	28890187	*NULL(d) - MTMR10(d)*	2	2	0
15q15.1	39159531	40134486	*INOC1(i) - PLAG2G4D(d)*	2	2	0
15q15.2 - 15.3	40915917	41817310	*TTBK2(i) - NULL(i)*	2	2	0
15q23	66413596	67236901	*ITGA11(i) - GLCE(u)*	2	2	0
15q25.1 - 25.2	78367393	80106823	*FAH(d) - MEX3B(d)*	2	2	0
17p13.3	450509	561244	*VPS53(i)*	2	2	0
17p13.2 - 13.1	6176952	9904211	*AIPL1(d) - GAS7(i)*	2	2	0
18q23	72120525	76068963	*LOC284274(u) - PARD6G(i)*	2	2	0
19p13.2	9464695	11658308	*ZNF560(i) - LOC401898(d)*	2	2	0
19p13.12 - 13.11	15579349	19682367	*CYP4F22(d) - ZNF14(3'UTR)*	2	2	0
19q13.11	39302438	39368822	*LSM14A(u-i)*	2	1	1
19q13.2 - 13.31	45796700	49174547	*LTBP4(i) - ZNF221(d)*	2	1	1
19q13.32	50478886	51019773	*MARK4(i) - SYMPK(i)*	2	1	1
19q13.32 - 13.43	53255346	63458980	*PLA2G4C(i) - ZNF544(i)*	2	2	0
20p13	2542190	2944423	*TMC2(i) - PTPRA(i)*	2	2	0
20p11.23 - 11.22	19508664	21313558	*SLC24A3(CDS) - XRN2(i)*	2	2	0
20p11.21 - 11.1	24480613	26148028	*C20orf39(i) - NULL(d)*	2	2	0
20q11.1 - 11.23	28084896	34443365	*NULL(d) - DLGAP4(i)*	2	2	0
20q13.13	46416394	49190813	*NULL(d) - KCNG1(u)*	2	2	0
20q13.32	56404776	56442694	*VAPB(i)*	2	1	1
20q13.33	59832199	62376958	*CDH4(i) - PCMTD2(3'UTR)*	2	2	0
21q22.13	37014570	37975732	*SIM2(i) - KCNJ6(i)*	2	2	0
21q22.2 - 22.3	41357397	46924583	*NULL(d) - PRMT2(d)*	2	1	1
22q11.1 - 11.22	15268577	20867581	*OR11H1(u) - NULL(u)*	2	2	0
22q12.1 - 12.2	27773709	28000939	*NULL(i) - EWSR1(i)*	2	1	1
22q13.31 - 13.32	45250436	48118190	*CELSR1(i) - FLJ44385(u)*	2	2	0

Genes in blue were validated by RT-PCR. bp = base pair, Total = number of samples with alteration, CN = copy number, u = upstream, d = downstream, i = intronic, CDS = coding region, 3'UTR = untranslated region, 5'UTR = 5' untranslated region.

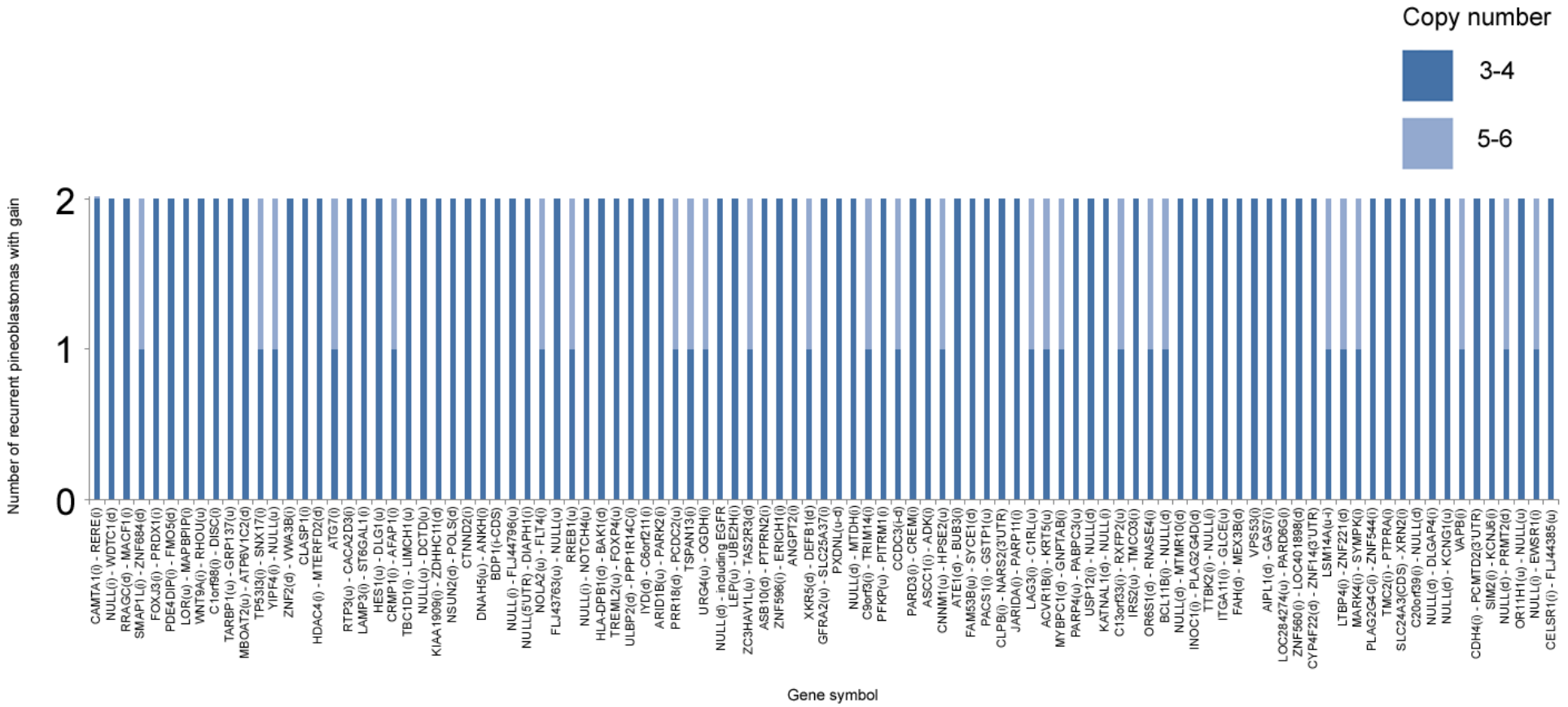

Figure 6.9 Graphical representation of increased gene copy numbers identified in 2 recurrent pineoblastomas using the 100K SNP array platform. u = upstream, d = downstream, i = intronic, 3'UTR = 3' untranslated region, 5'UTR = 5' untranslated region, CDS = coding region, NULL = no gene name.

6.3.1.10 Genomic regions encompassing candidate gene loss in primary pineoblastomas analysed using 100K SNP arrays

Loss of copy number was an infrequent event in the 2 recurrent pineoblastomas analysed. 6 focal regions of loss were identified in 1/2 (50%) recurrent pineoblastomas (Table 6.10).

Table 6.10 Regions of decreased copy number in 2 recurrent pineoblastomas identified using the 100K SNP array platform

Cytoband	Start (bp)	End (bp)	Gene symbol	Total	CN1	CN0
3q13.31	117791747	117991537	*NULL(d)*	1	1	0
7p11.2	56695043	57381007	*LOC401357(d) - NULL(d)*	1	1	0
11q22.3	103016430	103104927	*DDI1(u) - PDGFD(d)*	1	1	0
16q22.3	70732657	71151888	*PMFBP1(i) - NULL(u)*	1	1	0
18p11.21	12630421	12812702	*SPIRE1(i) - PTPN2(i)*	1	1	0
21q21.2	23436259	23619057	*NULL(u-d)*	1	1	0

bp = base pair, Total = number of samples with alteration, CN = copy number, u = upstream, d = downstream, i = intronic.

6.3.1.11 Identification of candidate regions of high level gain/amplification in CNS PNET and pineoblastoma

The high resolution, genome-wide approach taken in this thesis allowed the identification of candidate gene amplifications, in addition to hemizygous and homozygous deletions. Individual regions of high level gain identified (with a copy number of 6), contained at least 5 consecutive SNPs and are shown in Table 6.11. Gene copy number amplifications were identified at 17 distinct regions. CNS PNET17 had a large region of amplification located on 2p24.3 encompassing the proto-oncogene *MYCN*. A member of the *MYC* family, *MYCN* is most notably amplified in the extracranial solid tumour, neuroblastoma (Brouder, Seeger et al. 1984). Amplification of *MAP2* (2q34) was identified in case 11 (a pineoblastoma), with the encoded microtubule-associated protein involved in microtubule assembly, an essential step of neurogenesis (Farah, Liazoghli et al. 2005). In CNS PNET17 a region upstream of the caveolin gene (*CAV2*, 7q31.2, involved in cellular growth control and apoptosis) was

identified with high level gain (Figure 6.10a) (Carver, Schnitzer et al 2003). Amplification was also observed upstream of *LRIG3*, a gene with currently unknown functions and is shown in Figure 6.10b. CNS PNET28 had amplification of the gene, *NUAK1* (12q23.3), which has important roles in the phosphorylation of *ATM* and the suppression of fas-induced apoptosis by phosphorylation of *CASP6* (Suzuki, Kusakai et al. 2003). Of note, one recurrent tumour (CNS PNET21R) was found to have 2 novel regions of high level gain at 4q12 and 12q14.1, which were not present in the primary tumour (CNS PNET21P). The high level gain identified at 4q12 encompassed *PDGFRA*, encoding a cell surface tyrosine kinase receptor for the platelet derived growth factor family of mitogens, in addition to the co-amplification of the proto-oncogene *c-KIT* (*KIT*). Gene expression analysis performed for CNS PNET21R provided confirmation that the gene copy number amplification gave rise to an increase in *PDGFRA* expression (Figure 6.11).

Table 6.11 Candidate regions of amplification identified in CNS PNETs and pineoblastomas analysed using 100K and 500K SNP arrays

Cytoband	ID	Start (bp)	End (bp)	Gene symbol
1q42.13	8R	228504678	228534898	*NULL (i) - PGBD5 (i)*
2p24.3	17	1422483	15141791	*NULL (d) - NAG (d)*
2p24.3	17	15614969	15977810	*NAG (i) - NULL (d)*
2p25.2	17	6069283	6395879	*FLJ42418 (d)*
2p25.1	17	8228462	10265469	*C2orf46 (i-d)*
2q22.3	8R	145577586	145586350	*ZEB2 (u)*
2q33.1	22R	197195870	197200521	*HECW2 (u)*
2q31.1	28	170142309	170408666	*PPIG (u) - ZNF650 (u)*
2q33.3	28	208686042	208758663	*CRYGD (d) - NULL (i)*
2q34	11	209955206	209965782	*MAP2 (u)*
3p22.1	7	42966650	43523663	*NULL (d) - TMEM16K (i)*
4q12	21R	52379648	59114124	*DCUN1D4 (u) - NULL (u)*
7q31.2	17	114859395	114946242	*NULL (u)*
7q31.2	17	115918829	115951188	***CAV2 (u)***
12p13.31	28	8955641	8986493	*M6PR (i-d)*
12q14.1	21R	56263307	57836375	***LRIG3 (u)***
12q23.3	28	105149261	105198811	*NUAK1 (u) - CKAP4 (u)*

Regions of 5 consectutive SNPs with copy numbers of 6 were identified. Pineoblastoma ID underlined. Genes in bold are graphically represented in Figures 5.7a and 5.7b. R, recurrence. bp = base pair, NULL = no gene name, i = intronic, d = downstream, u = upstream.

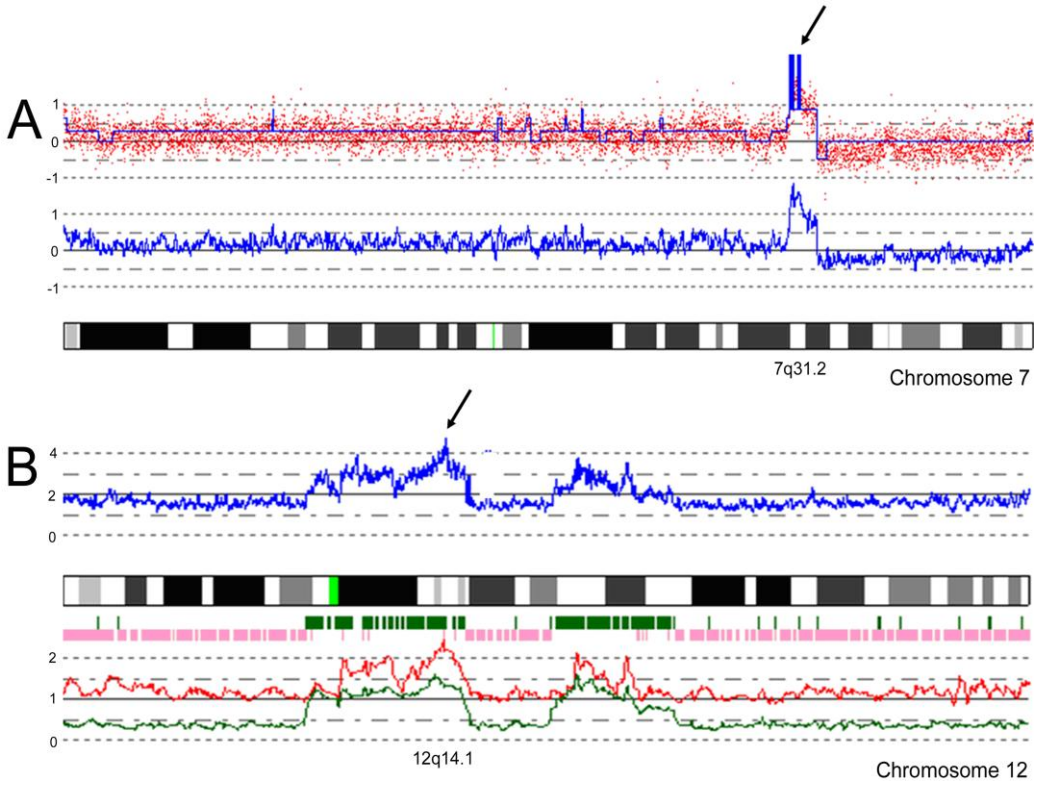

Figure 6.10a and 6.10b Amplifications identified in CNS PNET cases visualised in CNAG. (A) CNS PNET17 with potentially amplified region encompassing *CAV2*, (arrowed). Red dots = $\log_2$ ratios of each probe, blue line = averaged $\log_2$ ratios of probes. (B) CNS PNET21R with amplification of *LRIG3*, arrowed. Blue line = averaged copy number of probes, green bars = heterozygous probes, pink bars = LOH, green and red lines = allele-specific probe copy numbers.

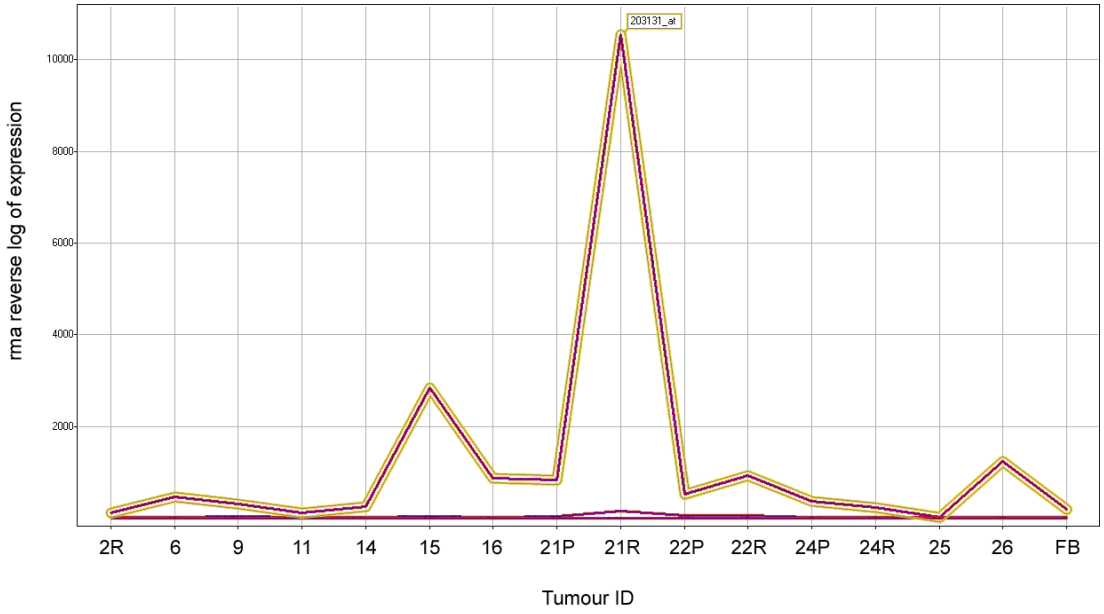

Figure 6.11 Affymetrix genechip U133 plus 2 expression array analysis for *PDGFRA* (probe 203131) in 15 CNS PNETs and Foetal Brain (FB). High level expression of *PDGFRA* was found in CNS PNET 21R following the identification of an amplicon at 4q12 using Affymetrix SNP array analysis. Gene expression analysis performed by Dr H. Rogers (CBTRC). P, primary; R, recurrence.

6.3.1.12 Identification of candidate regions of homozygous loss in CNS PNET and pineoblastoma

In this study, candidate regions of homozygous loss were more commonly observed than amplification. Individual homozygous deletions (with a copy number of 0), contained at least 5 consecutive SNPs and are shown in Table 6.12. No homozygous deletions were identified in the 6 primary and 2 recurrent pineoblastoma samples studied using the SNP array platform. CNS PNET34 contained homozygous loss of the glutamate receptor, *GRM7*, which is involved in glutamatergic neurotransmission in normal brain function (Figure 6.12a) (Makoff, Pilling et al. 1997). Loss of *IFT57* was identified in CNS PNET8P, encoding a protein with an indirect role in the sonic hedgehog pathway (SHH) pathway (Liu, Wang et al. 2005). Additionally, *IFT57* has pro-apoptotic functions via interactions with *HIP1*, which leads to the recruitment of *CASP8*, triggering apoptosis (Gervais, Singaraja et al. 2002). Whilst two olfactory receptor genes (*OR4A5* and *OR4K15*) were identified with homozygous loss in 2 separate CNS PNETs (4 and 39), *CCDC100* (encoding a protein which is not only involved in the positioning of neurons during brain development, but also is implicated in the migration and self renewal of neural progenitors) was lost in 2 CNS PNETs (Xie, Moy et al. 2007). A large region of 9p21.3 harboured homozygous copy number loss and was identified in 4 CNS PNETs. The loss encompassed *MTAP*, *CDKN2A*, *CDKN2B* and *DMRTA1* in 3 tumours (CNS PNETs 17, 24P and 24R), whilst a fourth tumour was identified with a smaller region of loss which involved only *MTAP*, *CDKN2A* and *CDKN2B* (CNS PNET 34). CNS PNET32 had lost both allele copies of *MRGPRX2* which has an involvement in the functioning of nociceptive neurons (Figure 6.12b), whilst CNS PNET41 had homozygous loss of the cadherin gene (*CDH7*) involved in cell-cell adhesion (Figure 6.12c) (Yang, Liu et al. 2005) (Vissers, Ravenswaaij et al. 2004). A region of homozygous loss at 22q11.23 was identified in 2 tumours, encompassing the putative tumour suppressor *INI1* (shown in Figures 6.12d and 6.12e).

Table 6.12 Candidate regions of homozygous loss identified in CNS PNETs analysed using 100K and 500K SNP arrays

Cytoband	ID	Start (bp)	End (bp)	Gene symbol
2q37.3	34	242567344	242663303	*FLJ33590 (d) - NULL (u)*
3p26.1	34	6976308	7067021	***GRM7 (i)***
3q13.12	8P	109375839	109390664	*IFT57 (i)*
4p16.3	8R	753229	1137333	*PCGF3 (3'UTR) - NULL (3'UTR)*
4q12	8P	58608814	58641115	*NULL (u)*
4q21.1	8P	78317830	78433089	*NULL (i) - CXCL13 (u)*
4q34.3	18	179450600	181288937	*NULL (u-d)*
4q34.3-35.1	18	181987214	183127745	*NULL (u-d)*
5q23.2	36	122724781	122733220	*CCDC100 (i)*
5q23.2	29	122724908	122733220	*CCDC100 (i)*
7p21.3	8P	11700038	11734963	*TMEM106B (u)*
7q11.21	29	61269841	62091131	*NULL (u-d)*
9p21.3	17	21647873	22537789	*NULL (u) - ELAVL2 (d)*
9p21.3	24P	21844199	23071563	*MTAP (i) - DMRTA1 (d)*
9p21.3	24R	21948524	23071563	*NULL (d) - DMRTA1 (d)*
9p21.3	34	21948524	21999960	*CDKN2A (i) - CDKN2B (3'UTR)*
9q34.11	41	132382895	132394715	*ASS1 (d)*
10q22.1	28	72515880	72592373	*PCBD1 (u)*
10q23.31	14	92423710	92456069	*NULL (d) – HTR7 (d)*
11p15.1	32	18907033	18916600	***MRGPRX1 (d) - MRGPRX2 (d)***
11p11.12	4	50585971	51230448	*OR4A5 (d)*
12q11-12	36	36391876	36711249	*NULL (u)*
12q12	8P	36588164	36903232	*NULL (u)*
14q11.2	39	19272965	19492423	*OR4Q3 (u) - OR4K15 (u)*
18q12.1	8P	26098054	26127599	*NULL (u-d)*
18q22.1	41	62058576	62062341	***CDH7 (d)***
20q13.2	33	52087236	52092000	*BCAS1 (i)*
22q11.23	6	21996929	22666327	***BCR (d) - GSTT2 (d)***
22q11.23	7	22038020	22833987	***FLJ31568 (d) - CABIN (i)***

Regions of 5 consectutive SNPs with copy numbers of 6 identified. Genes in bold are graphically represented in Figures 5.9a – e. P, primary; r, recurrence. bp = base pair, d = downstream, u = upstream, i = intronic, 3'UTR = 3' untranslated region.

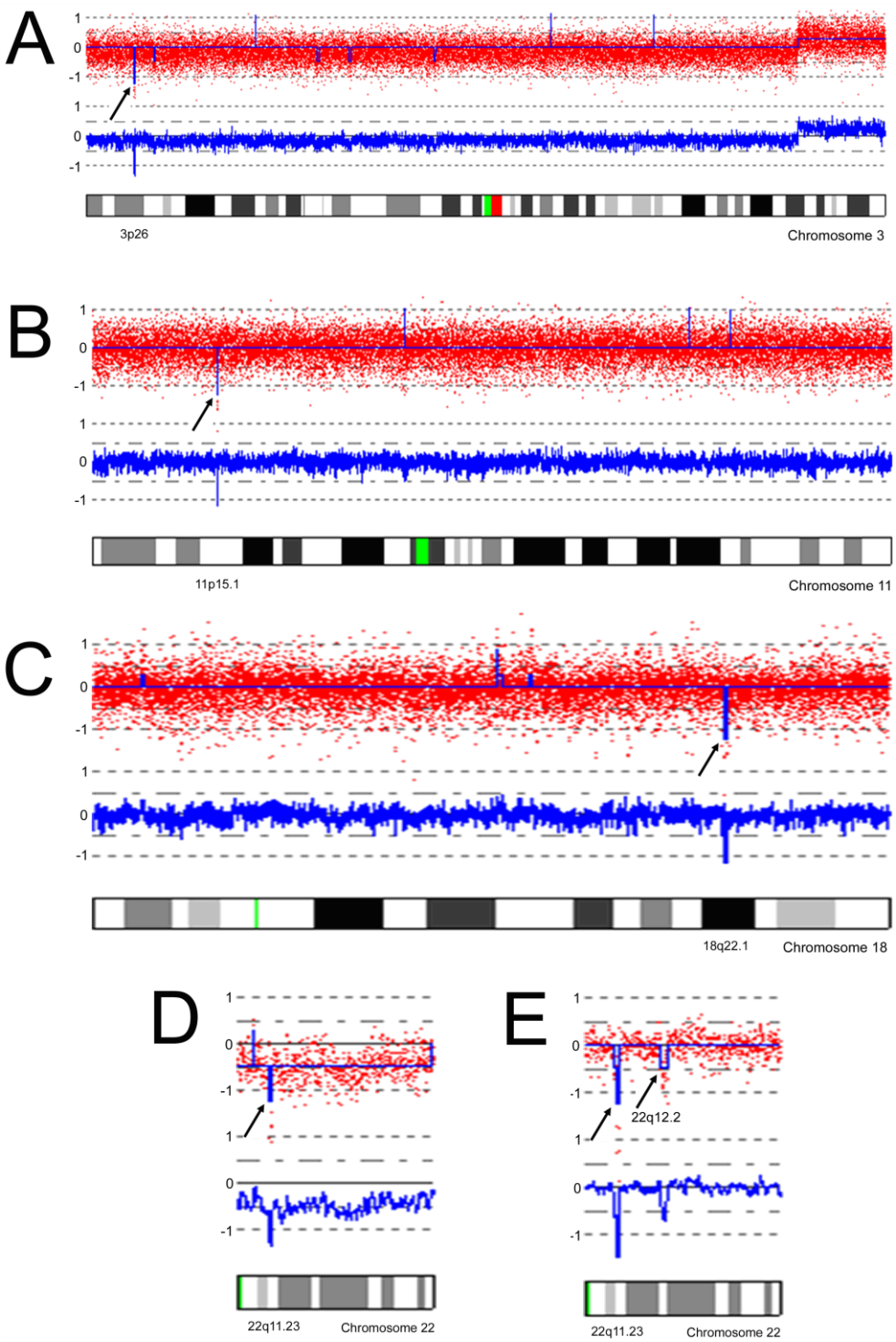

Figure 6.12A – 6.12E Homozygous deletions in CNS PNETs, visualised in CNAG. y axes = $\log_2$ ratio, x axis in top visualisations = probes (red) and normalised (blue), x axis in bottom visualisations = line graph of mean probe $\log_2$ ratio. CNS PNET34 with homozygous deletion of *GRM7* (A), CNS PNET32 with homozygous deletion of *MRGPRX2* (B), CNS PNET41 with homozygous deletion of *CDH7* (C), CNS PNET7 with the loss of one copy of the entire chromosome 22q (D), in addition to homozygous deletion of the region between *BCR* and *GSTT2* including *INI1* (*BAF47*), CNS PNET6 with homozygous deletion of the region between *FLJ31568* and *CABIN* (22q11.23) encompassing *INI1* (*BAF47/SMARCB1*) in addition to the loss of one copy at 22q12.2 (E). 22q12.2 encompasses the tumour suppressors, *EWSR1* (Ewings sarcoma region 1), *NF2* (Neurofibromatosis 2) and *LIF* (leukemia inhibitor factor). Genes identified with homozygous loss arrowed.

6.3.2 Combination of copy number and LOH results to identify candidate regions of aUPD in 15 paired CNS PNETs

SNP copy number and allele genotype results were combined to identify candidate regions of copy neutral LOH, also known as acquired uniparental disomy (aUPD). aUPD analysis was performed for tumours with matched constitutional blood sample SNP array data. Large regions of aUPD were identified in 5 CNS PNETs and were visualised following the generation of a heatmap in Spotfire® (Figure 6.13). In addition to identifying novel candidate regions of aUPD in CNS PNET, the LOH data generated using the SNP arrays also acted as a method of validation, confirming the loss in copy number generated by the SNP copy number algorithms. Where there is loss in copy number there should also subsequently be LOH at the same region. The results of copy number loss and LOH for the CNS PNETs showed a direct connection for all regions of copy number loss also harbouring LOH (however, only if the region was originally heterozygous), confirming that the loss in copy number at that region was correctly identified.

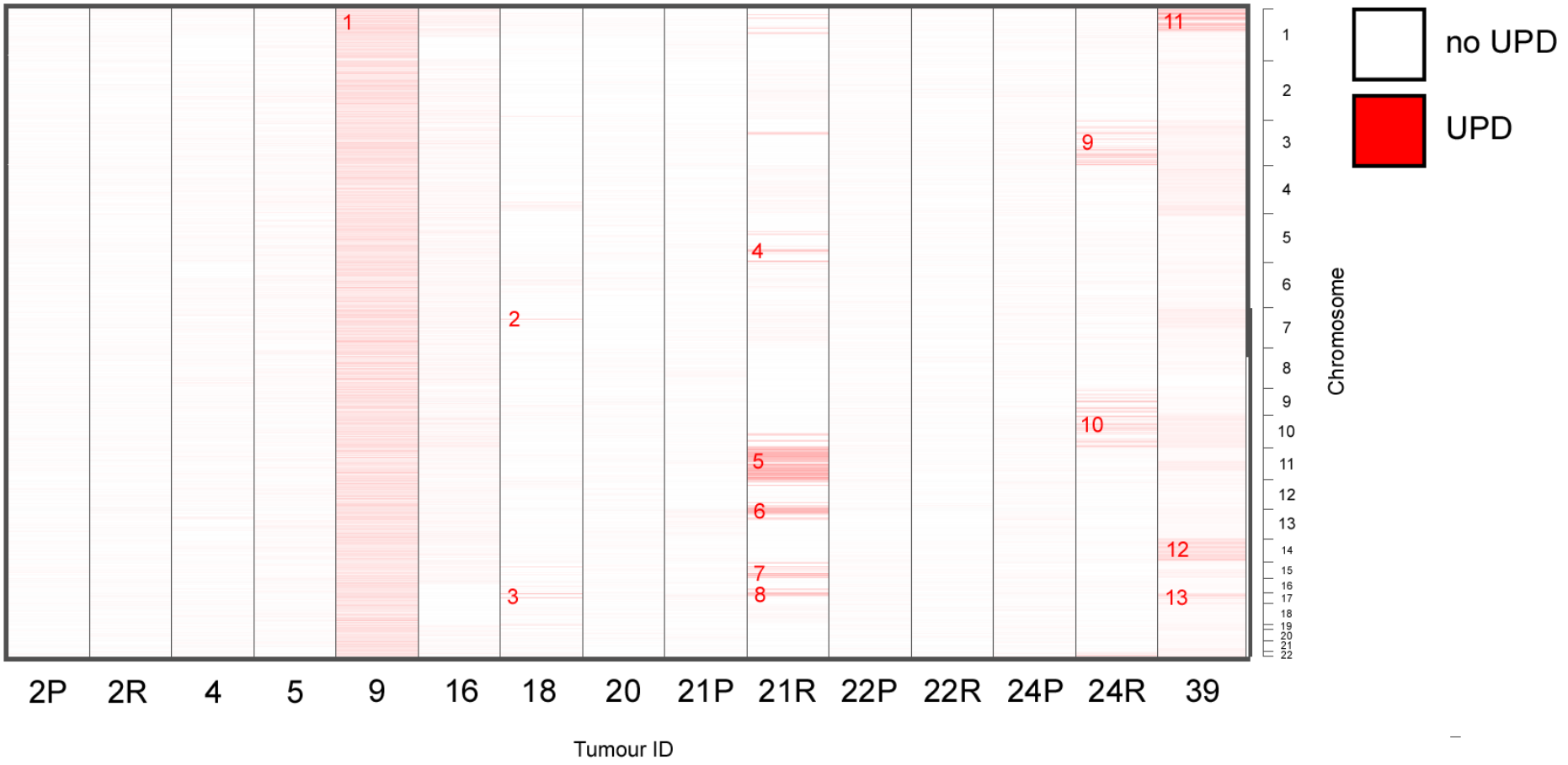

Figure 6.13 Genome-wide acquired uniparental disomy for 10 primary and 5 recurrent CNS PNETs. 9 primary and 5 recurrent CNS PNETs were analysed using the 100K mapping set and 1 primary CNS PNET was analysed using the 500K mapping set. Specific regions identified were genome-wide (1), 7p15.1(2), 17p13.3 and 17q13.1 (3), 5q31.1-2 (4), chromosome 11 (5), 13p (6), chromosome 15 (7), 16q and 17p (8), chromosome 3 (9), chromosomes 9 and 10 (10), 1p36.32 – 1p21.3 (11), chromsome 14 (12) and chromsome 17 (13). P, primary; R, recurrence.

The most common SNPs with aUPD identified in 14 CNS PNETs analysed using the 100K SNP arrays were summarised and ordered depending on frequency. Paired CNS PNETs (tumours with a matched blood samples) were used in this analysis, which combined the aUPD results of 9 primary and 5 recurrent CNS PNETs (Tables 6.13 and 6.14). Of the 9 primary CNS PNETs analysed for aUPD, the most common SNP identified with aUPD was located within the gene *CPNE4* (3q22.1), in 5/9 (55.6%) primary CNS PNETs. *CPNE4* is a member of the copine gene family which regulate molecular events between the cell membrane and cytoplasm (Creutz, Tomsig et al. 1998). 2 SNPs with aUPD were identified in the family with sequence similarity gene, *FAM3C* (7q31.31-32) in 4/9 (44.4%) primary CNS PNETs. Apart from chromosomes 18, 20 and 22, all chromosomes contained SNPs with aUPD in at least 3 primary CNS PNETs. The most frequent SNP with aUPD in 4/5 (80%) recurrent CNS PNETs, was located in the latrophilin gene, *LPHN3* (4q13.1), which has roles in cell adhesion and signal transduction (Hayflick, 2001). A SNP within another member of this gene family, *LPHN2* (1p31.1), was also identified with aUPD in 4/9 (44.4%) primary CNS PNETs. *TMEM16E* (encoding a transmembrane protein) contained 2 SNPs with aUPD in 3/5 (60%) recurrent CNS PNETs. Interestingly, on comparison of the aUPD data analyses of 9 primary and 5 recurrent CNS PNETs, SNPs located in 2 MAP kinases were identified with aUPD. Mitogen activated protein 6, (*MAPK6*) had aUPD in 3/9 (33.3%) primary CNS PNETs, whilst *MAP3K7* had aUPD in 3/5 (60%) recurrent CNS PNETs and in addition to regulating transcription and apoptosis, *MAP3K7* also has roles in cell response to environmental stress (Giroux, Iovanna et al. 2009).

Table 6.13 Most frequent regions of aUPD in 9 primary CNS PNETs analysed using the 100K SNP array platform

Affy SNP ID	Physical position	Gene symbol	Locus	CNS PNETs with aUPD
SNP_A-1641922	133413577	CPNE4	3q22.1	5
SNP_A-1664202	82979527	LPHN2	1p31.1	4
SNP_A-1714602	74769170	SEMA4F	2p13.1	4
SNP_A-1667870	56938384	NULL	3p14.3	4
SNP_A-1672738	100320269	COL8A1	3q12.1	4
SNP_A-1651362	102703417	SENP7	3q12.3	4
SNP_A-1694929	145731857	NULL	3q24	4
SNP_A-1693385	120891287	FAM3C	7q31.31	4
SNP_A-1749002	120908581	FAM3C	7q31.32	4
SNP_A-1657545	49836042	NULL	11p11.12	4
SNP_A-1685933	12707364	GPR19	12p13.1	4
SNP_A-1750672	75813311	KCTD12	13q22.2	4
SNP_A-1653480	29063506	NULL	16p11.2	4
SNP_A-1722617	48160014	NULL	1p33	3
SNP_A-1747804	67819113	NULL	1p31.3	3
SNP_A-1737168	94980112	F3	1p21.3	3
SNP_A-1747802	107760580	NTNG1	1p13.3	3
SNP_A-1642425	150306417	FLJ32955	2q23.3	3
SNP_A-1667539	156604052	NR4A2	2q24.1	3
SNP_A-1671509	195656938	NULL	2q32.3	3
SNP_A-1692706	225560060	DOCK10	2q36.2	3
SNP_A-1642728	57269125	APPL1	3p14.3	3
SNP_A-1662293	69614189	MITF	3p14.1	3
SNP_A-1684237	82472263	GBE1	3p12.2	3
SNP_A-1739300	98257090	NULL	3q11.2	3
SNP_A-1757192	118786353	IGSF11	3q13.31	3
SNP_A-1700536	139638966	FAM62C	3q22.3	3
SNP_A-1725891	174973217	NLGN1	3q26.31	3
SNP_A-1699225	58365751	NULL	4q12	3
SNP_A-1720690	58541512	NULL	4q12	3
SNP_A-1655440	64167920	SRD5A2L2	4q13.1	3
SNP_A-1703464	103504728	NFKB1	4q24	3
SNP_A-1671049	127592471	FAT4	4q28.1	3
SNP_A-1754737	156541333	MAP9	4q32.1	3
SNP_A-1740476	158200919	NULL	4q32.1	3
SNP_A-1693622	170314007	SH3RF1	4q32.3	3
SNP_A-1718502	76458973	PDE8B	5q14.1	3
SNP_A-1706802	77164460	AP3B1	5q14.1	3
SNP_A-1684735	88062905	MEF2C	5q14.3	3
SNP_A-1742221	98594496	NULL	5q21.1	3
SNP_A-1753573	109291709	MAN2A1	5q21.3	3
SNP_A-1688193	114012544	*TRIM36*	5q22.3	3
SNP_A-1710396	114600750	*PGGT1B*	5q22.3	3

SNP_A-1704037	167189249	*NULL*	5q34	3
SNP_A-1752176	168711427	*SLIT3*	5q35.1	3
SNP_A-1753494	179871	*DUSP22*	6p25.3	3
SNP_A-1710086	4498690	*KU-MEL-3*	6p25.1	3
SNP_A-1648685	65251864	*NULL*	6q12	3
SNP_A-1713213	69694649	*BAI3*	6q12	3
SNP_A-1708373	96531511	*FUT9*	6q16.1	3
SNP_A-1738259	125476732	*TPD52L1*	6q22.31	3
SNP_A-1732838	150740247	*IYD*	6q25.1	3
SNP_A-1745254	37891780	*TXNDC3*	7p14.1	3
SNP_A-1748516	78808419	*MAGI2*	7q21.11	3
SNP_A-1644229	131827984	*PLXNA4B*	7q32.3	3
SNP_A-1653132	155661372	*NULL*	7q36.3	3
SNP_A-1735982	4203725	*NULL*	8p23.2	3
SNP_A-1756787	5449404	*NULL*	8p23.2	3
SNP_A-1654954	21500160	*IFNE1*	9p21.3	3
SNP_A-1673709	87105129	*NTRK2*	9q21.33	3
SNP_A-1734914	25716374	*GPR158*	10p12.1	3
SNP_A-1729039	29067624	*BAMBI*	10p11.23	3
SNP_A-1743428	88064787	*GRID1*	10q23.2	3
SNP_A-1670777	92323480	*NULL*	10q23.31	3
SNP_A-1695228	15020214	*CALCA*	11p15.2	3
SNP_A-1747103	34575332	*EHF*	11p13	3
SNP_A-1681974	79704096	*NULL*	11q14.1	3
SNP_A-1698228	96617039	*NULL*	11q21	3
SNP_A-1646867	21931308	*ABCC9*	12p12.1	3
SNP_A-1694716	31278772	*FAM60A*	12p11.21	3
SNP_A-1659469	39831159	*CNTN1*	12q12	3
SNP_A-1663347	46298657	*RPAP3*	12q13.11	3
SNP_A-1711954	100634466	*CHPT1*	12q23.2	3
SNP_A-1674438	117345360	*SUDS3*	12q24.23	3
SNP_A-1688649	126305334	*NULL*	12q24.32	3
SNP_A-1729907	41875439	*TNFSF11*	13q14.11	3
SNP_A-1650955	59095730	*DIAPH3*	13q21.2	3
SNP_A-1664188	77151328	*SCEL*	13q22.3	3
SNP_A-1659121	28402188	*NULL*	14q12	3
SNP_A-1750836	48800555	*NULL*	14q22.1	3
SNP_A-1645503	57420370	*C14orf37*	14q23.1	3
SNP_A-1750520	69530362	*SMOC1*	14q24.2	3
SNP_A-1648674	98110674	*C14orf177*	14q32.2	3
SNP_A-1739774	37730935	*FSIP1*	15q14	3
SNP_A-1677793	38307000	*BUB1B*	15q15.1	3
SNP_A-1748134	45907658	*SEMA6D*	15q21.1	3
SNP_A-1666980	50105557	*MAPK6*	15q21.2	3
SNP_A-1691267	54077691	*NEDD4*	15q21.3	3
SNP_A-1677463	59051547	*RORA*	15q22.2	3
SNP_A-1677391	69978320	*MYO9A*	15q23	3

SNP_A-1701037	55508777	*HERPUD1*	16q13	3
SNP_A-1722762	55990324	*CX3CL1*	16q13	3
SNP_A-1661937	11109150	*FLJ45455*	17p13.1	3
SNP_A-1701579	36815436	*NULL*	17q21.2	3
SNP_A-1734707	22799865	*NULL*	19p12	3
SNP_A-1754365	18412764	*C21orf91*	21q21.1	3
SNP_A-1753608	30564119	*CLDN8*	21q22.11	3
SNP_A-1692489	31179148	*KRTAP11-1*	21q22.11	3
SNP_A-1686152	37975732	*KCNJ6*	21q22.13	3

Table 6.14 Most frequent regions of aUPD in 5 recurrent CNS PNETs analysed using the 100K SNP array platform

Probe set ID	Physical position	Gene symbol	Locus	CNS PNETs with UPD
SNP_A-1722415	62102021	*LPHN3*	4q13.1	4
SNP_A-1676915	63867199	*PGM1*	1p31.3	3
SNP_A-1700746	100896325	*GPR88*	1p21.2	3
SNP_A-1732022	36094650	*CRIM1*	2p22.3	3
SNP_A-1671135	141219342	*LRP1B*	2q22.1	3
SNP_A-1673725	145886958	*ZEB2*	2q22.3	3
SNP_A-1671967	126674361	*FAT4*	4q28.1	3
SNP_A-1748616	182262097	*NULL*	4q34.3	3
SNP_A-1676495	68042654	*PIK3R1*	5q13.1	3
SNP_A-1732933	48561782	*C6orf138*	6p12.3	3
SNP_A-1642162	91284402	*MAP3K7*	6q15	3
SNP_A-1732561	35475127	*HERPUD2*	7p14.3	3
SNP_A-1651849	60763957	*CA8*	8q12.1	3
SNP_A-1666345	83792383	*NRG3*	10q23.1	3
SNP_A-1706504	95040540	*CYP26A1*	10q23.33	3
SNP_A-1730221	4636495	*OR51E1*	11p15.4	3
SNP_A-1702308	21613794	*TMEM16E*	11p14.3	3
SNP_A-1702414	21614149	*TMEM16E*	11p14.3	3
SNP_A-1693305	108187879	*DDX10*	11q22.3	3
SNP_A-1693686	63152770	*DSEL*	18q22.1	3

Limited research into aUPD has been performed on solid tumours. This thesis presents the first indication that aUPD is involved in the pathogenesis of CNS PNET.

6.4 Discussion

The high resolution analysis undertaken in this thesis has identified novel candidate regions encompassing genes potentially involved in CNS PNET and pineoblastoma pathogenesis which warrant further investigation. In addition to the separate group-wise analysis of primary and recurrent CNS PNETs to identify potential genes involved in tumour initiation and subsequent progression, a further subset of 13 CNS PNETs analysed at a higher resolution led to other novel genomic changes being identified. Homozygous deletions and amplifications were found to be common events in 18/46 (39.1%) and 7/46 (15.2%) CNS PNETs, respectively. The combination of copy number and LOH data for each tumour, led to the identification of candidate regions of aUPD in the CNS PNET genome.

The most common chromosome arm gain identified in the CNS PNET and pineoblastoma cohort involved 1q (as shown in chapter 4). SNPs within genes located on 1q were frequently gained in both the primary and recurrent CNS PNETs analysed. In particular gain of SNPs in the intron of *FAM129A* was a common event shared by the primary and recurrent CNS PNETs (21/32 (65.6%) and 5/6 (83.3%, respectively). The encoded protein is involved in the endoplasmic reticulum stress response mechanisms and high expression has been identified in cancers of the thyroid (Matsumoto, Fujii et al. 2006). Immunohistochemical analysis of the FAM129A protein is now needed to elucidate firstly if the gain in copy number is maintained at the protein level, and secondly if a high expression is identified, are the tumours with high level expression related to a clinical group.

Gain of 5q31.3 was a common event in both the primary CNS PNETs and pineoblastomas analysed using the 100K SNP arrays (13/19 (68.4%) and 6/6 (100%), respectively). The protocadherin encoded by *PCDHGA3* has critical roles in the establishment and function of specific cell-cell connections in the brain (Morishita, Yagi et al. 2007).

SFRP1 (8p11.21), was identified with copy number gain in 8/13 (61.5%) primary CNS PNETs analysed using the 500K SNP arrays and has previously been investigated in other studies of CNS PNET (Chang, Pang et al 2005). Although only identified in 4/19 (21%) primary CNS PNETs analysed using the 100K SNP arrays (data not shown), this

difference could be due to the variation in SNP coverage of the 2 separate array platforms. Whilst the 100K SNP array contains 1 probe upstream and 1 probe downstream of *SFRP1*, the 500K SNP array has 12 probes either within the 3'UTR or intronically located in the gene, thus if tumours previously analysed using the 100K arrays were subsequently reanalysed using the 500K array platform, further CNS PNETs would potentially be identified with *SFRP1* copy number gain. The encoded secreted-frizzled related protein of *SFRP1* is involved in WNT signalling, is known to decrease intracellular β-catenin levels and plays a role in both cell growth and differentiation. Whilst a high proportion of the CNS PNETs analysed for this thesis were found to have gain of *SFRP1*, supportive of an oncogenic role for *SFRP1*, this is on the contrary to other studies which have hypothesised tumour suppressive roles, especially in bladder and liver cancers (Stoehr, Wissmann et al. 2004; Huang, Zhang et al. 2007). Moreover, a previous study of 9 CNS PNETs investigated the methylation status *SFRP1* and found 1/9 (11.1%) CNS PNETs with methylated *SFRP1*, further substantiating a tumour suppressive role for *SFRP1* (Chang, Pang et al. 2005). Although other studies have identified loss of *SFRP1* expression by either deletion or epigenetic silencing, a study by Lee *et al.,* identified an opposite result, whereby high level expression of *SFRP1* was identified in medulloblastoma (Lee, Miller et al. 2003). The gain in copy number of *SFRP1* identified within the present study needs further validation (particularly at the gene expression level) and its role in the pathogenesis of CNS PNET needs to be investigated further. Functional exploration is needed to better understand the involvement of this gene in cancer with respects to its oncogenic and tumour suppressive roles specific to cancers of different tissues.

The most common chromosome arm loss identified in the CNS PNETs and pineoblastomas involved 16q, in 5/46 tumours (as shown in chapter 4) and many genes located on 16q were identified with copy number loss within the present chapter. Loss of SNPs downstream of *SALL1* was a frequent event in both the primary CNS PNETs and pineoblastomas analysed using the 100K SNP arrays (5/19 (26.3%) and 2/6 (33.3%), respectively). Loss of SNPs downstream of *OR4C12* (11p11.12), encoding an olfactory receptor, was a common event in the primary CNS PNETs and pineoblastomas studied (13/32, 40.6% and 3/6, 50%, respectively). Loss of *OR4C12* was also a common event in recurrent CNS PNETs (3/6, 50%). Situated in a gene cluster of olfactory receptors located on chromosome 11p, little is currently understood of the roles played by *OR4C12* in the normal brain or when lost, its potential role in

tumourigenesis. Loss of *CADPS* (3p14.2) was identified as a frequent event in the primary and recurrent CNS PNETs (6/19, 31.6%) and 4/6, 66.7%, respectively). Validation of *SALL1, OR4C12* and *CADPS* copy number loss now needs to be performed to verify the SNP array results.

Group-wise analysis of primary and recurrent CNS PNET and pineoblastomas has led to the identification of a number of candidate genes potentially involved in tumourigenesis. Currently, softwares for SNP array copy number analysis do not have inbuilt statistical support, thus we were unable to identify events which were significantly higher or lower within the primary or recurrent tumour cohorts. Therefore, the analysis so far has provided only potential regions encompassing genes of interest, potentially involved in tumour initiation and tumour recurrence. The release of a new software Genespring GX11 (Agilent, 2010) will enable such analysis to be performed and assist in the identfication of gene copy number alterations associated with primary or recurrent CNS PNETs.

The tumour suppressors, *CDKN2A* and *CDKN2B,* were identified with copy number loss in 7/38 (18.4%) CNS PNETs. 1 primary and 2 recurrent CNS PNETs harboured hemizygous loss of *CDKN2A* and *CDKN2B* (9p21.3), whilst 3 primary and 1 recurrent CNS PNETs had homozygously lost this region. Loss of 9p21.3 was not an event in any of the 8 pineoblastomas studied. Encoding cyclin dependent kinase inhibitors 2A and 2B, the 2 tumour suppressors have previously been identified as lost in a number of CNS PNETs, in addition to a variety of other tumours. Most recently identified in a study by Pfister *et al,* which involved both aCGH and FISH analyses, loss of *CDKN2A* and *CDKN2B* was observed in 7/21 (33%) CNS PNETs (Pfister, Remke et al. 2007). 4/21 (19%) of the deletions identified at 9p21.3 involved both allele copies. A separate study by McCabe *et al.,* identified homozygous loss at 9p21.3 in a single CNS PNET (McCabe, Ichimura et al. 2006). Together, this data highlights the loss of *CDKN2A* and *CDKN2B* as a frequent event in CNS PNETs and suggests a potential role for these genes in the pathogenesis of a subset of CNS PNETs. In the present study, the most common region of homozygous loss involved 9p21.3 in 4/38 (10.5%) CNS PNETs. Whilst both allele copies of *MTAP, CDKN2A, CDKN2B* and *DMRTA1* were lost in 3 CNS PNETs, a fourth tumour had loss of *MTAP, CDKN2A* and *CDKN2B* (Figure 6.14).

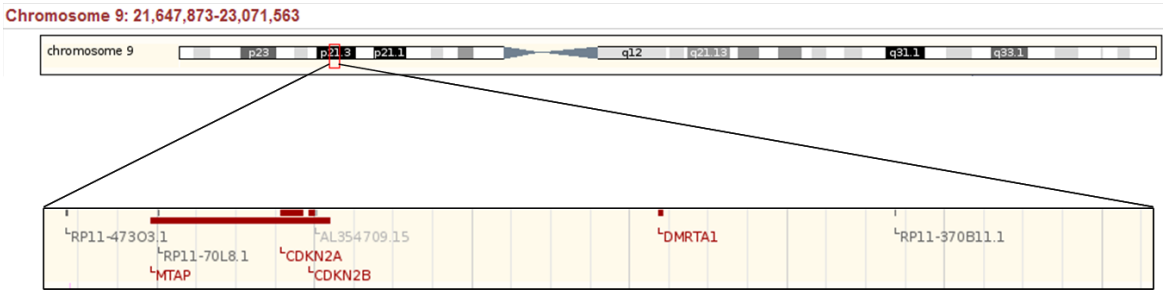

www.ensembl.org

Figure 6.14 The 9p21.3 locus. The region (21647873 – 23071563bp) encompasses *MTAP, CDKN2A, CDKN2B* and *DMRTA1*.

The loss of *CDKN2A, CDKN2B* and *MTAP* copy number is a well documented feature in cancer. Interestingly, *MTAP* (methylthio adenosine phosphorylase), is a potential novel target for therapy with the ability to interfere with methionine utilization (Chen, Zhang et al. 1996; Wong, Chung et al. 1998; Harasawa, Yamada et al. 2002). Since both primary and recurrent samples for patient 24 had lost both copies of *CDKN2A* and *CDKN2B*, the loss of both tumour suppressor genes seems to have occurred early in the tumour's development. Further investigation into the loss of *CDKN2A, CDKN2B* and *MTAP* in CNS PNET is needed to elucidate their potential roles played in tumour development and progression. An increased understanding of their roles in tumourigenesis will also potentially highlight pathways which could be targeted for therapeutic exploitation.

The SNP array data was used to identify high level gains (amplification) and homozygous deletions in individual CNS PNETs and pineoblastomas. Amplification of *MYCN* was identified in a single tumour of the present study (CNS PNET17) and has previously been identified in one CNS PNET (Kagawa, Maruno et al. 2006). *MYCN* amplification is commonly found in ~25% neuroblastomas, a tumour of neural crest origin. High level gain of the oncogene *MYCN* has been shown to lead to an increase in both *MYCN* mRNA and protein expression levels (Kohl, Gee et al. 1984; Nisen, Waber et al. 1988; Seeger, Wada et al. 1988; Slavc, Ellenbogen et al. 1990). The amplicon has also been identified as a rare event in medulloblastoma (Aldosari, Bigner et al. 2002). Amplification of *MYCN* in neuroblastoma is associated with a clinically aggressive tumour and patients have a poor outcome, with 5 year overall survival rates of 33%

(Minard, Hartmann et al. 2000; Fix, Lucchesi et al. 2008; Canete, Gerrard et al. 2009). Interestingly, the 3rd and current 4th editions of the WHO classification of nervous/ central nervous system tumours termed one type of CNS PNET as the 'cerebral neuroblastoma' (Kleihues, 2000; Louis, 2007). CNS PNET17 is a potential candidate for this rare classification. Similar to the poor prognosis of neuroblastoma patients with *MYCN* amplification, the CNS PNET patient with amplification of *MYCN* also had a very poor outcome with the tumour recurring 7 months following the first surgery and the patient died 2 months after tumour relapse. The identification of *MYCN* amplification in CNS PNET17, also highlighted the coamplification of the gene, *NAG* (neuroblastoma amplified gene), which is located upstream of *MYCN*. Hence, *NAG* could be a seperate candidate oncogene located on chromosome 2p24.3, involved in a small subset of CNS PNETs. Coamplification of *NAG* has previously been identified in CNS PNETs (Fruhwald, O'Dorisio et al. 2000).

Amplification of *PDGFRA* and *KIT* (4q12) was observed in CNS PNET21R. Interestingly, the patient died 3 months post recurrent surgery which is comparable to literature of other brain tumours with *PDGFRA* amplification, with patients having a very poor outcome and an aggressive tumour phenotype. Amplification of 4q12 has previously been identified in 2 CNS PNETs (Russo, Pellarin et al. 1999; McCabe, Ichimura et al. 2006), in addition to other paediatric brain tumours, including both glioma and medulloblastoma (Michiels, Weiss et al. 2002; Tong, Hui et al. 2004; Inda, Perot et al. 2005; Sihto, Sarlomo-Rikala et al. 2005; Puputti, Tynninen et al. 2006; Rossi, Conroy et al. 2006). Over-expression of PDGF receptors has previously been associated with metastatic medulloblastomas with worse prognoses (MacDonald, Brown et al. 2001; Gilbertson and Clifford 2003). Amplification of the region 12q13.3-14.1 was identified in the same CNS PNET (21R). Encompassing genes *GLI1* and *CDK4*, this aberration has formerly been identified in glioma (Collins 1995). The present study is the first to report this amplicon in a CNS PNET. Both the 4q12 and the 12q13.3-14.1 amplifications occurred in the same recurrent tumour and not the primary sample, highlighting the alterations as late events potentially involved in the pathogenesis of CNS PNET, with possible roles in tumour progression and relapse. The amplification identified at 4q12, encompassing both *PDGFRA* and *KIT* is of clinical interest due to the application of anti-KIT receptor tyrosine kinase inhibitors, used to inhibit the overexpression of *KIT* caused by the genes amplification. Whilst the present and 5 previous genetic studies have identified regions of amplification in CNS PNET

(Nicholson, Ross et al. 1999; Rickert, Simon et al. 2001; Inda, Perot et al. 2005; Kagawa, Maruno et al. 2006; McCabe, Ichimura et al. 2006), one recent report did not identify a single amplicon in any of the 10 CNS PNETs analysed using aCGH (Pfister, Remke et al. 2007). This discrepancy could be due to the different patient populations used, in addition to the genetic heterogeneity within the CNS PNET genome. A separate issue to consider when comparing studies of genome-wide copy number is the resolution of the platform used. With CGH, aCGH and SNP array technologies providing different levels of coverage across the genome, it is important to note that the different results identified in seperate CNS PNET genetic studies do play a role in the variable results reported. Even within the dataset presented for this thesis, the results were dependent on the cut offs used. For the identification of regions of interest, the cut of was 5 consectutive SNPs with a copy number gain or loss. Identifying regions of copy number alteration using 5 consectutive SNPs has previously been performed in other studies showing that the SNP array results were valid and false positive results were minimal (Northcott, Nakahara et al 2009). This further highlights the need for independent validation using different methods. Although other studies of CNS PNET copy number alterations have not used independent validation of genome-wide copy number results using a different technology, in chapter 7, the results of CGH validation for a small number of tumours will show confirmation of broad regions of copy number alteration also identified from the SNP array analysis.

24 distinct regions of homozygous loss were identified in the CNS PNET and pineoblastoma cohort. A previously unreported candidate homozygous deletion of *GRM7* was discovered in a single CNS PNET. Encoding a glutamate receptor with important roles in neurotransmission within the CNS, the loss of *GRM7*, has previously also been identified in other cancers (Choi, Bae et al. 2007). The identification of homozygous loss of *CCDC100* (5q23.2) in 2 CNS PNETs was intriguing, however, with limited gene information available, further research into this genes' potential involvement in CNS PNET is needed. Homozygous loss of *INI1* was identified in 2 CNS PNETs. More commonly involved in the pathogenesis of a separate classification of paediatric brain tumour; the loss is a feature of ~25% of cases of ATRT (Tekautz, Fuller et al. 2005; Biegel 2006). Interestingly, one CNS PNET (CNS PNET6) which had lost both allelic copies of *INI1* also contained some histological features consistent with the diagnosis of ATRT, due to the existence of small numbers of cells possessing rhabdoid morphology. Although originally diagnosed as a CNS PNET, this tumour

highlights the difficulties in correctly classifying tumours containing similar cellular morphologies and shows the importance of histopathological tumour review by a group of neuropathologists. Characterisation of paediatric brain tumours at the molecular genetic level will undoubtedly aid in the future classification systems of paediatric brain tumours.

Genome-wide investigations to identify regions of LOH in CNS PNETs has not previously been performed. The SNP array analysis presented here provides the first information on regions of LOH in the CNS PNET genome. When analysed alongside each other, the LOH and copy number data for each SNP enabled the identification of candidate areas of aUPD (copy neutral LOH) across the entire genome. Intriguingly, on comparison of primary and recurrent patient samples, 2 primary samples which were heterozygous at specific regions had acquired regions of UPD at recurrence, highlighting a potential role of aUPD in tumour recurrence. Whilst the primary samples CNS PNET21P and CNS PNET24P did not harbour regions of aUPD, at recurrence, CNS PNET 21R had aUPD on chromosomes 5q, 11, 13, 15, 16q and 17p, whilst CNS PNET 24R had regions of aUPD on chromosomes 3, 9 and 10. Interestingly, aUPD on chromosome 11 has previously been identified in other cancers including AML and Wilms tumour and is also associated with Beckwith-Weidemann syndrome (Slatter, Elliott et al. 1994; Gupta, Raghavan et al. 2008; Raghavan, Smith et al. 2008). To identify the most frequent regions of aUPD in the CNS PNET cohort, the combined copy number and LOH data was ordered by frequency, which revealed *CPNE4* (3q22.1) was the most common candidate region harbouring aUPD in 5/9 (55.6%) primary CNS PNETs. Two genes within the same gene family were identified with potential aUPD. 4/9 (44.4%) primary CNS PNETs had aUPD involving *LPHN2* (1p31.1), whilst 4/5 (80%) of the recurrent CNS PNETs analysed had aUPD for *LPHN3* (4q13.1). LOH of *LPHN2* has previously been identified in a high frequency of breast cancers (White, Varley et al. 1998). Latrophilins (LPHNs) have been hypothesised to play roles in both signal transduction and cell adhesion. In addition, two gene members of the MAP kinase family were identified with aUPD in the CNS PNET cohort. A third of primary CNS PNETs had aUPD of *MAPK6* (15q21.2), whilst 60% of the recurrent CNS PNETs analysed had aUPD of *MAP3K7* (6q15). MAP kinases respond to mitogens and regulate many cellular activities including gene expression, mitosis, cell differentiation, survival and apoptosis. The deregulation of the MAPK pathway in CNS PNET (by aUPD and other mechanisms) will be an important

area for future research. Genes identified with aUPD in the present study need to be confirmed in a larger series of CNS PNETs. Further investigation into the potential roles played by the genes identified with aUPD will undoubtedly improve the understanding of this genetic mechanism in the involvement of CNS PNET development and progression. Group-wise analysis of the aUPD in primary and recurrent CNS PNETs led to the identification of a number of candidate regions potentially involved in the pathogenesis of CNS PNET, however, with current softwares available we were not able to identify events which were significantly higher or lower within the primary or recurrent tumour cohorts. Therefore, the analysis so far has provided only potential regions of interest with aUPD, involved in tumour initiation and tumour recurrence.

CHAPTER 7

CONFIRMATION OF CHROMOSOMAL REGIONS AND GENES OF INTEREST

7.1 Introduction

Validation of the SNP array results was an important part of the present study. As a relatively new technology, the confirmation of copy number alterations was essential to test the reliability and accuracy of the data generated. The use of the hidden markov model (HMM, an algorithm to predict inferred copy number and LOH inference from haplotype information of the raw data) can lead to the identification of false positives; hence, validation excludes the possibility of taking anomalous results forward. A number of techniques were used to validate the SNP array data. aCGH is a well recognised, reliable platform used in the identification of copy number gain and loss across the entire genome. DNA of a tumour sample previously analysed using the SNP array platform was subsequently examined using a different genome-wide technique to test the reliability of overall results. In part, confirmation of the SNP array results was achieved on comparison of the aCGH profile generated from the same patients' tumour DNA. Secondly, to validate copy number imbalance at the gene level, real time PCR was used to quantify the actual copy number of the gene of interest. Real time PCR also confirms the reliability of the SNP array platform by testing the SNP copy numbers generated when using the HMM. Hence, an accurate discrimination between the copy numbers predicted in CNAG (0, 1, 2, 3, 4, 5 and 6) was made. Lastly, immunohistochemistry was performed to determine if the altered gene copy numbers identified by the SNP array analysis led to changes in the encoded protein's expression. The construction of a tissue microarray array (TMA) to examine the protein expression of many different FFPE tumour samples in a single experiment was an invaluable research tool. Moreover, immunohistochemistry is a reproducible technique in histopathological laboratories and the discovery of a diagnostic or prognostic result could therefore easily be integrated into the clinical diagnostic setting. SNP array data published to date, establishes the technology to be accurate, reliable and informative when validated by real time PCR, fluorescence in situ hybridisation, and immunohistochemical analyses (Hu, Wang et al. 2005; Kotliarov, Steed et al. 2006; Harada, Chelala et al. 2008).

7.2 Materials and methods

7.2.1 aCGH and SNP array result comparison

Agilent 44K CGH arrays were previously processed and analysed by Dr Sara Dyer for a subset of 9 CNS PNETs (1, 2R, 9, 14, 20, 21P, 21R, 22P and 24R) (Dyer 2008). Comparisons of the regions of imbalance were then made between the aCGH and SNP array results for each CNS PNET.

7.2.2 Real time qPCR validation

SNP array copy number results for genes of interest (identified in chapter 6, Section 6.3) were derived using CNAG (as detailed in chapter 2, Section 2.4.13). Real time qPCR validation of the copy numbers of genes of interest was performed (detailed in chapter 2.5). Gene copy numbers derived using the SNP array and real time qPCR methods were compared. Statistical associations were identified using methods detailed in chapter 2, Section 2.8.

7.2.3 p15INK4B immunohistochemistry

Immunohistochemical staining for p15INK4B was performed as stated in chapter 2, Section 2.6. 33 tumours had scorable results for p15INK4B (as defined in chapter 2, Section 2.6). 28 CNS PNETs and 5 pineoblastomas were included (Table 7.1). Of the clinical information available for the 28 CNS PNETs, 15 patients were male and 13 female. 22 samples were primary tumours whilst 6 were taken at relapse. Patient age ranges between 6 – 149 months, with mean and median ages of 76.6 and 73.5 months, respectively. 7 had metastatic disease at diagnosis whilst 17 were metastasis free. Patient follow-up ranged from day of diagnosis to 108 months, with a mean and median follow-up of 34.59 and 21 months, respectively. 21 patients with scorable p15INK4B results had died, however, presently 6 are still current alive. Of the clinical information available for the 5 pineoblastomas, 4 patients were male and 1 female. All 5 were primary tumours from patients aged between 5 – 183 months. Mean and median pineoblastoma patients ages were 67.8 and 29 months, respectively. 4 had metastatic disease at diagnosis whilst 1 was metastasis free. Pineoblastoma patient follow-up

ranged from 14 – 180 months, with mean and median follow-ups of 61 and 37 months, respectively. Whilst 5 pineoblastoma patients had died, 1 patient is presently alive. Examples of negative, weak, moderate and strong p15INK4B staining is shown in Figure 7.1a-d.

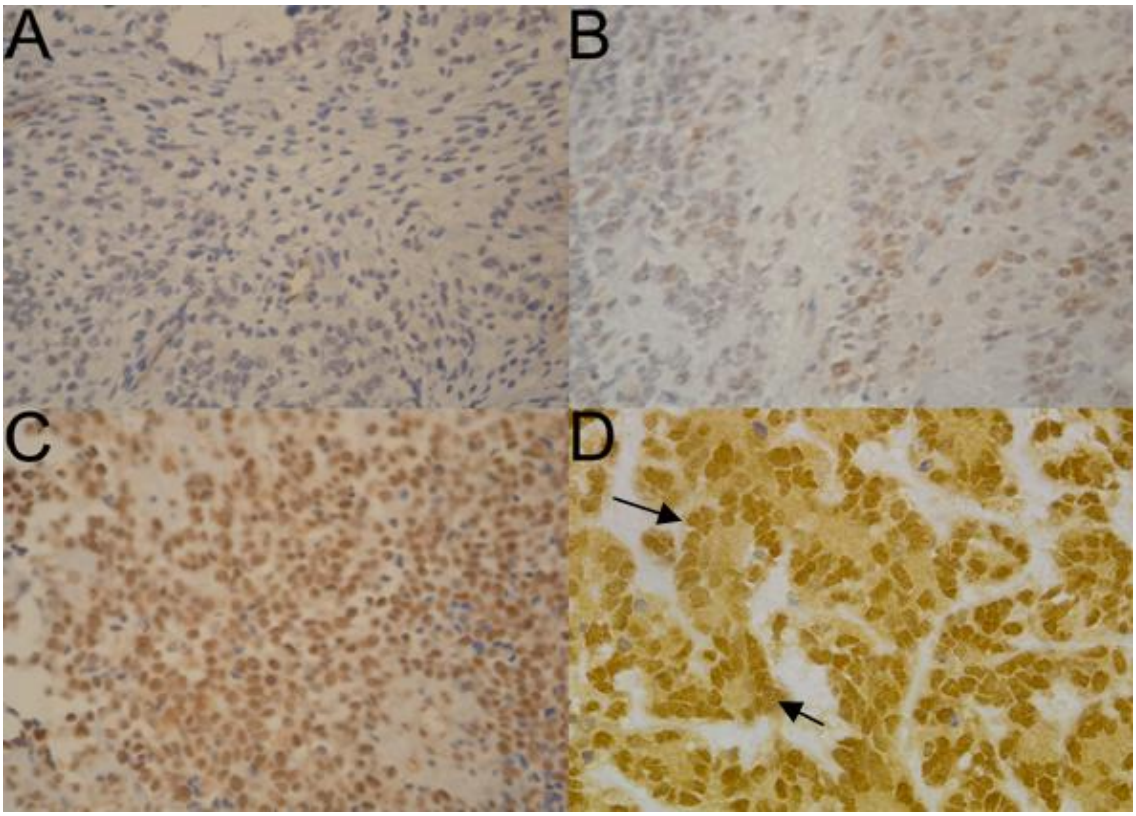

1:200 magnification

Figure 7.1a-d p15INK4B (encoded by *CDKN2B*) staining intensities of CNS PNET tissue. Tumours were scored as negative, with no protein present (A), weak, <50% cells with low intensity nuclear staining (B), moderate, >50% cells with low intensity nuclear staining (C) or strong (D), with >50% cells with intense nuclear staining. Homer-wright rosettes arrowed.

Table 7.1 Clinical information for tumour samples entered into immunohistochemical analyses of p15INK4B and INI1

ID	Gender	Primary/ rec	Age (m)	Location	Metastasis	Follow up (m)	Censor	*CDKN2B* SNP CN	p15INK4B IHC	*INI1* SNP CN	INI1 IHC
42	F	P	5	PR	M2	14	D	-	Weak	-	-
43	M	P	6	CR	-	-	-	-	Neg	-	Pos
1*	F	P	6	PR	M3	10	D	2	-	2	Neg
2P*	F	P	10	CR - Pa	M2	41	D	2	-	3	Pos
2R*	F	R	10	CR – Fr	M2	41	D	2	Strong	2	Pos
44	M	P	12	CR - T, Pa	M3	8	D	-	Mod	-	Neg
6*	F	P	19	CR - Fr	M2	3	D	2	-	0	Neg
9*	F	P	20	CR - Fr	M0	0	D	2	Mod	2	Pos
10*	F	P	24	CR - T	M0	3	D	2	Weak	2	-
11*	M	P	24	PR	M0	180	A	2	Mod	3	Pos
45	M	P	27	CR	M0	38	D	-	Strong	-	Pos
46	M	P	29	PR	M2	15	D	-	Mod	-	Neg
47	M	P	30	CR - Pa	M0	6	D	-	Neg	-	Neg
14*	M	P	37	CR - T	M4	6	D	2	Weak	2	Neg
48	F	P	38	CR - LV	M0	16	D	-	Weak	-	-
49	F	P	46	CR	M0	11	D	-	Weak	-	-
16*	F	P	53	CR - Fr, T, Pa	M0	21	A	2	Strong	4	Pos
17*	M	P	59	CR - Mi, Fr	M2	9	D	0	Neg	2	Pos
18*	M	P	61	CR - Fr	M0	21	D	2	Strong	2	Pos
50	M	P	62	CR - Fr	M0	38	D	-	Strong	-	Pos
20*	F	P	85	CR - Fr	M0	83	A	1	Strong	3	Pos
51	F	P	87	CR - Pa	M0	10	D	-	Mod	-	-
52	M	P	98	PR	M3	59	D	-	Strong	-	Pos
53	F	P	99	CR - Pa	M0	8	D	-	-	-	Pos
54P	F	P	101	CR - Pa	-	108	A	-	Neg	-	-
54R	F	R	101	CR - Pa	-	108	A	-	Weak	-	-
21P*	M	P	107	CR	M2	71	D	2	Mod	2	Pos
21R*	M	R	107	CR, PF	M2	71	D	3	Strong	3	Pos
22P*	M	P	122	CR - Pa	M0	58	A	2	Strong	2	Pos
22R*	M	R	122	CR - Pa	M0	58	A	1	Neg	2	Pos
55	M	P	123	CR - H	M0	16	D	-	Strong	-	-
56	F	P	126	CR	M0	0	D	-	Strong	-	Neg
57	F	P	141	CR	M4	58	D	-	Neg	-	Pos
25*	M	P	142	CR	M0	0	D	2	Neg	3	-
26*	F	R	148	CR - Fr, Pa	-	36	D	1	Mod	1	Neg
58	M	R	149	CR	M0	39	D	-	Mod	-	Neg
59	M	P	183	PR	M3	37	D	-	Neg	-	-
60	M	P	186	CR - Pa	M0	219	A	-	-	-	Pos

Clinical information is ordered by age. F = female, M = male, P = primary tumour, R = recurrent tumour, PR = pineoblastoma, CR = CNS PNET, Fr = frontal lobe, T = temporal lobe, Pa = parietal lobe, LV = lateral ventricle, Mi = midline, PF = posterior fossa, H = hemispheric, D = deceased, A = alive, Neg = negative, Mod = moderate, Pos = positive, metastasis based on Chang staging (Chang 1969), - information unavailable. * denotes tumours analysed in both SNP array and immunohistochemical analyses.

Statistical associations linking p15INK4B staining and patient clinical factors were investigated. The Fisher's exact test was used to investigate whether negative, weak, moderate, strong, negative/weak and moderate strong p15INK4B staining were associated with (i) tumour location (primary CNS PNET vs pineoblastoma), (ii) tumour recurrence (primary CNS PNET vs recurrent CNS PNET) and (iii) metastatic disease (metastasis at diagnosis vs metastatic-free). To test whether negative, weak, moderate, strong, negative/weak and moderate strong p15INK4B staining patterns were associated with patient age for the primary CNS PNETs, independent samples t-tests were performed. Finally to test whether p15INK4B staining could potentially be used as a marker of prognosis, univariate survival curves were made using the Kaplan-Meier method and univariate comparisons were made by the log-rank test.

7.2.4 INI1 immunohistochemistry

Immunohistochemical staining for INI1 was performed as stated in chapter 2, Section 2.6. 24 CNS PNETs and 4 pineoblastomas had scorable results for INI1 protein expression (Table 7.1). Of the clinical information available for the 24 CNS PNETs, 14 patients were male and 10 female. 19 samples were primary CNS PNETs, whilst 5 were taken at relapse. CNS PNET patient ages ranged from 6 – 186 months, with mean and median ages of 75 and 61.5 months, respectively. 9 had metastatic disease at diagnosis and 13 were metastasis free. Patient follow-up ranged from the day of diagnosis to 219 months, with mean and median follow-ups of 40.5 and 30 months, respectively. 18 CNS PNET patients had died and 5 are presently alive. Of the 4 pineoblastomas included in the immunohistochemical study of INI1, 3 patients were male and 1 female. All 4 pineoblastoma samples were from primary tumours of patients aged between 6 and 98 months (with mean and median ages of 39.3 and 26.5 months, respectively). 3 had metastatic disease at diagnosis and 1 was metastasis free. Pineoblastoma patient follow-up ranged from 10 – 180 months (with mean and median follow-ups of 66 and 37 months, respectively). 3 pineoblastoma patients had died and 1 is presently alive. Statistical associations linking INI1 staining and patient clinical factors were investigated. The Fisher's exact test was used to investigate whether negative or positive staining was associated with (i) tumour location (primary CNS PNET vs pineoblastoma), (ii) tumour recurrence (primary CNS PNET vs recurrent CNS PNET) and (iii) metastatic disease (metastasis at diagnosis vs metastatic-free). To test whether negative or positive INI1 staining was associated with patient age for the

primary CNS PNETs, an independent samples t-tests was performed. Finally to test whether INI1 staining was linked to patient prognosis, univariate survival curves were made using the Kaplan-Meier method and univariate comparisons were made by the log-rank test.

7.2.5 INI1 Sequencing

Sequencing of exons 5 and 9 of the *INI1* gene was performed as detailed in chapter 2, Section 2.7.

7.3 Results

7.3.1 aCGH comparison of CNS PNETs analysed on the Affymetrix SNP array platform

A subset of 9 CNS PNETs (1, 2R, 9, 14, 20, 21P, 21R, 22P and 24R) were analysed using the Agilent 44K array CGH platform (Dyer 2008) and the results mirrored the findings of the SNP array results (Figures 7.2A-D). However, the increased resolution of the SNP array analysis defined the precise boundaries between regions of normal and aberrant copy number, for example, CNS PNET21R was analysed using both the aCGH and SNP array platforms. Using aCGH, an 8.5Mb amplicon located on chromosome 4 (52404033 – 60955374) was identified, though using the higher resolution SNP arrays, the same amplicon was identified with a size of 6.7Mb (52379648 – 59114124) (Figures 7.2A and 7.2B). Additionally, CNS PNET24R was also analysed using both the aCGH and SNP array platforms. Using aCGH a homozygous deletion of 5Mb located on chromosome 9 (20648308 – 25668319) was identified, whilst on analysis using the SNP arrays the same region of loss was refined to between (21948524 – 23071563) with a size of 1.1Mb (Figures 7.2C and 7.2D).

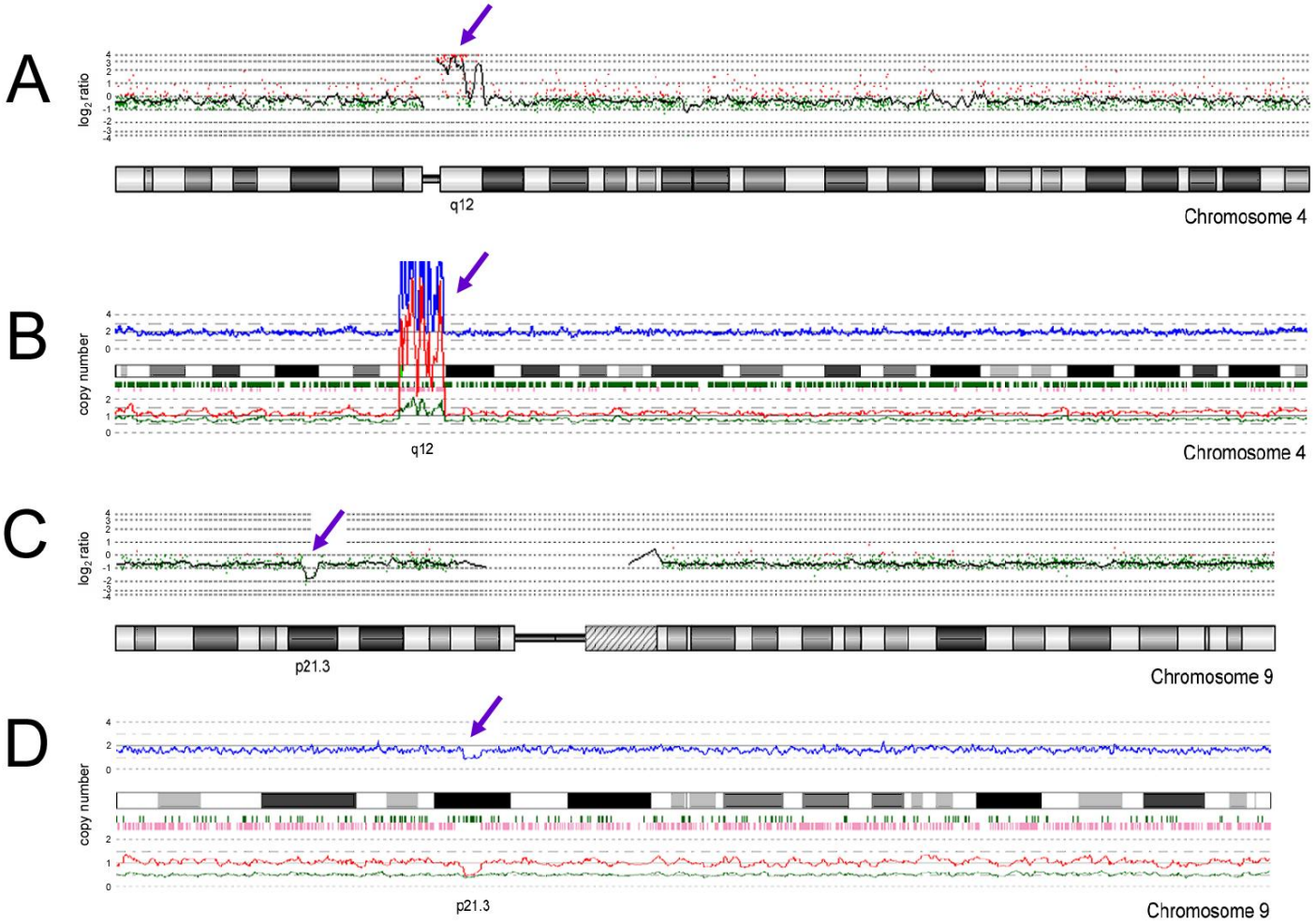

Figure 7.2a-d Two examples of regions of copy number alteration identified from the Affymetrix SNP array analysis confirmed using the Agilent 44K aCGH platform. aCGH illustration of the *PDGFRA/KIT* amplicon (4q12) in CNS PNET 21R (A). SNP array illustration of the same amplicon (B). aCGH depiction of loss of one copy of chromosome 9 with homozygous loss of 9p21.3 in CNS PNET 24R, harbouring genes *CDKN2A* and *CDKN2B* (C). SNP array illustration of the 9p21.3 deletion (D). For the aCGH data, gained probes are shown in red, whereas lost probes are shown in green, with a black line depicting the moving average of the $\log_2$ratio. For the SNP array data, allele specific probe copy numbers are represented as red and green lines with the blue line, the moving average. Purple arrows indicate regions of copy number alteration.

7.3.2 Real time qPCR validation of SNP array results

Real time qPCR was performed to validate genes of interest which were found to have alterations in copy number, as identified from the SNP array analysis. Candidate genes chosen for validation were either the most frequently occurring within all tumour samples investigated, or the gene copy number alterations were commonly identified in tumours of a clinically relevant patient group. A subset of nine candidate genes (*PCDHGA3*, *FAM129A*, *PDGFRA*, *MYCN*, *OR4C12*, *CADPS*, *SALL1*, *CDKN2A* and *CDKN2B*) were identified for verification studies (Figures 7.2 – 7.11).

7.3.2.1 Real time qPCR validation of *PCDHGA3* gain

30/46 (65.4%) tumours analysed using the SNP arrays were available for *PCDHGA3* copy number verification by real time qPCR (Figure 7.3). From the SNP array analyses, 26 tumours were identified with gain of copy number, 10/26 (38.5%) were verified by qPCR whilst 16/26 (61.5%) were not. Of 4 tumours identified with a normal copy number for *PCDHGA3*, 2/4 (50%) were verified by qPCR, whilst 2/4 (50%) were not validated by qPCR.

7.3.2.2 Real time PCR validation of *FAM129A* gain

25/46 (54.3%) tumours analysed using the SNP arrays were available for *FAM129A* copy number verification by real time qPCR (Figure 7.4). From the SNP array analyses, 16 tumours were identified with gain of *FAM129A* copy number, 7/16 (43.8%) were verified by qPCR whilst 9/16 (56.2%) were not. Of 9 tumours identified with a normal copy number for *FAM129A*, 8/9 (89%) were verified by qPCR, whilst 1/9 (11.1%) was not validated by qPCR.

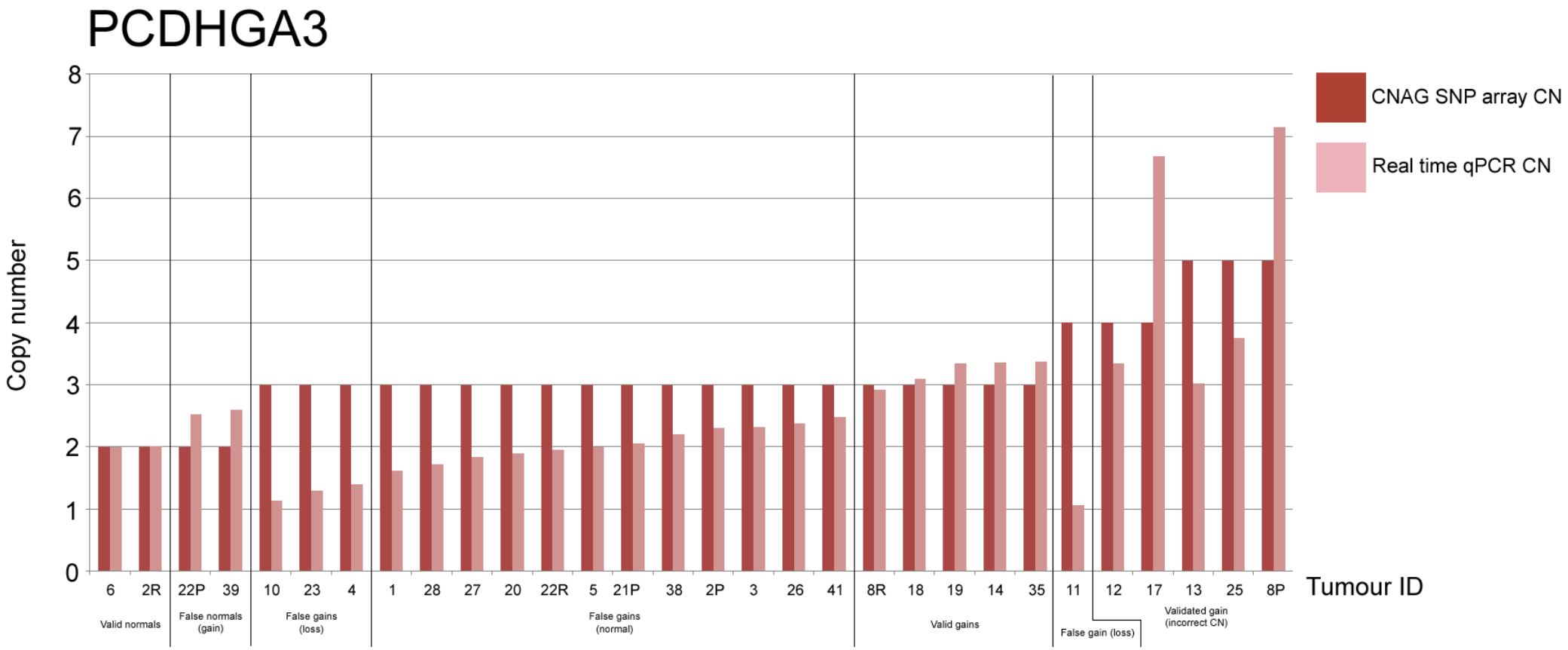

Figure 7.3 Real time PCR validation of *PCDHGA3* gene copy number. P, primary; R, recurrence.

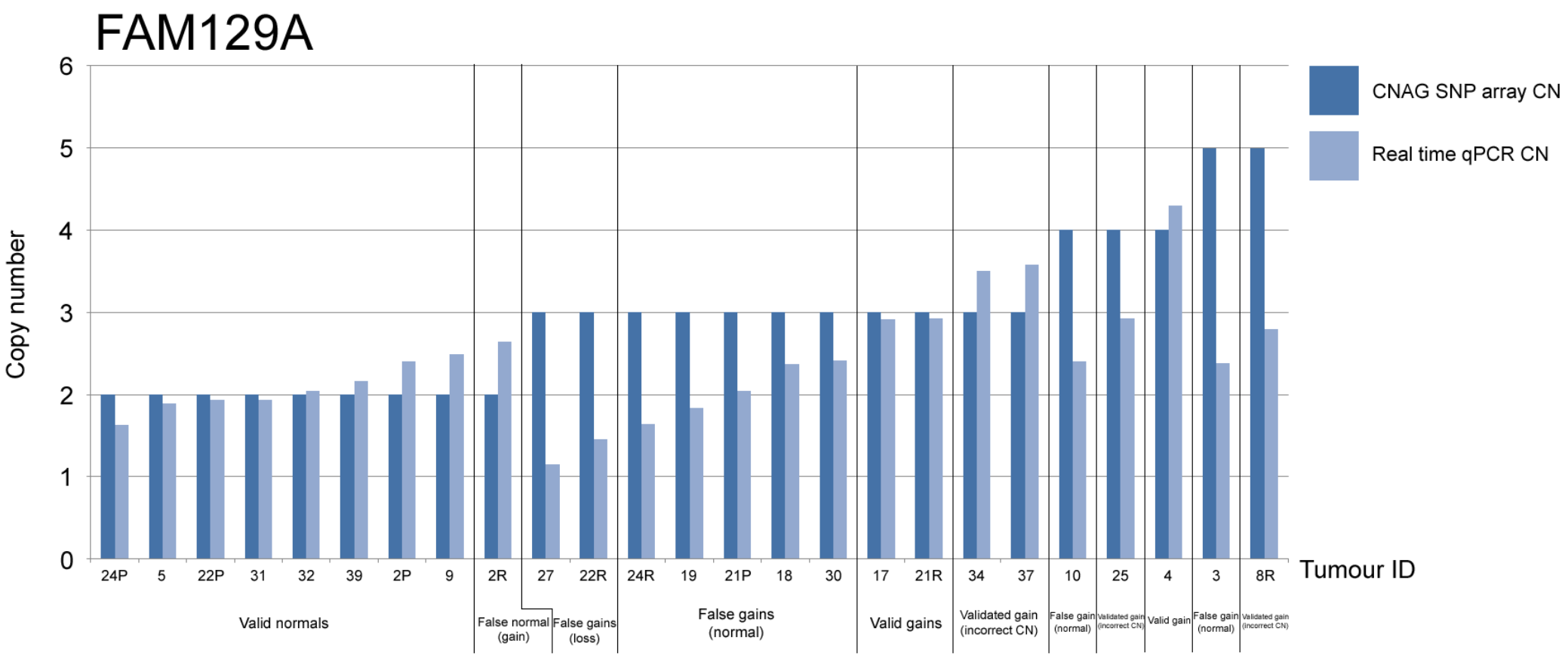

Figure 7.4 Real time PCR validation of *FAM129A* gene copy number. Copy number gains verified (arrowed). P, primary; R, recurrence.

7.3.2.3 Real time PCR validation of *PDGFRA* amplification

To validate regions of amplification, real time PCR was used to confirm the high level gain encompassing *PDGFRA* (4q12). 7/46 (15.2%) tumours analysed using the SNP arrays were available for *PDGFRA* copy number verification by real time qPCR (Figure 7.5). The SNP array analyses revealed a potential amplification of *PDGFRA* in CNS PNET 21R. Whilst the HMM implemented in CNAG gives a maximum copy number of 6 for SNP array data, the amplification was validated by qPCR which identified 33 copies of the *PDGFRA* gene. One other tumour was identified with gain by the SNP array analysis, however when analysed by qPCR this result was not validated. 4/5 (80%) tumours with a normal copy number for *PDGFRA* by the SNP array analyses also had a normal copy number by qPCR whilst in 1/5 (20%) the normal result was not validated.

7.3.2.4 Real time PCR validation of *MYCN* amplification

11/46 (23.9%) tumours analysed using the SNP arrays were available for *MYCN* copy number verification by real time qPCR. The SNP array analyses revealed a potential amplification of *MYCN* in CNS PNET 17. Whilst the HMM implemented in CNAG gives a maximum copy number of 6 for SNP array data, the amplification was validated by qPCR which identified 54 copies of the *MYCN* gene (Figure 7.6). Of 5 other tumours identified with gain by the SNP array analyses, when analysed by qPCR, 2/5 (40%) tumours with gain of MYCN were validated and 3/5 (60%) did not validate.

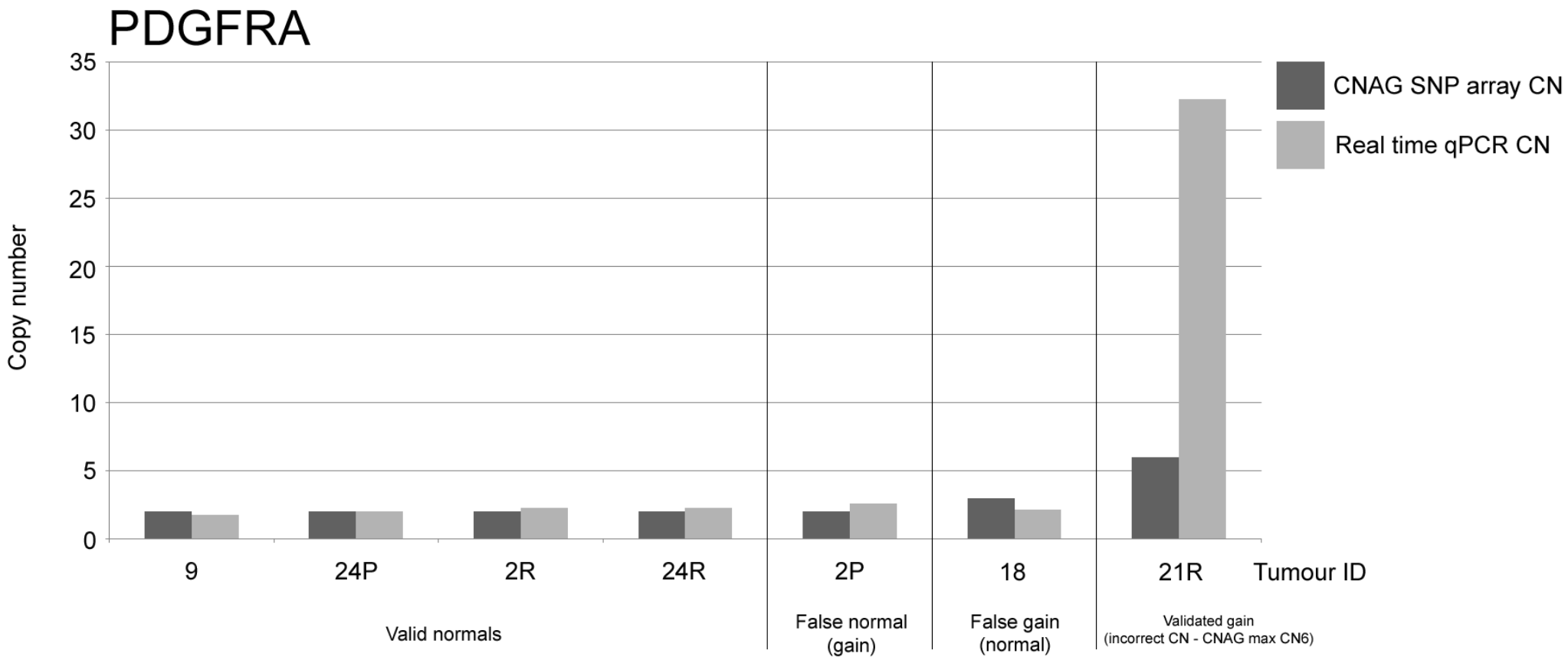

Figure 7.5 Real time PCR validation of *PDGFRA* gene copy number. Amplification (arrowed). P, primary; R, recurrence.

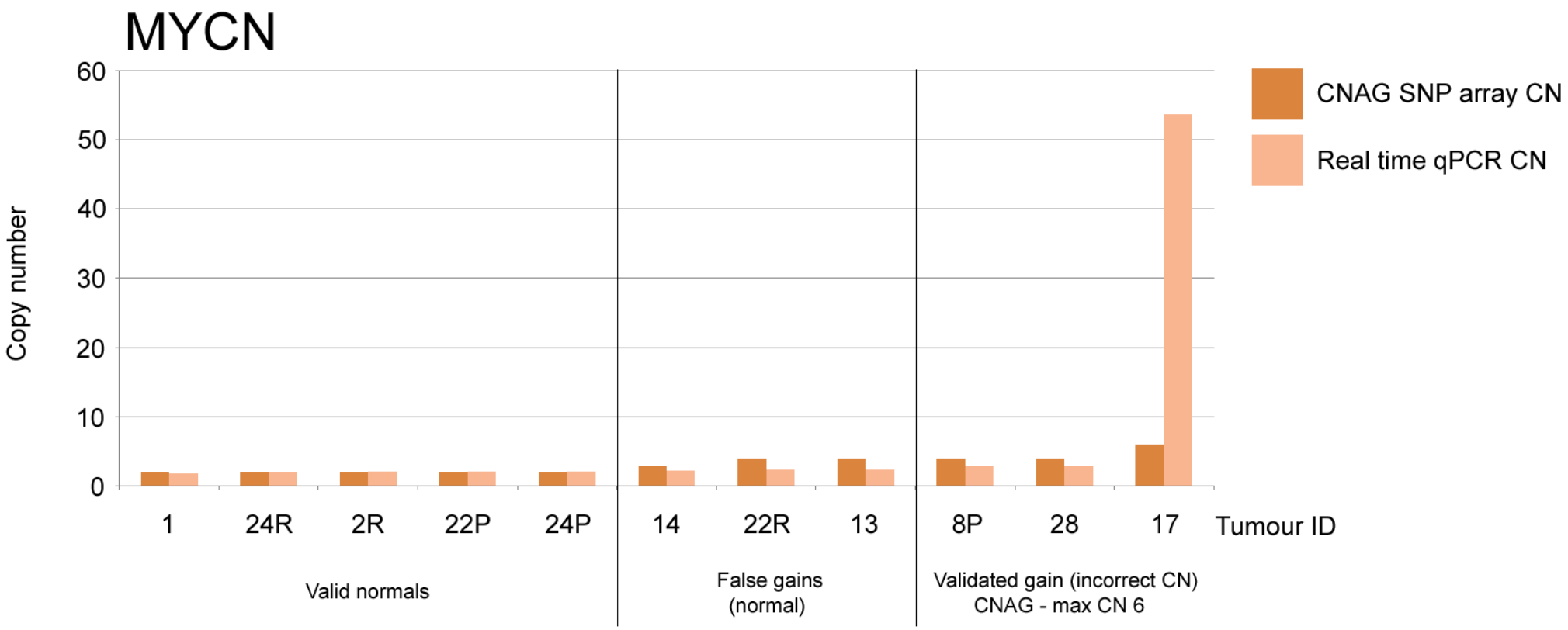

Figure 7.6 Real time PCR validation of *MYCN* gene copy number. P, primary; R, recurrence.

7.3.2.5 Real time PCR validation of *OR4C12* loss

29/46 (63%) tumours analysed using the SNP arrays were available for *OR4C12* copy number verification by real time qPCR. From the SNP array analyses, 14 tumours were identified with loss in *SALL1* copy number, 6/14 (42.9%) were verified by qPCR whilst 8/14 (57.1%) were not validated (Figure 7.7). Of 15 tumours identified with a normal copy number for *OR4C12*, 8/15 (53%) were verified by qPCR, whilst 7/15 (47%) were not validated by qPCR.

7.3.2.6 Real time PCR validation of *CADPS* loss

16/46 (34.8%) tumours analysed using the SNP arrays were available for *CADPS* copy number verification by real time qPCR. From the SNP array analyses, 4 tumours were identified with loss in *SALL1* copy number and were subsequently validated by real time qPCR (Figure 7.8). Of 12 tumours identified with normal copy number, 7/12 (58.3%) were verified by qPCR, whilst 5/12 (41.7%) were not validated qPCR.

7.3.2.7 Real time PCR validation of *SALL1* loss

25/46 (54.3%) tumours analysed using the SNP arrays were available for *SALL1* copy number verification by real time qPCR. From the SNP array analyses, 7 tumours were identified with loss of *SALL1* and were subsequently validated by real time qPCR (Figure 7.9). Of 17 tumours identified with normal copy number, 9/17 (52.9%) were verified by qPCR, whilst 8/17 (20%) were not validated qPCR. Additionally, a single gain of *SALL1* was validated for 1 tumour.

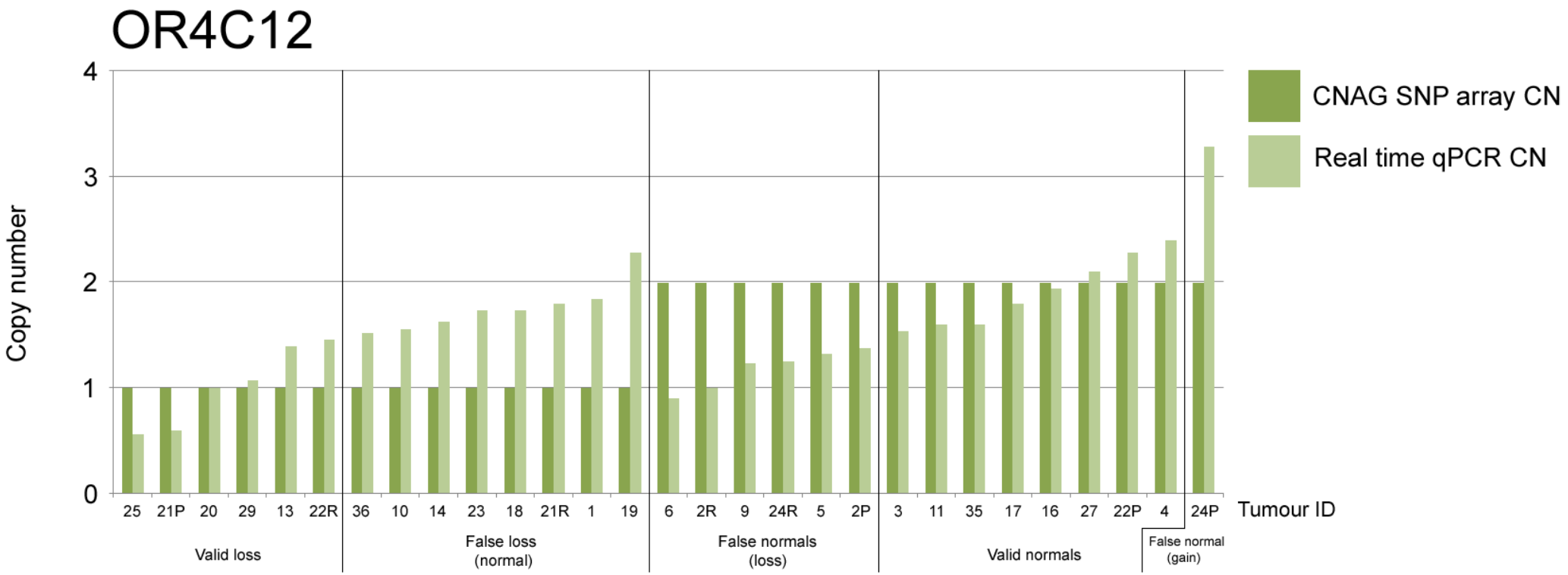

Figure 7.7 Real time PCR validation of *OR4C12* gene copy number. Copy number losses verified (arrowed). P, primary; R, recurrence.

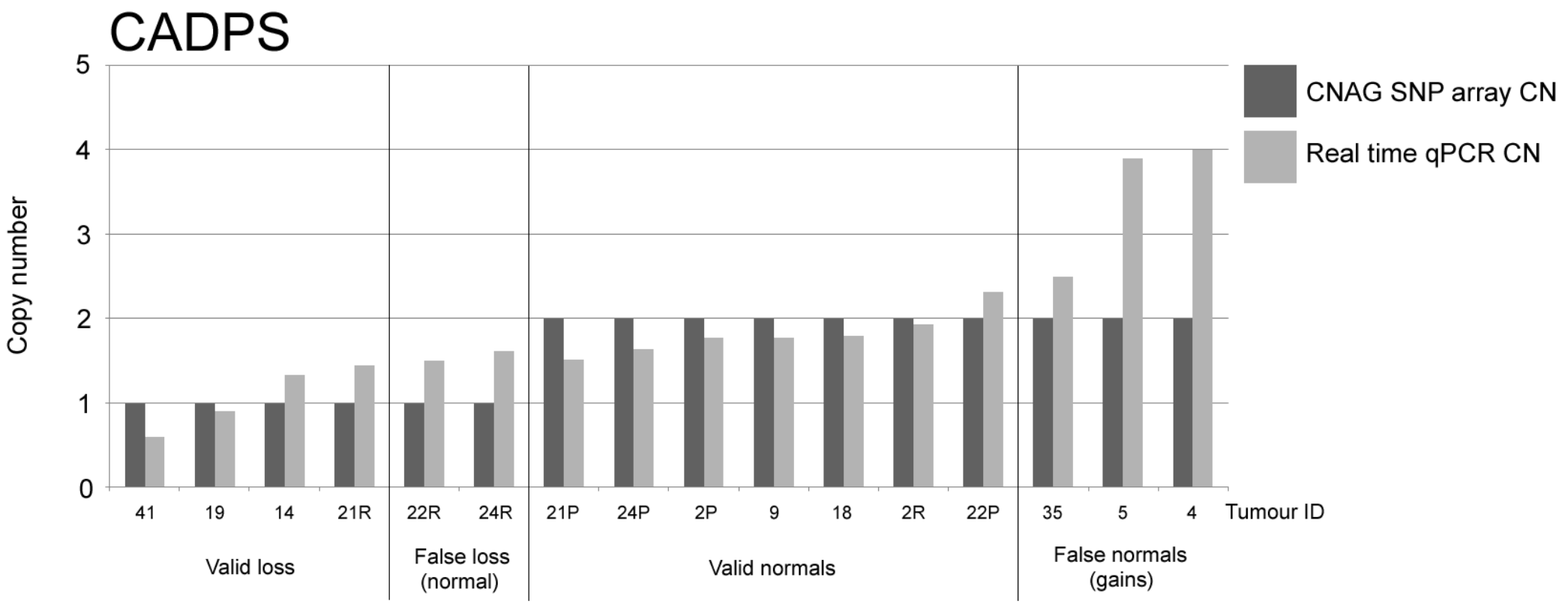

Figure 7.8 Real time PCR validation of *CADPS* gene copy number. Copy number losses verified (arrowed). P, primary; R, recurrence.

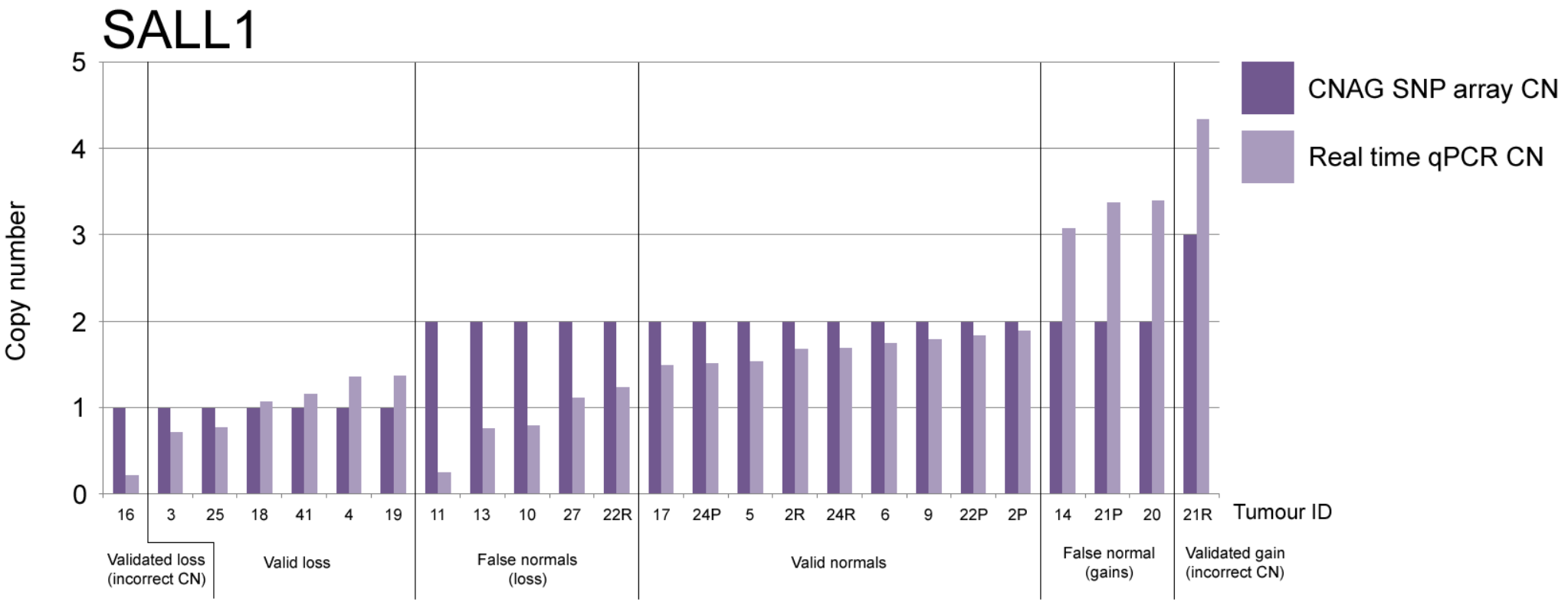

Figure 7.9 Real time PCR validation of *SALL1* gene copy number. Copy number losses verified (arrowed). P, primary; R, recurrence.

7.3.2.8 Real time PCR validation of *CDKN2A* loss

28/46 (60.9%) tumours analysed using the SNP arrays were available for *CDKN2A* copy number verification by real time qPCR. From the SNP array analyses, 7 tumours were identified with loss of *CDKN2A* and were subsequently validated by real time qPCR (Figure 7.10). Of 20 tumours identified with normal copy number for *CDKN2A*, 16/20 (80%) were verified by qPCR, whilst 14/20 (20%) were not validated as diploid by qPCR. Additionally, a single gain of *CDKN2B* was validated for 1 tumour.

7.3.2.9 Real time PCR validation of *CDKN2B* loss

34/46 (73.9%) tumours analysed using the SNP arrays were available for *CDKN2B* copy number verification by real time qPCR. From the SNP array analyses, 7 tumours were identified with loss of *CDKN2B.* 7/7 (100%) were subsequently validated by real time qPCR (Figure 7.11). Of 26 tumours identified with normal copy number for *CDKN2B*, 16/26 (61.5%) were verified by qPCR, whilst 10/26 (38.5%) were not validated as normal by qPCR. Additionally, a single gain of *CDKN2B* was validated for 1 tumour.

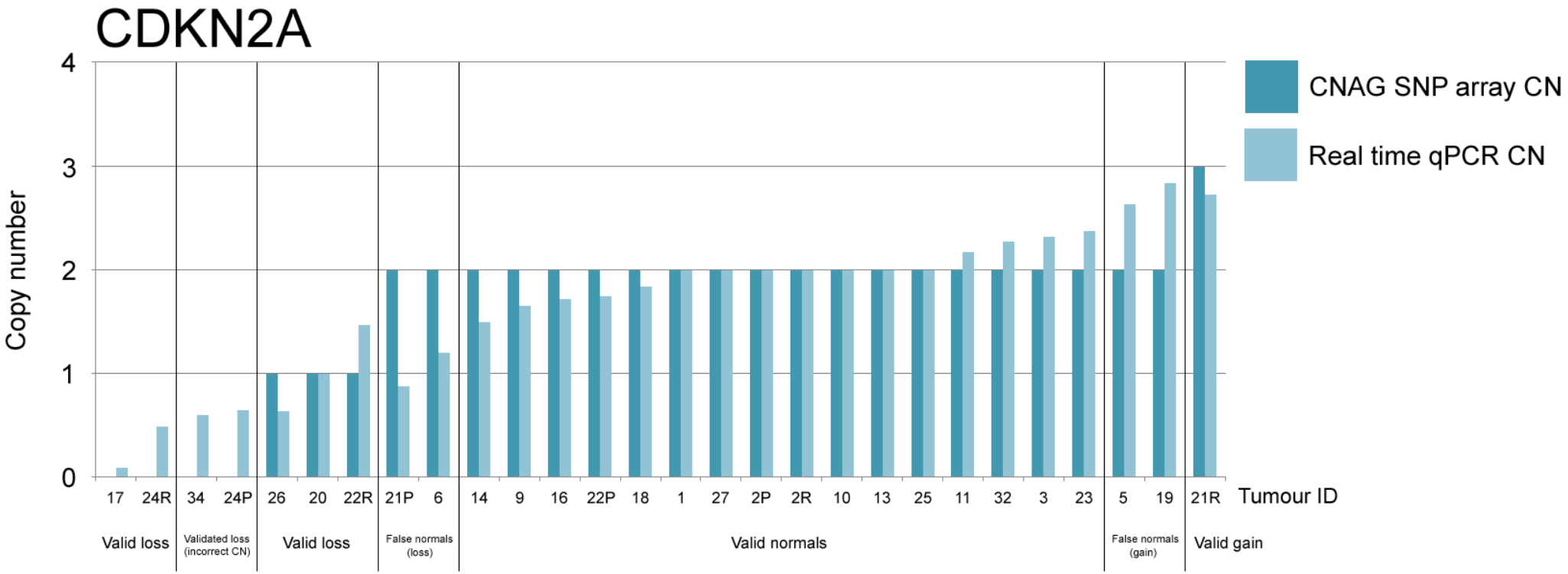

Figure 7.10 Real time PCR validation of *CDKN2A* gene copy number. Copy number losses verified (arrowed). P, primary; R, recurrence.

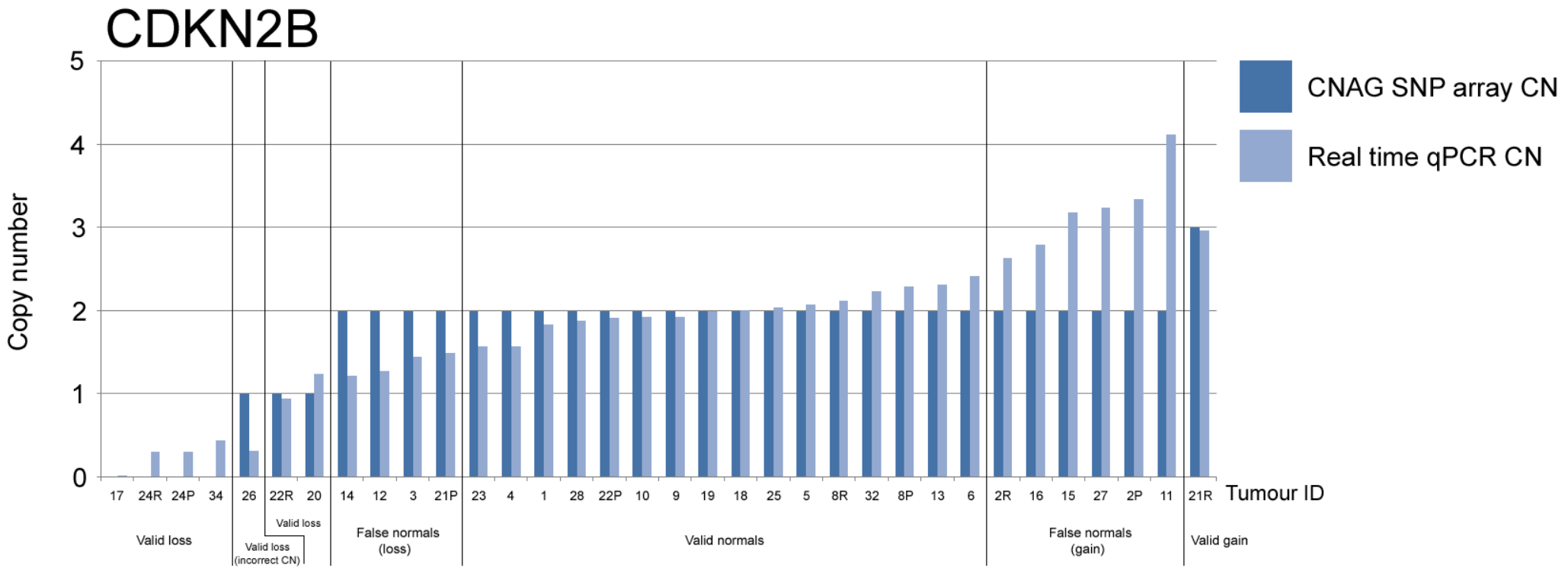

Figure 7.11 Real time PCR validation of *CDKN2B* gene copy number. Copy number losses verified (arrowed). P, primary; R, recurrence.

7.3.3 Statistical associations identified between SNP array and real time qPCR derived gene copy number alterations and tumour patient clinical characteristics

Statistical analysis was performed to assess whether patient clinical characteristics were associated to specific gene copy number alterations identified in both the SNP array and real time qPCR analyses (Table 7.2). On comparison of tumour location (cerebral - CNS PNET vs pineoblastoma) and gene copy number alterations, trends were identified from both the SNP array and real time qPCR derived gene copy number alterations, revealing a potential link between gain of *PCDHGA3* and pineoblastomas ($p = 0.076$ and $p = 0.052$, respectively). When comparing primary and recurrent tumours for loss of *CADPS*, a marginally significant results was found in the SNP array analyses linking *CADPS* loss with primary tumours ($p = 0.066$), however, this result was not verified on statistical analysis of the qPCR derived *CADPS* copy numbers of tumours ($p = 1$). A second trend was identified when comparing primary and recurrent CNS PNETs, with recurrent CNS PNETs more commonly having loss of *CDKN2A* and *CDKN2B* ($p = 0.063$), however this was not validated in the statistical analyses of the qPCR results ($p = 0.609$). 2 significant associations were identified on the comparison of gene copy number alterations and metastatic disease status. Gain of *PCDHGA3* gain was associated with metastatic disease at diagnosis when using SNP derived gene copy number alterations ($p = 0.05$), however this was not verified when using the gene copy numbers of tumours used in the qPCR analyses ($p = 1$). Using the qPCR derived copy numbers for *SALL1*, loss of the gene was linked to metastatic status ($p = 0.03$), although this association was not identified for the tumours analysed in the SNP array analyses ($p = 0.12$). On comparison of gene copy number alterations and patient survival, a single significant result was identified. Loss of *CADPS* was linked to poor prognosis when using the *CADPS* gene copy numbers derived from both SNP array and real time qPCR analyses ($p = 0.033$ and $p = 0.046$, respectively). This result is however, only suggestive, as the tumour cohort was retrospectively collected and tumours not uniformly treated.

Table 7.2 Statistical analyses of CNS PNET and pineoblastoma patient clinical information and gene copy number alteration identified using SNP array and real time qPCR.

Clinical variable →	**Primary tumour location**		**CNS PNET primary/recurrence**		**Primary CNS PNET survival**		**Primary CNS PNET metastasis**		**Primary CNS PNET age**	
Method of CN estimation →	SNP	qPCR	SNP	qPCR	SNP	qPCR	SNP	qPCR	SNP	qPCR
↓ Gene - *PCDHGA3* gain	0.076	0.052	1	0.59	0.497	0.231	0.05	1	0.48	0.85
***FAM129A* gain**	0.65	1	0.64	0.28	0.554	0.404	0.44	1	0.9	0.33
***OR4C12* loss**	1	0.128	0.369	0.586	0.432	0.73	0.41	1	0.77	0.32
***CADPS* loss**	1	1	0.066	1	0.033	0.046	1	1	0.51	0.3
***SALL1* loss**	0.587	0.094	0.56	0.61	0.559	0.234	0.12	0.03	0.81	0.7
***CDKN2A* and *CDKN2B* loss**	0.6	0.266	0.063	0.609	0.455	0.408	0.6	0.12	0.276	0.241

Primary tumour locations were either cerebral/suprasellar (CNS PNET) or pineal (pineoblastoma). All recurrences were 1st recurrences. Metastasis was either present (M1-4) or absent (M0) as staged using the Chang staging system (Chang 1969). Two-sided Fisher's exact tests were performed to compare tumour location, primary/recurrent tumours and metastatic status at diagnosis with gene copy number alterations identified from either the SNP array or real time qPCR analyses. Univariate survival curves were made using the Kaplan-Meier method and comparisons tested using log-rank tests to assess whether gene copy number alterations were linked to prognosis. Independent sample t-tests were performed to identify associations between patient age and gene copy number alterations. P values are shown for both SNP and real time qPCR derived gene copy numbers. Statistically significant results are highlighted in green, whilst marginally significant results (trends) are highlighted in yellow.

7.3.4 Immunohistochemistry of *CDKN2B* (p15INK4B)

To further investigate the loss of *CDKN2B* gene copy number identified by the SNP array analysis, (and subsequently validated by the real time qPCR analysis), immunohistochemistry was performed to evaluate the expression level of the encoded protein (p15INK4B). The production of a TMA led to the compilation of a large cohort of CNS PNETs and pineoblastomas for immunohistochemical analysis (Table 7.1). 7/28 (25%) CNS PNETs were negative for p15INK4B staining, 5/28 (17.9%) CNS PNETs had weak staining, 6/28 (21.4%) CNS PNETs showed moderate staining and 10/28 (35.7%) CNS PNETs had strong staining for p15INK4B. For *CDKN2B*, 14 CNS PNET cases had both a SNP array result and a scorable immunohistochemical result for the encoded protein, p15INK4B. 3 CNS PNETs negative for p15INK4B staining had a copy number result for *CDKN2B* from the SNP array analysis. Whilst 1 CNS PNET absent of p15INK4B protein expression had a normal copy number of 2 identified in the SNP array analysis (Figure 7.12b), 2 further CNS PNETs absent of p15INK4B expression both had deletions of *CDKN2B*, 1 CNS PNET with hemizygous loss (Figure 7.12c) and 1 with homozygous loss. 2 CNS PNETs with weak p15INK4B staining had retained normal gene copy number for *CDKN2B* (from the SNP array analysis). 3 CNS PNETs with moderate staining for p15INK4B had SNP array copy number results; 2 moderately staining CNS PNETs had retained normal gene copy number for *CDKN2B* whilst a third moderately staining CNS PNET had lost a single copy of *CDKN2B*. 6 CNS PNETs with strong staining for p15INK4B had *CDKN2B* copy number results from the SNP array analyses; gain of a single copy of *CDKN2B* was identified in 1 CNS PNET, a normal copy number of 2 was identified in 4 CNS PNETs with strong staining for p15INK4B (Figure 7.12a), whilst a single CNS PNET with strong p15INK4B staining had lost one allelic copy of *CDKN2B*. Of the 5 pineoblastomas included in the immunohistochemical evaluation of p15INK4B protein expression, 1/5 (20%) pineoblastoma was negative, 1/5 (20%) pineoblastomas showed weak staining, 2/5 (40%) pineoblastomas had moderate staining and 1/5 (20%) strongly stained for p15INK4B expression. 1 pineoblastoma case had both a SNP array copy number result for *CDKN2B* and an immunohistochemical result for p15INK4B. The tumour retained both allele copies of *CDKN2B* and showed moderate staining for p15INK4B.

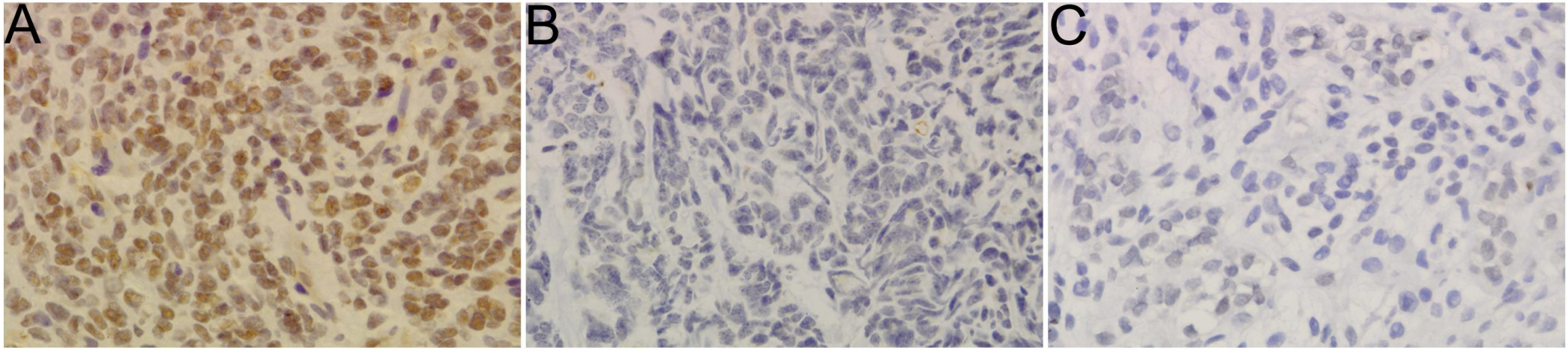

Figure 7.12a-c p15INK4B (encoded by *CDKN2B*) protein expression in CNS PNETs, determined by immunohistochemistry. Magification 1:200. CNS PNET 22P retained both copies of *CDKN2B* and displayed strong positive nuclear protein expression for p15INK4B (A). CNS PNET 25 also retained biallelic expression of the *CDKN2B* gene, however, showed no nuclear protein expression for p15INK4B (B). CNS PNET 22R had a single allele present due to the loss of one copy of *CDKN2B* and showed no nuclear protein expression of p15INK4B (C).

Statistical comparisons (as defined in chapter 2, Section 2.8) were made to test whether p15INK4B immunohistochemical results were associated with patient clinical groups and survival; however no statistically significant results were identified.

7.3.5 Immunohistochemistry of INI1

Loss of INI1 (22q11.23) protein expression is a prominent feature of ATRT and has also been detected in other paediatric brain tumours. To investigate if loss of INI1 protein expression was a feature of the tumours in our cohort, we examined INI1 protein expression on a TMA of CNS PNET and pineoblastoma cases. 7/24 (29.2%) CNS PNETs were negative for INI1 staining and 17/24 (70.8%) were positive for INI1 staining. 14 CNS PNETs had both a SNP array result and FFPE tissue available for inclusion on a TMA for immunohistochemical evaluation. 3 CNS PNETs negative for INI1 staining had a copy number result for *INI1* (from the SNP array analysis). One INI1-negative CNS PNET had retained both copies of *INI1*, whilst 2 INI1-negative CNS PNETs showed hemizygous and homozygous loss of *INI1* (Figures 7.13b and 7.13c, respectively). 11 INI1-positive CNS PNETs had a SNP array copy number result for the *INI1* gene. Whilst 7 INI1-positive CNS PNETs had retained both allele copies of *INI1* (one example shown in Figure 7.13a), 3 had gained a single copy of *INI1* and 1 CNS PNET had gained 2 copies of *INI1*. Of the 4 pineoblastomas included in the 2/4 (50%) were INI1-positive and 2/4 (50%) were negative. 2 pineoblastomas had both a SNP copy number and immunohistochemical result for INI1. 1 INI-negative pineoblastoma had retained both allele copies of *INI*1 and 1 INI1-positive had gained a single copy of the *INI1*.

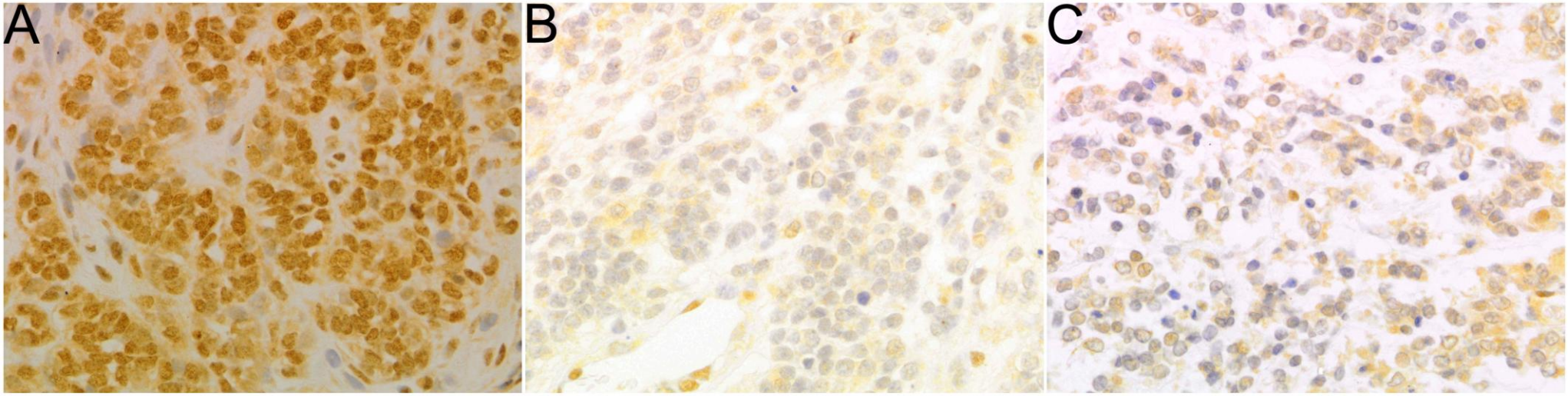

Figure 7.13a-c INI1 protein expression for CNS PNETs, determined by immunohistochemistry. Magnification 1:200. CNS PNET 22P which retained both alleles of the *INI1* gene (as identified by the SNP array analysis) displayed positive staining for the protein (A). CNS PNET 26 which had lost one copy of the *INI1* gene showed the protein to be absent (B). CNS PNET 6 (reclassified as ATRT) had a homozygous deletion of the *INI1* gene and showed no protein expression for INI1 (C).

Statistical comparisons (as defined in chapter 2, Section 2.8) were made to test whether INI1 immunohistochemical results were associated with patient clinical groups and survival. A single statistically significant result was identified, where the INI1-negative patients had a significantly poorer prognosis ($p < 0.0001$), (Figure 7.14). The CNS PNET patients were however not uniformly treated as part of a clinical trial and this result is spectulative and needs to be confirmed in a larger set of CNS PNETs treated uniformly as part of a trial.

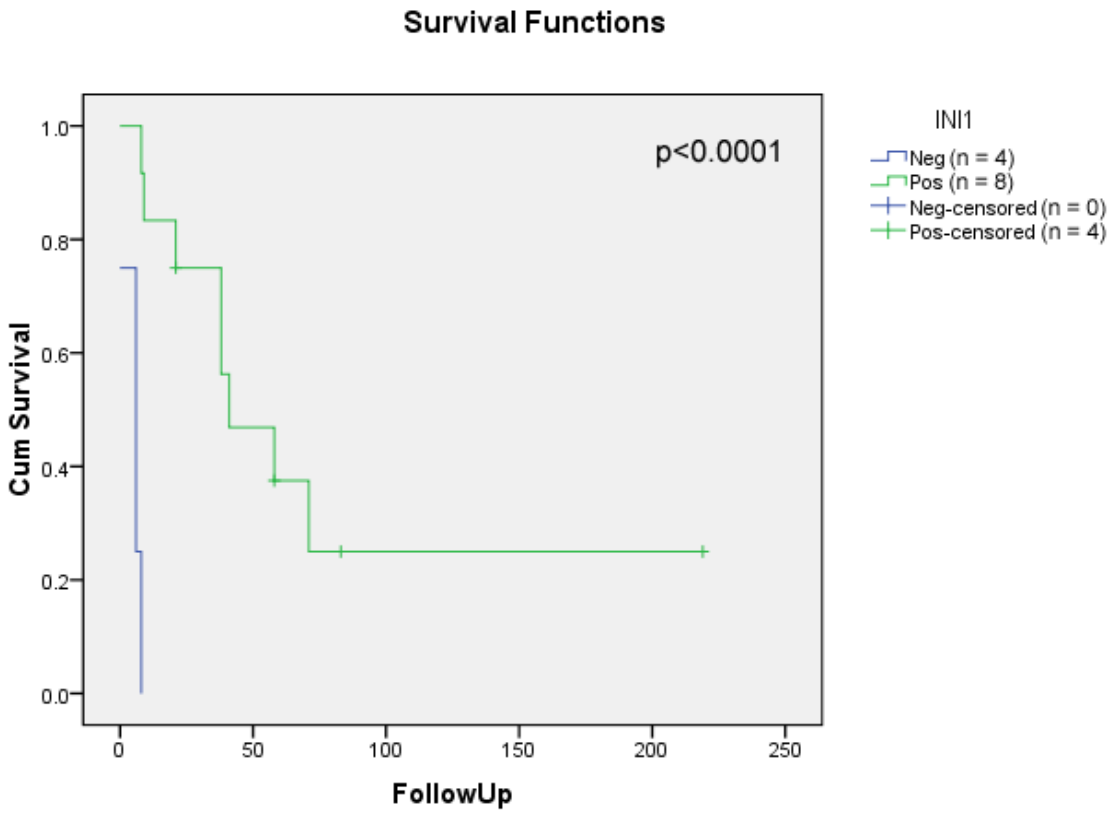

Figure 7.14 Kaplan-Meier survival analysis (using the log-rank test) of primary CNS PNETs tested for immunohistochemical staining of INI1. INI1-negative CNS PNET patients have a poorer prognosis than those with INI1-positive tumours. Follow up (months).

7.3.6 *INI1* sequencing

A mutational screen was performed for exons 5 and 9 of the *INI1* gene to identify if *INI1* gene mutation was an event in the pathogenesis of CNS PNET and pineoblastoma. Mutational hotspots on exons 5 and 9 have frequently been identified

in other paediatric brain tumours, especially ATRT (Versteege, Severnet et al. 1998; Severnet, Sheridan et al. 1999; Schmitz, Mueller et al. 2001, Biegel , Tan et al. 2002; Haberler, Laggner et al. 2006; Janson, Nedzi et al. 2006; Bourdeaut, Freneaux et al. 2007). Therefore we sequenced *INI1* exons 5 and 9 in 28 CNS PNET and 7 paired constitutional blood samples, however no mutations were identified (Table 7.3). Sequencing for exon 5 and exon 9 of individual CNS PNET cases are shown in Figures 7.15 and 7.16, respectively.

Table 7.3 CNS PNETs and pineoblastomas screened for mutations in exons 5 and 9 of the *INI1* gene. All 19 CNS PNETs, 8 pineoblastomas and 7 paired constitutional samples showed no mutations present. Wt = Wildtype, * Constitutional blood also analysed alongside tumour sample.

ID	1	2P	2R	3	4	5	8P	8R	9	11	12	13	14
***INI1* seq**	Wt	Wt*	Wt	Wt	Wt*	Wt*	Wt	Wt	Wt	Wt	Wt	Wt	Wt

16	17	18	19	21P	21R	22P	22R	23	24P	24R	25	26	27
Wt*	Wt	Wt*	Wt	Wt	Wt	Wt*	Wt	Wt	Wt*	Wt	Wt	Wt	Wt

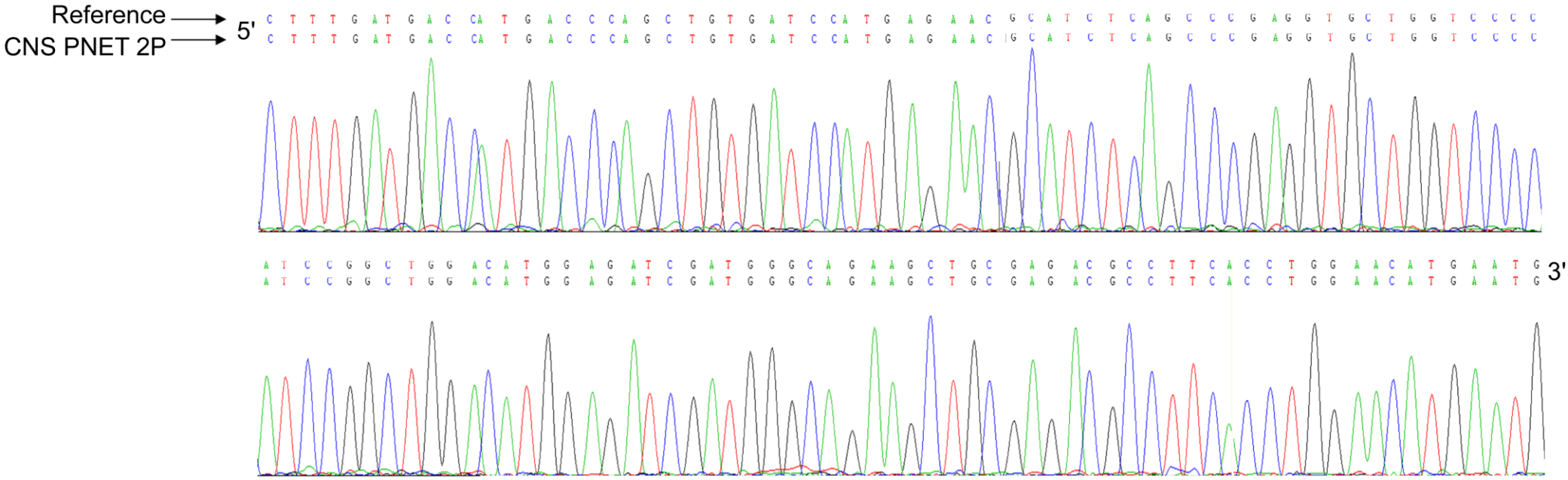

Figure 7.15 Sequencing of *INI1* exon 5. No mutation was identified for CNS PNET2P. Reference sequence taken from human genome build 19, Chromosome 22, 24,145,482 – 24,145,609 bp.

Figure 7.16 Sequencing of *INI1* exon 9. No mutation was identified for CNS PNET18.Reference sequence taken from human genome build 19, Chromosome 22, 24,176,328 – 24,176,703 bp.

7.4 Discussion

The copy number data generated for 46 CNS PNETs and pineoblastomas using the SNP array analysis was validated using both aCGH and real time PCR analyses. Furthermore, utilizing FFPE CNS PNET samples for the construction of a TMA, a larger CNS PNET sample cohort was available for immunohistochemical investigation of proteins encoded by candidate genes identified by the SNP array analysis.

9 CNS PNETs were jointly analysed using both aCGH and SNP array platforms to assess the reliability and accuracy of the SNP array results. The aCGH results confirmed the genomic regions of gain and loss identified by the SNP array analysis and on comparison of the 2 platforms, the higher resolution SNP array data more precisely defined the boundaries between normal and aberrant regions of copy number.

The real time qPCR analyses of 9 candidate genes demonstrated the importance of validating the SNP array copy number results. Although there was a positive correlation between the CNAG SNP array derived copy number results and the real time qPCR derived copy number results (Figure 7.17) this correlation was relatively weak. Using Spearman's rank test, a significant correlation was identified between the copy numbers derived from the two seperate methods ($r = 0.619$, (significant at the 0.01 level, 2 tailed)).

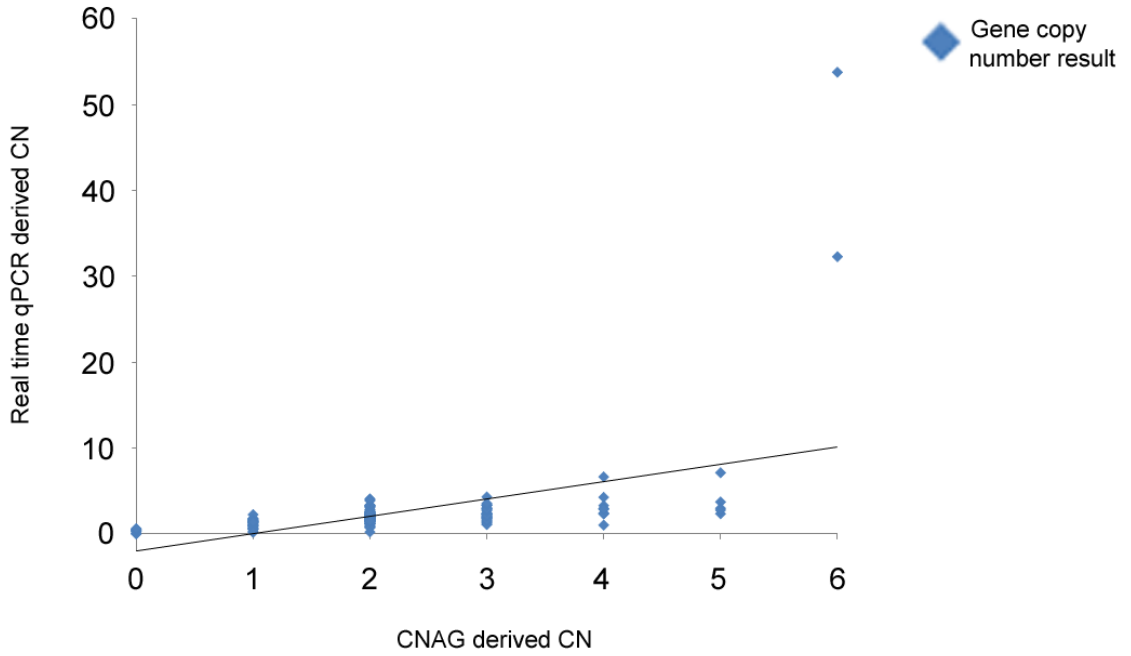

Figure 7.17 Comparison of SNP array derived copy number results (using CNAG) and real time qPCR derived copy number results for 9 candidate genes of interest in CNS PNETs and pineoblastomas. A weak positive correlation was identified. CN = copy number.

Overall, the majority of gene copy number loss identified in the SNP array analysis was validated by real time qPCR. Of the tumours available for validation of gene copy number loss, 27/41 (65.9%) losses identified from the SNP array analysis were verified by real time qPCR with the correct copy number, 4/41 (9.7%) losses were validated however with an incorrect amount of loss and 10/41 (24.4%) of copy number loss was not validated and had a normal SNP copy number by real time qPCR. Of the gene copy number gains identified in the genes of interest from the SNP array analysis, less than half were verified by real time qPCR. 10/53 (18.9%) of gene copy number gains were validated with the correct gene copy number, 14/53 (26.4%) of gains were validated, however, the extent of gain was inaccurate by the SNP array analysis. 23/53 (43.4%) of gains identified by the SNP array analysis were false positives and had normal copy numbers by real time qPCR and lastly, 6/53 (11.3%) of gains identified had copy number loss when analysed by real time qPCR. It was also important to include tumours with a normal copy number for the gene being validated. Overall, of the 9 genes investigated, 75/111 (67.6%) of tumours with normal gene copy number identified from the SNP array analysis, also had a normal gene copy number by real time qPCR. False normals were however identified, with 19/111 (17.1%) of normal gene copy numbers by SNP array showing gain by qPCR and 17/111 (15.3%) showing

loss. Thus, whilst amplifications and homozygous deletions identified using the SNP arrays were verified in the real time qPCR analyses, validation of single copy gains and losses revealed inaccuracies in the SNP array derived gene copy numbers. Ideally, real time qPCR experiments should be replicated, however due to limitations in the amounts of DNA available for the project, this was not achieved, although in each experiment the sample was analysed in triplicate and the mean taken. Potentially FISH might be a better indicator of single copy alterations.

Two amplifications were validated by real time PCR. High level gains of *PDGFRA* and *MYCN* were identified in 2 separate CNS PNETs, with 32 and 54 copies of *PDGFRA* and *MYCN*, respectively. Although only identified in a single CNS PNET, amplifications involving *PDGFRA* and *MYCN* have been identified in previous studies (Inda, Perot et al. 2005; Kagawa, Maruno et al. 2006; McCabe, Ichimura et al. 2006; Pfister, Remke et al. 2007). As high level gain of *PDGFRA* is a feature of a subset of CNS PNETs, this highlights the need for further investigation into the PDGFR-RAS-RAF-MAPK pathway. Gene copy number gain was a more frequent event than loss potentially indicating that oncogene activation is the more prevalent mechanism of tumorigenesis in CNS PNET, rather than tumour suppressor gene inactivation. The loss in copy number involving tumour suppressors *CDKN2A* and *CDKN2B* were also validated by real time PCR and previous studies have also identified the loss of 9p21.3 encompassing *CDKN2A* and *CDKN2B* in CNS PNETs (McCabe, Ichimura et al. 2006; Pfister, Remke et al. 2007).

Statistical analysis identified a single significant result identified in the tumours of both the SNP array and real time qPCR analyses: - loss of *CADPS* (3p14.2) was associated with patients with a poor prognosis, ($p = 0.033$ and $p = 0.046$, respectively). This result now needs to be verified in a larger collection of CNS PNETs in a patient cohort which has been uniformly treated to identify if *CADPS* is indeed a potential marker of prognosis in CNS PNET patients.

Due to time constraints, validation of the candidate regions of aUPD identified in CNS PNET and pineoblastomas (chapter 6, Section 6.3.2) was not performed. Sequencing the regions of aUPD identified from the SNP array analysis could potentially reveal mutations in genes involved in the pathogenesis of CNS PNET and pineoblastoma.

Validation of candidate regions of aUPD in CNS PNET and pineoblastoma will be a key area of future work.

Immunohistochemistry was performed to test whether the loss in gene copy number involving *CDKN2A* and *CDKN2B* had altered the encoded proteins expression. Limitations in the optimal use of *CDKN2A* (P16INK4A) antibodies led to the assessment of only p15INK4B expression (encoded by *CDKN2B*). The first P16INK4A antibody selected was used in a recent publication by Pfister *et al.*, however has subsequently been withdrawn (mouse monoclonal, AB7; 16P07, Neomarkers, Fremont, CA) (Pfister, Remke et al. 2007). Optimisation of a second antibody for *CDKN2A* (P16INK4A, Cat No. 551153, Clone G175-405, BD Biosciences/Pharmingen), showed unspecific binding preventing the antibodies correct usage, hence the protein expression of p15INK4B (encoded by *CDKN2B*) was therefore evaluated in a large cohort of CNS PNETs and pineoblastomas. Although *CDKN2B* copy number loss (identified in the SNP array analysis) was limited to the CNS PNETs of the cohort, loss of p15INK4B expression was identified in both CNS PNETs and pineoblastomas. 7/28 (25%) CNS PNETs and 1/5 (20%) pineoblastomas were p15INK4B-negative and 5/28 (17.9%) CNS PNETs and 1/5 (20%) pineoblastomas had weak staining for p15INK4B. CNS PNETs identified with *CDKN2B* loss analysed using the SNP arrays either had weak or negative protein expression for p15INK4B, therefore verifying the loss in gene dosage. Additional CNS PNETs and pineoblastomas with normal copy number results (from the SNP array analyses) were found to be p15INK4B-negative or had weak staining. This suggests that other mechanisms as well as copy number loss are inhibiting gene and protein expression of *CDKN2B*/p15INK4B within this subset of CNS PNETs and pineoblastomas. Possible mechanisms for this include (i) alterations in DNA methylation resulting in gene silencing, (ii) aberrant expression of miRNAs altering gene expression and thus protein expression levels or (iii) mutations within the gene sequence. Previous studies have identified the methylation of *CDKN2A* and *CDKN2B* in other brain tumours (Rousseau, Ruchoux et al. 2003; Muhlisch, Bajanowski et al. 2007). Promoter methylation of *CDKN2B* has been observed in 23/71 (32.4%) ependymomas, whilst methylation of P16INK4A and P14ARF (both encoded by *CDKN2A*) was identified in 17/43 (39.5%) and 11/42 (26.2%) medulloblastomas, respectively. Genome-wide expression and methylation profiling of the CNS PNETs and pineoblastomas of this study will add a further level of analysis to the investigation of candidate genes involved in pathogenesis. Mutational screening of selected

candidate genes would also further compliment the analyses undertaken. Compilation of SNP array copy number and LOH data, as well as methylation and gene expression profiles would offer a comprehensive picture of the genes and pathways involved in CNS PNET and pineoblastoma development and progression. Due to the small number of p15INK4B-negative tumours in the present study, a statistically significant correlation linking p15INK4B-negative CNS PNETs and a clinically relevant patient group was not possible. This highlights the need for a larger collection of CNS PNETs and pineoblastomas for immunohistochemical investigation to distinguish if p15INK4B-negativity could be linked to a clinically related patient group or potentially patient prognosis.

ATRT, CNS PNET, medulloblastoma and high grade glioma can on occasion appear very similar upon histological examination. INI1 immunohistochemistry can be used to distinguish between ATRT and other paediatric high grade brain tumours, therefore we investigated INI1 protein expression in the CNS PNET and pineoblastoma cohort. A number of previous studies have identified loss of INI1 in paediatric brain tumours that have not been classified as ATRTs (by neuropathologists) due to the absence of rhabdoid cells (Haberler, Laggner et al. 2006; Bourdeaut, Freneaux et al. 2007). In the present study, 7 CNS PNETs and 2 pineoblastomas were found to lack INI1 protein expression. Although the sample set included cases diagnosed over a wide period of time, only 1 case was reclassified as ATRT (CNS PNET6) based on morphology (by a neuropathological review panel) and that lack of INI1 expression was confirmed. The tumour remained in the tumour cohort of this thesis because it was originally classified as a CNS PNET, however, the loss of INI1 identified by the SNP array analysis provided evidence on which to question the original diagnosis. This result highlights an important role of genetic diagnostics in the correct classification of brain tumours. Six additional CNS PNETs and 2 pineoblastomas were identified with loss of INI1 protein expression; however these tumours lacked rhabdoid morphology associated with ATRT. The tumour samples were carefully reviewed independently by more than one neuropathologist and the likelihood that rhabdoid features were missed due to a sampling error is low, although cannot be excluded. In addition to the immunohistochemical results for INI1 validating the gene copy number loss identified in the SNP array analysis, the results also showed a subset of tumours (which had retained both allele copies of *INI1*) had lost INI1 protein expression. This result highlights other mechanisms other than copy number loss to have a potential role in the

loss of INI1 protein expression identified in this subset of CNS PNETs and pineoblastomas.

Other studies have identified INI1 immunonegative paediatric brain tumours which lack the morphologically characteristic features of ATRT (Haberler, Laggner et al. 2006; Bourdeaut, Freneaux et al. 2007). Haberler *et al*, identified 9/26 (34%) cases with INI1 immunonegativity. This finding is proportional to the number of INI1 negative paediatric brain tumours in the present study, however, no genetic analysis was undertaken to test for *INI1* gene deletion or mutation. In the present study no mutations of exon 5 or 9 were identified. In a more recent paper, Bourdeaut *et al.*, identified a smaller proportion of brain tumours, 4/39 (10%), with loss of INI1 protein expression that lacked rhabdoid features (Bourdeaut, Freneaux et al. 2007). Interestingly the study did not find mutations/deletions of the *INI1* gene. Together, these findings highlight a subset of CNS PNETs lacking both rhabdoid morphology and INI1 protein expression, with no evidence of *INI1* mutation. This raises the possibility of alternate mechanisms preventing the expression of INI1. One potential mechanism is the methylation of promoter CpG islands causing silencing of *INI1* gene expression, although further work is needed to provide evidence for this. Taken together, this thesis provides evidence to support the notion that high grade embryonal tumours are a spectrum of diseases rather than being clearly defined entities.

Statistical analysis of immunohistochemical results for INI1 protein expression and CNS PNET and pineoblastoma patient clinical characteristics led to the identification of a single statistically significant result. Primary CNS PNETs with immunonegativity for the INI1 protein had a poor survival ($p < 0.0001$). Interestingly, all tumour samples of the 6 patients presently alive had positive staining for INI1. These results suggests that evaluating INI1 protein expression levels in all brain tumours, independent of classification, could potentially be used as a marker of prognosis. The inactivation of INI1 could potentially be involved in the pathogenesis of CNS PNET and pineoblastoma, warranting further investigation in a larger cohort of samples.

CHAPTER 8

SUMMARY AND CONCLUSIONS

8.1 Final Discussion

Most of our therapies for childhood and adult cancers are based on empiricism and not an understanding of the underlying tumour biology, thereby enabling us to use directed rather than generic therapies. Present management of childhood brain tumours remains a challenge and there is need to identify novel targets for therapeutic intervention, as current therapies have limited success rates and can cause unaccepTable levels of morbidity. CNS PNETs can arise in many areas of the brain including both cerebral and suprasellar regions, whilst pineoblastoma arises in the pineal region. Frequently these tumours arise in deep seated brain locations and incomplete resections of CNS PNETs and pineoblastomas are common. The extensive disruption of normal brain tissue alongside neoplastic areas can cause severe life long morbidity. The use of adjuvant therapies to treat CNS PNET and pineoblastoma has had limited rates of success. Firstly, the blood brain barrier (BBB) (usually an essential defender against toxins and infections), obstructs the optimal use of chemotherapy to the brain (Schinkel 1999) and secondly, craniospinal iradiation is mostly limited to brain tumour patients over the age of 3 years due to late effects in very young children. Moreover, there is a close balance between advantageous use and neurotoxicity, thus to increase the prognoses of paediatric patients with brain tumours, novel targets for therapy need to be elucidated.

The understanding of genetic and biological mechanisms leading to tumourigenesis in solid tissues and their successful treatment has consistently lagged behind those of paediatric haematological malignancies. Whereas the mortality rates of paediatric leukaemia have substantially dropped over the last 20 years, this is not the case for children diagnosed with a brain tumour (Ries 1999). In patients with chronic myeloid leukaemia (CML) the improvement in prognosis is ultimately due to an increased knowledge of the underlying genetic alterations leading to leukaemogenesis. The Philadelphia chromosome was first discovered in 1960 (Nowell and Hungerford 1960). Later in 1973, Rowley identified the mechanism by which the Philadelphia chromosome arises as a translocation between chromosomes 9 and 22 (Rowley 1973). 95% of CML patients harbour the Philadelphia chromosome, characterised by the reciprocal translocation, (t(9;22)(q34;q11), which causes the production of a *BCR-ABL* fusion gene. This fusion gene subsequently encodes a chimeric oncoprotein with deregulated constitutive tyrosine kinase activity. Clinical trials led by Drs Druker,

Sawyer and Talpaz used a novel therapeutic agent (STI-571 or Imatinib, later known as Gleevec) to inhibit the proliferation of BCR-ABL expressing hematopoetic cells. The relatively specific BCR-ABL tyrosine kinase inhibitor targets the enzymatic activity of the BCR-ABL protein and causes a disruption in the oncogenic signal (Schindler, Bornmann et al. 2000). The drug showed striking efficacy, little toxicity and increased the survival of patients greatly. Thus, a better understanding of the underlying genetics leading to leukaemogenesis has led to the development of a novel, targeted therapy increasing the survival rates of leukaemia patients. Translating this success story into the field of paediatric brain tumours, similar improvements in patient outcome may become apparent in the not too distant future. However, this can only be achieved once comprehensive genetic analyses of paediatric brain tumours have been performed.

For this thesis, CNS PNET and pineoblastoma samples were collected from 60 patients alongside clinical information. The large clinical dataset was firstly utilized to identify relationships between clinical attributes (chapter 3, Section 3.2) and secondly to identify alterations at the chromosome arm (chapter 4, Section 4.3.1), gene (chapter 6, Section 6.3.1) and protein levels (chapter 7, Sections 7.3.4 and 7.3.5) associated with clinically relevant patient groups. Global genetic changes were analysed in a cohort of 46 fresh-frozen tumour samples (32 primary CNS PNETs, 6 recurrent CNS PNETs, 6 primary pineoblastomas and 2 recurrent pineoblastomas) using high resolution SNP arrays and the data generated revealed the complex underlying genetics within these tumours, agreeing with previous genetic studies (Inda, Perot et al. 2005; McCabe, Ichimura et al. 2006; Pfister, Remke et al. 2007). Reminiscent of earlier studies, few shared genetic alterations were identified between the CNS PNETs of the present study and tumours harboured many separate genomic abnormalities to one another (Russo, Pellarin et al. 1999; Pomeroy, Tamayo et al. 2002; McCabe, Ichimura et al. 2006; Pfister, Remke et al. 2007). Owing to the complexity of the CNS PNET genome it is not presently known which of the many genetic alterations within CNS PNET are disease causing or are subsequent genetic events caused by an increase in genomic instability.

As SNP array technology is a relatively new technique, this thesis is one of the first to genetically characterise CNS PNETs and pineoblastomas using this platform, therefore validation of the results was an essential part of the study. The SNP array analysis of this relatively large cohort of tumours provided the most common copy number

alterations across the genome, whereas previous lower resolution studies with less than 10 CNS PNET samples have only provided few regions of interest, mainly in single tumours (McCabe, Ichimura et al. 2006; Pfister, Remke et al. 2007). Gain of 1q, 2p and loss of 16q were the most frequent chromosome arm imbalances identified in the CNS PNETs of the present study and will need to be validated, potentially using FISH. Gain of 1q is a common event in high grade paediatric brain tumours (Reardon, Michalkiewicz et al. 1997; Avet-Loiseau, Venuat et al. 1999; Nicholson, Ross et al. 1999; Hirose, Aldape et al. 2001; Rickert, Simon et al. 2001; Ward, Harding et al. 2001; Carter, Nicholson et al. 2002; Inda, Perot et al. 2005; Mendrzyk, Korshunov et al. 2006; Dyer 2007; Pfister, Remke et al. 2007). The role of gain of 1q in CNS PNET patheogenesis remains unclear, however, the high resolution approach taken within this thesis has identified a number of candidate oncogenes potentially involved in tumorigenesis, particularly *FAM129A* (1q25.3). The loss of 16q was additionally a frequent event in the CNS PNET cohort of the present study and has previously been reported in both CNS PNETs and medulloblastomas (Kagawa, Maruno et al. 2006; Rossi, Conroy et al. 2006; Lo, Rossi et al. 2007; Pfister, Remke et al. 2007). A number of candidate tumour suppressor genes located on 16q were identified, in particular the loss of *SALL1* (16q12.1) and *WWOX* (16q23.1), with the loss of *WWOX* already a prominent feature identified in other cancers (Hezova, Ehrmann et al. 2007; Jenner, Leone et al. 2007; Pimenta, Cordeiro et al. 2008).

Unsupervised hierarchical clustering of the SNP array copy number data was performed to test whether the CNS PNETs shared similarities in genetic profiles. 4 distinct groups of CNS PNETs were identified reflecting the genetic heterogeneity of CNS PNETs (chapter 4, Section 4.3.2). Group 1 was characterised by many whole chromosome arm imbalances; group 2 by many small regions of loss and gain, group 3 by few whole chromosome arm imbalances; (with all pineoblastomas clustering within this group, (Fisher's exact test, $p = 0.005$)) and group 4 harboured copy number 'balanced' genomes. These groupings are reminiscent of those identified in ependymoma (Dyer, Prebble et al. 2002), but unlike ependymoma, no clear clinical correlations of tumours harbouring similar genetic signatures within groups were made for CNS PNET. This may perhaps reflect the small sample size, as found initially for childhood ependymoma, warranting the study of larger CNS PNET cohorts.

The present study has delivered a new level of genetic information in CNS PNETs. As well as identifying copy number alterations, the SNP arrays were used to identify regions of LOH. Utilizing both copy number and LOH results, regions of aUPD (copy neutral LOH) were identified (chapter 6, Section 6.3.2). As previous CGH and aCGH analyses of CNS PNET were unable to identify aUPD, this is the first study to present data for aUPD across the CNS PNET genome and validation of the copy neutral LOH identified from the SNP array analysis will be essential in the confirmation of regions of aUPD in CNS PNET.

Previous reports have included only few samples with limited clinical information. The collection of a comprehensive clinical dataset alongside genetic data was essential in the identification of genetic alterations arising in clinically relevant groups. The aim of this thesis was to characterise the genetics of a relatively large cohort of CNS PNETs and pineoblastomas and to link genetic alterations to clinically relevant groups. Differences in the underlying genetics of CNS PNET and pineoblastomas were identified in addition to genetic differences associated to patient age, tumour relapse, metastatic disease and patient survival.

8.1.1 CNS PNETs arising in patients of different ages are genetically distinct

This thesis has provided many lines of evidence to suggest CNS PNETs arising in children of different ages are genetically distinct. Comparison of the amount of chromosome arm alteration revealed age dependent patterns, with primary CNS PNETs in patients under the age of 3 years at diagnosis, having 4 times fewer chromosomal arm imbalances than patients over the age of 3 years (18 chromosome arm alterations vs 72, respectively). This finding is consistent with the hypothesis that brain tumours arising in very young children are biologically distinct from those occurring in older children, with fewer genetic events needed to initiate malignant change (Dyer, Prebble et al. 2002). From the SNP array analysis, 5 CNS PNETs were identified with no copy number imbalance and interestingly, all 5 patients were under the age of 5 years. The apparent relationship between balanced tumours and young patient age has previously been reported in ependymomas (Dyer 2008). Further investigation into global gene expression, methylation and mutational screening is needed for these 5 CNS PNETs to identify alterations in other genetic mechanisms causing tumuorigenesis in copy neutral

tumours. Further evidence is needed in a larger sample size to complement this initial work, which shows that the genetics driving CNS PNETs in older children is potentially distinct to the genetics in tumours of younger children.

8.1.2 CNS PNET and pineoblastoma are genetically distinct

Both CNS PNETs and pineoblastomas were included in the study cohort, firstly to identify whether any clinical factors were associated to tumour classification and secondly to investigate if specific genetic alterations were linked to a diagnosis of either CNS PNET or pineoblastoma. We identified, of the patients in our study cohort, children under the age of 3 years were more commonly diagnosed with pineoblastoma, whereas older patients (over the age of 3 years) were associated with CNS PNETs. The age dependent localisation of PNETs could be due to differences in the cell of origin of pineoblastoma and CNS PNET and warrants further investigation. Although a number of observations were made linking chromosome arm imbalance with tumour location, these did not reach statistical significance. Larger cohorts of CNS PNETs and pineoblastomas need to be analysed at the genetic level, potentially providing further evidence to link individual chromosome arm imbalances with a clinical characteristic or with patient survival. The comparison of the genetic imbalances found in CNS PNETs and pineoblastomas showed a site-specific difference in the genetic alterations identified. One observation made was the potential association of gain of chromosome arms 2p, 2q and 21q arising in the CNS PNETs. Additionally, the primary CNS PNETs were found to contain 18 times as many allelic changes as primary pineoblastoma (arising in the pineal region), (90 chromosome arm alterations vs 5, respectively). Providing evidence that the cells of origin are site specific for CNS PNETs and pineoblastomas will be a fascinating area for future work and can only be achieved upon the inclusion of many more genetic profiles of pineoblastoma, in addition to the establishment of pineoblastoma cell lines. It has previously been shown that histologically similar brain tumours (for example ependymoma) which arise in different brain regions are in fact molecularly distinct, in addition to arising from different populations of site-restricted progenitor cells (Taylor, Poppleton et al. 2005; Gilbertson and Gutmann 2007; Sharma, Mansur et al. 2007). Further evidence separating the genetic profiles of CNS PNET and pineoblastoma was provided by Spotfire® cluster analysis of 25 primary tumours analysed using the 100K SNP arrays. Whereas the primary CNS PNETs more often had complex genomes with many

genetic alterations, the pineoblastomas contained fewer alterations, mostly whole chromosome arm defects. Whilst the pineoblastomas clustered together in cluster group 3 (Fisher's exact etst, $p = 0.005$), near to the 4th cluster group containing CNS PNETs with no copy number alteration, the majority of CNS PNETs clustered separately to the pineoblastomas, either clustering in groups 1 and 2 (which contained tumours with chaotic genomic change).

Overall, 5 CNS PNETs (4 primary and 1 recurrent) were identified with a balanced genome (at the 100K/500K resolution). As tumour viability was checked before extracting DNA from tumour tissue, it is unlikely that normal brain tissue contaminated the sample, resulting in an apparently balanced genome. This suggests mechanisms other than aberrant DNA copy number to be important in the pathology of a subset of CNS PNETs. Other series have also reported a minority of CNS PNETs with balanced profiles analysed at high resolution (Pfister, Remke et al. 2007; Lee 2008). Epigenetic studies, alongside gene expression will be crucial in identifying the mechanisms involved in the pathogenesis of these tumours. Although an original hypothesis of this thesis was to provide evidence that CNS PNETs and pineoblastomas are genetically distinct, a number of similarities in chromosome arm alterations were identified. 1/6 (16.7%) primary pineoblastomas contained gain of 1q, which was also identified in 7/32 (28.9%) primary CNS PNETs and 2/6 (33.3%) recurrent CNS PNETs. Loss of 16q was also an event shared between a subset of CNS PNETs and pineoblastomas, (2/6 (33.3%) primary pineoblastomas and 3/32 (9.4%) primary CNS PNETs, respectively. In agreement, one other study in this limited field of research also found gain of 1q in a single pineoblastoma suggesting gain of 1q is also a factor of pineoblastoma pathogenesis (Rickert, Simon et al. 2001). Further analysis of the genes gained on 1q and lost on 16q is needed to decipher if CNS PNETs and pineoblastomas share genetic alterations and have similar pathogenic pathways involved in tumourigenesis. Presenting evidence to support the hypothesis that CNS PNETs and pineoblastomas are genetically distinct was hampered by the small sample size of only 8 pineoblastoma (6 primary and 2 recurrences in the present study). Further analysis of a larger sample set of pineoblastoma will undoubtedly provide additional evidence that CNS PNET and pineoblastoma are potentially genetically distinct.

8.1.3 Characterising the genetic alterations of recurrent CNS PNETs will identify genes involved in tumour progression and biologically adverse behaviour

Tumour recurrence is common feature in patients diagnosed with CNS PNET. Maximising the use of the data collected for the recurrent CNS PNETs, 2 separate analyses were performed. Firstly a group-wise analysis was performed comparing the genetic alterations identified in 6 recurrent CNS PNETs, to those identified in 32 primary CNS PNETs. Further validation and statistical analysis is needed to identify genes with copy number imbalance which is statistically different on comparison of the primary and recurrent CNS PNET groups. Secondly the comparison of genetic alterations identified in 5 primary and recurrent CNS PNET pairs was performed. 4/5 (80%) paired recurrences showed marked gain in copy number when compared to the paired primary tumour. The pattern of genetic alteration within the recurrent tumours raises two possibilities, either current therapy used to treat CNS PNET promotes genetic gain rather than loss at relapse or that oncogene activation is the main mechanism for progression/relapse rather than tumour suppressor inactivation in CNS PNET recurrence. Regions of maintained copy number imbalance were identified potentially highlighting important regions encompassing candidate genes involved in the initiation of tumourigenesis. We identified a region of maintained gain involving 2p21 in 4/5 (80%) CNS PNET pairs. 2p21 encompasses *ABCG5* and *ABCG8* which encode for ATP-binding cassette proteins. With tumour recurrence occurring due to resistance of current therapies, elucidating the roles played by these potential drug transporters will be an interest area for future work. Regions of acquired copy number imbalance specific to the recurrent CNS PNET (not previously found in the primary tumour) potentially show regions encompassing candidate genes involved in aggressive biological behaviour and tumour progression. These in turn could potentially be markers of poor prognosis in CNS PNET. Further work is needed on the acquired alterations identified at relapse however, to distinguish between the alterations driving tumour recurrence.

Although the analysis of the present study concentrated on the maintained and acquired alterations at relapse, regions that were present in the primary but not at relapse are also important. These regions could potentially be involved in tumour initiation but are not needed for tumour progression and subsequent relapse. A seperate theory is that the

genomic regions altered in the primary and not present at relapse could be 'passenger' alterations which arise due to the increased genomic instabily of the tumour's genome. Validation and characterisation of these regions will allow us to identify whether these regions are important to tumour initiation or whether alterations identified in the primary tumour but not present at relapse are merely due to the unsTable genome. Although the data is not shown, gain of heterozygosity (GOH) analysis was performed to identify regions of GOH in the recurrent CNS PNETs not present in the primary CNS PNETs; however no regions of GOH were identified. Consideration of whether the recurrent tumours were relapses of the primary tumour and not a different lesion is important. From the molecular data, regions of maintained copy number alteration were identified in 4/5 (80%) primary and recurrent tumour pairs. Secondary brain tumours can arise due to the irradiation of a primary brain tumour. As only 2/8 (25%) recurrent tumours were irradiated, it is unlikely that the majority of relapsed tumours were separate irradiation-induced lesions. Another important factor to consider is that radiation-induced tumours usually take at least 5 years to occur and in the present study cohort only a single case (CNS PNET 21R) recurred 5 years post-diagnosis.

8.1.4 Characterising the genetic alterations of metastatic CNS PNETs will identify genes involved in the development of metastatic disease

Although metastasis is common in CNS PNET and pineoblastoma, very little is understood about the biology and genetics promoting tumour dissemination. Initial assessment of the clinical information collected for CNS PNET and pineoblastoma patients of this study cohort showed that metastatic disease at diagnosis was more common in primary pineoblastoma patients (Fisher's exact test, $p = 0.0035$). The relationship between metastasis and patients with pineoblastoma warrants further investigation, with pineal tumour location, young patient age and the presence of metastatic disease all factors of poor patient prognosis (Geyer, Zeltzer et al. 1994; Albright, Wisoff et al. 1995; Cohen, Zeltzer et al. 1995; Jakacki, Zeltzer et al. 1995; Dirks, Harris et al. 1996; Reddy, Janss et al. 2000; Hong, Mehta et al. 2004; Fangusaro, Finlay et al. 2008). Little research has been performed to identify genetic alterations correlating with metastatic disease; however, one previous genetic study identified a trend whereby loss of *CDKN2A* (9p21.3) was associated with CNS PNETs with metastatic disease (Pfister, Remke et al. 2007). Although this association was not identified for the metastatic CNS PNETs of the present study, upon

immunohistochemical evaluation, it was noted that tumours with strong staining for p15INK4B (encoded by *CDKN2B*) tendered not to have metastatic disease. The analysis of new CNS PNET cases will further justify the involvements of *CDKN2B*/p15INK4B in the metastatic disease of CNS PNET.

In the present study, only associations between a patient's metastatic status and the genetics of the primary tumour were evaluated. To get a clearer picture of the genetic alterations involved in metastasis and to identify biomarkers of disease progression, it will be important for future studies to investigate the genetics of metastatic deposits of CNS PNET and pineoblastoma and compare this data to the genetics of the primary tumour. In the management of CNS PNET and pineoblastoma, biopsy/resection of the metastatic deposit is not usually in the patients' interest, and therefore no metastatic tumour samples were available for inclusion within the present study. It is also important to note that when CNS PNETs and pineoblastomas do metastasise, often there are many small metastatic deposits within the brain of which surgical resection would not be an option, thus CNS PNET and pineoblastoma metastatic tissue samples are rarely available to research.

8.1.5 CNS PNETs and medulloblastomas are distinct entities at the genetic level

Previous CGH and aCGH analyses in the literature have compared the genetic profiles of CNS PNETs and medulloblastomas and identified different genetic alterations in each. To confirm the results of previous studies, the SNP array data for the CNS PNETs presented here needs to be directly compared to a large cohort of medulloblastomas genetically analysed using the same platform. Although no medulloblastoma SNP array results were available for comparison during the time frame or scope of this thesis, a very recent report released has identified the genetic alterations of 212 paediatric medulloblastomas using a combination of 100K and 500K SNP array analysis (Northcott, Nakahara et al. 2009). A collaborative study utilizing both high resolution datasets will undoubtedly add to the current genetic information further separating the 2 PNET classifications. Clustering analysis will also be an invaluable tool in uncovering whether the tumours cluster separately, as is hypothesised due to differences in their site-specific genetic signatures. On comparison

of the genetic data of CNS PNETs within this thesis and previous genetic imbalances identified in medulloblastoma, the present study provides further evidence to suggest that CNS PNETs are genetically distinct to medulloblastomas at the genome wide level. Overall the CNS PNET genome is characterised by more frequent partial chromosome gain than that of medulloblastoma.

Gain of chromosome arm 1q was the most frequent genetic alteration identified in CNS PNET from the SNP array analysis, occurring in 7/32 (%) and 2/6 (33.3%), primary and recurrent CNS PNETs, respectively. Interestingly, one report has shown the gain of 1q is more frequent in CNS PNETs than medulloblastoma suggesting genes located on 1q have important oncogenic roles in CNS PNET (Inda, Perot et al. 2005). A recent genetic study of CNS PNETs identified the loss of the telomeric end of chromosome 13q (13q34) was a common event in CNS PNET but not medulloblastoma (McCabe, Ichimura et al. 2006). On the contrary, 3 CNS PNETs of the present study contained gain of chromosome 13q and no loss of chromosome 13q was identified. The previous study also hypothesised that CNS PNETs were more likely to contain regions of amplification than medulloblastomas. Many regions of amplifications were identified in the CNS PNETs of this thesis supporting this concept, however still needing validation. Amplification at 4q12 (involving *PDGFRA* and *KIT*) was identified in a single CNS PNET of the present study and has previously been identified in other paediatric brain tumours (including medulloblastoma) and highlights the over-activity of PDGF pathways as an event in paediatric brain tumours (Inda, Perot et al. 2005; McCabe, Ichimura et al. 2006; Holtkamp, Ziegenhagen et al. 2007). Amplification of *MYC* (8q24) and *MYCN* (2p24.3) have been detected in 5-10% of medulloblastomas and has been associated with a poor prognosis (Aldosari, Bigner et al. 2002; Eberhart, Kratz et al. 2002; Neben, Korshunov et al. 2004; Mendrzyk, Radlwimmer et al. 2005). A single *MYCN* amplification was identified in a CNS PNET of the present study. The amplification of *MYC*, however, was not a feature of the CNS PNETs, adding to the evidence that CNS PNETs and medulloblastomas are potentially genetically distinct.
Isochromosome 17q is a frequent cytogenetic alteration in medulloblastoma, but was not found in the CNS PNETs of this study. A recent aCGH study by Lo *et al.*, identified i17q in 24/72 (33.3%) medulloblastomas consistent with earlier reports (Biegel, Rorke et al. 1989; Michiels, Weiss et al. 2002; Inda, Perot et al. 2005; Mendrzyk, Radlwimmer et al. 2005; Lo, Rossi et al. 2007). A separate study found i17q to be a negative prognostic marker in poor-risk medulloblastomas (Pan, Pellarin et

al. 2005). Although gain of 17q was identified in 3 CNS PNETs of the present study, the imbalance was an isolated event, not associated with the loss of 17p. Three previous genetic studies of CNS PNET and medulloblastoma have identified gain of 17q to occur more commonly in medulloblastoma than CNS PNET and the SNP array results of this thesis is also supportive, with only 3/46 (6.5%) CNS PNETs identified with gain of 17q (Inda, Perot et al. 2005; McCabe, Ichimura et al. 2006; Pfister, Remke et al. 2007).

Loss of tumour suppressor genes *CDKN2A* and *CDKN2B* (9p21.3) was found in 7/38 (18.4%) CNS PNETs of the present study. One previous study has found the loss of *CDKN2A* to be a more frequent event in CNS PNET than medulloblastoma (Pfister, Remke et al. 2007). Genetic studies of medulloblastoma have corroborated this, with the loss of *CDKN2A* and *CDKN2B* only rarely found in medulloblastoma (Mendrzyk, Radlwimmer et al. 2005; Rossi, Conroy et al. 2006).

The WNT/β-catenin pathway has been implicated in various tumour types, including medulloblastoma (Morin, et al. 1997; Iwao, et al. 1998; Voeller, et al 1998; Koch, et al. 1999; Koesters, et al. 1999; Ogasawara, et al. 2006). Pathway upregulation has previously been observed in medulloblastomas with mutations in key pathways components *CTNNB1* and *APC* (Hamilton, et al. 1995; Eberhart, et al. 2000; Koch, et al. 2001; Ellison, et al. 2005; Clifford, et al. 2006; Gajjar, et al. 2004; Thompson, et al 2006). Recently, the WNT/β-catenin pathway has been investigated in CNS PNETs. Activation of the WNT/β-catenin pathway was identified in over a third of CNS PNETs using immunohistochemical analysis of *CTNNB1* and a link between an active WNT/β-catenin pathway and a favourable prognosis was identified (Rogers, Miller et al. 2009). In the majority of medulloblastoma cases the aberrant activity of the WNT/β-catenin pathway was caused by activating mutations in *CTNNB1*, which was in contrast to the CNS PNETs of the study, where only a single mutation was identified. Previously a small study of 4 CNS PNETs also identified a single mutation in *CTNNB1* (Koch, Waha et al. 2001). The results of the study suggest the WNT/β-catenin pathway plays an important role in CNS PNET pathogenesis, but whereas in the majority of medulloblastomas the aberrant activation of the WNT/β-catenin pathway is caused by activating mutations in *CTNNB1*, this was not the case for the majority of CNS PNET cases and further investigation is needed to identify the underlying causes altering the WNT/β-catenin pathway activity. An association between WNT/β-catenin pathway

activation and chromosome 6 loss has previously been identified in a subset of medulloblastomas with favourable prognosis (Clifford, Lusher et al. 2006; Thompson, Fuller et al. 2006). A comparison was made, testing for the association in the CNS PNETs of this thesis. An overlap of 12 CNS PNETs had both SNP array data for chromosome 6 and an immunohistochemical result for *CTNNB1* to test for WNT/β-catenin pathway activation (Rogers, Miller et al. 2009). 6/12 (50%) CNS PNETs showed nuclear staining for *CTNNB1* (signifying an active WNT/ β-catenin pathway status), whilst a further 6/12 (50%) had cytoplasmic staining for *CTNNB1* (signifying an inactive WNT/β-catenin pathway status). Only 1/12 (8.3%) CNS PNETs harboured allelic loss of chromosome 6 (however, only involving the long arm of the chromosome) and the tumour had cytoplasmic staining for *CTNNB1*. Thus, the link between WNT/β-catenin pathway activation and the loss of chromosome 6 is a distinct feature of a subset of medulloblastomas and is not present in the CNS PNETs of this thesis.

Taken together the evidence discussed here suggests that CNS PNETs are genetically distinct to their cerebellar counterparts and that both tumours warrant specific evidence based therapies depending on their genetic and biological composition (Bigner, McLendon et al. 1997; Burnett, White et al. 1997; Biegel 1999; Russo, Pellarin et al. 1999; Inda, Perot et al. 2005; McCabe, Ichimura et al. 2006; Rossi, Conroy et al. 2006; Pfister, Remke et al. 2007).

8.1.6 Paediatric embryonal brain tumours are a spectrum of diseases and not clearly defined entities

To further discriminate between the diagnoses of the embryonal brain tumours, CNS PNET, pineoblastoma and ATRT, an immunohistochemical and mutational screen of INI1 was performed. Known to be deleted in the majority of paediatric ATRTs, this gene has only been analysed in limited numbers of brain tumours previously (Judkins, et al. 2004, Haberler, et al. 2006, Bourdeaut, et al. 2007). In the present study, CNS PNETs and pineoblastomas lacking rhabdoid features were found to have lost INI1 protein expression, indicating that the loss of INI1 was not purely associated with the rhabdoid cell phenotype. The lack of INI1 protein expression was also identified as a marker of poor prognosis in primary CNS PNET patients ($p < 0.0001$). Thus,

independent of a correct tumour classification between the CNS PNET and ATRT entities, INI1 protein negativity was linked to a poor prognosis and should be taken into account by clinicians when considering treatment options and possible outcomes. Mutational analysis did not identify mutations within the mutational hotspots of the *INI1* gene (exons 5 and 9); raising the possibility of an alternative mechanism for the inactivation of *INI1* in the subset of CNS PNETs lacking INI1 protein expression which did not harbour gene copy number loss. Screening of the 7 remaining exons would further confirm whether *INI1* gene mutation was a component of the lost protein expression within this subset of CNS PNETs.

8.2 Study limitations

The greatest limitation of the present study was the rarity of CNS PNET and pineoblastoma samples available for genetic analysis. In the UK, of 450 children a year diagnosed with a brain tumour, only a small fraction (2-4%) have a CNS PNET or pineoblastoma. Whilst the majority of CNS PNET and pineoblastoma patients whom have their tumours surgically resected and consent to the sample being used for research, a small majority do not and quite often when a child is very sick it is not always appropriate to ask the family for consent. Even when a tumour sample is donated for research, it may not be of adequate size or quality to extract DNA from. For DNA extraction of high quality frozen tissue, the sample needs to be at least 5mg. Neurosurgeons sometimes use a CUSA™ trap (ultrasonic surgical aspirator) to extract cancerous brain tissue and due to the contamination of tumour tissue with blood and normal brain tissue, the sample is unable to be used in genetic studies.

The power of statistical associations between alterations at the gene/protein level and clinical variables for the CNS PNETs and pineoblastomas of this study was hampered by the relatively small number of samples in the cohort. On comparison of the gene copy number results and patient clinical characteristics, only a single association was identified in both SNP array and real time qPCR analyses. Loss of *CADPS* was linked with poor survival in primary CNS PNETs when analysed using both the SNP array and real time qPCR methods ($p = 0.033$ and $p = 0.046$, respectively). When a significant result has not been identified, the use of power statistics can aid in the estimation of sample number needed to provide a statistically significant result. From the immunohistochemical investigation we identified patients with primary CNS

PNETs which had negative/weak p15INK4B expression had a poorer prognosis than those with moderate/strong p15INK4B expression, however this result did not reach significance due to low sample number ($p = 0.187$). For this result to reach significance, power statistics (as detailed in chapter 2, Section 2.8.6) were used to show a total of 60 samples (25 with negative/weak p15INK4B staining and 35 with moderate/strong p15INK4B staining) would be needed to reach significance.

The CNS PNETs and pineoblastomas of this study were not uniformly treated; therefore when investigating factors related to patient survival, the associations identified here will still need to be validated in samples of a uniformly treated patient cohort. The CNS PNETs and pineoblastoma samples used in the present study were collected from 7 CCLG centres in the UK and the CHTN in America across a large time frame (1993 – 2008, (15 years) for samples included in the SNP array analysis and 1972 – 2007, (35 years) for samples included on the TMA for immunohistochemical analysis) and were therefore not treated using the same guidelines. An ideal cohort would contain a large number of samples which well represented each clinical patient group to produce statistically significant results.

Although there is a strong compulsion for researchers to use newly released, high resolution technologies to compete with other research groups and keep up to date within the cancer research environment, typically these new platforms have underdeveloped softwares which are not easy to use and are not tailored to answer specific scientific questions. The use of high resolution SNP arrays in the present study led to the generation of a vast amount of genetic data which was manually interpreted to identify novel genes and regions of interest. With limited software available to analyse and compare the genetics of the CNS PNETs in the study, the program Spotfire® was used to visually analyse the data of all the tumours at one time. As a visualisation program, Spotfire® is not a genetic analysis software and lacked many features needed to analyse the SNP array data fully. Although the heatmaps generated in Spotfire® were informative; they are not straightforward to interpret. Thus, due to the difficulties facing SNP array analysis, a bioinformatic collaboration was set up to produce new software (SNPview). Though not completed in time for the majority of the SNP array analysis performed for the present study, a number of Figures were produced which delivered the SNP array data in a more uncomplicated and informative manner. Additionally, Spotfire® had limitations in the amount of memory available for

cluster analysis of the SNP array data. Originally, Spotfire® was not designed to hold or cluster such massive amounts of data, hence the cluster analysis was limited to fewer than 30 CNS PNET samples and was restricted to a cytoband only basis. The development of computer programs capable to hold, combine and cluster data needs more focus in the future. Other factors which need to be incorporated into new SNP array analysis softwares include patient clinical information and details of the differences in tumour histologies. Thus, future comparisons between chromosome arm alterations, patient clinical information and tumour histologies will be made highlighting possibly associations.

Combining the complete datasets of the CNS PNETs analysed using the 100K and 500K SNP arrays was not possible due to the differences in the probe sets for each SNP array. The development of SNPview, (a collaboration with Dr Alain Pitiot and Francois Morvillier, The Brain and Body Centre, University of Nottingham. UK) led to the ability to analyse both SNP array platforms at once, however, this achievement occurred late into the present study and will be utilised in future work. The comparison of tumour genetics and patient clinical information was manually executed due to the lack of software supporting both SNP array data and patient clinical information. For this thesis, the comparisons between genetic alterations (chromosome arm or gene imbalance) against clinical characteristics was manually performed and the statistical comparisons were identified using the separate statistical package, SPSS. Although too late for this thesis, the collaborative SNPview project has been established to produce a software package (SNPview version 2) which is capable of holding genetic, clinical and histological data for large sample sets. The program also has the additional feature of clustering large datasets at full resolution. A comprehensive set of statistical tools within a data analysis software would be advantageous for SNP array data analysis. One example of where statistical support is needed is within the group-wise analysis of the primary and recurrent tumours. The generation of gene lists which are statistically associated to either the primary of recurrent tumours is needed. Thus, further efforts to include statistical tests within the SNPview version 2 program would be beneficial and will be an area for future collaborative work.

A number of CNS PNETs and pineoblastomas analysed as part of this thesis have gene expression array results. The combination of SNP array and gene expression array datasets will enable the identification of copy number alterations which directly alter

the level of gene expression, thus biologically relevant targets will be identified through the combination of these datasets and provide candidates to be taken forward for immunohistochemical evaluation. February 2010 saw the release of Genespring GX11 (Agilent) which can combine both the SNP array and gene expression datasets of Affymetrix arrays. Combining the SNP array and gene expression datasets within this new software will be a key area of future work to maximise the data collected for this set of CNS PNETs and pineoblastomas.

A separate limitation in the analysis of the present study was the inability to analyse the X chromosome due to the scarcity of sex-matched constitutional blood samples. For unpaired analysis of the SNP array data both genders were used providing unusable X chromosome results. The addition of increased cohort numbers of paired samples will provide a better focus on candidate regions/genes located on the X chromosome linked to the tumourigenesis of CNS PNET. The deposition of SNP array data within publically available domains (which is now widely performed within the research community) will add to the efficient normalisation of SNP array data. Although the X chromosome was not analysed for this thesis, on evaluation of the quality of SNP array data, an interesting result was found for the X chromosome of a CNS PNET patient which had a constitutional blood sample also available for analysis. The association of brain tumours arising as part of a genetic syndrome has greatly increased the understanding of the pathways involved in brain tumourigenesis. Patient CNS PNET9 had monosomy of the X chromosome in both the tumour and constitutional blood samples. This cytogenetic abnormality is indicative of Turner's syndrome, and additionally the patient's tumour sample contained aUPD across the majority of the tumour genome. This novel finding is the first CNS PNET patient identified with turners syndrome and emphasizes the importance of genetically analysing the sex chromosomes of brain tumour patients. The finding also raises the importance of collecting patient blood samples alongside the tumour sample and clinicians and scientists need to make a collaborative effort to obtain these for research.

8.3 Future work

Further validation of the SNP array results is required to confirm the copy number alterations of candidate genes identified in this thesis. Real time PCR validation of gene copy numbers and immunohistochemistry of the proteins encoded by candidate

genes is necessary to further confirm the SNP array data. Additionally, fluorescence in situ hybridisation (FISH) is required to validate the chromosome arm imbalances identified. FISH confirmation of the gain of chromosome arm 1q and the loss of 16q will supplement the present validation of the SNP array data. The use of FISH to validate the single gene copy number alterations identified in the SNP array analysis also needs to be performed. Although the real time qPCR results confirmed gene amplifications and homozygous deletion, single copy number alterations were harder to validate and FISH confirmation is better suited for the validation of single gene copy number alterations.

Functional analysis of the most commonly lost and gained genes identified in the CNS PNET cohort, *OR4C12* and *PCDHGA3*, respectively, will provide evidence for their roles in pathogenesis. Currently 1 in house CNS PNET cell line and 1 commercial cell line (PFSK1), which have been characterised (Hussain et al 2010, unpublished), are available for use. To investigate either the overexpression or knockdown of candidate genes involved in CNS PNET pathogenesis, transient transfections and RNAi (potentially using siRNA) of these cell lines could be performed. Downstream effects on the cell cycle, apoptosis, drug resistance, proliferation and cell migration can therefore be assessed. If the *in vitro* work provides evidence for tumourigenic roles of the candidate genes tested, cells stably lacking or overexpressing candidate genes could be implanted into nude/SCID mice to test if these cells have the capacity to form xenograft tumours when injected both subcutaneously and orthotopically. Immunohistochemical staining of xenograft tumours from sacrificed mice can then be assessed to see if the cells of xenograft tumours represent those of CNS PNET classification. In the long term, if xenograft tumours are formed in mice from cells overexpressing/lacking candidate genes, the use of genetically engineered mouse (GEM) models could provide further evidence of the tumourigenic role of a candidate gene. If the transgenic mouse is viable and a tumour of the correct classification is formed, this provides an opportunity to identify which therapies are optimal in shrinking the tumour with the least side effects, however, as this is a mouse model, the same results might not arise if tested in humans, although at present the use of mouse models is an excellent way of better understanding the functions of candidate genes. Thus, the results from these analyses could potentially be used to both determine the role played by these genes in tumourigenesis and to identify potential therapeutic targets.

Although the present study analysed the largest cohort of CNS PNETs to date, few statistically significant results were identified. The rarity of CNS PNET tissue available for genetic and immunohistochemical analysis limited the statistical testing. The collection of a larger sample set adding to the current study will potentially advance the statistically significant results in the study of CNS PNETs, relating clinical characteristics and prognosis with the genetic alterations identified. Difficulties in obtaining fresh frozen material, particularly from pineal based tumours, has led to the exploration of using Formalin Fixed Paraffin Embedded (FFPE) tissue in the future study of CNS PNET. Existing high resolution systems which could be used to analyse the DNA extracted from FFPE tissues include Agilent 244K aCGH and Affymetrix SNP6 platforms providing good quality genetic data (Thompson, Herbert et al. 2005; Johnson, Hamoudi et al. 2006; Tuefferd, De Bondt et al. 2008).

In order to identify whether the gene copy number changes found in the present study have altered gene expression levels, the SNP array data and gene expression array data of corresponding CNS PNET samples (performed within the CBTRC group, Rogers H unpublished) will be combined. The translation of candidate genes will in turn be investigated at the protein level by immunohistochemistry, with results linked to clinical information to provide diagnostic and prognostic markers in CNS PNET. DNA methylation studies in CNS PNET are also required to unravel if the genetic silencing of genes is involved in tumour pathogenesis. A subset of CNS PNETs analysed using SNP and gene expression arrays are currently being analysed for global methylation patterns using Illumina Golden Gate methylation arrays in a collaborative study with the Northern Institute of Cancer Research (Clifford S, Hayden J, unpublished). Interrogating over 1500 CpG residues in >800 cancer-related genes, the combination of epigenetic profiles alongside gene expression will play an important role in establishing alterations in the CNS PNETs with copy neutral genomes. Candidate genes identified from genome-wide methylation analysis may warrant further investigation and the use of DNA methyltransferases to reverse a gene's methylation status could be used in function studies (Karpf 2007).

Histopathological classification of brain tumours containing primitive cells (which include medulloblastoma, CNS PNET, pineoblastoma, GBM and ATRT) is difficult. Understanding the genetic alterations of each tumour type and identifying markers of

prognosis will be essential in the molecular classification of brain tumours which reflect the underlying genetics. It remains to be identified whether histological sub-groups are present in CNS PNETs and if potential sub-groups provide information on patient prognoses, however, with the majority of CNS PNETs having a poor prognosis overall, if present, these sub-groups may not be of substantial prognostic value. The cell(s) of origin of CNS PNET remains elusive. At present, little research has been performed to answer this question; however, historically the cell of origin is thought to be primitive, of neuronal lineage, arising from the ectoderm during development of the CNS, with little or no differentiation. It has been proposed in current literature that the tumour cells have arisen through genetic alteration of normal cells located to specific brain regions and the results of this thesis suggest differences in the genetic alterations between CNS PNETs and pineoblastomas, which could signify different cells of origin for each. It still remains unclear whether paediatric brain tumours have separate cells of origin, although evidence now suggests medulloblastomas arise from progenitor cells of the cerebellar granule layer whereas ependymomas arise from the radioglial cell (Dahmane and Ruiz i Altaba 1999; Dahmane, Sanchez et al. 2001; Taylor, Poppleton et al. 2005). Further characterisation of the underlying genetics of CNS PNET will be crucial to decipher the cell of origin. Gene expression analyses will be vital in the investigation of the cell of origin, as similarities between the tumours expression profile and the normal tissue from which it arose could potentially be identified.

Our ability to achieve significant advances in the diagnosis, prognosis and therapy of CNS PNETs relies on gaining a better understanding of the underlying biology through high resolution molecular characterisation of these tumours. The results of this thesis and the future work hereafter will provide a genetic basis to diagnose CNS PNETs more accurately and understand the underlying biology driving these tumours. Novel targets for therapy will be identified providing CNS PNET patients with better treatments and an increased survival. Making use of this new data increasing our understanding of this tumour can therefore be used to develop better understanding of the origin of CNS PNET. Finally, key molecular events in CNS PNET pathogenesis are predictive of their clinical behaviour and the increase of CNS PNET cohort numbers is required for high quality, statistically relevant results. Further work is needed to better understand the relationships between the cell of origin, the tumours microenvironment and the genetic defects causing the development and progression of CNS PNET.

BIBLIOGRAPHY

Affymetrix Genechip Human Mapping 100K Set.

Affymetrix Genechip Mapping 100K Assay Protocol.

Agamanolis, D. P. and J. M. Malone (1995). "Chromosomal abnormalities in 47 pediatric brain tumors." Cancer Genet Cytogenet **81**(2): 125-34.

Albright, A. L., J. H. Wisoff, et al. (1995). "Prognostic factors in children with supratentorial (nonpineal) primitive neuroectodermal tumors. A neurosurgical perspective from the Children's Cancer Group." Pediatr Neurosurg **22**(1): 1-7.

Aldosari, N., S. H. Bigner, et al. (2002). "MYCC and MYCN oncogene amplification in medulloblastoma. A fluorescence in situ hybridization study on paraffin Sections from the Children's Oncology Group." Arch Pathol Lab Med **126**(5): 540-4.

Amoaku, W. M., H. E. Willshaw, et al. (1996). "Trilateral retinoblastoma: A report of five patients." Cancer **78** (4): 858-63.

Andersson, U., D. Guo, et al. (2004). "Epidermal growth factor receptor family (EGFR, ErbB2-4) in gliomas and meningiomas." Acta Neuropathol **108**(2): 135-42.

Ater, J. L., J. van Eys, et al. (1997). "MOPP chemotherapy without irradiation as primary postsurgical therapy for brain tumors in infants and young children." J Neurooncol **32**(3): 243-52.

Avet-Loiseau, H., A. M. Venuat, et al. (1999). "Comparative genomic hybridization detects many recurrent imbalances in central nervous system primitive neuroectodermal tumours in children." Br J Cancer **79**(11-12): 1843-7.

Badiali, M., A. Pession, et al. (1991). "N-myc and c-myc oncogenes amplification in medulloblastomas. Evidence of particularly aggressive behavior of a tumor with c-myc amplification." Tumori **77**(2): 118-21.

Baker, S. J., S, Markowitz, et al. (1990). "Suppression of human colorectal carcinoma cell growth by wild-type p53." Science **249**(4971): 912-5.

Batanian, J. R., N. Havlioglu, et al. (2003). "Unusual aberration involving the short arm of chromosome 11 in an 8-month-old patient with a supratentorial primitive neuroectodermal tumor." Cancer Genet Cytogenet **141**(2): 143-7.

Batra, S. K., R. E. McLendon, et al. (1995). "Prognostic implications of chromosome 17p deletions in human medulloblastomas." J Neurooncol **24**(1): 39-45.

Bayani, J., M. Zielenska, et al. (2000). "Molecular cytogenetic analysis of medulloblastomas and supratentorial primitive neuroectodermal tumors by using conventional banding, comparative genomic hybridization, and spectral karyotyping." J Neurosurg **93**(3): 437-48.

Beckwith, J. B. and N. F. Palmer (1978). "Histopathology and prognosis of Wilms tumors: results from the First National Wilms' Tumor Study." Cancer **41**(5): 1937-48.

Beier, D., P. Hau, et al. (2007). "CD133(+) and CD133(-) glioblastoma-derived cancer stem cells show differential growth characteristics and molecular profiles." Cancer Res **67**(9): 4010-5.

Bhattacharjee, M., J. Hicks, et al. (1997). "Central nervous system atypical teratoid/rhabdoid tumors of infancy and childhood." Ultrastruct Pathol **21**(4): 369-78.

Bhattacharjee, M. B., D. D. Armstrong, et al. (1997). "Cytogenetic analysis of 120 primary pediatric brain tumors and literature review." Cancer Genet Cytogenet **97**(1): 39-53.

Biegel, J. A. (1999). "Cytogenetics and molecular genetics of childhood brain tumors." Neuro Oncol **1**(2): 139-51.

Biegel, J. A. (2006). "Molecular genetics of atypical teratoid/rhabdoid tumor." Neurosurg Focus **20**(1): E11.

Biegel, J. A., L, Tan, et al. (2002) "Alterations of the hSNF5/INI1 gene in central nervous system atypical teratoid/rhabdoid tumors and renal and extrarenal rhabdoid tumors." Clin Cancer Res **8**(11): 3467.
Biegel, J. A., L. B. Rorke, et al. (1989). "Isochromosome 17q in primitive neuroectodermal tumors of the central nervous system." Genes Chromosomes Cancer **1**(2): 139-47.
Biegel, J. A., A. J. Janss, et al. (1997). "Prognostic significance of chromosome 17q deletions in childhood primitive neuroectodermal tumours (medulloblastoma) of the central nervous system." Clin Cancer Res **3**(3): 473-8.
Bigner, S. H., H. S. Friedman, et al. (1990). "Amplification of the c-myc gene in human medulloblastoma cell lines and xenografts." Cancer Res **50**(8): 2347-50.
Bigner, S. H., J. Mark, et al. (1988). "Structural chromosomal abnormalities in human medulloblastoma." Cancer Genet Cytogenet **30**(1): 91-101.
Bigner, S. H., R. E. McLendon, et al. (1997). "Chromosomal characteristics of childhood brain tumors." Cancer Genet Cytogenet **97**(2): 125-34.
Birch, J. M., V. Blair, et al. (1998). "Cancer phenotype correlates with constitutional TP53 genotype in families with the Li-Fraumeni syndrome." Oncogene **17**(9): 1061-8.
Brodeut, G. M, R. C. Seeger, et al. (1984). "Amplification of N-myc in untreated human neuroblastomas correlates with advanced disease stage." Science **224**(4653): 1121-4.
Bourdeaut, F., P. Freneaux, et al. (2007). "hSNF5/INI1-deficient tumours and rhabdoid tumours are convergent but not fully overlapping entities." J Pathol **211**(3): 323-30.
Brown, A. E., K. Leibundgut, et al. (2006). "Cytogenetics of pineoblastoma: four new cases and a literature review." Cancer Genet Cytogenet **170**(2): 175-9.
Bruses, J. L. (2000). "Cadherin-mediated adhesion at the interneuronal synapse." Curr Opin Cell Biol **12**(5): 593-7.
Burnett, M. E., E. C. White, et al. (1997). "Chromosome arm 17p deletion analysis reveals molecular genetic heterogeneity in supratentorial and infratentorial primitive neuroectodermal tumors of the central nervous system." Cancer Genet Cytogenet **97**(1): 25-31.
Cairncross, J. G., K, Ueki., et al. (1998). "Specific genetic predictors of chemotherapeutic response and survival in patients with anaplastic oligodendrogliomas." **90**(19): 1473-9.
Canete, A., M. Gerrard, et al. (2009). "Poor survival for infants with MYCN-amplified metastatic neuroblastoma despite intensified treatment: the International Society of Paediatric Oncology European Neuroblastoma Experience." J Clin Oncol **27**(7): 1014-9.
Caren, H., J. Erichsen, et al. (2008). "High-resolution array copy number analyses for detection of deletion, gain, amplification and copy-neutral LOH in primary neuroblastoma tumors: four cases of homozygous deletions of the CDKN2A gene." BMC Genomics **9**: 353.
Carter, M., J. Nicholson, et al. (2002). "Genetic abnormalities detected in ependymomas by comparative genomic hybridisation." Br J Cancer **86**(6): 929-39.
Carvalho, B., E. Ouwerkerk, et al. (2004). "High resolution microarray comparative genomic hybridisation analysis using spotted oligonucleotides." J Clin Pathol **57**(6): 644-6.
Carver, L. A., J. E. Schnitzer, et al. (2003). "Caveolae: mining little caves for new cancer targets." Nat Rev Cancer **3**(8): 571-581.
Chadduck, W. M., F. A. Boop, et al. (1991). "Cytogenetic studies of pediatric brain and spinal cord tumors." Pediatr Neurosurg **17**(2): 57-65.
Chang, C. H., E. M. Housepian, et al. (1969). "An operative staging system and a megavoltage radiotherapeutic technic for cerebellar medulloblastomas." Radiology **93**(6): 1351-9.
Chang, Q., J. C. Pang, et al. (2005). "Promoter hypermethylation profile of RASSF1A, FHIT, and SFRP1 in intracranial primitive neuroectodermal tumors." Hum Pathol **36**(12): 1265-72.

Chen, M. L., J. G. McComb, et al. (2005). "Atypical teratoid/rhabdoid tumors of the central nervous system: management and outcomes." Neurosurg Focus **18**(6A): E8.
Chen, Z. H., H. Zhang, et al. (1996). "Gene deletion chemoselectivity: codeletion of the genes for p16(INK4), methylthioadenosine phosphorylase, and the alpha- and beta-interferons in human pancreatic cell carcinoma lines and its implications for chemotherapy." Cancer Res **56**(5): 1083-90.
Chintagumpala, M., T. Hassall, et al. (2008). "A pilot study of risk adapted radiotherapy and chemotherapy in patients with supratentorial PNET." Neuro Oncol.
Choi, Y. W., S. M. Bae, et al. (2007). "Gene expression profiles in squamous cell cervical carcinoma using array-based comparative genomic hybridization analysis." Int J Gynecol Cancer **17**(3): 687-96.
Clifford, S. C., M. E. Lusher, et al. (2006). "Wnt/Wingless pathway activation and chromosome 6 loss characterize a distinct molecular sub-group of medulloblastomas associated with a favorable prognosis." Cell Cycle **5**(22): 2666-70.
Cogen, P. H. (1991). "Prognostic significance of molecular genetic markers in childhood brain tumors." Pediatr Neurosurg **17**(5): 245-50.
Cogen, P. H., L, Daneshvar, et al. (1992). "Involvement of multiple chromosome 17p loci in medulloblastoma tumorigenesis." Am J Hum Genet **50**(3): 584-9.
Cohen, B. H., P. M. Zeltzer, et al. (1995). "Prognostic factors and treatment results for supratentorial primitive neuroectodermal tumors in children using radiation and chemotherapy: a Childrens Cancer Group randomized trial." J Clin Oncol **13**(7): 1687-96.
Collins, V. P. (1995). "Gene amplification in human gliomas." Glia **15**(3): 289-96.
Copeland, D. R., C. deMoor, et al. (1999). "Neurocognitive development of children after a cerebellar tumor in infancy: A longitudinal study." J Clin Oncol **17**(11): 3476-86.
Corder, E. H., A. M. Saunders, et al. (1993). "Gene dose of apolipoprotein E type 4 allele and the risk of Alzheimer's disease in late onset families." Science **261**(5123): 921-3.
Cowell, J. K., S. Matsui, et al. (2004). "Application of bacterial artificial chromosome array-based comparative genomic hybridization and spectral karyotyping to the analysis of glioblastoma multiforme." Cancer Genet Cytogenet **151**(1): 36-51.
Creutz, C. E., J. l. Tomsig, et al. (1998). "The copines, a novel class of C2 domain-containing, calcium-dependent, phospholipid-binding proteins conserved from Paramecium to humans." J Biol Chem **273**(3): 1393-402.
Dahmane, N. and A. Ruiz i Altaba (1999). "Sonic hedgehog regulates the growth and patterning of the cerebellum." Development **126**(14): 3089-100.
Dahmane, N., P. Sanchez, et al. (2001). "The Sonic Hedgehog-Gli pathway regulates dorsal brain growth and tumorigenesis." Development **128**(24): 5201-12.
Dai, A. I., J. W. Backstrom, et al. (2003). "Supratentorial primitive neuroectodermal tumors of infancy: clinical and radiologic findings." Pediatr Neurol **29**(5): 430-4.
De Potter, P., C. L. Shields, et al. (1994). "Clinical variations of trilateral retinoblastoma: a report of 13 cases." J Pediatr Opthalmol Strabismus **31** (1): 26-31.
De Vos, M., B. E. Hayward, et al. (2004). "Novel PMS2 pseudogenes can conceal recessive mutations causing a distinctive childhood cancer syndrome." Am J Hum Genet **74**(5): 954-64.
Dewire, M. D., D, W, Ellison, et al. (2009). "Fancomi anemia and biallelic *BRCA2* mutation diagnosed in a young child with an embryonal CNS tumor." Pediatr Blood Cancer **53**(6): 1140-2.
Didiano, D., T. Shalaby, et al. (2004). "Telomere maintenance in childhood primitive neuroectodermal brain tumors." Neuro Oncol **6**(1): 1-8.
Dirks, P. B., L. Harris, et al. (1996). "Supratentorial primitive neuroectodermal tumors in children." J Neurooncol **29**(1): 75-84.

Dohrmann, G. J., J. R. Farwell, et al. (1976). "Glioblastoma multiforme in children." J Neurosurg **44**(4): 442-8.
Dong, S., E. Wang, et al. (2001). "Flexible use of high-density oligonucleotide arrays for single-nucleotide polymorphism discovery and validation." Genome Res **11**(8): 1418-24.
Donson, A. M., S. O. Addo-Yobo, et al. (2007). "MGMT promoter methylation correlates with survival benefit and sensitivity to temozolomide in pediatric glioblastoma." Pediatr Blood Cancer **48**(4): 403-7.
Dreyer, W. J. and J. Roman-Dreyer (1999). "Cell-surface area codes: mobile-element related gene switches generate precise and heriTable cell-surface displays of address molecules that are used for constructing embryos." Genetica **107**(1-3): 249-59.
Duffner, P. K., M. E. Horowitz, et al. (1999). "The treatment of malignant brain tumors in infants and very young children: an update of the Pediatric Oncology Group experience." Neuro Oncol **1**(2): 152-61.
Duffner, P. K., M. E. Horowitz, et al. (1993). "Postoperative chemotherapy and delayed radiation in children less than three years of age with malignant brain tumors." N Engl J Med **328**(24): 1725-31.
Duffner, P. K., J. P. Krischer, et al. (1998). "Second malignancies in young children with primary brain tumors following treatment with prolonged postoperative chemotherapy and delayed irradiation: a Pediatric Oncology Group study." Ann Neurol **44**(3): 313-6.
Dupont, W.D., W.D., Plummer. (1990). "Power and sample size calculations : a review and computer program." Controlled clinical trials **11**:116-28.
Dyer, S. (2008). Cytogenetic and Molecular Cytogenetic Characterisation of Paediatric Brain Tumours. Division of Reproductive and Child Health, Birmingham. **PhD**.
Dyer, S., E. Prebble, et al. (2002). "Genomic imbalances in pediatric intracranial ependymomas define clinically relevant groups." Am J Pathol **161**(6): 2133-41.
Easton, D. F., K. A. Pooley, et al. (2007). "Genome-wide association study identifies novel breast cancer susceptibility loci." Nature **447**(7148): 1087-93.
Eberhart, C. G., A. Chaudhry, et al. (2005). "Increased p53 immunopositivity in anaplastic medulloblastoma and supratentorial PNET is not caused by JC virus." BMC Cancer **5**: 19.
Eberhart, C. G., J. L. Kepner, et al. (2002). "Histopathologic grading of medulloblastomas: a Pediatric Oncology Group study." Cancer **94**(2): 552-60.
Eberhart, C. G., J. Kratz, et al. (2004). "Histopathological and molecular prognostic markers in medulloblastoma: c-myc, N-myc, TrkC, and anaplasia." J Neuropathol Exp Neurol **63**(5): 441-9.
Eberhart, C. G., J. E. Kratz, et al. (2002). "Comparative genomic hybridization detects an increased number of chromosomal alterations in large cell/anaplastic medulloblastomas." Brain Pathol **12**(1): 36-44.
Eberhart, C. G., T. Tihan, et al. (2000). "Nuclear localization and mutation of beta-catenin in medulloblastomas." J. Neuropathol Exp Neurol **59**(4): 333-7.
Efferth, T., T. Ramirez, et al. (2004). "Combination treatment of glioblastoma multiforme cell lines with the anti-malarial artesunate and the epidermal growth factor receptor tyrosine kinase inhibitor OSI-774." Biochem Pharmacol **67**(9): 1689-700.
Egger, G., G. Liang, et al. (2004). "Epigenetics in human disease and prospects for epigenetic therapy." Nature **429**(6990): 457-63.
Ellison, D. (2002). "Classifying the medulloblastoma: insights from morphology and molecular genetics." Neuropathol Appl Neurobiol **28**(4): 257-82.
Ellison, D. W., O. E. Onilude, et al. (2005). "beta-Catenin status predicts a favorable outcome in childhood medulloblastoma: the United Kingdom Children's Cancer Study Group Brain Tumour Committee." J Clin Oncol **23**(31): 7951-7.

Emadian, S. M., J. D. McDonald, et al. (1996). "Correlation of chromosome 17p loss with clinical outcome in medulloblastoma." Clin Cancer Res **2**(9): 1559-64.
Esteller, M. (2002). "CpG island hypermethylation and tumor suppressor genes: a booming present, a brighter future." Oncogene **21**(35): 5427-40.
Evans, G., L, Burnell, et al. (1993). "Congenital anomalies and genetic syndromes in 173 cases of medulloblastoma." Med Pediatr Oncol **21**(6): 433-4.
Fan, X., I. Mikolaenko, et al. (2004). "Notch1 and notch2 have opposite effects on embryonal brain tumor growth." Cancer Res **64**(21): 7787-93.
Fan, X., Y. Wang, et al. (2003). "hTERT gene amplification and increased mRNA expression in central nervous system embryonal tumors." Am J Pathol **162**(6): 1763-9.
Fangusaro, J., J. Finlay, et al. (2008). "Intensive chemotherapy followed by consolidative myeloablative chemotherapy with autologous hematopoietic cell rescue (AuHCR) in young children with newly diagnosed supratentorial primitive neuroectodermal tumors (sPNETs): report of the Head Start I and II experience." Pediatr Blood Cancer **50**(2): 312-8.
Farah, C. A., D. Liazoghli, et al. (2005). "Interactions of microtubule-associated protein-2 and p63: a new link between microtubules and rough endoplasmic reticulum membranes in neurons." J Biol Chem **280**(10): 9439-49.
Fernandez, C., C. Bouvier, et al. (2002). "Congenital disseminated malignant rhabdoid tumor and cerebellar tumor mimicking medulloblastoma in monozygotic twins: pathologic and molecular diagnosis." Am J Surg Pathol **26**(2): 266-70.
Fero, M. L., E, Randel, et al. (1998). "p27Kip1 is haplo-insufficient for tumour suppression." Nature **396**(6707): 177-80.
Fitzgibbon, J., S. Iqbal, et al. (2007). "Genome-wide detection of recurring sites of uniparental disomy in follicular and transformed follicular lymphoma." Leukemia **21**(7): 1514-20.
Fix, A., C. Lucchesi, et al. (2008). "Characterization of amplicons in neuroblastoma: high-resolution mapping using DNA microarrays, relationship with outcome, and identification of overexpressed genes." Genes Chromosomes Cancer **47**(10): 819-34.
Fleming, T. P., A. Saxena, et al. (1992). "Amplification and/or overexpression of platelet-derived growth factor receptors and epidermal growth factor receptor in human glial tumors." Cancer Res **52**(16): 4550-3.
Frebourg, T., N. Barbier, et al. (1995). "Germ-line p53 mutations in 15 families with Li-Fraumeni syndrome." Am J Hum Genet **56**(3): 608-15.
Fruhwald, M. C., M. S. O'Dorisio, et al. (2000). "Gene amplification in PNETs/medulloblastomas: mapping of a novel amplified gene within the MYCN amplicon." J Med Genet **37**(7): 501-9.
Fujii, Y., T. Hongo, et al. (1994). "Chromosome analysis of brain tumors in childhood." Genes Chromosomes Cancer **11**(4): 205-15.
Gajjar, A., R, Hernan, et al. (2004). "Clinical, histopathological and molecular markers of prognosis: toward a new disease stratification system for medulloblastoma." J Clin Oncol **22**(6): 984-93.
Gervais, F. G., R. Singaraja, et al. (2002). "Recruitment and activation of caspase-8 by the Huntingtin-interactering protein Hip-1 and novel partner Hippi." Nat Cell Biol **4** 95-105.
Gessi, M., F. Giangaspero, et al. (2003). "Atypical teratoid/rhabdoid tumors and choroid plexus tumors: when genetics "surprise" pathology." Brain Pathol **13**(3): 409-14.
Geyer, J. R., R. Sposto, et al. (2005). "Multiagent chemotherapy and deferred radiotherapy in infants with malignant brain tumors: a report from the Children's Cancer Group." J Clin Oncol **23**(30): 7621-31.
Geyer, J. R., P. M. Zeltzer, et al. (1994). "Survival of infants with primitive neuroectodermal tumors or malignant ependymomas of the CNS treated with eight drugs in 1 day: a report from the Childrens Cancer Group." J Clin Oncol **12**(8): 1607-15.

Giangaspero, F., G. Perilongo, et al. (1999). "Medulloblastoma with extensive nodularity: a variant with favorable prognosis." J Neurosurg **91**(6): 971-7.
Giangaspero, F., L. Rigobello, et al. (1992). "Large-cell medulloblastomas. A distinct variant with highly aggressive behavior." Am J Surg Pathol **16**(7): 687-93.
Gilbertson, R., C. Wickramasinghe, et al. (2001). "Clinical and molecular stratification of disease risk in medulloblastoma." Br J Cancer **85**(5): 705-12.
Gilbertson, R. J. and S. C. Clifford (2003). "PDGFRB is overexpressed in metastatic medulloblastoma." Nat Genet **35**(3): 197-8.
Gilbertson, R. J. and D. W. Ellison (2008). "The origins of medulloblastoma subtypes." Annu Rev Pathol **3**: 341-65.
Gilbertson, R. J. and D. H. Gutmann (2007). "Tumorigenesis in the brain: location, location, location." Cancer Res **67**(12): 5579-82.
Gilheeney, S. W., A. Saad, et al. (2008). "Outcome of pediatric pineoblastoma after surgery, radiation and chemotherapy." J Neurooncol **89**(1): 89-95.
Giroux, V., J. L. Iovanna, et al. (2009). "Combined inhibition of PAK7, MAP3K7 and CK2alpha kinases inhibits the growth of MiaPaCa2 pancreatic cancer cell xenografts." Cancer Gene Ther **16**(9): 731-40.
Goelz, S. E., B, Vogelstein, et al. (1985). "Hypomethylation of DNA from benign and malignant human colon neoplasms." Science **228** (4696): 187-96.
Griffin, C. A., A. L. Hawkins, et al. (1988). "Chromosome abnormalities in pediatric brain tumors." Cancer Res **48**(1): 175-80.
Gupta, M., M. Raghavan, et al. (2008). "Novel regions of acquired uniparental disomy discovered in acute myeloid leukemia." Genes Chromosomes Cancer **47**(9): 729-39.
Haberler, C., U. Laggner, et al. (2006). "Immunohistochemical analysis of INI1 protein in malignant pediatric CNS tumors: Lack of INI1 in atypical teratoid/rhabdoid tumors and in a fraction of primitive neuroectodermal tumors without rhabdoid phenotype." Am J Surg Pathol **30**(11): 1462-8.
Halatsch, M. E., E. E. Gehrke, et al. (2004). "Inverse correlation of epidermal growth factor receptor messenger RNA induction and suppression of anchorage-independent growth by OSI-774, an epidermal growth factor receptor tyrosine kinase inhibitor, in glioblastoma multiforme cell lines." J Neurosurg **100**(3): 523-33.
Halatsch, M. E., U. Schmidt, et al. (2006). "Epidermal growth factor receptor inhibition for the treatment of glioblastoma multiforme and other malignant brain tumours." Cancer Treat Rev **32**(2): 74-89.
Hamilton, R. L. and I. F. Pollack (1997). "The molecular biology of ependymomas." Brain Pathol **7**(2): 807-22.
Hamilton, S. R., B. Liu, et al. (1995). "The molecular basis of Turcot's syndrome." N Engl J Med **332**(13): 839-47.
Harada, K., S. Toyooka, et al. (2002). "Aberrant promoter methylation and silencing of the RASSF1A gene in pediatric tumors and cell lines." Oncogene **21**(27): 4345-9.
Harada, T., C. Chelala, et al. (2008). "Genome-wide DNA copy number analysis in pancreatic cancer using high-density single nucleotide polymorphism arrays." Oncogene **27**(13): 1951-60.
Harasawa, H., Y. Yamada, et al. (2002). "Chemotherapy targeting methylthioadenosine phosphorylase (MTAP) deficiency in adult T cell leukemia (ATL)." Leukemia **16**(9): 1799-807.
Hart, M. N. and K. M. Earle (1973). "Primitive neuroectodermal tumors of the brain in children." Cancer **32**(4): 890-7.
Hayflick, J. S., (2001). " A family of heptahelical receptors with adhesion-like domains: a marriage between two super families." J Recept Sig Transduct Res **20**(2-3): 119-31.
Hegi, M. E., A. C. Diserens, et al. (2005). "MGMT gene silencing and benefit from temozolomide in glioblastoma." N Engl J Med **352**(10): 997-1003.

Hemmati, H. D., I. Nakano, et al. (2003). "Cancerous stem cells can arise from pediatric brain tumors." Proc Natl Acad Sci U S A **100**(25): 15178-83.
Herman, J. G. and S. B. Baylin (2003). "Gene silencing in cancer in association with promoter hypermethylation." N Engl J Med **349**(21): 2042-54.
Herman, J. G., A. Umar, et al. (1998). "Incidence and functional consequences of hMLH1 promoter hypermethylation in colorectal carcinoma." Proc Natl Acad Sci U S A **95**(12): 6870-5.
Hermanson, M., K. Funa, et al. (1996). "Association of loss of heterozygosity on chromosome 17p with high platelet-derived growth factor alpha receptor expression in human malignant gliomas." Cancer Res **56**(1): 164-71.
Herr, A., R. Grutzmann, et al. (2005). "High-resolution analysis of chromosomal imbalances using the Affymetrix 10K SNP genotyping chip." Genomics **85**(3): 392-400.
Hezova, R., J. Ehrmann, et al. (2007). "WWOX, a new potential tumor suppressor gene." Biomed Pap Med Fac Univ Palacky Olomouc Czech Repub **151**(1): 11-5.
Hing, S., Y. J. Lu, et al. (2001). "Gain of 1q is associated with adverse outcome in favorable histology Wilms' tumors." Am J Pathol **158**(2): 393-8.
Hirai, M., S. Yoshida, et al. (1999). "1q23 gain is associated with progressive neuroblastoma resistant to aggressive treatment." Genes Chromosomes Cancer **25**(3): 261-9.
Hirose, Y., K. Aldape, et al. (2001). "Chromosomal abnormalities subdivide ependymal tumors into clinically relevant groups." Am J Pathol **158**(3): 1137-43.
Holtkamp, N., N. Ziegenhagen, et al. (2007). "Characterization of the amplicon on chromosomal segment 4q12 in glioblastoma multiforme." Neuro Oncol **9**(3): 291-7.
Hong, T. S., M. P. Mehta, et al. (2004). "Patterns of failure in supratentorial primitive neuroectodermal tumors treated in Children's Cancer Group Study 921, a phase III combined modality study." Int J Radiat Oncol Biol Phys **60**(1): 204-13.
Hostettler, L., I, Zlobec, et al. (2010). "ABCG5-positivity in tumor buds is an indicator of poor prognosis in node-negative colorectal cancer patients." World J Gastroenterol **16**(6): 732-9.
Hu, N., C. Wang, et al. (2005). "Genome-wide association study in esophageal cancer using GeneChip mapping 10K array." Cancer Res **65**(7): 2542-6.
Hu, X. F., E. Yang, et al. (2006). "MUC1 cytoplasmic tail: a potential therapeutic target for ovarian carcinoma." Expert Rev Anticancer Ther **6**(8): 1261-71.
Huang, J., Y. L. Zhang, et al. (2007). "Down-regulation of SFRP1 as a putative tumor suppressor gene can contribute to human hepatocellular carcinoma." BMC Cancer **7**: 126.
Hussain, D., W, Punjaruk et al. (2010). "Pediatric brain tumor cancer stem cells: cell cycle dynamics, DNA repair and etoposide extrusion." Submitted to Neuro-Oncology
Iafrate, A. J., L. Feuk, et al. (2004). "Detection of large-scale variation in the human genome." Nat Genet **36**(9): 949-51.
Inda, M. M. and J. S. Castresana (2007). "RASSF1A promoter is highly methylated in primitive neuroectodermal tumors of the central nervous system." Neuropathology **27**(4): 341-6.
Inda, M. M., J. Munoz, et al. (2006). "High promoter hypermethylation frequency of p14/ARF in supratentorial PNET but not in medulloblastoma." Histopathology **48**(5): 579-87.
Inda, M. M., C. Perot, et al. (2005). "Genetic heterogeneity in supratentorial and infratentorial primitive neuroectodermal tumours of the central nervous system." Histopathology **47**(6): 631-7.
Ishibashi, M., K. Moriyoshi, et al. (1994). "Persistent expression of helix-loop-helix factor HES-1 prevents mammalian neural differentiation in the central nervous system." EMBO J **13**(8): 1799-805.

Iwao, K., S. Kakaamori, et al. (1998). "Activation of the beta-catenin gene by interstitial deletions involving exon 3 in primary colorectal carcinoma without adenomatous polyposis coli mutations." Cancer Res **58** (5): 1021-6.
Jakacki, R. I., P. M. Zeltzer, et al. (1995). "Survival and prognostic factors following radiation and/or chemotherapy for primitive neuroectodermal tumors of the pineal region in infants and children: a report of the Childrens Cancer Group." J Clin Oncol **13**(6): 1377-83.
Janson, K., L. A. Nedzi, et al. (2006). "Predisposition to atypical teratoid/rhabdoid tumor due to an inherited INI1 mutation." Pediatr Blood Cancer **47**(3): 279-84.
Jenner, M. W., P. E. Leone, et al. (2007). "Gene mapping and expression analysis of 16q loss of heterozygosity identifies WWOX and CYLD as being important in determining clinical outcome in multiple myeloma." Blood **110**(9): 3291-300.
Johnson, N. A., R. A. Hamoudi, et al. (2006). "Application of array CGH on archival formalin-fixed paraffin-embedded tissues including small numbers of microdissected cells." Lab Invest **86**(9): 968-78.
Johnston, D. L., D. Keene, et al. (2009). "Medulloblastoma in children under the age of three years: a retrospective Canadian review." J Neurooncol.
Johnston, D. L., D. L. Keene, et al. (2008). "Supratentorial primitive neuroectodermal tumors: a Canadian pediatric brain tumor consortium report." J Neurooncol **86**(1): 101-8.
Jones, D. T., K. Ichimura, et al. (2006). "Genomic analysis of pilocytic astrocytomas at 0.97 Mb resolution shows an increasing tendency toward chromosomal copy number change with age." J Neuropathol Exp Neurol **65**(11): 1049-58.
Jones, P. A. and P. W. Laird (1999). "Cancer epigenetics comes of age." Nat Genet **21**(2): 163-7.
Judkins, A. R., J. Mauger, et al. (2004). "Immunohistochemical analysis of hSNF5/INI1 in pediatric CNS neoplasms." Am J Surg Pathol **28**(5): 644-50.
Kagawa, N., M. Maruno, et al. (2006). "Detection of genetic and chromosomal aberrations in medulloblastomas and primitive neuroectodermal tumors with DNA microarrays." Brain Tumor Pathol **23**(1): 41-7.
Kallioniemi, A., O. P. Kallioniemi, et al. (1992). "Comparative genomic hybridization for molecular cytogenetic analysis of solid tumors." Science **258**(5083): 818-21.
Kane, M. F., M. Loda, et al. (1997). "Methylation of the hMLH1 promoter correlates with lack of expression of hMLH1 in sporadic colon tumors and mismatch repair-defective human tumor cell lines." Cancer Res **57**(5): 808-11.
Karpf, A. R. (2007). "Epigenomic reactivation screening to identify genes silenced by DNA hypermethylation in human cancer." Curr Opin Mol Ther **9**(3): 231-41.
Kim, D. G., D. Y. Lee, et al. (2002). "Supratentorial primitive neuroectodermal tumors in adults." J Neurooncol **60**(1): 43-52.
King, R. (2000). Cancer Biology, Pearson Education Limited.
Kleihues, P., P. C. Burger, et al. (1993). "The new WHO classification of brain tumours." Brain Pathol **3**(3): 255-68.
Kleihues, P., Cavenee, W. (2000). Tumours of the Nervous System, IARC.
Kleihues, P., D. N. Louis, et al. (2002). "The WHO classification of tumors of the nervous system." J Neuropathol Exp Neurol **61**(3): 215-25; discussion 226-9.
Knudson, A. G., Jr. (1971). "Mutation and cancer: statistical study of retinoblastoma." Proc Natl Acad Sci U S A **68**(4): 820-3.
Koch, A., D. Denkhaus, et al. (1999). "Childhood hepatoblastomas frequently carry a mutated degradation targeting box of the beta-catenin gene." Cancer Res **59**(2): 269-73.
Koch, A., A. Waha, et al. (2001). "Somatic mutations of WNT/wingless signaling pathway components in primitive neuroectodermal tumors." Int J Cancer **93**(3): 445-9.

Koesters, R., R. Ridder, et al. (1999). "Mutational activation of the beta-catenin proto-oncogene is a common event in the development of Wilm's tumors." Cancer Res **59**(16): 3880-2.
Kohl, N. E., C. E. Gee, et al. (1984). "Activated expression of the N-myc gene in human neuroblastomas and related tumors." Science **226**(4680): 1335-7.
Korshunov, A., A. Benner, et al. (2008). "Accumulation of genomic aberrations during clinical progression of medulloblastoma." Acta Neuropathol **116**(4): 383-90.
Kotliarov, Y., M. E. Steed, et al. (2006). "High-resolution global genomic survey of 178 gliomas reveals novel regions of copy number alteration and allelic imbalances." Cancer Res **66**(19): 9428-36.
Kraus, J. A., J. Felsberg, et al. (2002). "Molecular genetic analysis of the TP53, PTEN, CDKN2A, EGFR, CDK4 and MDM2 tumour-associated genes in supratentorial primitive neuroectodermal tumours and glioblastomas of childhood." Neuropathol Appl Neurobiol **28**(4): 325-33.
Kuhl, J. (1998). "Modern treatment strategies in medulloblastoma." Childs Nerv Syst **14**(1-2): 2-5.
Kuhn, S. A., U. K. Hanisch, et al. (2007). "A paediatric supratentorial primitive neuroectodermal tumour associated with malignant astrocytic transformation and a clonal origin of both components." Neurosurg Rev **30**(2): 143-9; discussion 149.
Kumar, K. S., J. Sonnemann, et al. (2006). "Histone deacetylase inhibitors induce cell death in supratentorial primitive neuroectodermal tumor cells." Oncol Rep **16**(5): 1047-52.
Ladd-Acosta, C., J. Pevsner, et al. (2007). "DNA methylation signatures within the human brain." Am J Hum Genet **81**(6): 1304-15.
Lamlum, H., M. Ilyas, et al. (1999). "The type of somatic mutation at APC in familial adenomatous polyposis is determined by the site of the germline mutation: a new facet to Knudson's 'two-hit' hypothesis." Nat Med **5**(9): 1071-5.
Lamont, J. M., C. S. McManamy, et al. (2004). "Combined histopathological and molecular cytogenetic stratification of medulloblastoma patients." Clin Cancer Res **10**(16): 5482-93.
Lander, E. S., L. M. Linton, et al. (2001). "Initial sequencing and analysis of the human genome." Nature **409**(6822): 860-921.
Lannering, B., I. Marky, et al. (1990). "Long-term sequelae after pediatric brain tumors: their effect on disability and quality of life." Med Pediatr Oncol **18**(4): 304-10.
Larsen, W. (1993). Human Embryology. The fourth week. Churchill Livingstone, New York.
Larsen, W. (1993). Human Embryology. The development of the brain and cranial nerves. Churchill Livingstone, New York.
Lasser, D. M., D. C. DeVivo, et al. (1994). "Turcot's syndrome: evidence for linkage to the adenomatous polyposis coli (APC) locus." Neurology **44**(6): 1083-6.
Lee, K., M. Li, C. Eberhart, C. Lau, S. Pomeroy, P. Collins, P. Modena, A. Gajjar, E. Bouffet, M. Taylor, C. Hawkins, A. Huang. (2008). High resolution genomic analysis identifies distinct groups of pediatric supratentorial primitive neuroectodermal tumors. ISPNO. Chicago.
Lee, Y., H. L. Miller, et al. (2003). "A molecular fingerprint for medulloblastoma." Cancer Res **63**(17): 5428-37.
Li, M. H., E. Bouffet, et al. (2005). "Molecular genetics of supratentorial primitive neuroectodermal tumors and pineoblastoma." Neurosurg Focus **19**(5): E3.
Li, Y. and P. J. Cozzi (2007). "MUC1 is a promising therapeutic target for prostate cancer therapy." Curr Cancer Drug Targets **7**(3): 259-71.
Liu, A., B. Wang, et al. (2005). "Mouse intraflagellar transport proteins regulate both the activator and repressor functions of Gli transcription factors." Development **132** 3103-3111.

Lindsey, J. C., M. E. Lusher, et al. (2006). "Epigenetic inactivation of MCJ (DNAJD1) in malignant paediatric brain tumours." Int J Cancer **118**(2): 346-52.
Ling, V. (1997). "Multidrug resistance: molecular mechanisms and clinical relevance." Cancer Chemother Pharmacol **40**(Suppl): S3 - S8.
Lo, K. C., M. R. Rossi, et al. (2007). "Genome wide copy number abnormalities in pediatric medulloblastomas as assessed by array comparative genome hybridization." Brain Pathol **17**(3): 282-96.
Louis, D. N., H. Ohgaki, O. Wiestler, W. Cavenee. (2007). WHO Classification of Tumours of the Central Nervous System, IARC.
Louis, D. N., H. Ohgaki, et al. (2007). "The 2007 WHO classification of tumours of the central nervous system." Acta Neuropathol **114**(2): 97-109.
Lusher, M. E., J. C. Lindsey, et al. (2002). "Biallelic epigenetic inactivation of the RASSF1A tumor suppressor gene in medulloblastoma development." Cancer Res **62**(20): 5906-11.
MacDonald, T. J., K. M. Brown, et al. (2001). "Expression profiling of medulloblastoma: PDGFRA and the RAS/MAPK pathway as therapeutic targets for metastatic disease." Nat Genet **29**(2): 143-52.
MacDonald, T. J., B. R. Rood, et al. (2003). "Advances in the diagnosis, molecular genetics, and treatment of pediatric embryonal CNS tumors." Oncologist **8**(2): 174-86.
Makoff, A., C. Pilling, et al. (1997). "Human metabotropic glutamate receptor type 7: molecular cloning and mRNA distribution in the CNS." Brain Res Mol Brain Res **40**(1): 165-70.
Malkin, D., F. P. Li, et al. (1990). "Germ line p53 mutations in a familial syndrome of breast cancer, sarcomas, and other neoplasms." Science **250**(4985): 1233-8.
Marec-Berard, P., A. Jouvet, et al. (2002). "Supratentorial embryonal tumors in children under 5 years of age: an SFOP study of treatment with postoperative chemotherapy alone." Med Pediatr Oncol **38**(2): 83-90.
Marino, S., M. Vooijs, et al. (2000). "Induction of medulloblastomas in p53-null mutant mice by somatic inactivation of Rb in the external granular layer cells of the cerebellum." Genes Dev **14**(8): 994-1004.
Mason, W. P., A. Grovas, et al. (1998). "Intensive chemotherapy and bone marrow rescue for young children with newly diagnosed malignant brain tumors." J Clin Oncol **16**(1): 210-21.
Matallanas, D., D. Romano, et al. (2007). "RASSF1A elicits apoptosis through an MST2 pathway directing proapoptotic transcription by the p73 tumor suppressor protein." Mol Cell **27**(6): 962-75.
Matsumoto, F., H. Fujii, et al. (2006). "A novel tumor marker, Niban, is expressed in subsets of thyroid tumors and Hashimoto's thyroiditis." Hum Pathol **37**(12): 1592-600.
McBride, S. M., S. M. Daganzo, et al. (2008). "Radiation is an Important Component of Multimodality Therapy for Pediatric Non-Pineal Supratentorial Primitive Neuroectodermal Tumors." Int J Radiat Oncol Biol Phys.
McCabe, M. G., K. Ichimura, et al. (2006). "High-resolution array-based comparative genomic hybridization of medulloblastomas and supratentorial primitive neuroectodermal tumors." J Neuropathol Exp Neurol **65**(6): 549-61.
McKinney, P. A. (2004). "Brain tumours: incidence, survival, and aetiology." J Neurol Neurosurg Psychiatry **75 Suppl 2**: ii12-7.
McManamy, C. S., J. M. Lamont, et al. (2003). "Morphophenotypic variation predicts clinical behavior in childhood non-desmoplastic medulloblastomas." J Neuropathol Exp Neurol **62**(6): 627-32.
McManamy, C. S., J. Pears, et al. (2007). "Nodule formation and desmoplasia in medulloblastomas-defining the nodular/desmoplastic variant and its biological behavior." Brain Pathol **17**(2): 151-64.

McNeil, D. E., T. R. Cote, et al. (2002). "Incidence and trends in pediatric malignancies medulloblastoma/primitive neuroectodermal tumor: a SEER update. Surveillance Epidemiology and End Results." Med Pediatr Oncol **39**(3): 190-4.
Mendrzyk, F., A. Korshunov, et al. (2006). "Identification of gains on 1q and epidermal growth factor receptor overexpression as independent prognostic markers in intracranial ependymoma." Clin Cancer Res **12**(7 Pt 1): 2070-9.
Mendrzyk, F., B. Radlwimmer, et al. (2005). "Genomic and protein expression profiling identifies CDK6 as novel independent prognostic marker in medulloblastoma." J Clin Oncol **23**(34): 8853-62.
Merchant, T. E., C. Li, et al. (2009). "Conformal radiotherapy after surgery for paediatric ependymoma: a prospective study." Lancet Oncol **10**(3): 258-66.
Merlo, A., J. G. Herman, et al. (1995). "5' CpG island methylation is associated with transcriptional silencing of the tumour suppressor p16/CDKN2/MTS1 in human cancers." Nat Med **1**(7): 686-92.
Mertens, F., B. Johansson, et al. (1994). "Isochromosomes in neoplasia." Genes Chromosomes Cancer **10**(4): 221-30.
Michiels, E. M., M. M. Weiss, et al. (2002). "Genetic alterations in childhood medulloblastoma analyzed by comparative genomic hybridization." J Pediatr Hematol Oncol **24**(3): 205-10.
Minard, V., O. Hartmann, et al. (2000). "Adverse outcome of infants with metastatic neuroblastoma, MYCN amplification and/or bone lesions: results of the French society of pediatric oncology." Br J Cancer **83**(8): 973-9.
Miyaki, M., M. Konishi, et al. (1994). "Characteristics of somatic mutation of the adenomatous polyposis coli gene in colorectal tumors." Cancer Res **54**(11): 3011-20.
Molloy, P. T., A. T. Yachnis, et al. (1996). "Central nervous system medulloepithelioma: a series of eight cases including two arising in the pons." J Neurosurg **84**(3): 430-6.
Momota, H., A. H. Shih, et al. (2008). "c-Myc and beta-catenin cooperate with loss of p53 to generate multiple members of the primitive neuroectodermal tumor family in mice." Oncogene **27**(32): 4392-401.
Momparler, R. L. and V. Boveni. (2000). "DNA methylation and cancer." J Cell Physiol **183** (2): 145-54.
Morin, P., A. B. Sparks, et al. (1997). "Activation of beta-catenin-Tcf signalling in colon cancer by mutations in beta-catenin or APC." Science **275** (5307): 1787-90.
Morishita, H., T. Yagi, et al. (2007). "Protocadherin family: diversity, structure and function." Curr Opin Biol **19**: 584-592.
Muhlisch, J., T. Bajanowski, et al. (2007). "Frequent but borderline methylation of p16 (INK4a) and TIMP3 in medulloblastoma and sPNET revealed by quantitative analyses." J Neurooncol **83**(1): 17-29.
Muhlisch, J., A. Schwering, et al. (2006). "Epigenetic repression of RASSF1A but not CASP8 in supratentorial PNET (sPNET) and atypical teratoid/rhabdoid tumors (AT/RT) of childhood." Oncogene **25**(7): 1111-7.
Mulhern, R. K., T. E. Merchant, et al. (2004). "Late neurocognitive sequelae in survivors of brain tumours in childhood." Lancet Oncol **5**(7): 399-408.
Murone, M., A. Rosenthal, et al. (1999). "Sonic hedgehog signaling by the patched-smoothened receptor complex." Curr Biol **9**(2): 76-84.
Nannya, Y., M. Sanada, et al. (2005). "A robust algorithm for copy number detection using high-density oligonucleotide single nucleotide polymorphism genotyping arrays." Cancer Res **65**(14): 6071-9.
Neben, K., A. Korshunov, et al. (2004). "Microarray-based screening for molecular markers in medulloblastoma revealed STK15 as independent predictor for survival." Cancer Res **64**(9): 3103-11.

Ng, I. O., Z. D. Liang, et al. (2000). "DLC-1 is deleted in primary hepatocellular carcinoma and exerts inhibitory effects on the proliferation of hepatoma cell lines with deleted DLC-1." Cancer Res **60**(23): 6581-4.
Nicholson, J. C., F. M. Ross, et al. (1999). "Comparative genomic hybridization and histological variation in primitive neuroectodermal tumours." Br J Cancer **80**(9): 1322-31.
Nisen, P. D., P. G. Waber, et al. (1988). "N-myc oncogene RNA expression in neuroblastoma." J Natl Cancer Inst **80**(20): 1633-7.
Norris, L. S., S. Snodgrass, et al. (2005). "Recurrent central nervous system medulloepithelioma: response and outcome following marrow-ablative chemotherapy with stem cell rescue." J Pediatr Hematol Oncol **27**(5): 264-6.
Northcott, P. A., Y. Nakahara, et al. (2009). "Multiple recurrent genetic events converge on control of histone lysine methylation in medulloblastoma." Nat Genet **41**(4): 465-72.
Nowell, P. C. and D. A. Hungerford (1960). "Chromosome studies on normal and leukemic human leukocytes." J Natl Cancer Inst **25**: 85-109.
O'Shea, D., C. O'Riain, et al. (2009). "Regions of acquired uniparental disomy at diagnosis of follicular lymphoma are associated with both overall survival and risk of transformation." Blood **113**(10): 2298-301.
Ogasawara, N., T, Tsukamoto, et al. (2006). "Mutations and nucleic accumulation of beta-catenin correlate with intestinal phenotype expression in human gastric cancer." Histopathology **49** (6): 612-21.
Ohba, S., K. Yoshida, et al. (2008). "A supratentorial primitive neuroectodermal tumor in an adult: a case report and review of the literature." J Neurooncol **86**(2): 217-24.
Ohgaki, H., P. Dessen, et al. (2004). "Genetic pathways to glioblastoma: a population-based study." Cancer Res **64**(19): 6892-9.
Ohgaki, H., R. H. Eibl, et al. (1993). "Mutations of the p53 tumor suppressor gene in neoplasms of the human nervous system." Mol Carcinog **8**(2): 74-80.
Ohgaki, H., R. H. Eibl, et al. (1991). "p53 mutations in nonastrocytic human brain tumors." Cancer Res **51**(22): 6202-5.
Oyharcabal-Bourden, V., C. Kalifa, et al. (2005). "Standard-risk medulloblastoma treated by adjuvant chemotherapy followed by reduced-dose craniospinal radiation therapy: a French Society of Pediatric Oncology Study." J Clin Oncol **23**(21): 4726-34.
Ozaki, T., M. Paulussen, et al. (2001). "Genetic imbalances revealed by comparative genomic hybridization in Ewing tumors." Genes Chromosomes Cancer **32**(2): 164-71.
Packer, R. J., J. A. Biegel, et al. (2002). "Atypical teratoid/rhabdoid tumor of the central nervous system: report on workshop." J Pediatr Hematol Oncol **24**(5): 337-42.
Pan, E., M. Pellarin, et al. (2005). "Isochromosome 17q is a negative prognostic factor in poor-risk childhood medulloblastoma patients." Clin Cancer Res **11**(13): 4733-40.
Pang, J. C., Q. Chang, et al. (2005). "Epigenetic inactivation of DLC-1 in supratentorial primitive neuroectodermal tumor." Hum Pathol **36**(1): 36-43.
Parnavelas, J. G. and B. Nadarajah (2001). "Radial glial cells. are they really glia?" Neuron **31**(6): 881-4.
Paulino, A. C. and E. Melian (1999). "Medulloblastoma and supratentorial primitive neuroectodermal tumors: an institutional experience." Cancer **86**(1): 142-8.
Pelengaris, S. (2007). "The molecular biology of cancer." Oxford, Blackwell.
Pfaffl, M. W. (2001). "A new mathematical model for relative quantification in real-time RT-PCR." Nucleic Acids Res **29**(9): e45.
Pfister, S., M. Remke, et al. (2007). "Supratentorial primitive neuroectodermal tumors of the central nervous system frequently harbor deletions of the CDKN2A locus and other genomic aberrations distinct from medulloblastomas." Genes Chromosomes Cancer **46**(9): 839-51.

Pfister, S., M. Remke, et al (2009). "Outcome prediction in pediatric medulloblastoma based on DNA copy-number aberrations of chromosomes 6q and 17q and the MYC and MYCN loci." J Clin Oncol **27**(10): 1627-36.
Pietsch, T., A. Waha, et al. (1997). "Medulloblastomas of the desmoplastic variant carry mutations of the human homologue of Drosophila patched." Cancer Res **57**(11): 2085-8.
Pimenta, F. J., G. T. Cordeiro, et al. (2008). "Molecular alterations in the tumor suppressor gene WWOX in oral leukoplakias." Oral Oncol **44**(8): 753-8.
Pizer, B. L., C. L. Weston, et al. (2006). "Analysis of patients with supratentorial primitive neuro-ectodermal tumours entered into the SIOP/UKCCSG PNET 3 study." Eur J Cancer **42**(8): 1120-8.
Pomeroy, S. L., P. Tamayo, et al. (2002). "Prediction of central nervous system embryonal tumour outcome based on gene expression." Nature **415**(6870): 436-42.
Postovsky, S., M. W. Ben Arush, et al. (2003). "A novel case of a CAT to AAT transversion in codon 179 of the p53 gene in a supratentorial primitive neuroectodermal tumor harbored by a young girl. Case report and review of the literature." Oncology **65**(1): 46-51.
Proust, F., A. Laquerriere, et al. (1999). "Simultaneous presentation of atypical teratoid/rhabdoid tumor in siblings." J Neurooncol **43**(1): 63-70.
Puget, S., J, Grill, et al. (2009). "Candidate genes on chromosome 9q33-34 involved in the progression of childhood ependymomas." J Clin Oncol **27**(11): 1884 - 92.
Puputti, M., O. Tynninen, et al. (2006). "Amplification of KIT, PDGFRA, VEGFR2, and EGFR in gliomas." Mol Cancer Res **4**(12): 927-34.
Raffel, C., R. B. Jenkins, et al. (1997). "Sporadic medulloblastomas contain PTCH mutations." Cancer Res **57**(5): 842-5.
Raghavan, M., L. L. Smith, et al. (2008). "Segmental uniparental disomy is a commonly acquired genetic event in relapsed acute myeloid leukemia." Blood **112**(3): 814-21.
Raizer, J. J. (2005). "HER1/EGFR tyrosine kinase inhibitors for the treatment of glioblastoma multiforme." J Neurooncol **74**(1): 77-86.
Ramos, D. and C. M. Aldaz (2006). "WWOX, a chromosomal fragile site gene and its role in cancer." Adv Exp Med Biol **587**: 149-59.
Reardon, D. A., E. Michalkiewicz, et al. (1997). "Extensive genomic abnormalities in childhood medulloblastoma by comparative genomic hybridization." Cancer Res **57**(18): 4042-7.
Reddy, A. T., A. J. Janss, et al. (2000). "Outcome for children with supratentorial primitive neuroectodermal tumors treated with surgery, radiation, and chemotherapy." Cancer **88**(9): 2189-93.
Reifenberger, J., G. Janssen, et al. (1998). "Primitive neuroectodermal tumors of the cerebral hemispheres in two siblings with TP53 germline mutation." J Neuropathol Exp Neurol **57**(2): 179-87.
Reifenberger, J., M. Wolter, et al. (1998). "Missense mutations in SMOH in sporadic basal cell carcinomas of the skin and primitive neuroectodermal tumors of the central nervous system." Cancer Res **58**(9): 1798-803.
Reifenberger, J., G, Reifenberger, et al. (1994). "Molecular genetic analysis of oligodendroglial tumors shows preferential allelic deletions on 19q and 1p." **145**(5): 1175-90.
Rickert, C. H. and W. Paulus (2004). "Comparative genomic hybridization in central and peripheral nervous system tumors of childhood and adolescence." J Neuropathol Exp Neurol **63**(5): 399-417.
Rickert, C. H., R. Simon, et al. (2001). "Comparative genomic hybridization in pineal parenchymal tumors." Genes Chromosomes Cancer **30**(1): 99-104.

Ries, L. A., M. A. Smith (1999). Cancer Incidence and Survival among Children and Adolescents: United States SEER Program 1975-1995.
Riva, D. and C. Giorgi (2000). "The neurodevelopmental price of survival in children with malignant brain tumours." Childs Nerv Syst **16**(10-11): 751-4.
Roberts, P., P. D. Chumas, et al. (2001). "A review of the cytogenetics of 58 pediatric brain tumors." Cancer Genet Cytogenet **131**(1): 1-12.
Rogers, H. A., S. Miller, et al. (2009). "An investigation of WNT pathway activation and association with survival in central nervous system primitive neuroectodermal tumours (CNS PNET)." Br J Cancer **100**(8): 1292-302.
Romer, J. T., H. Kimura, et al. (2004). "Suppression of the Shh pathway using a small molecule inhibitor eliminates medulloblastoma in Ptc1(+/-)p53(-/-) mice." Cancer Cell **6**(3): 229-40.
Rong, R., W. Jin, et al. (2004). "Tumor suppressor RASSF1A is a microtubule-binding protein that stabilizes microtubules and induces G2/M arrest." Oncogene **23**(50): 8216-30.
Rorke, L. B. (1983). "The cerebellar medulloblastoma and its relationship to primitive neuroectodermal tumors." J Neuropathol Exp Neurol **42**(1): 1-15.
Rorke, L. B., R. J. Packer, et al. (1996). "Central nervous system atypical teratoid/rhabdoid tumors of infancy and childhood: definition of an entity." J Neurosurg **85**(1): 56-65.
Rorke, L. B., J. Q. Trojanowski, et al. (1997). "Primitive neuroectodermal tumors of the central nervous system." Brain Pathol **7**(2): 765-84.
Rossi, M. R., J. Conroy, et al. (2006). "Array CGH analysis of pediatric medulloblastomas." Genes Chromosomes Cancer **45**(3): 290-303.
Rostomily, R. C., O. Bermingham-McDonogh, et al. (1997). "Expression of neurogenic basic helix-loop-helix genes in primitive neuroectodermal tumors." Cancer Res **57**(16): 3526-31.
Rousseau, E., M. M. Ruchoux, et al. (2003). "CDKN2A, CDKN2B and p14ARF are frequently and differentially methylated in ependymal tumours." Neuropathol Appl Neurobiol **29**(6): 574-83.
Rowley, J. D. (1973). "Letter: A new consistent chromosomal abnormality in chronic myelogenous leukaemia identified by quinacrine fluorescence and Giemsa staining." Nature **243**(5405): 290-3.
Russo, C., M. Pellarin, et al. (1999). "Comparative genomic hybridization in patients with supratentorial and infratentorial primitive neuroectodermal tumors." Cancer **86**(2): 331-9.
Sakariassen, P. O., H., Immervoll et al. (2007). "Cancer stem cells as mediators of treatment resistance in brain tumors: status and controversies." Neoplasia **9** (11): 882-92.
Sarkar, C., P. Deb, et al. (2005). "Recent advances in embryonal tumours of the central nervous system." Childs Nerv Syst **21**(4): 272-93.
Sari, N., C, Akyuz et al. (2009). "Wilms tumor, AML and medulloblastoma in a child with cancer prone syndrome of total premature chromatid separation and Fancomi anemia." Pediatr Blood Cancer **53**(2): 208-10.
Sawyer, J. R., G. Sammartino, et al. (2003). "Constitutional t(16;22)(p13.3;q11.2 approximately 12) in a primitive neuroectodermal tumor of the pineal region." Cancer Genet Cytogenet **142**(1): 73-6.
Scheurlen, W. G., G. C. Schwabe, et al. (1998). "Molecular analysis of childhood primitive neuroectodermal tumors defines markers associated with poor outcome." J Clin Oncol **16**(7): 2478-85.
Schindler, T., W. Bornmann, et al. (2000). "Structural mechanism for STI-571 inhibition of abelson tyrosine kinase." Science **289**(5486): 1938-42.
Schinkel, A. H. (1999). "P-Glycoprotein, a gatekeeper in the blood-brain barrier." Adv Drug Deliv Rev **36**(2-3): 179-194.

Schlosser, S., S, Wagner, et al. (2010). "MGMT as a potential stratification marker in relasped high-grade glioma of children: the HIT-GBM experience." Pediatr Blood Cancer **54**(2): 228-37.
Schmitz, U., W. Mueller, et al. (2001). "INI1 mutations in meningiomas at a potential hotspot in exon 9." Br J Cancer **84**(2): 199-201.
Scotting, P. J., V. Appleby. (2004). Neuroembryology. Brain and spinal tumours of childhood. D. Walker, J. Punt and R. Taylor, London, Arnold.
Scotting, P. J., D. A. Walker, et al. (2005). "Childhood solid tumours: a developmental disorder." Nat Rev Cancer **5**(6): 481-8.
Sebat, J., B. Lakshmi, et al. (2004). "Large-scale copy number polymorphism in the human genome." Science **305**(5683): 525-8.
Seeger, R. C., R. Wada, et al. (1988). "Expression of N-myc by neuroblastomas with one or multiple copies of the oncogene." Prog Clin Biol Res **271**: 41-9.
Sevenet, N., E. Sheridan, et al. (1999). "Constitutional mutations of the hSNF5/INI1 gene predispose to a variety of cancers." Am J Hum Genet **65**(5): 1342-8.
Shaffer, L. G., Slovak, M. L., Campbell, L. J. (2009) "ISCN: International system for human cytogenetic nomenclature." Karger.
Shapiro, L. and D. R. Colman (1999). "The diversity of cadherins and implications for a synaptic adhesive code in the CNS." Neuron **23**(3): 427-30.
Sharma, M. C., A. K. Mahapatra, et al. (1998). "Pigmented medulloepithelioma: report of a case and review of the literature." Childs Nerv Syst **14**(1-2): 74-8.
Sharma, M. K., D. B. Mansur, et al. (2007). "Distinct genetic signatures among pilocytic astrocytomas relate to their brain region origin." Cancer Res **67**(3): 890-900.
Shinojima, N., K. Tada, et al. (2003). "Prognostic value of epidermal growth factor receptor in patients with glioblastoma multiforme." Cancer Res **63**(20): 6962-70.
Shivakumar, L., J. Minna, et al. (2002). "The RASSF1A tumor suppressor blocks cell cycle progression and inhibits cyclin D1 accumulation." Mol Cell Biol **22**(12): 4309-18.
Shridhar, V., K. C. Bible, et al. (2001). "Loss of expression of a new member of the DNAJ protein family confers resistance to chemotherapeutic agents used in the treatment of ovarian cancer." Cancer Res **61**(10): 4258-65.
Sihto, H., M. Sarlomo-Rikala, et al. (2005). "KIT and platelet-derived growth factor receptor alpha tyrosine kinase gene mutations and KIT amplifications in human solid tumors." J Clin Oncol **23**(1): 49-57.
Simpkins, S. B., T. Bocker, et al. (1999). "MLH1 promoter methylation and gene silencing is the primary cause of microsatellite instability in sporadic endometrial cancers." Hum Mol Genet **8**(4): 661-6.
Singh, S. K., I. D. Clarke, et al. (2003). "Identification of a cancer stem cell in human brain tumors." Cancer Res **63**(18): 5821-8.
Singh, S. K., C. Hawkins, et al. (2004). "Identification of human brain tumour initiating cells." Nature **432**(7015): 396-401.
Slater, H. R., D. K. Bailey, et al. (2005). "High-resolution identification of chromosomal abnormalities using oligonucleotide arrays containing 116,204 SNPs." Am J Hum Genet **77**(5): 709-26.
Slatter, R. E., M. Elliott, et al. (1994). "Mosaic uniparental disomy in Beckwith-Wiedemann syndrome." J Med Genet **31**(10): 749-53.
Slavc, I., R. Ellenbogen, et al. (1990). "myc gene amplification and expression in primary human neuroblastoma." Cancer Res **50**(5): 1459-63.
Spiegler, B. J., E. Bouffet, et al. (2004). "Change in neurocognitive functioning after treatment with cranial radiation in childhood." J Clin Oncol **22**(4): 706-13.
Spirio, L. N., W. Samowitz, et al. (1998). "Alleles of APC modulate the frequency and classes of mutations that lead to colon polyps." Nat Genet **20**(4): 385-8.

Spoudeaus, H. a. F. J. K. (2004). Toxicity and late effects. Brain and spinal tumours of childhood. A. G. P. D. Walker, J. Punt and R. Taylor, London, Arnold.
Sreekantaiah, C., H. Jockin, et al. (1989). "Interstitial deletion of chromosome 11q in a pineoblastoma." Cancer Genet Cytogenet **39**(1): 125-31.
Sriuranpong, V., M. W. Borges, et al. (2002). "Notch signaling induces rapid degradation of achaete-scute homolog 1." Mol Cell Biol **22**(9): 3129-39.
Stea, B., R. Falsey, et al. (2003). "Time and dose-dependent radiosensitization of the glioblastoma multiforme U251 cells by the EGF receptor tyrosine kinase inhibitor ZD1839 ('Iressa')." Cancer Lett **202**(1): 43-51.
Steinberg, M. S. and P. M. McNutt (1999). "Cadherins and their connections: adhesion junctions have broader functions." Curr Opin Cell Biol **11**(5): 554-60.
Stiller, C. A. (2004). "Epidemiology and genetics of childhood cancer." Oncogene **23**(38): 6429-44.
Stiller, C. A. and K. J. Bunch (1992). "Brain and spinal tumours in children aged under two years: incidence and survival in Britain, 1971-85." Br J Cancer Suppl **18**: S50-3.
Stoehr, R., C. Wissmann, et al. (2004). "Deletions of chromosome 8p and loss of SFRP1 expression are progression markers of papillary bladder cancer." Lab Invest **84**(4): 465-78.
Sung, K. W., K. H. Yoo, et al. (2007). "High-dose chemotherapy and autologous stem cell rescue in children with newly diagnosed high-risk or relapsed medulloblastoma or supratentorial primitive neuroectodermal tumor." Pediatr Blood Cancer **48**(4): 408-15.
Suzuki, A., G. Kusakai, et al. (2003). "Identification of a novel protein kinase mediating Akt survival signalling to the ATM protein." J Biol Chem **278**(1): 48-53.
Suzuki, M., M. Kato, et al. (2008). "Whole-genome profiling of chromosomal aberrations in hepatoblastoma using high-density single-nucleotide polymorphism genotyping microarrays." Cancer Sci **99**(3): 564-70.
Tamarin, R. (2002). Prinicples of Genetics, McGraw-Hill.
Taylor, M. D., N. Gokgoz, et al. (2000). "Familial posterior fossa brain tumors of infancy secondary to germline mutation of the hSNF5 gene." Am J Hum Genet **66**(4): 1403-6.
Taylor, M. D., H. Poppleton, et al. (2005). "Radial glia cells are candidate stem cells of ependymoma." Cancer Cell **8**(4): 323-35.
Tekautz, T. M., C. E. Fuller, et al. (2005). "Atypical teratoid/rhabdoid tumors (ATRT): improved survival in children 3 years of age and older with radiation therapy and high-dose alkylator-based chemotherapy." J Clin Oncol **23**(7): 1491-9.
Thompson, E. R., S. C. Herbert, et al. (2005). "Whole genome SNP arrays using DNA derived from formalin-fixed, paraffin-embedded ovarian tumor tissue." Hum Mutat **26**(4): 384-9.
Thompson, M. C., C. Fuller, et al. (2006). "Genomics identifies medulloblastoma subgroups that are enriched for specific genetic alterations." J Clin Oncol **24**(12): 1924-31.
Timmermann, B., R. D. Kortmann, et al. (2002). "Role of radiotherapy in the treatment of supratentorial primitive neuroectodermal tumors in childhood: results of the prospective German brain tumor trials HIT 88/89 and 91." J Clin Oncol **20**(3): 842-9.
Timmermann, B., R. D. Kortmann, et al. (2006). "Role of radiotherapy in supratentorial primitive neuroectodermal tumor in young children: results of the German HIT-SKK87 and HIT-SKK92 trials." J Clin Oncol **24**(10): 1554-60.
Tischkowitz, M. D., J, Chisholm, et al. (2004). "Medulloblastoma as a first presentation of fancomi anemia." J Pediatr Hematol Oncol **26**(1): 52-5.
Tomlinson, I. P., R. Roylance, et al. (2001). "Two hits revisited again." J Med Genet **38**(2): 81-5.
Tong, C. Y., A. B. Hui, et al. (2004). "Detection of oncogene amplifications in medulloblastomas by comparative genomic hybridization and array-based comparative genomic hybridization." J Neurosurg **100**(2 Suppl Pediatrics): 187-93.

Tuefferd, M., A. De Bondt, et al. (2008). "Genome-wide copy number alterations detection in fresh frozen and matched FFPE samples using SNP 6.0 arrays." Genes Chromosomes Cancer **47**(11): 957-64.
Uematsu, Y., R. Takehara, et al. (2002). "Pleomorphic primitive neuroectodermal tumor with glial and neuronal differentiation: clinical, pathological, cultural, and chromosomal analysis of a case." J Neurooncol **59**(1): 71-9.
Vagner-Capodano, A. M., J. C. Gentet, et al. (1992). "Cytogenetic studies in 45 pediatric brain tumors." Pediatr Hematol Oncol **9**(3): 223-35.
Valent, A., G. Le Roux, et al. (2002). "MYCN gene overrepresentation detected in primary neuroblastoma tumour cells without amplification." J Pathol **198**(4): 495-501.
Varley, J. M., G. McGown, et al. (1999). "Are there low-penetrance TP53 Alleles? evidence from childhood adrenocortical tumors." Am J Hum Genet **65**(4): 995-1006.
Varley, J. M., G. McGown, et al. (1997). "Germ-line mutations of TP53 in Li-Fraumeni families: an extended study of 39 families." Cancer Res **57**(15): 3245-52.
Varley, J. M., M. Thorncroft, et al. (1997). "A detailed study of loss of heterozygosity on chromosome 17 in tumours from Li-Fraumeni patients carrying a mutation to the TP53 gene." Oncogene **14**(7): 865-71.
Versteege, I., N. Sevenet, et al. (1998). "Truncating mutations of hSNF5/INI1 in aggressive paediatric cancer." Nature **394**(6689): 203-6.
Vescovi, A. L., R. Galli, et al. (2006). "Brain tumour stem cells." Nat Rev Cancer **6**(6): 425-36.
Vincent, S., P. Dhellemmes, et al. (2002). "Intracerebral medulloepithelioma with a long survival." Clin Neuropathol **21**(5): 197-205.
Vissers, L. E., C. M. Ravenswaaij, et al. (2004). "Mutations in a new member of the chromodomain gene family cause CHARGE syndrome." Nat Genet **36**(9): 955-57.
Voeller, H. J., C. I. Truica, et al. (1998). "Beta-catenin mutations in human prostate cancer." Cancer Res **58**(12): 2520-3.
Vorechovsky, I., O. Tingby, et al. (1997). "Somatic mutations in the human homologue of Drosophila patched in primitive neuroectodermal tumours." Oncogene **15**(3): 361-6.
Vrieling, H. (2001). "Mitotic maneuvers in the light." Nat Genet **28**(2): 101-2.
Walter, A. W., R. K. Mulhern, et al. (1999). "Survival and neurodevelopmental outcome of young children with medulloblastoma at St Jude Children's Research Hospital." J Clin Oncol **17**(12): 3720-8.
Ward, S., B. Harding, et al. (2001). "Gain of 1q and loss of 22 are the most common changes detected by comparative genomic hybridisation in paediatric ependymoma." Genes Chromosomes Cancer **32**(1): 59-66.
Weeks, D. A., J. B. Beckwith, et al. (1989). "Rhabdoid tumor of kidney. A report of 111 cases from the National Wilms' Tumor Study Pathology Center." Am J Surg Pathol **13**(6): 439-58.
White, G. R., J. M. Varley, et al. (1998). "Isolation and characterization of a human homologue of the latrophilin gene from a region of 1p31.1 implicated in breast cancer." Oncogene **17**(26): 3513-9.
Wolter, M., J. Reifenberger, et al. (1997). "Mutations in the human homologue of the Drosophila segment polarity gene patched (PTCH) in sporadic basal cell carcinomas of the skin and primitive neuroectodermal tumors of the central nervous system." Cancer Res **57**(13): 2581-5.
Wong, Y. F., T. K. Chung, et al. (1998). "MTAP gene deletion in endometrial cancer." Gynecol Obstet Invest **45**(4): 272-6.
Xie, J., R. L. Johnson, et al. (1997). "Mutations of the PATCHED gene in several types of sporadic extracutaneous tumors." Cancer Res **57**(12): 2369-72.
Xie, Z., L. Y. Moy, et al. (2007). "Cep120 and TACCs control, interkinetic nuclear migration and the neural progenitor pool." Neuron **4**(56): 79-93.

Yagi, T. and M. Takeichi (2000). "Cadherin superfamily genes: functions, genomic organization, and neurologic diversity." Genes Dev **14**(10): 1169-80.
Yan, P.S., C. M. Chen, et al. (2001). "Dissecting complex epigenetic alterations in breast cancer using CpG island microarrays." Cancer Res **61**(23): 8375-80.
Yang, S., Y. Liu, et al. (2005). "Adaptive evolution of MRGX2, a human sensory neuron specific gene involved in nociception." Gene **6**(352): 30-5.
Yarden, Y. and M. X. Sliwkowski (2001). "Untangling the ErbB signalling network." Nat Rev Mol Cell Biol **2**(2): 127-37.
Yuan, B. Z., A. M. Jefferson, et al. (2004). "DLC-1 operates as a tumor suppressor gene in human non-small cell lung carcinomas." Oncogene **23**(7): 1405-11.
Yuan, B. Z., M. J. Miller, et al. (1998). "Cloning, characterization, and chromosomal localization of a gene frequently deleted in human liver cancer (DLC-1) homologous to rat RhoGAP." Cancer Res **58**(10): 2196-9.
Yuan, B. Z., X. Zhou, et al. (2003). "DLC-1 gene inhibits human breast cancer cell growth and in vivo tumorigenicity." Oncogene **22**(3): 445-50.
Zhang, J., A. Lindroos, et al. (2006). "Gene conversion is a frequent mechanism of inactivation of the wild-type allele in cancers from MLH1/MSH2 deletion carriers." Cancer Res **66**(2): 659-64.
Zhao, X., C. Li, et al. (2004). "An integrated view of copy number and allelic alterations in the cancer genome using single nucleotide polymorphism arrays." Cancer Res **64**(9): 3060-71.
Zheng, X., G. Shen, et al. (2007). "Most C6 cells are cancer stem cells: evidence from clonal and population analyses." Cancer Res **67**(8): 3691-7.
Zhou, X., S. S. Thorgeirsson, et al. (2004). "Restoration of DLC-1 gene expression induces apoptosis and inhibits both cell growth and tumorigenicity in human hepatocellular carcinoma cells." Oncogene **23**(6): 1308-13.
Zulch, K. J. (1979). Histological typing of tumours of the centra nervous system. Geneva, World Health Organisation.
Zurawel, R. H., C. Allen, et al. (2000). "Analysis of PTCH/SMO/SHH pathway genes in medulloblastoma." Genes Chromosomes Cancer **27**(1): 44-51.
Zurawel, R. H., S. A. Chiappa, et al. (1998). "Sporadic medulloblastomas contain oncogenic beta-catenin mutations." Cancer Res **58**(5): 896-9.
Zuzak, T. J., D. F. Steinhoff, et al. (2002). "Loss of caspase-8 mRNA expression is common in childhood primitive neuroectodermal brain tumour/medulloblastoma." Eur J Cancer **38**(1): 83-91.

APPENDIX